Iranica Journal of Energy & Environment 5 (2): 101-112, 2014
ISSN 2079-2115
IJEE an Official Peer Reviewed Journal of Babol Noshirvani University of Technology
DOI: 10.5829/idosi.ijee.2014.05.02.01

BUT

Process Analysis and Optimization of Industrial Estate Wastewater Treatment Using Conventional and Compartmentalized Membrane Bioreactor: A Comparative Study

G.R. Ghalekhani and A.A.L. Zinatizadeh

Water and Wastewater Research Center (WWRC), Department of Applied Chemistry, Faculty of Chemistry, Razi University, Kermanshah, Iran

Received: January 12, 2014; **Accepted** in Revised Form: June 11, 2014

Abstract: Membrane bioreactor (MBR) technology isan integrated combined system ofbiological and membrane processes to treat wastewater. MBR competently removes organic mattersand suspended solids from any type of wastewater. This study is aimed to evaluate and compare the performance of conventional and compartmentalized lab-scale MBR in treating an industrial estate wastewater (Faraman Industrial Estate, Kermanshah, Iran). The MBR systems were operated in two conditions; one in a completely stirred regime(conventional activated sludge (AS) system) and the other one in a semi plug flow regime(compartmentalized activated sludge (CAS) system). Experimental design was performed by response surface methodology (RSM) to assess the effect of two independent numerical factors *i.e.* hydraulic retention time (HRT) and mixed liquor volatile suspended solids (MLVSS) on nine responses.From the overall results, it was found that CAS-MBR performed better than AS-MBR.The CAS-MBR achieved 94.9% of TCOD removal efficiency at 24 h of HRT and MLVSS concentration of 10000 $mg.L^{-1}$. Compared to AS-MBR, CAS-MBR showed higher percentage of removal efficiency for total nitrogen andtotal Kjeldahl nitrogen. Moreover, CAS-MBR recorded the lowest SVI value of 55 $mL.mg^{-1}$compared to AS-MBR. Additional microfiltration has increased the TCOD removal in both systems. As a conclusion, the CAS-MBR operated at the same condition showed higher treatment capacityin compare to AS-MBR.

Key words: Industrial estate wastewater treatment · Conventional and compartmentalized MBR · Response surface methodology (RSM)

INTRODUCTION

As industries are rapidly developing, various kinds of wastewater discharged from the plants include high concentration organics and nutrients. The composition of industrial effluents is characterized by the high structural diversity of constituents and their high concentration level. Industrial wastewaters may be a severe hazard to receive waters and their plants and fauna. One of the major problems associated with the biological treatment of industrial wastewater is its slow and non-biodegradable fraction of chemical oxygen demand (COD) which inhibits the treatment performance of the bioreactors. Biological oxygen demand (BOD_5) per COD ratio (BOD_5/COD) constitutes a good measurement of the biodegradability of a wastewater and contaminants with a ratio of BOD_5/COD =0.4 are generally accepted as biodegradable [1]. From a review, the BOD_5/COD ratio for industrial estate wastewaters is varied from 0.17 to 0.74 [2]. Therefore, industries should attempt to treat its wastewater that will yield a satisfactory effluent for the particular receiving stream, which may necessitate considerable study, research and pilot investigations. The composition of industrial effluents is characterized by diverse in constituents with high concentration level [3]. High strength municipal wastewater [4] and complex composition of the industrial wastewater [5] accounts for, in some cases, unpredictable toxicological and ecotoxicological effects. In addition, slowly biodegradable chemical oxygen demand (sbCOD) is the major problem

Corresponding Author: A.A.L. Zinatizadeh, Water and Wastewater Research Center (WWRC), Faculty of Chemistry, Razi University, Kermanshah, Iran. E-mail: zinatizadeh@gmail.com; zinatizadeh@razi.ac.ir.

Please cite this article as: Ghalekhani, G.R. and A.A.L. Zinatizadeh, 2014. Process analysis and optimization of industrial estate wastewater treatment using conventional and compartmentalized membrane bioreactor: A comparative study. Iranica Journal of Energy and Environment, 5 (2): 101-112

Table 1: Summary of results from MBR studies on wastewater reuse

No.	Objective	MBR system details	MBR effluent quality	Ref.
1	Comparison of the performance of direct membrane filtration and MBR systems for municipal wastewater	MLSS: 4000–7000 mg/L Submerged hollow fibers Pore size:0.1 μm	COD_e: < 9 mg/L TSS: < 0.3 mg/L Turbidity: < 0.1 NTU	[15]
2	Effect of MLSS and organic loading rate on system performance for synthetic wastewater	MLSS: 3000–15000 mg/L Submerged tubular Pore size:20–40 μm	COD_e: 18–224 mg/L TSS: 0 mg/L	[16]
3	Effectiveness of MBR at COD and N removal at different HRTs for municipal wastewater	MLSS: 4200–8700 mg/L Flat sheet Pore size:0.45 μm	COD: 94–97% removal TSS: 100% removal TN: 62–76% removal	[17]
4	Effects of high MLVSS, sludge age and bioreactor configuration on MBR treating municipal wastewater	MLSS: 5000–15000 mg/L Submerged hollow fiber Pore size: 0.1 μm	COD: 96% removal TSS: 100% removal TN: 36–80% removal	[18]
5	Feasibility of MBR application in wastewater reuse for municipal wastewater	MLSS: 4800–9000 mg/L Submerged hollow fibers Pore size:0.04 μm	COD_e: 4–11 mg/L TSS: 0 mg/L TN: 1.1–5.4 mg/L	[19]
6	Influence of activated sludge characteristics on membrane fouling in a hybrid membrane bioreactor	MLSS: 12000 mg/L Submerged hollow fiber Pore size: 0.04 μm	COD_e: 12.9±3 mg/L TN: 8.1±4.5 mg/L Turbidity: <1 NTU	[20]
7	Effect of SRT and MLSS on performance of an MBR treating municipal wastewater	MLSS: 4000–17000 mg/L Submerged hollow fiber Pore size: 0.02 μm	COD_e: 19–40 mg/L TSS: 0 mg/L TN: 6.2–13.3 mg/L	[21]
8	Effects of operating parameters on MBR performance with respect to the removal of persistent organic pollutants	MLSS: 200–430 mg/L Flat sheet Pore size:0.4 μm	COD_e: 2.5–31 mg/L Turbidity: 0.2 NTU	[22]

associated with industrial wastewaters that are not typically considered in conventional treatment processes design. One solution for the aforementioned problem is to develop a bio process with high biomass concentration to provide a competitive microbial media.

Response surface methodology (RSM) is a combination of mathematical and statistical techniques used for developing, improving and optimizing the processes and it is used to evaluate the relative significance of several factors even in the presence of complex interactions. This methodology is widely used in chemical engineering, notably to optimize process variables. Optimization of biological treatment of industrial estate wastewater in a sequence batch reactor (SBR) [6], analysis of the interactive effects of cell concentration and light intensity on hydrogen production by *Rhodopseudomonas capsulate* [7]. Optimization of medium for phenylalanine ammonia lyase production in *Escherichia coli* [8], acidogenesis of cheese-whey wastewater to acetic and butyric acids [9], powdered activated carbon augmented activated sludge process for treatment of semi-aerobic landfill leachate [10], Fenton and photo-fenton treatment of distillery effluent and optimization of treatment conditions [11], process modeling and analysis of palm oil mill effluent treatment in an up-flow anaerobic sludge fixed film bioreactor [12], for optimization of electrospunnanofiber formation process [13], process modeling and analysis of biological nutrients removal in an integrated RBC-AS system using response surface methodology [14] are the examples of the RSM applications.

Membrane bioreactor (MBR) technology, which combines biological-activated sludge and membrane processes. For the treatment of many types of wastewaters, filtration has become more popular, abundant and accepted in recent years. Conventional activated sludge (CAS) process cannot cope with either composition of wastewater or fluctuations of wastewater flow rate. MBR technology is also used in cases where demand on the quality of effluent exceeds the capability of CAS. Although MBR capital and operational costs exceed the costs of conventional process, it seems that the upgrade of conventional process occurs even in cases when conventional treatment works well. Use of MBRs for wastewater reuse applications is still in its infancy and research teams worldwide are focusing their attention on characterizing the performance of MBRs for wastewater reuse and developing approaches to optimize the treatment efficacy. Table 1 summarizes the results from some recent studies on the use of MBRs for wastewater reuse applications.

The focus of the present study is to evaluate the performance of two types of lab-scale membrane bioreactors (MBR) in treating Faraman industrial wastewater (FIW). The MBR systems were operated in a completely stirred activated sludge (AS-MBR) and a semi plug flow compartmentalized activated sludge (CAS-MBR). For both systems, the output was analysed based on the interactive effect of two process variables *i.e.*mixed liquor volatile suspended solids (MLVSS) concentration and hydraulic retention time (HRT). Nine main parameters *i.e.* total chemical oxygen demand (TCOD) removal, rapid biodegradable chemical oxygen demand (rbCOD) removal, slowly biodegradable COD (sbCOD) removal, total effluent nitrate (NO_3^-) (TEN) concentration, total kjeldahl nitrogen (TKN) removal, total nitrogen (TN) removal, total phosphorous (TP) removal, sludge volume index (SVI) and effluent turbidity were measured and calculated as process responses. Response surface methodology (RSM) was used to analyse the collecteddata. Finally the process parameters were optimized.

MATERIALS AND METHODS

Wastewater Characteristics: Untreated wastewater samples were taken from Faraman Industrial Zone, Kermanshah, Iran. Table 2 shows the characteristics of this wastewater. The samples were stored in a cold room (4°C) before use and this step had no observable effect on its composition. Different dilutions of Faraman industrial wastewater (FIW) were prepared using tap water. Supplementary nutrients such as nitrogen (NH_4Cl) and phosphorous (KH_2PO_4) were added to give a ratio of COD: N: P of 1000:50:20.

Table 2: Faraman Industrial wastewater (FIW) characteristics

Parameter	Unit	Range
TCOD	$mg.L^{-1}$	800-1600
BOD_5	$mg.L^{-1}$	220-500
nbCOD*	$mg.L^{-1}$	35
sbCOD	$mg.L^{-1}$	450-750
TN	$mg.L^{-1}$	200-300
TP	$mg.L^{-1}$	40-60
TSS	$mg.L^{-1}$	100-400
pH	-	7.0-7.6

*The nbCOD was anticipated to be about 35 mg/l as intercept of (effluent COD) versus (1/HRT) plot.

Bioreactor Configuration and Start up: Figs. 1a and 1b illustrate the schematic drawings of lab-scale AS-MBR and CAS-MBR bioreactor set-up, respectively. Both set-ups have three basic vessels, *i.e.* an aeration tank, a settling tank and a membrane chamber. The working volume of the aeration tank in both systems was 3030±15 mL. The membrane chamber's working volume was 4150±15 mL cylindrical vessel including a submerged metallic membrane holder as shown in Fig. 2. Two units of

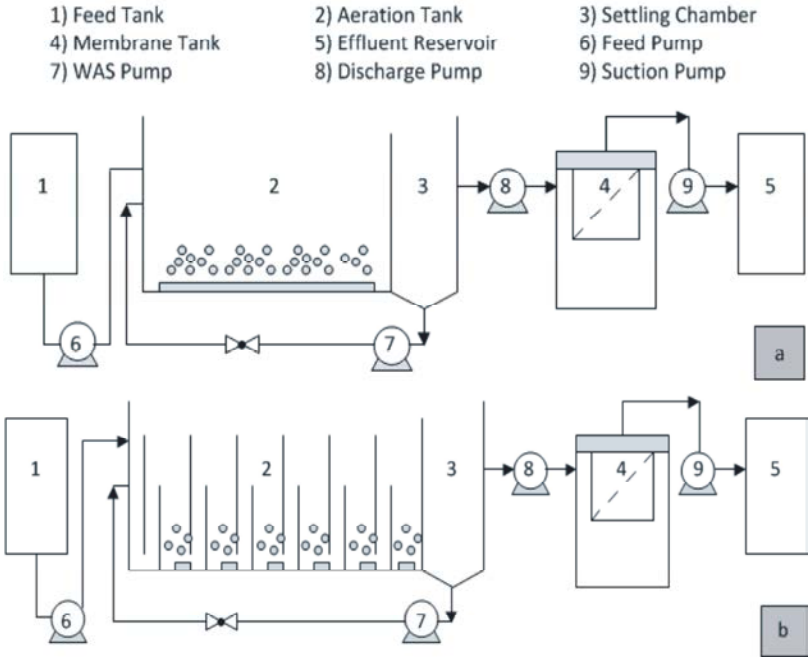

Fig. 1: Schematic diagram of (a) AS-MBR set-up and (b) CAS-MBR set-up.

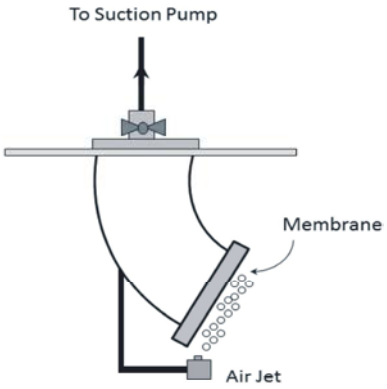

Fig. 2: Submerged membrane holder

Table 3: Experimental conditions.

Type of bioreactor	Run No.	MLVSS (B) (mg.L-1)	HRT (A) (h)
AS-MBR	1	4000	4
	2		8
	3		12
	4		36
	5	6000	24
	6	8000	18
	7		24
			24
			24
			24
			24
	8		30
	9	10000	24
	10	12000	4
	11		12
	12		36
CAS-MBR	1	4000	4
	2		8
	3		12
	4		36
	5	6000	24
	6	8000	18
	7		24
			24
			24
			24
			24
	8		30
	9	10000	24
	10	12000	4
	11		12
	12		36

adjustable speed peristaltic pump (PD5201, Heidolph, Germany) were used to feed and apply trans-membrane pressure to the membrane tanks. In order to control the dissolved oxygen (DO) level in aeration tank, DO was monitored in all experiments.

To start up the systems, the reactor was continuously fedby FIWwith 1.0 g $COD.L^{-1}d^{-1}$ of initial organic loading rate (OLR) for 24 h of HRT. The HRT and OLR were maintained constantly for 7 days throughout the start-up procedure. During this period, COD and BOD reduction were monitored.

Experimental Design and Mathematical Model

Variables: A general factorial design of RSM was used in this study. The design involves one categorical factor *i.e.* type of hydraulic regime (AS-MBR and CAS-MBR) and two different numerical factors *i.e* HRT (12-36h at 7 levels) and MLVSS (4000-12000 $mg.L^{-1}$ at 5 levels). The range was selected based on preliminary studies.

Design of Experiments: The biological treatment process was evaluated based on the number of experiments suggested by the factorial design as shown in Table 3. A total of 32 experiments were designed with 8 replicates to verify the results and errors. Due to industrial characteristics of FIW, rbCOD and sb CODfractionations were also monitored throughout the experiments. Therefore, total of nine parameters were identified as the responses. Following are the parameters; TCOD removal,rbCOD removal, sbCOD removal,TEN concentrations, TKN removal, TN removal, TP removal, SVI and effluent turbidity. Design of experiment (DOE) statistically minimizes the number of experimentsand eliminates experimental errors systematically.

Mathematical Modeling: After conducting the experiments, the coefficients of the polynomial model were calculated using the following equation [23].

$$R = \beta_0 + \sum \beta_i X_i + \sum \beta_{ij} X_i X_j + \sum \beta_{11} X_I^2 + \varepsilon$$

where R is the response,β_0 is the constant term, β_i representsthe coefficients of the linear parameters, β_{ii} represents the coefficients of the quadratic parameter, β_{ij}represents the coefficients of the interaction parameters X_i and X_j and $i < j$, X_i and X_j represents the variablesand åis the random error or noise to the response. The results were completely analyzed using analysis of variance (ANOVA) automatically performed by Design Expert software (Stat-Ease Inc., version 7.0.0). The Design Expert

software is a windows-compatible software which provides efficient design of experiments for the identification of vital factors that affect the process and uses response surface methodology (RSM) to determine optimal operational conditions. The results can be obtained as 3D presentations for visualization and also as contours to study the effect of system variables on responses. From these three-dimensional plots, the simultaneous interaction of the two factors on the responses was studied. The optimum region was also identified based on the main parameters in the overlay plot.

Analytical Methods: The concentrations of TCOD, BOD and TEN, the removal of TKN, TN and TP, SVIand MLVSS of the systems were determined using standard methods for water and wastewater testing [24]. For COD, a colorimetric method with closed reflux procedure was used. To measure the absorbance of COD samples, a spectrophotometer (model 6320D, Jenway, USA) at 600 nm was used. TKN was determined using TKN meter Gerhardt (model Vapodest10) and the turbidity was measured usingturbidimeter (model 2100P, Hach Co.).

RESULTS AND DISCUSSION

Statistical Analysis: The ANOVA results for the responses are summarized in Table 4. In this study, various responses were investigated; therefore, different degree of polynomial models was used for data fitting. The regression equations obtained are presented in Table 4. In order to quantify the curvature effects, the data from the experimental results were fitted to higher degree polynomial equations, *i.e.* two-factor interaction (2FI) and quadratic. The model terms in the equations are generated after eliminating the insignificant variables. Based on the statistical analysis, the models were highly significant with very low probability values (<0.0010). Table 4 shows that the model terms of independent variables were significant at the 95% confidence level. The square of correlation coefficient for each response was computed as coefficient of determination (R^2). It showed a good agreement between actual and predicted values.

Adequate precision (AP) is a measurement in a certain range to predict response relative to its associated error or, in other words, a signal-to-noise ratio. The values of AP should be 4.00 or more [23]. Table 4 shows that th values of AP for all the models were satisfactory. Conversely, low values of the coefficient of variation (CV) (1.74-12.96%) indicates good precision and reliability of the experiments as suggested by Kuehl and Khuri and Cornell [23-26].

AS-MBR and CAS-MBR Performance CODRemoval: COD removal for both systems were quantified using three different parameters *i.e.* TCOD,rbCOD and sbCOD. Due to industrial characteristics of FIW, rapid (rbCOD) and slow (sbCOD) biodegradable COD fractionations were also monitored throughout the experiments.

TCOD Removal: Two modified quadratic models were developed to describe the variation of the TCOD removal efficiency as a function of the variables (HRT=A and MLVSS=B) in both systems as shown in Table 4. The significance of each coefficient was determined by *F*-value and *P*-value. From Table 4, it was noticed that A, B and A^2 are the significant model terms for the both systems. Figs. 3a and 3b illustrate the effects HRT and

Table 4: ANOVA results for the responses studied

Type of bioreactor	Response	Modified equations with significant terms*	Probability	R^2	Adj.R^2	Adeq. Precision	S.D	CV
AS-MBR	TCOD removal	$88.21+8.41A+3.46B-11.98A^2$	0.0008	0.7415	0.6769	9.898	5.44	6.49
	Effluent NO_3^-	$35.45+0.84A+5.56B-5.42B^2-0.86AB$	< 0.0001	0.9877	0.9816	38.860	0.59	1.74
	TKN removal	$14.96+1.31A+5.05B$	< 0.0001	0.8529	0.8234	18.215	1.45	9.71
	TP removal	$10.86+1.84A+2.82B-1.65B^2-0.90AB$	< 0.0001	0.9888	0.9832	51.105	0.29	2.86
	SVI	$106.97-53.92B+20.65B^2$	< 0.0001	0.9305	0.9166	21.814	10.29	9.02
	Effluent Turbidity	$7.84-0.53A-6.94B+2.21A^2+3.05B^2$	< 0.0001	0.9885	0.9843	39.745	0.71	6.78
CAS-MBR	TCOD removal	$89.21+7.29A+8.22B-9A^2$	< 0.0001	0.8182	0.7727	13.150	4.72	5.51
	Effluent NO_3^-	$34.67+1.23A+5.94B-4.93B^2$	< 0.0001	0.9594	0.9459	24.964	1.03	3.14
	TKN removal	$15.38+7.03B$	< 0.0001	0.8678	0.8558	20.425	1.75	11.41
	TP removal	$10.28+1.84A+2.82B-0.90AB$	0.0002	0.8765	0.8353	18.231	0.92	8.97
	SVI	$107.69+2.54A-58.74B+8.24B^2$	< 0.0001	0.9972	0.9962	99.478	2.22	2.01
	Effluent Turbidity	$7.45-5.96B+3.05B^2$	< 0.0001	0.9443	0.9357	22.947	1.20	12.96

* A and B are HRT and MLVSS, respectively.

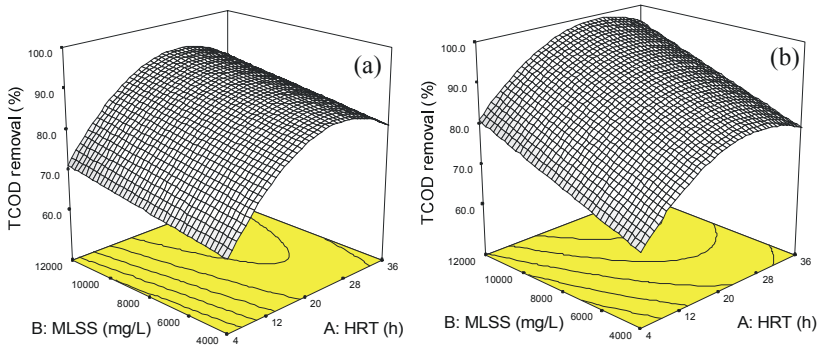

Fig. 3: Response surface plots for TCOD removal; (a) AS-MBR, (b) CAS-MBR.

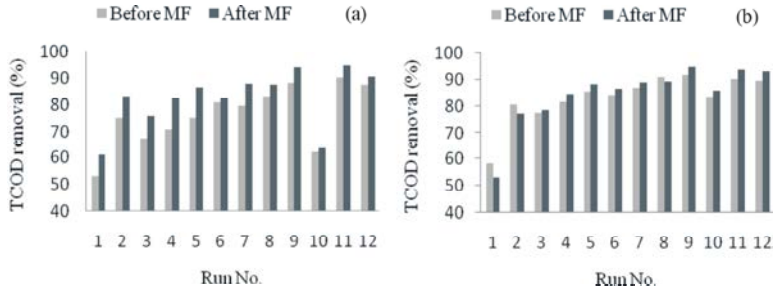

Fig. 4: Effect of microfiltration on the TCOD removal; (a) AS-MBR, (b) CAS-MBR.

MLVSS on the removal of TCOD in the AS-MBR and CAS-MBR, respectively. An increasing trend in TCOD removal percentage was observed with an increase in HRT and MLVSS concentration.

As expected, CAS-MBR system showed a better performance of TCOD removal compared to AS-MBR. Maximum TCOD removal efficiency for AS–MBR was 94.7% at HRT of 24h and MLVSS of 12000 mg.L^{-1}, while for CAS-MBR it was more than 98% at HRT of 24h and MLVSS of 12000 mg.L^{-1}. At lower HRT and MLVSS values, (4h and 4000 mg.L^{-1}), minimum removal of TCOD was recorded for both systems *i.e.* 61.0% for AS-MBR and 53.1% for CAS-MBR.

In order to analyze the performance of the biological treatment, TCOD removal measurements were also taken before and after microfiltration (MF). Figs. 4a and 4b show the effects of TCOD removal with and without membrane microfiltration in AS-MBR and CAS-MBR systems, respectively. The data have been plot according to the number of experiments in Table 3. Microfiltration showed a good improvement in TCOD removal efficiencies for both systems. It showed about 1.5 to 11.7% and 1.0 to 3.6% increase in TCOD removal for AS-MBR and CAS-MBR systems, respectively. These results prove that microfiltration enhances AS-MBR to remove its TCOD content. Therefore, the need for microfiltration in CAS-MBR is less than AS-MBR.

rbCODand sbCOD Removal: Fig. 5a shows rbCOD removal efficiencies for AS-MBR and CAS-MBR systems. Highest rbCOD removal was achieved at HRT of 20 and 12hwith the MLVSS concentration of 8000 mg.L^{-1} and 12000 mg.L^{-1} for CAS-MBR system and AS-MBR system respectively. A minimum removal of rbCOD was recorded at HRT of 4h and MLVSS concentration of 4000 mg.L^{-1} for both systems. CAS-MBR system showed higher (92%) average removal of rbCOD compared to AS-MBR (87%). This is because of the semi plug-flow regime in CAS-MBR provides additional area for reaction to take place along the reactor and it has significant low dead zone. In overall, both bioreactors showed a good performance of rbCOD removal.

One of the major problems associated with biological treatment of industrial wastewaters is non-biodegradable (nbCOD) and slow biodegradable (sbCOD) fraction of COD. Both COD's inhibit the performance of bioreactors [1]. BOD/COD ratio represents a good measurement for biodegradability of a wastewater. Contaminants with a ratio of BOD_5/COD ≥0.4 are generally accepted as biodegradable [1]. The ratio of FIW was in the range of 0.22-0.35. Fig. 5b shows the removal efficiencies of sbCOD in AS-MBR and CAS-MBR systems. Atthe highest operating condition of HRT (36 h) and MLVSS concentration (12000 mg.L^{-1}), the maximum removal efficiency for AS-MBR and CAS-MBR systems were

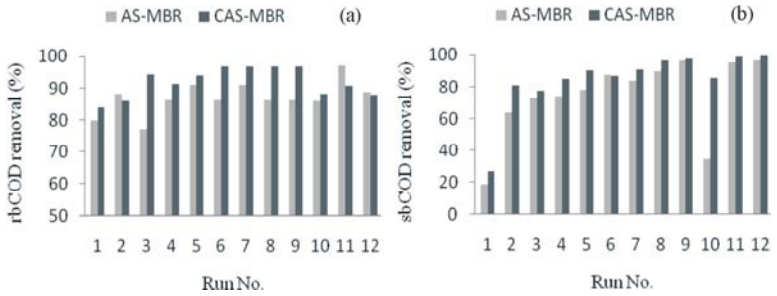

Fig. 5: Evaluation of (a) rbCOD removal and (b) sbCOD removal efficiency in the AS-MBR and CAS-MBR.

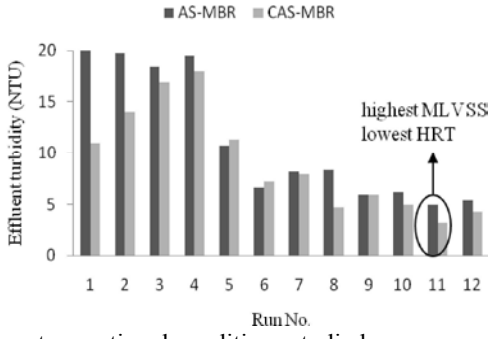

Fig. 6: Effluent turbidity under different operational conditions studied.

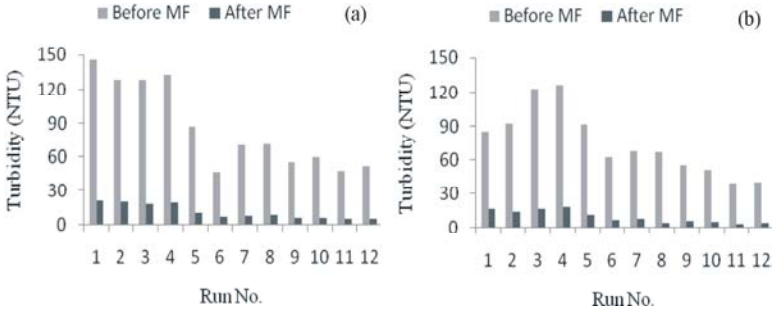

Fig. 7: Effect of microfiltration on the turbidity reduction; (a) AS-MBR, (b) CAS-MBR.

recorded as 96.6 and 99.7%, respectively. On the hand, CAS-MBR was more efficient than AS-MBR in terms of sbCOD removal and it was merely due to its specific hydraulic regime.

Effluent Turbidity: Effluent turbidity measurement is used to indicate the clarity of treated wastewater with respect to colloidal and residual particulate matter. Thus, in this study the potential of the membrane bioreactors to reduce the initial turbidity of the influent (~ 700-1000 NTU) was analyzed. Fig. 6 shows the trend of effluent turbidity for both systems according to the number of runs in Table 3.

Minimum value of turbidity was achieved at the highest MLVSS concentration (12000 $mg.L^{-1}$) and lowest HRT (12 h). The range of the effluent turbidity achieved was 5.0 - 21.0 NTU and 4.1 - 18.0 NTU for AS-MBR and CAS-MBR, respectively. Both systems managed to clarify the effluent efficiently. However, it was observed that at certain MLVSS concentration, if the HRT is increased there was a drastic change in turbidity for both systems. Higher values of turbidity in AS-MBR system was observed compared to CAS-MBR and this could be due to cell debris during the biological treatment.

Figs. 7a and 7b show the effect of microfiltration in turbidity reduction for AS-MBR and CAS-MBR systems. The data is presented based on the number of runs in Table 3. Microfiltration showed a significant improvement in turbidity reduction for both systems. The figures show about 84.5-89.7% and 80.0-91.8% increase in turbidity reduction for AS-MBR and CAS-MBR systems, respectively. AS-MBR and CAS-MBR (97.00-99.50 and 97.43-99.68%, respectively) have sufficiently reduced turbidity in all the experiments studied.

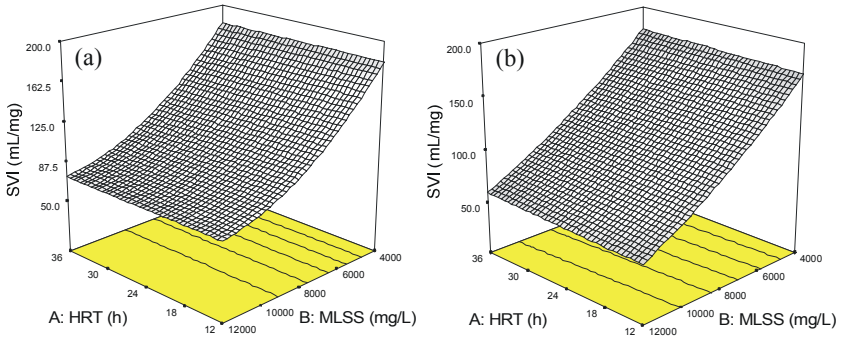

Fig. 8: Response surface plots for SVI; (a) AS-MBR, (b) CAS-MBR.

Sludge Volume Index (SVI): The SVI was reported as milliliter of settled volume per gram of MLVSS. SVI readings are used to identify the settling and compaction characteristics of sludge and determine the effects of the variables on the sludge characteristics. From the literature it is known that SVI< 80, 80≤ SVI ≥150 and SVI > 150 indicates excellent, moderate and poor settling and compacting characteristics respectively. From the ANOVA results in Table 4, the significant model terms for SVI was identified as a function of B and B^2 for AS-MBR and A, B and $B^2$for CAS-MBR. Figs. 8a and 8b depict the dependency of SVI with variables in AS-MBR and CAS-MBR, respectively. The SVI values are in between 70.8-185 $mL.mg^{-1}$ and 55-177.5 $mL.mg^{-1}$ for AS-MBR and CAS-MBR, respectively.

The results also showed that for CAS-MBR, SVI decreased intensively when MLVSS concentration increases from 4000 to 12000 $mg.L^{-1}$, indicating favored conditions for microbial aggregation at a lower food to microorganisms (F/M) ratio [27] in the plug-flow hydraulic regime. An insignificant effect on SVI was noticed with changes in HRT for the range tested, although at certain MLVSS concentration (8000 $mg.L^{-1}$ for run numbers 6, 7 and 8) increase in HRT led to a slight increase in the response. This could be related to excessive growth of filamentous bacteria in low F/M ratio [27].

Total Nitrogen (TN) Removal: Due to the usage of high concentrations of MLVSS and longer period of HRT in this study (12000 $mg.L^{-1}$ and 36h, respectively), the nitrogen fractionation and phosphorus concentration were monitored to find out the probability of the biological nutrient nitrogen and phosphorus removal.

Total Effluent Nitrate (NO_3^-)(TEN) Concentration: Nitrate (NO_3-N) is the most oxidized form of nitrogen found in wastewater. In Iran, standard limit of nitrogen has been set to50 $mg.L^{-1}$ as NO_3^- in primary drinking water becauseof its serious health effects and occasionally fatal effects on infants.

The regression results for the effluent NO_3^- data are presented in Table 4. A, B, B^2 and AB were significant model terms for the AS-MBR, while for CAS-MBR were A, B and B^2, indicating that MLVSS concentration (B) is more effective than HRT (A) on the response in the both types of hydraulic regimes. It was observed that an increase in the variables caused an increase in the responses in the both systems due to an increase in oxidation potential that favored the nitrification process [5]. Effluent NO_3^- concentration increased from 22.49 to 35.87 $mg.L^{-1}$and 21.35 to 35.98 $mg.L^{-1}$ for AS-MBR and CAS-MBR, respectively. Maximum values of NO_3^- were obtained at maximum HRT and MLVSS concentration in both systems. Low F/M value at high MLVSS concentrations and low BOD loading rate at the high HRTs (≤ 0.16 $g.L^{-1}.d^{-1}$ at HRT≥ 18h) in the AS-MBR and CAS-MBR systems resulted the high nitrification rate. A similar finding was reported by Farizoglu and his colleagues [28]. Furthermore, in this study higher dosage of dissolved oxygen (DO) was applied (5-7 $mg.L^{-1}$) and this could also indirectly enhances the nitrification process.

Total Kjeldahl Nitrogen (TKN) Removal: Removal of TKN is essential to control the release of organic nitrogen to the medium. The TKN removal data was fitted with two modified linear models as shown in Table 4. Aand B were the significant model terms for AS-MBR and only B for CAS-MBR. It was noticed that for CAS-MBR system the response was independent of HRT. This difference was attributed due to the carbon source which was consumed in the first compartments of the CAS-MBR system, while effective nitrification has been occurred at the last ones. In other words, because of low F/M values in last compartments of CAS-MBR system, microorganisms were

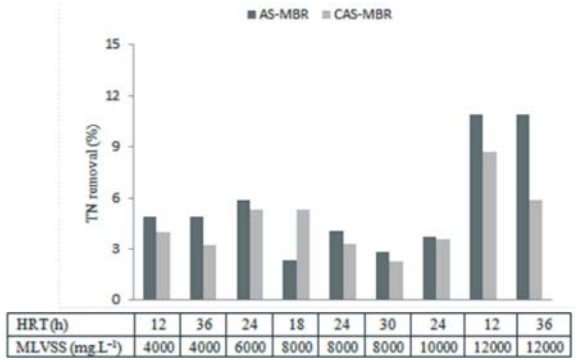

HRT (h)	12	36	24	18	24	30	24	12	36
MLVSS (mg L^{-1})	4000	4000	6000	8000	8000	8000	10000	12000	12000

Fig. 9: TN removal under different operational conditions studied.

forced to use nitrogenous source as food. The amount of 21.1 and 22.1% were found as the maximum TKN removal for the AS-MBR and CAS-MBR, respectively.

Total Nitrogen (TN) Removal: In conventionally treatment processes, biological nitrogen removal is achieved by nitrification followed by a denitrification process, *i.e.* (a) aerobic nitrification of NH_4^+ by chemolithoautotrophic bacteria to NO_2^- or NO_3^- with O_2 as the electron acceptor and (b) anoxic denitrification of NO_2^- or NO_3^- to gaseous N_2 by heterotrophic microorganism using organic matter as carbon and energy source [29].

Fig. 9 shows the TN removal for all experiments in the AS-MBR and CAS-MBR. Maximum values of TN removal (10.94% in the AS-MBR and 8.70% in CAS-MBR) were obtained at the highest MLVSS concentration of 12000 mg.L^{-1} in the both systems. The TN removal percentage in the AS-MBR was higher comparatively to CAS-MBR and this is attributed to the endogenous respiration in the low F/M ratios in the system [27]. Moreover, 11-12% of microbial cell content was composed of nitrogen and the total nitrogen used for cell generation was greater than the amount of TN removed. This might be due to the release of nitrogen gas from cells during microbial dissimilation.

Total Phosphorous (TP) Removal: Phosphorus removal in biological treatment process can be done by repeating anaerobic and aerobic steps and this will lead to phosphorus accumulating organisms (PAOs) in the form of polyphosphate. ANOVA results in Table 4 shows that A, B, B^2 and AB were significant model terms for AS-MBR, whereas for CAS-MBR it was A, B and AB for TP removal. It was found that both systems, at the operating conditions applied, did not show good removal of TP. The maximum removal of TP achieved by AS-MBR and CAS-MBR was about 13.0 and 13.3% respectively. Low percentage of TP removal is expected due to the low influent BOD/COD ratio (0.22-0.35) and high concentration of NO_3^- (21-36 mg.L^{-1}) and PO_4^{3-}(8.6-9.8 mg.L^{-1}) ions in both systems. It is known that $NO_3^-$and PO_4^{3-} ions could interfere as an oxidative agent [30, 31]. However, there was a small increase in TP removal with increasing HRT and MLVSS concentration in the both systems. This is mainly because of increasing COD removal at high values of HRT and MLVSS concentration. Furthermore, in this condition, microorganisms use phosphorus for their cell growth [5].

Amount of TP used for cell generation was also calculated based on 1% phosphorous content of cells. Similar to nitrogen, results showed that in low MLVSS concentrations, the TP used for cell generation was greater than TP removed. Probably, it was related to partial anaerobic and/or anoxic conditions were occurred during retention in the settling chamber. In the described conditions, phosphorous was released from cell as polyhydroxybutyrate (PHB) [5]. Moreover, high level of DO and continuous aeration, could be the reason for low nutrients removal in the MBR systems [32]. Therefore, for the systems with the aim of nutrient removal, the intermittent aeration and/or lower aeration rate is strongly recommended.

Process Optimization: From the study, it was found that TCOD removal, rbCOD removal, sbCOD removal and effluent turbidity were the most critical responses to achieve a highly treated effluent. Thus, to optimize the process, TCOD and effluent turbidity wereconsidered as main parameters to provide two groups *i.e.* Group 1 with COD removal ≥ 80% and Group 2 with COD removal ≥ 90% and each group investigated at three levels of the effluent turbidity (5, 10 and 15 NTU). Fig. 10 shows graphical optimization, which display the area of feasible response values (shaded portion) in the factors space. The graphical optimization results allow visual inspection to choose the optimum operating conditions.

Fig. 10 displays the overlay plot forCOD removal ≥ 90% and Fig. 11 for COD removal ≥ 80% for both systems. For COD removal ≥ 90%, an optimum condition was not found for AS-MBR (Figs. 10a1, 10a2 and 10a3); however, for CAS-MBRan optimum region covered by HRT of 12-35 h and MLVSS more than 10000 mg.L^{-1} was found (Figs. 10b1, 10b2 and 10b3). For COD removal ≥ 80% an optimum region was found for both systems (Fig. 11). As a conclusion, the CAS-MBR showed higher treatment capacity at the same condition compared to AS-MBR.

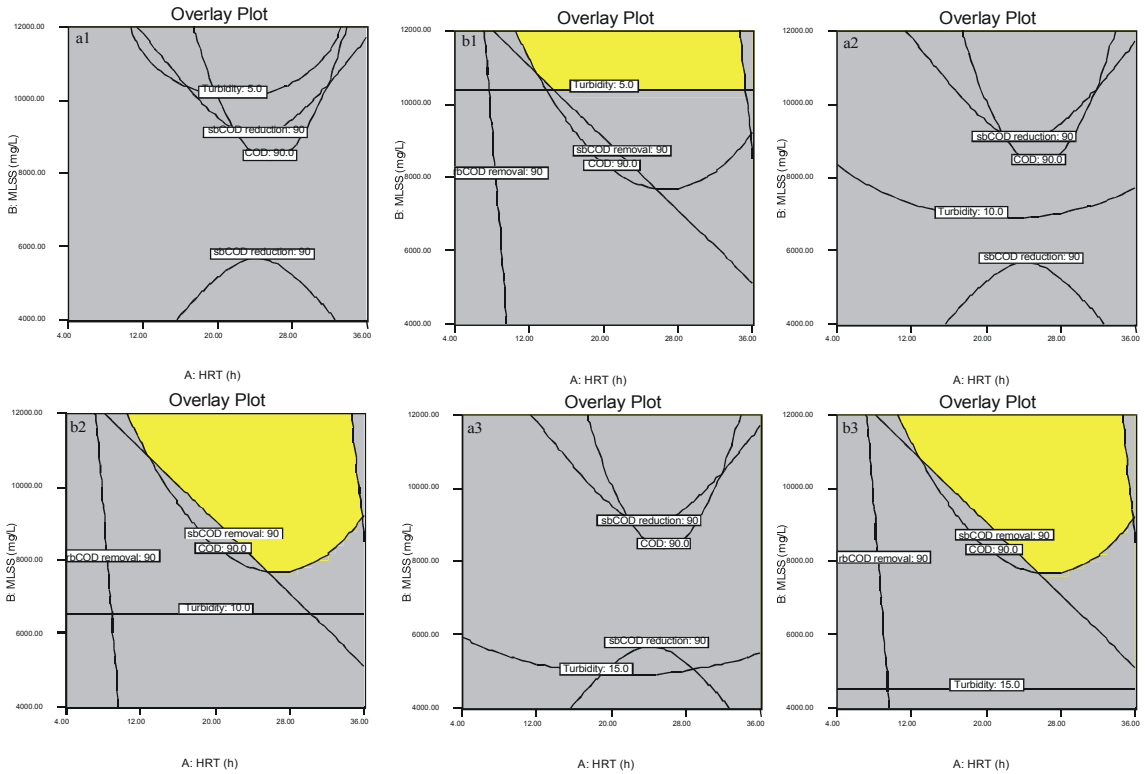

Fig. 10: Overlay plots for the optimal region with 90% COD removal at three levels of effluent turbidity (5, 10 and 15 NTU): (a) AS-MBR, (b) CAS-MBR.

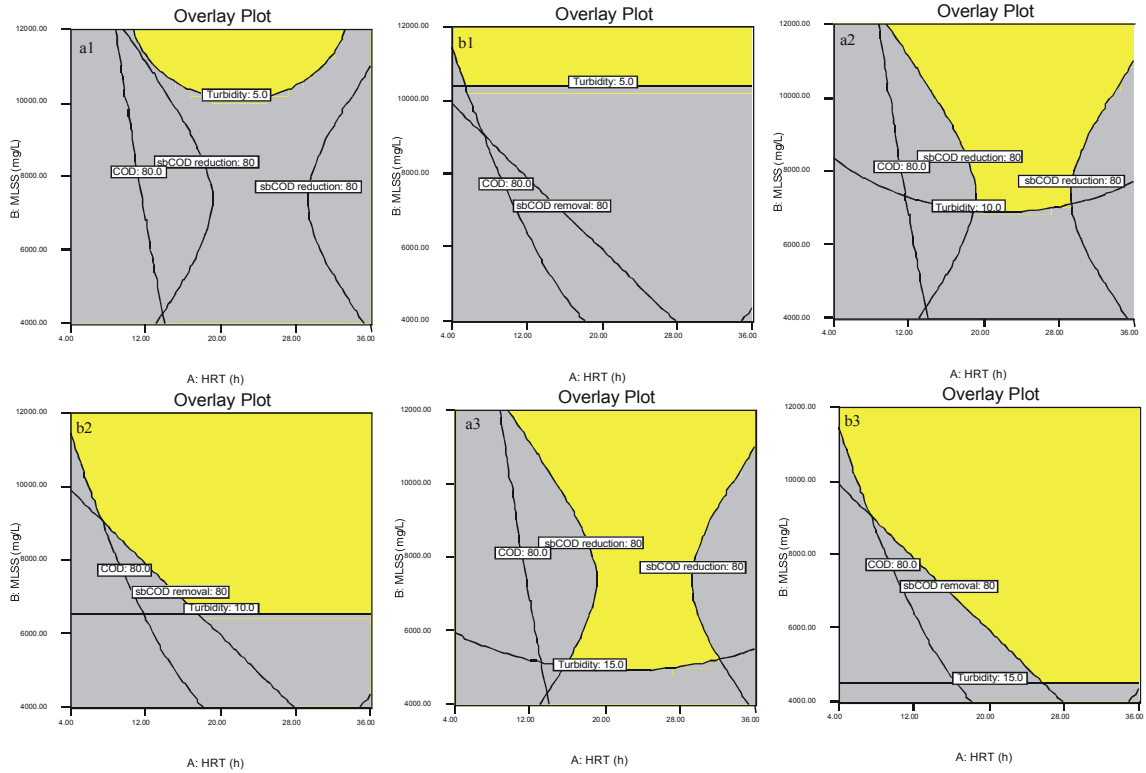

Fig. 11: Overlay plots for the optimal regionwith 80% COD removal at three levels of effluent turbidity (5, 10, 15 NTU): (a) AS-MBR, (b) CAS-MBR.

CONCLUSION

Two lab-scale membrane bioreactor with different hydraulic flow regimes (AS-MBR and CAS-MBR) were successfully designed and operated for FIW treatment. Maximum TCOD removal efficiency for AS–MBR was 94% at HRT of 24h and MLVSS of 12000 $mg.L^{-1}$; while for CAS-MBR it was more than 98% at the same condition. CAS-MBR was more efficient than AS-MBR in terms of sbCOD removal due to the specific regime. Microfiltration showed a significant effect in turbidity reduction; however, the need for microfiltration in CAS-MBR was less than AS-MBR. The optimum region for CAS-MBR is at HRT 12-35 h and MLVSS of more than 10000 mg/l. AS-MBR could not achieve COD removal higher than 90% with an effluent turbidity less than 15 NTU while CAS-MBR was able to achieve COD removal higher than 90% with an effluent turbidity even less than 5 NTU. As a conclusion, the CAS-MBR showed higher treatment capacity at the same condition compared to AS-MBR.An intermittent aeration and/or lower aeration rate are recommended for both systems as an effective strategy to remove nutrients.

REFERENCES

1. Sajjadi, B., M.K. Moraveji and R. Davarnejad, 2011. Investigation of Temperature and Influent Load on Nitrifying Treatment of Using Wastewater CFD. Iranica Journal of Energy and Environment, 2: 08-17.
2. Chan, Y.J., M.F. Chong, C.L. Law and D. Hassell, 2009. A review on anaerobic–aerobic treatment of industrial and municipal wastewater. Chemical Engineering Journal, 155(1): 1-18.
3. Chelliapan, S., S.B. Mahat, M.F.M. Din, A. Yuzir and N. Othman, 2012. Anaerobic digestion of paper mill wastewater. Iranica Journal of Energy & Environment, 3(2): 85-90.
4. Birima, A.H., T.A. Mohammed, M.J. Megat Mohd Noor, S.A. Muyibi, A. Idris, H. Nagaoka, J. Ahmed and L. Abdul Ghani, 2009. Membrane fouling in a submerged membrane bioreactor treating high strength municipal wastewater. Desalination and Water Treatment, 7(1-3): 267-274.
5. Metcalf, I. and H. Eddy, Wastewater engineering; treatment and reuse. Vol. 346. 2003: McGraw-Hill New York.
6. Asadi, A. and A. Ziantizadeh, 2011. Statistical Analysis and Optimization of an Aerobic SBR Treating an Industrial Estate Wastewater Using Response Surface Methodology (RSM). Iranica Journal of Energy & Environment, 24: 356-365.
7. Zheng, Y.M., H.Q. Yu and G.P. Sheng, 2005. Physical and chemical characteristics of granular activated sludge from a sequencing batch airlift reactor. Process biochemistry, 40(2): 645-650.
8. Cui, J.D., 2010. Optimization of medium for phenylalanine ammonia lyase production in E. coli using response surface methodology. Korean journal of chemical engineering, 27(1): 174-178.
9. Yang, K., Y. Yu and S. Hwang, 2003. Selective optimization in thermophilic acidogenesis of cheese-whey wastewater to acetic and butyric acids: partial acidification and methanation. Water Research, 37(10): 2467-2477.
10. Aghamohammadi, N., H.b.A. Aziz, M.H. Isa and A.A. Zinatizadeh, 2007. Powdered activated carbon augmented activated sludge process for treatment of semi-aerobic landfill leachate using response surface methodology. Bioresource Technology, 98(18): 3570-3578.
11. Hadavifar, M., A.A. Zinatizadeh, H. Younesi and M. Galehdar, 2010. Fenton and photo-Fenton treatment of distillery effluent and optimization of treatment conditions with response surface methodology. Asia-Pacific Journal of Chemical Engineering, 5(3): 454-464.
12. Zinatizadeh, A.A., A. Mohamed, A. Abdullah, M. Mashitah, M. Hasnain Isa and G. Najafpour, 2006. Process modeling and analysis of palm oil mill effluent treatment in an up-flow anaerobic sludge fixed film bioreactor using response surface methodology (RSM). Water Research, 40(17): 3193-3208.
13. Ziabari, M., V. Mottaghitalab and A.K. Haghi, 2010. A new approach for optimization of electrospun nanofiber formation process. Korean Journal of Chemical Engineering, 27(1): 340-354.
14. Akhbari, A., A.A. Zinatizadeh, P. Mohammadi, M. Irandoust and Y. Mansouri, 2011. Process modeling and analysis of biological nutrients removal in an integrated RBC-AS system using response surface methodology. Chemical Engineering Journal, 168(1): 269-279.

15. Ahn, K.H., K. Song, I. Yeom and K. Park, 2001. Performance comparison of direct membrane separation and membrane bioreactor for domestic wastewater treatment and reuse. Water Science and technology: Water Supply, 1: 5-6.
16. Al-Malack, M.H., 2007. Performance of an immersed membrane bioreactor (IMBR). Desalination, 214(1): 112-127.
17. Chae, S., S. Kang, S. Lee, E. Lee, S. Oh, Y. Watanabe and H. Shin, 2007. High reuse potential of effluent from an innovative vertical submerged membrane bioreactor treating municipal wastewater. Desalination, 202(1): 83-89.
18. Côté, P., H. Buisson, C. Pound and G. Arakaki, 1997. Immersed membrane activated sludge for the reuse of municipal wastewater. Desalination, 113(2): 189-196.
19. Fatone, F., P. Battistoni, P. Pavan and F. Cecchi, 2006. Application of a membrane bioreactor for the treatment of low loaded domestic wastewater for water re-use. Water Science & Technology, 53(9): 111-121.
20. Wang, X.C., Y.S. Hu and Q. Liu, 2012. Influence of activated sludge characteristics on membrane fouling in a hybrid membrane bioreactor. Desalination and Water Treatment, 42(1-3): 30-36.
21. Innocenti, L., D. Bolzonella, P. Pavan and F. Cecchi, 2002. Effect of sludge age on the performance of a membrane bioreactor: influence on nutrient and metals removal. Desalination, 146(1): 467-474.
22. Lipp, P., K. Kreißel, S. Meuler, F. Bischof and A. Tiehm, 2009. Influencing parameters for the operation of an MBR with respect to the removal of persistent organic pollutants. Desalination and Water Treatment, 6(1-3): 102-107.
23. Kuri, A. and J. Cornell, 1996. Response Surfaces. Design and Analyses, 1996, Marcel Dekker, Inc., New York. Second Edition, Revised and Expanded.
24. APHA, 1998. Standard methods for the examination of water and wastewater. American Public Health Association, Washington, DC.
25. Noordin, M.Y., V.C. Venkatesh, S. Sharif, S. Elting and A. Abdullah, 2004. Application of response surface methodology in describing the performance of coated carbide tools when turning AISI 1045 steel. Journal of Materials Processing Technology, 145(1): 46-58.
26. Kuehl, R., 2000. Design of experiments: statistical principles of research design and analysis, 2000, Pacific Grove, CA, USA: Duxberry Press.
27. Chua, H., H. Peter, S.N. Sin and K.N. Tan. Effect of food: microorganism ratio in activated sludge foam control. in Twenty-First Symposium on Biotechnology for Fuels and Chemicals. 2000. Springer.
28. Farizoglu, B., B. Keskinler, E. Yildiz and A. Nuhoglu, 2007. Simultaneous removal of C, N, P from cheese whey by jet loop membrane bioreactor (JLMBR). Journal of hazardous materials, 146(1): 399-407.
29. Golbabaei Kootenaei, F. and H. Amini Rad, 2013. Removal of nutrients from hospital wastewater by novel nano-filtration membrane bioreactor (NF-MBR). Iranica Journal of Energy & Environment, 4(1): 60-67.
30. Kuba, T., A. Wachtmeister, M. Van Loosdrecht and J. Heijnen, 1994. Effect of nitrate on phosphorus release in biological phosphorus removal systems. Water Science and Technology, 30(6): 263-269.
31. Chang, H.N., R.K. Moon, B.G. Park, S.J. Lim, D.W. Choi, W.G. Lee, S.L. Song and Y.H. Ahn, 2000. Simulation of sequential batch reactor (SBR) operation for simultaneous removal of nitrogen and phosphorus. Bioprocess Engineering, 23(5): 513-521.
32. Third, K.A., M. Newland and R. Cord-Ruwisch, 2003. The effect of dissolved oxygen on PHB accumulation in activated sludge cultures. Biotechnology and Bioengineering, 82(2): 238-250.

Persian Abstract

DOI: 10.5829/idosi.ijee.2014.05.02.01

چکیده

در این مطالعه، حذف همزمان کربن، نیتروژن و فسفر از فاضلاب سنتزی در یک بیوراکتور با جریان رو به بالای هوازی/انوکسیک با فیلم ثابت لجن (UAASFF) مورد بررسی قرار گرفت. تحلیل سینتیکی با استفاده از داده های آزمایشگاهی به دست آمده از مطالعه قبلی که در آن بیوراکتور UAASFF تحت شرایط راهبری مختلف با تغییر سه متغیر مستقل HRT ، نسبت COD:N:P و زمان هوادهی مورد آزمایش قرار گرفته بود، انجام شد. در این تحلیل مدل های مختلف سینتیکی (مونود، درجه اول، درجه دوم؛ و استوور کین کنن) مورد ارزیابی قرار گرفتند. حداکثر راندمان حذف برای COD، نیتروژن کل (TN) و فسفر کل(TP) به ترتیب ۹۵/۴۲، ۷۹ و ۷۹/۱٪ به دست آمد. تمام مدل های آزمایش شده، ضرایب همبستگی بالایی را برای حذف کربن، نیتروژن و فسفر نشان دادند. ضرائب سینتیکی به دست آمده در این مطالعه به صورت زیر می باشند:

$Y= 0.417\text{-}0.496$ g VSS/g COD, $k_d= 0.027\text{-}0.053$ d^{-1}, μ_{max} =1.36 g VSS /g VSS.d, K_B=37.96 g/l.d, U_{max}=38.46 g/l.d, $K_B(N)$ =0.271-7.2 g/l.d 6, $U_{max}(N)$ =0.33-5.4 g/l.d, $K_B(P)$=0.09-0.89 g/l.d, $U_{max}(P)$=0.07-0.42 g/l.d

Iranica Journal of Energy & Environment 5 (2): 113-123, 2014
ISSN 2079-2115
IJEE an Official Peer Reviewed Journal of Babol Noshirvani University of Technology
DOI: 10.5829/idosi.ijee.2014.05.02.02

BUT

A Novel Approach to Investigate Adsorption of Crystal Violet from Aqueous Solutions Using Peels of *Annona squamosa*

K. Mahalakshmi, S.K. Suja, K. Yazhini, S. Mathiya and G. Jayanthi Kalaivani

Department of Chemistry, Lady Doak College, Madurai, Tamilnadu, India

Received: April 12, 2014; **Accepted** in Revised Form: June 11, 2014

Abstract: An effective and economical adsorbent was prepared from the peels of *Annonasquamosa*for the removal of crystal violet from aqueous solutions. Adsorption studies were carried out using batch experiments. The dependence of initial dye concentration, pH, contact time, particle size and temperature on the adsorption process was studied. The crystal violet was found to be electroactive and hence electrochemical studies were also performed. The study showed that the equilibrium was achieved within 60 min for the different initial concentrations (10 to 30 $mg.l^{-1}$). The equilibrium adsorption data were analyzed using various isotherm models and they were found to fit Langmuir, Freundlich, Temkin and Harkins-Jura isotherm models in varying orders of magnitude. The maximum dye adsorption capacitiesfor cyclic voltammetry and spectral studiesat 303 K were found to be 5.6818×10^{-4} $A.g^{-1}$(in terms of current)and 5×10^{4} $mg.g^{-1}$(in terms of weight),respectively. The data suggested that the adsorption kinetics was best represented by pseudo-second order kinetic model. The thermodynamic parameters including ΔG, ΔH and ΔS for the adsorption process have also been evaluated using which it was concluded that the process of adsorption was spontaneous and endothermic. The cyclic voltammetricand spectral studies yielded similar results. Furthermore, statistical analysis also showed the absence of any significant difference between the two methods.

Key words: Adsorption · Crystal Violet · *Annonasquamosa* · Cyclic voltammetry

INTRODUCTION

At present, most of the developing countries like India are facing a major problem viz. pollution. This may be due to the population outburst and industrial growth.Many industries use toxic and hazardous chemicals for manufacturing their finished products. The waste products (effluents) discharged by those industries contain toxic heavy metals, dyes, hazardous chemicals that may affect our environment even if they are present at low concentrations[1]. The use of various dyes has become popular among many industries such as paper, textile, leather, food, cosmetics and pharmaceuticals [2]. These industries generate coloured effluents which are directly discharged into the natural water sources like river, lakes etc. They cause adverse effects to the aquatic plants by reducing the light penetration through the water and thereby inhibiting photosynthetic process [3]. Crystal violet, a well known basic dye, belonging to triphenylmethane group, is used as biological stain, veterinary medicine, additive to poultry feed to inhibit propagation of mould, intestinal parasites and fungus, textile dying and paper printing [4]. It is harmful upon inhalation, ingestion and skin contact and also has been found to cause cancer and severe eye irritation [5]. Basic dyes have high brilliance, intense colours and are highly visible even in very low concentration [6]. Such dyes are poorly degraded by microbial enzyme and can persist in a variety of environment. The treatment of the dye effluents before being discharged into water sources is therefore a concern environmental protection. Among the various effluent treatment processes, adsorption is found to be the most economical and efficient process [7]. Several adsorbents have been used for the removal of crystal violet such as grapefruit peel [8], tamarind seed

Corresponding Author: S.K. Suja, Department of Chemistry, Lady Doak College, Madurai, Tamilnadu, India.
E-mail senthija2007@gmail.com.

Please cite this article as: Mahalakshmi, K., S.K. Suja, K.Yazhini, S. Mathiya and G. Jayanthi Kalaivani, 2014. A novel approach to investigate adsorption of crystal violet from aqueous solutions using peels of Annona squamosa. Iranica Journal of Energy and Environment, 5(2): 113-123

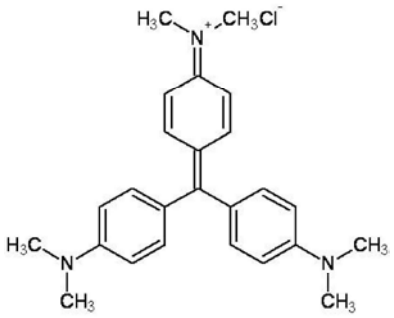

Fig. 1: Structure of crystal violet

powder [9], coniferous pinus bark powder [10], treated ginger waste [11], spent tea leaves (STL) [12], male flowers of coconut tree [13], coconut bunch waste [14], pumpkinseed hull [4], agricultural waste [16], citric acid modified rice straw [17], date palm fiber [18], leaf biomass of *Calotropisprocera* [19] , *Ricinus Communis* pericarpcarbon [20], citrulluslanatus rind [21], bottom ash [22], pretreated walnut shell [23].

Watermelon shell [24], cassava peels [25], polyanilinenanocomposite coated on rice husk [26], chitosan [27], etc., had been evaluated as effective adsorbent for the removal of metal ions.

Annonasquamosa peels have been evaluated as a low cost adsorbent for the removal of lead and cadmium ions from water [28]. However, it has not been used for the removal of crystal violet dye. Moreover, electrochemical studies on the adsorption of crystal violet dye from aqueous solutions have not yet been reported. Our studies were aimed at the removal of crystal violet dye from aqueous solutions under different experimental conditions using *Annonasquamosa*peels along with the exploration of adsorption kinetics and isotherms using both electrochemical and spectral studies. Fig. 1 shows aromatic structure of crystal violet.

MATERIALS AND METHODS

Adsorbent: Peels of *Annonasquamosa*(*PAS*) collected were thoroughly washed with distilled water to remove the dirt adhering to the surface. It was then dried, powdered and sieved to a size of 250 -300 µm and stored in an air tight container till further use. No other physical or chemical treatment was done prior to adsorption experiment.

Adsorbate Solution: Crystal violet (CV) used for this study was received from Sigma Aldrich (CI-42555, molecular formula – $C_{25}H_{30}N_3Cl$, molecular weight – 408 $gmol^{-1}$, λ_{max}– 584 nm) and used without further purification. A stock of 1000 $mg.l^{-1}$ dye solution was prepared using deionized water. Different concentrations of dye solution were prepared by appropriate dilution from the stock solution.

Instruments Used: The absorbance of dye solutions at the desired wavelength was determined using Thermo Scientific Helious Alpha UV-Visible spectrophotometer. Cyclic voltammetric studies were carried out using CHI 6063C – Electrochemical analyzer.The FT-IR spectra of *PAS* before and after adsorption were recorded using FT-IR spectrophotometer (Thermofisher) using KBr pellet method.

Electrochemical Measurements: All voltammetric experiments were performed in the single compartment cell with a volume of 5 ml at 30°C. The working electrode was glassy carbon. Ag/AgCl electrode was used as a reference electrode and a platinum wire served as the counter electrode.

Batch Adsorption Studies: Adsorption of CV dye solution was carried out using batch experiments and the effect of various parameters like contact time (10-60 min), pH (2-12), initial dye concentration (10-30$mg.l^{-1}$), particle size (150µm, 250µm and 300µm) and temperature (30-50°C) on the removal of CV were studied.

The adsorption studies were carried out by adding varying amounts of adsorbent to 50 ml of dye solution of known concentrations. The solutions were agitated at 160 rpm using shaker to attain equilibrium at predetermined time intervals. The samples were taken and the supernatant solution was separated from the adsorbent by centrifugation for 5 minutes. The supernatant solutions wereused to obtain reduction peak current (i_p) values as a function of the concentration of CV dye remaining after adsorption, using electrochemical analyzer. The same solutions were used to measure the absorbance of the solutions, using UV-Visible spectrophotometer.

For cyclic voltammetric studies, amount adsorbed at equil um e calculated as:

$$q_e = \frac{(i_{po} - i_{pe})V}{W} \quad (1)$$

where i_{Po} is the initial reduction peak current of the dye solution (µA), and i_{Pe} is the reduction peak current of the dye solution at equilibrium (µA).

The percentage dye removal was calculated using

$$\% \text{ removal} = \frac{(i_{po} - i_{pe})}{i_{po}} \times 100 \quad (2)$$

For spectral studies, amount of dye adsorbed at equilibrium was given by,

$$q_e = \frac{(C_o - C_e)V}{W} \quad (3)$$

where C_o is the initial concentration of the dye (mg.l^{-1}), C_e is the concentration of dye at equilibrium (mg.l^{-1}), V is the volume of the solution (l), W is the weight of adsorbent (g)

The percentage dye removal was calculated using

$$\% \text{ removal} = \frac{(C_o - C_e)}{Co} \times 100 \quad (4)$$

RESULTS AND DISCUSSION

Spectral Characterization of the Adsorbent: The FTIR spectra of *PAS* before and after adsorption were studiedin order to explore the surface porosity of the adsorbent in the range of 400-4000 cm^{-1}. The FTIR spectrum of *PAS* shows peaks at 614.8cm^{-1}, 771.1cm^{-1}, 823.8cm^{-1}, 1059.0cm^{-1}, 1446.3cm^{-1}, 1618.7cm^{-1}, 3418.3 cm^{-1}. Since the adsorbent shows a large number of peaks, it is evident that the adsorbent is complex in nature. Comparing Figs. 2a and 2b, it can be noted that some of the above mentioned peaks are shifted (1446.3cm^{-1}and 1618.7cm^{-1}) or disappeared (614.8cm^{-1}and 771.1 cm^{-1}) and some new peaks (456.7cm^{-1} and 466.6 cm^{-1}) are also formed. Hence from the spectrum it is obvious that there is possible involvement of those functional groups on the surface of *PAS* in the adsorption process [21].

Effect of pH on Adsorption of CV: The pH of dye solution is an important parameter in adsorption process which affects the surface binding sites of the adsorbent and the degree of ionization of the dye in solution. In order to understand the effect of pH, the equilibrium adsorption studies were carried out at a concentration of 10mg.l^{-1} dye solutions at pH ranging from 2 to 12. The percentage removal of dye was found to be marginally greater at pH 8 (Fig. 3), which is indeed the pH of the dye solution itself. Hence further studies were carried out without adjusting the pH of the dye solution.

Cyclic Voltammetric Studies on CV: The electrochemical behaviour of CV dye was examined over a potential range from-1.5V to +1.5V (vs. Ag/AgCl) with a scan rate of 100 mVs^{-1}. The cyclic voltammogram of CV dye was shown in Fig. 4. A reduction peak was observed at -0.756V which indicated that the CV dye was electroactive [28].

Effect of Contact Time and Initial Dye Concentration: The effect of initial dye concentration onto adsorption of CV by *PAS* was studied at different initial concentrations (10 - 30 mg.l^{-1}) at 303 K and the results were shown in Fig. 5.

The reduction peak current (i_p) values at various time intervals for different initial concentrations of CV dye solutions were noted. It was found that the i_p values decreased as the time of contact between the CV dye solution and PAS increased and reached a constant value indicating an increase in the percentage removal of CV.

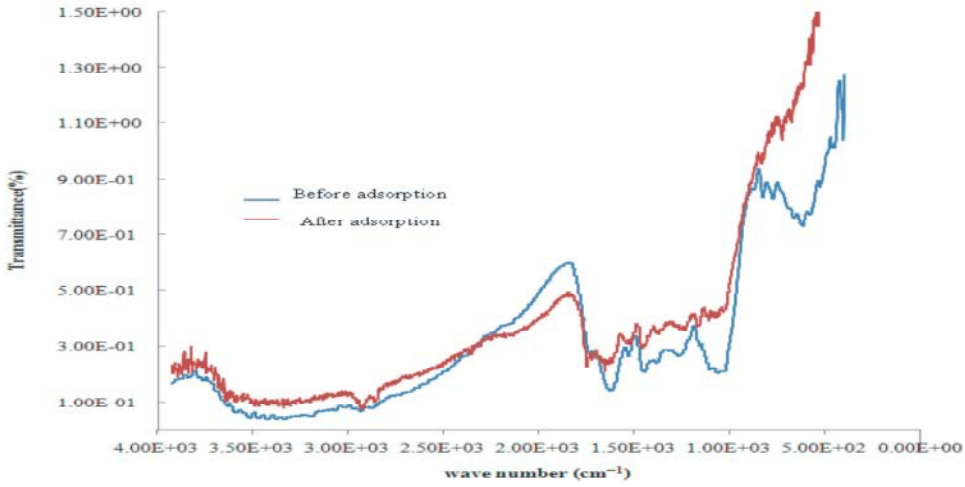

Fig. 2: FTIR spectrum of *PAS* adsorbent before (a) and after (b) adsorption.

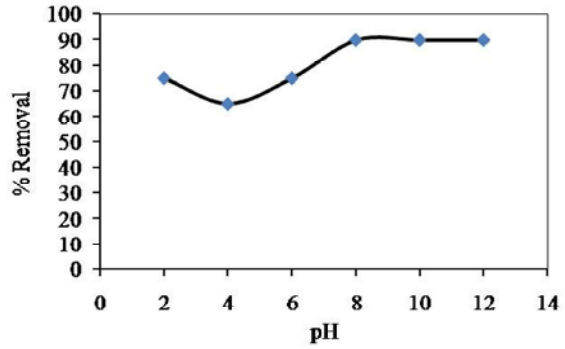

Fig. 3: Effect of pH on adsorption of CV onto *PAS* (Concentration of CV: 10mg.l^{-1}, adsorbent dose: 0.2g; particle size:200-250 µm; agitation speed:160 rpm; temperature:30°C)

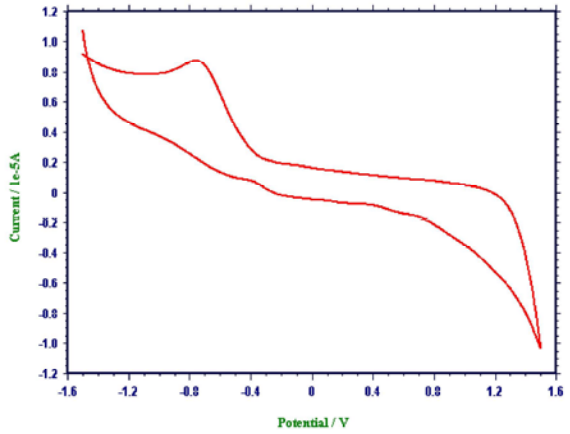

Fig. 4: Cyclic voltammogram of CV dye.

The $\Delta i_p = (i_{po}-i_{pe})$ values were found to increase as the initial concentrations of CV increased. This indicated that the percentage removal of dye also increased (from 92 to 98 %) with increasing concentrations.Similar results were also observed in spectral studies.

As the initial concentration of CV increased, the percentage removal increased from 92 to 98 %. This is due the fact that increase in concentration enhances the interaction between the dye and the adsorbent despite the necessary driving force to overcome the resistance to mass transfer of dye [19]. The uptake of CV increased rapidly during initial stages and reached a constant value beyond 40 min for all the initial concentrations studied.

Adsorption Kinetics: The mechanism of adsorption and the potential rate controlling steps involved in the process of adsorption had been investigated using kinetic models such as pseudo-first-order, pseudo-second-order andintraparticle diffusion model [19]. The linear form of these models is given by equations (5), (6) and (7), respectively.

$$\log (q_e - q_t) = \log q_e - \frac{k_1 t}{2.303} \quad (5)$$

$$\frac{t}{q_t} = \frac{1}{k_2 q_e^2} + \frac{1}{q_e} t \quad (6)$$

$$q_t = k_{id} t^{\frac{1}{2}} + C \quad (7)$$

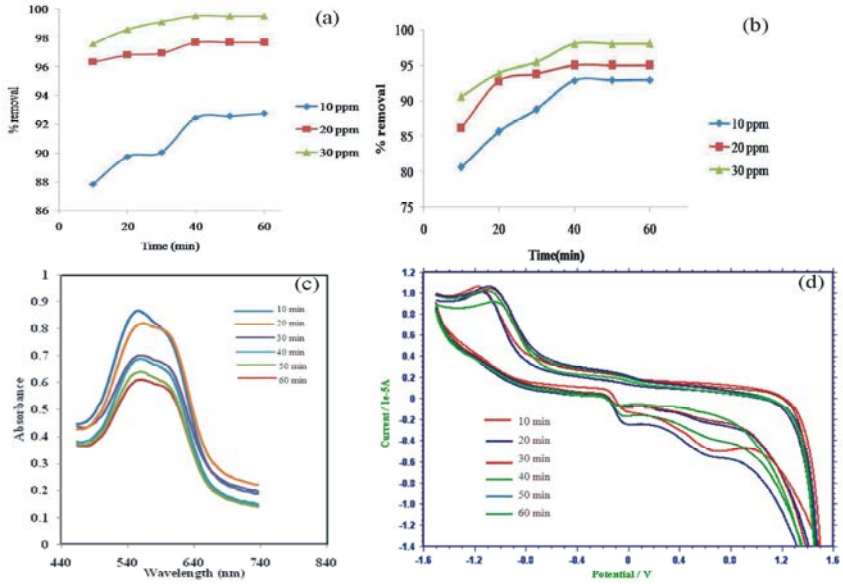

Fig. 5: Effect of contact time on adsorption of CV onto *PAS* at different initial concentrations (adsorbent dose: 0.2 g; particle size: 200-250 µm; agitation speed: 160 rpm; temperature: 30°C) (a) and (c) Spectral studies (b) & (d) Cyclic Voltammetric studies

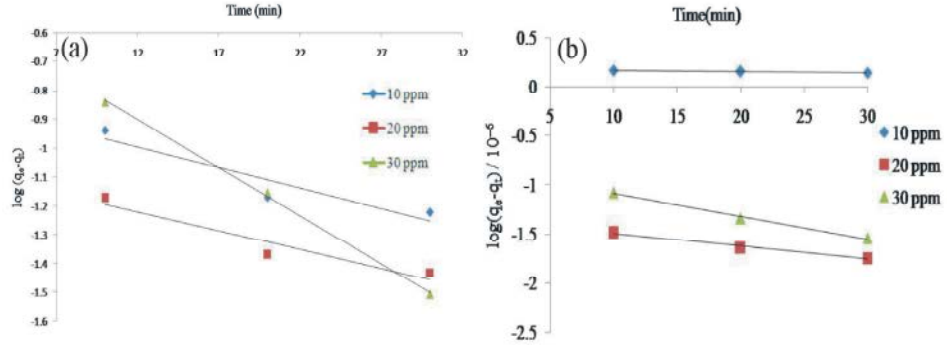

Fig. 6: Pseudo-first order kinetic plot for adsorption of CV onto PAS at different initial concentrations (particle size: 200-250 µm, agitation speed: 160 rpm, temperature: 30°C) (a) Spectral studies (b) Cyclic Voltammetric studies

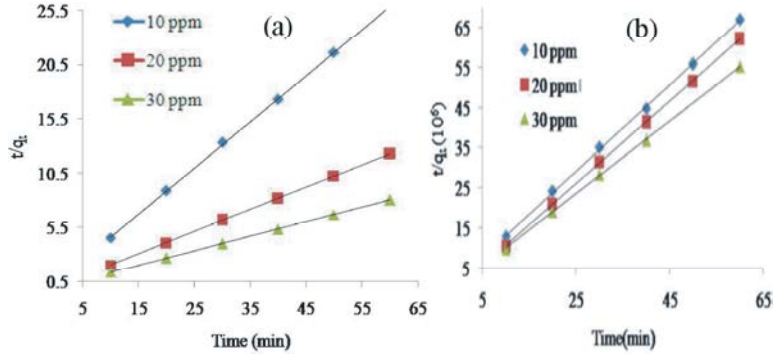

Fig. 7: Pseudo-second-order kinetic plots for adsorption of CV onto *PAS* at different initial concentrations (particle size: 200-250 µm, agitation speed: 160 rpm, temperature: 30°C) (a) Spectral studies (b) Cyclic Voltammetricstudies

where q_t and q_e ($mg.g^{-1}$) are the adsorption capacities at time t and at equilibrium, respectively k_1 (min^{-1}) and k_2 ($mg.(g.min)^{-1}$) are pseudo-first and pseudo-second order rate constants; k_{id} is the intraparticle diffusion rate constants ($mg.g^{-1}$ $min^{-0.5}$) and C is the intercept which gives an idea about the boundary layer thickness.

The pseudo second-order model was developed based on the assumption that the rate-controlling step is chemisorption involving valence force due to sharing or exchange of electrons between adsorbent and adsorbate molecules [5]. Fig. 6 presents the pseudo-first order kinetic plot for adsorption of CV onto PAS at different initial concentrations. The higher R^2 (>0.98) for the pseudo-second order kinetics (Fig.7), indicated the fitness of this model and it was suggested that chemisorption might be a rate-controlling step[5]. Moreover the $q_e$valuescalculated using pseudo second-order equation agreed well with the experimental q_e indicating that the adsorption of CV onto *PAS* could be well represented using the pseudo second order kinetic model. These results were in accordance with those obtained using cyclic voltammetric studies.

Intraparticle diffusion is a transport process involving movement of species from the bulk of the solution to the solid phase. In a well stirred batch adsorption system, the intraparticle diffusion model has been used to describe the adsorption process occurring on a porous adsorbent. Accordingto intraparticle diffusion model, a plot of q_t versus $\sqrt{t}$ should give a straight line with a slope k_p and an intercept of zero if the adsorption limited by an internal diffusion process. The relationship between qt and $\sqrt{t}$ at different concentrations was studied (Figs. 8a and 8b).

The plot in this analysis revealed a linear step,corresponding to fast uptake of sorbate. The line inthe initial stage does not pass through the origin. This revealed that the uptake is dominated by film diffusion than it does for the intraparticle diffusionprocess. Tables 1 and 2 summarizedadsorption kinetic model parameters using spectral and cyclic voltammetric studies, respectively.

Adsorption Isotherms: The adsorption isotherm establishes a relationship between the amount of dye molecules adsorbed onto the adsorbent and the

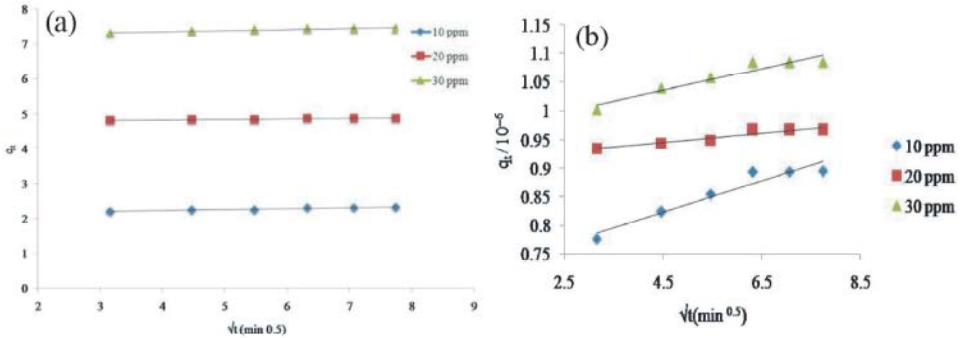

Fig. 8: Intra particle diffusion plot for adsorption of CV onto *PAS* at different initial concentrations (particle size: 200-250 µm, agitation speed: 160 rpm, temperature: 30°C) (a) Spectral studies (b) Cyclic Voltammetric studies

Table 1: Adsorption kinetic model parameters obtained using spectral studies

C_o mg/ L	q_e (exp) mg/g	Pseudo First- order Kinetic model			Pseudo Second- order Kinetic model			Intra particle diffusion Model		
		q_e(cal) mg/g	k_1 (min^{-1})	R^2	q_e(cal) mg/g	k_2 (mg /(g min)	R^2	k_{id}	C	R^2
10	2.4596	1.9275	0.1059	0.946	2.3474	0.4985	0.999	0.027	2.240	0.881
20	2.4611	15.922	0.3224	0.839	2.4096	0.8401	0.999	0.016	2.267	0.910
30	2.4249	6.8706	0.3155	0.787	2.5063	0.4990	1.0	0.031	2.116	0.909

Table 2: Adsorption kinetic model parameters obtained using cyclic voltammetric studies

C_o mg/ L	q_e (exp) µA/g	Pseudo First- order Kinetic model			Pseudo Second- order Kinetic model			Intra particle diffusion Model		
		q_e(cal) µA/g	k_1 (min^{-1})	R^2	q_e(cal) µA/g	k_2 (10^6A/(g min)	R^2	k_{id} 10^{-8}	C 10^{-7}	R^2
10	0.89575	1.0544	0.1519	0.886	1.000	0.5	0.999	3	7	0.926
20	0.96725	0.37932	0.1358	0.928	1.000	1	0.999	2	8	0.760
30	1.0862	0.88511	0.1635	0.877	1.1100	0.008	0.999	2	10	0.921

equilibrium concentration of the dye molecules in solution at a given temperature. The fitness of the equilibrium data obtained for the adsorption of CV onto *PAS* was analyzed using various models viz.,Freundlich, Langmuir, Temkin and Harkins-Jura adsorption isotherm models.

Freundlich Isotherm: The Freundlich isotherm is suitable for heterogenous surface [16] and its logarithmic form can be expressed as

$$\log q_e = \log k + \frac{1}{n}\log C_e \quad (8)$$

where k and n are Freundlich constants related to adsorption capacity and adsorption intensity, respectively.

Freundlich plots for the adsorption of CV onto *PAS* using spectral and cyclic voltammetric studies were shown in Fig. 9 (a) and Fig. 10 (a), respectively. The constants k and n values were determined from the intercept and slope of the plots, respectively. If n value was found to be 1, it indicates that the partition between the two phases were independent of the concentration of the dye [29]. The R^2 values were found to be 1 indicating the fitness of the Freundlich model with the equilibrium data.

Langmuir Isotherm: The Langmuir isotherm assumes monolayer adsorption process. The linear form of it can be expressed as

$$\frac{1}{X/M} = \frac{1}{q_{max}} + \frac{1}{q_{max} b}\frac{1}{C_e} \quad (9)$$

where q_{max} is the maximum monolayer dye concentration in the solid phase ($mg.g^{-1}$), C_e is the equilibrium dye concentration in the aqueous phase ($mg.l^{-1}$), X/M= q_e is

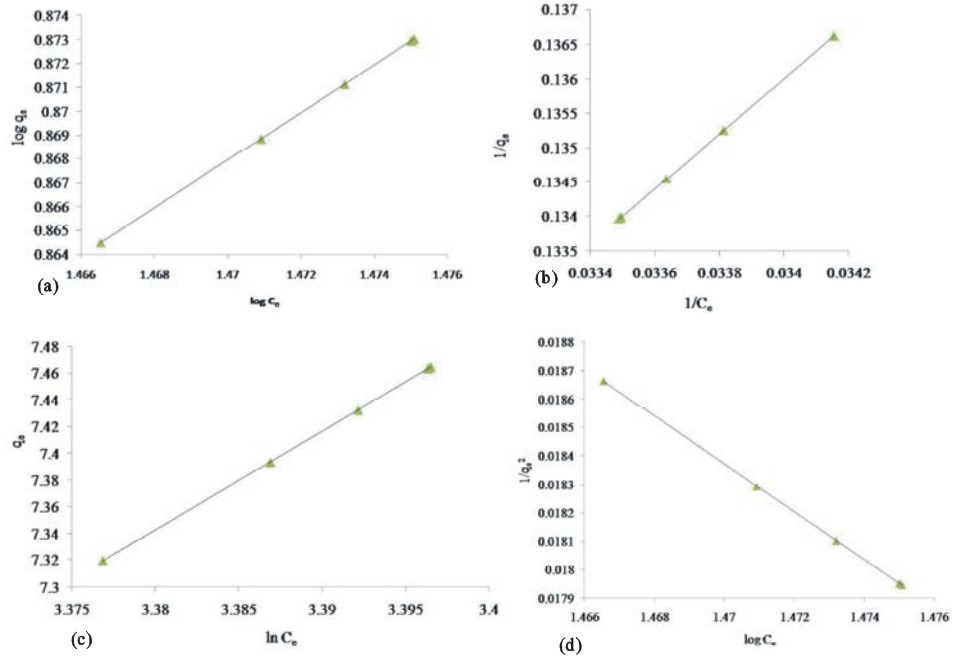

Fig 9: (a) Freundlich(b) Langmuir (c) Temkin (d) Harkin-Jura adsorption isotherm plots for the adsorption of CV by *PAS* (Concentration of CV: 20 mg.l^{-1}; adsorbent dose: 0.2g ; particle size: 200-250 µm; agitation speed: 160 rpm; temperature: 30°C) using Spectral studies

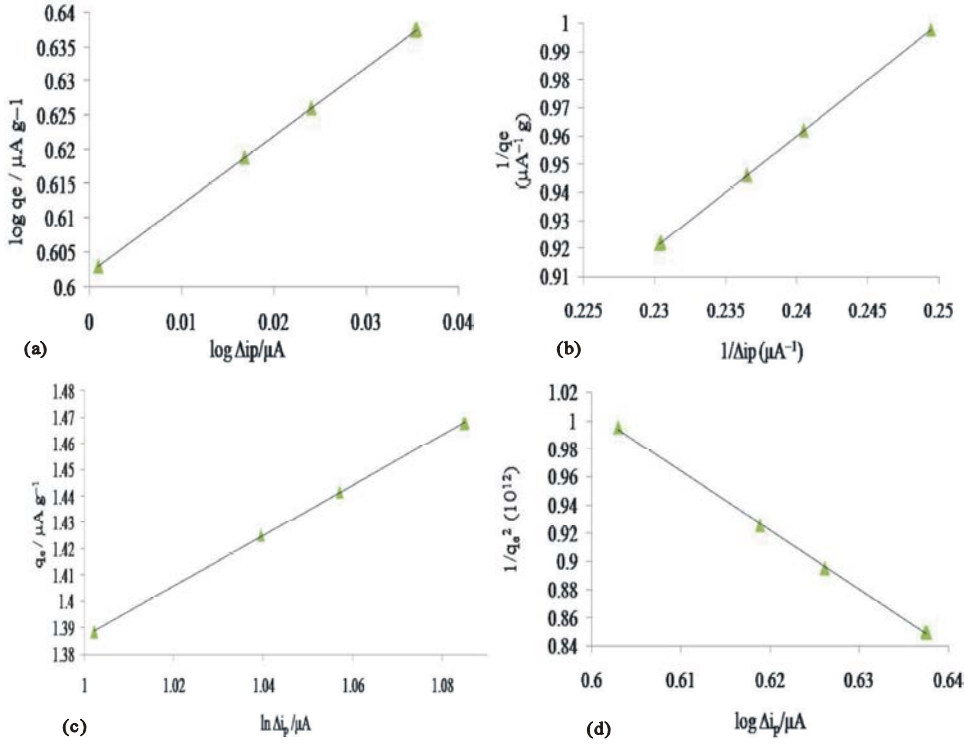

Fig 10: (a) Freundlich(b) Langmuir (c) Temkin (d) Harkin-Jura adsorption isotherm plots for the adsorption of CV by *PAS* (Concentration of CV: 20 mg.l^{-1}; adsorbent dose: 0.2g ; particle size: 200-250 µm; agitation speed: 160 rpm; temperature: 30°C) using cyclic voltammetric studies

Table 3: Adsorption isotherm model parameters based on spectral studies

T (K)	Langmuir isotherm model			Freundlich isotherm model			Temkin isotherm Model			Harkin Jura isotherm model		
	q_{max} (mg/g)	b (L/mg)	R^2	k (mg/g)	n	R^2	A_T (L/mg)	B_T (J/mg)	R^2	A	B	R^2
303	5×10^{4}	2×10^{5}	1	3.9994	1	1	2248.59	0.227	0.974	2.8985	1.4840	0.946

Table 4: Adsorption isotherm model parameters based on cyclic voltammetric studies

T (K)	Langmuir isotherm model			Freundlich isotherm model			Temkin isotherm Model			Harkin Jura isotherm model		
	q_{max} (μA/g)	b (L/ μA)	R^2	k (μA /g)	n	R^2	A_T (L/ μA)	B_T (J/ μA)	R^2	A	B	R^2
303	5.6818×10^{-4}	2.275×10^{-3}	0.999	3.8815	0.9980	0.999	1.0000	1×10^{6}	0.998	2×10^{-13}	4.0	0.997

the equilibrium dye concentration in the solid phase ($mg.g^{-1}$) and b is the Langmuir equilibrium constant ($l.mg^{-1}$).

Langmuir plots for the adsorption of CV onto *PAS* using spectral and cyclic voltammetric studies were shown in Fig. 9(b) and Fig. 10 (b), respectively. The constants q_{max} and b obtained from spectral and cyclic voltammetric studies for three different concentrations (10-30 ppm) were presented in Tables 3 and 4, respectively. The dimensionless constant separation factor (R_L) which indicates whether the adsorption process is unfavourable ($R_L > 1$), linear ($R_L = 1$), favourable ($0 < R_L < 1$) or irreversible ($R_L = 0$) can be calculated as

$$R_L = \frac{1}{1+bC_o} \quad (10)$$

The R_L values were found to be less than 1 indicating that the adsorption process was favourable [21]. The R^2 values were to be 1 indicating the fitness of the Langmuir model with the equilibrium data.

Temkin Isotherm: Temkin isotherm suggests that sorption energy decreases as the degree of completion of the sorptionalcenters of an adsorbent is increased [21].

$$q_e = B_T(\ln A_T + \ln C_e) \quad (11)$$

where, $B_T = RT/b$ is the absolute temperature (K), R is the gas constant ($8.314 J.mol^{-1}K^{-1}$), A_T is the equilibrium binding constants ($l.mg^{-1}$) and B_T is related to the heat of adsorption ($J.mol^{-1}$).

Temkin plots for the adsorption of CV onto *PAS* using spectral and cyclic voltammetric studies were shown in Fig. 9(c) and Fig. 10(c), respectively. The constants A_T and B_T values were determined from the intercept and slope of the plots, respectively. The R^2 values were in the range 0.999 to 1.0 indicating the fitness of the model with the equilibrium data.

Harkin-Jura Isotherm: Harkins-Jura adsorption isotherm accounts for multilayer adsorption and can be explained with the existence of heterogeneous pore distribution. It can be expressed as

$$\frac{1}{q_e^2} = \frac{B}{A} - \frac{1}{A}\log C_e \quad (12)$$

where B and A are the isotherm constants.

Harkins-Jura plots for the adsorption of CV onto *PAS* using spectral and cyclic voltammetric studies were shown in Fig. 9(d) and Fig. 10 (d), respectively. The constants A and B values were determined from the slope and intercept of the plots, respectively. The R^2 values were in the range 0.999 to 1.0 indicating the fitness of the model with the equilibrium data. Hence there could be a possibility of multilayer adsorption to occur [21].

Effect of Particle Size: Adsorption of CV onto *PAS* of three different particle sizes (200-250, 250-300, 300-500 μm) was studied by keeping all other parameters constant. The variation of particle size on the adsorption process monitored byspectral technique was shown in Fig.11. As particle size was decreased, the adsorption efficiency of *PAS* increased. This could be due to increase in the total surface area with decrease in particle size leading to increase in the adsorption efficiency of the adsorbent [21].

In Cyclic voltammetric studies, a drastic change in the peak potential was observed on changing the mesh size of the adsorbent. This may be due to the involvement of H^+ ions during the electro-oxidation process. Negative shift in the peak potential which may be due to intercalative mode of interaction between the adsorbent and the dye was observed.

Effect of Temperature: Temperature has a significant effect on the process of adsorption. Adsorption of CV onto *PAS* was studied at three different temperatures (303 K, 313 K and 323 K) for 10 $mg.l^{-1}$ initial concentration

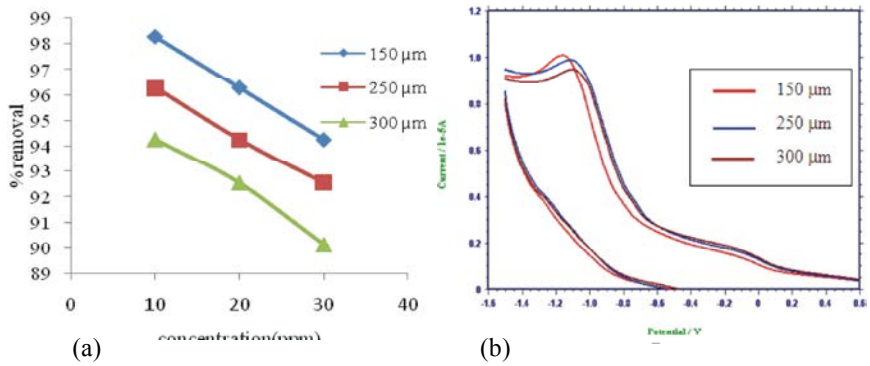

(a) (b)

Fig. 11: Effect of particle size on adsorption of CV onto PAS (adsorbent dose: 0.2 g; contact time: 60 min; agitation speed: 160 rpm; temperature: 30°C) (a) spectral studies (b) cyclicvoltammetric studies.

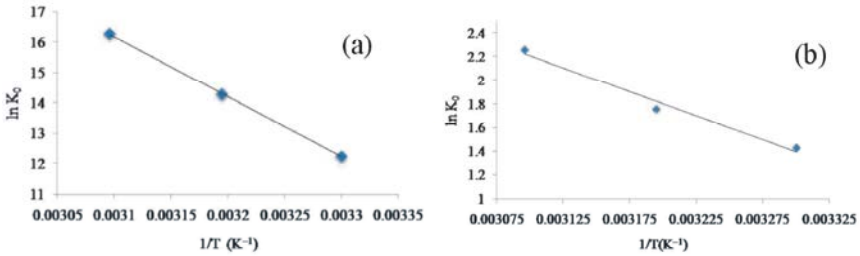

Fig. 12: Van't Hoff plot for effect of temperature on the adsorption of CV(a) Spectral studies (b) Cyclic Voltammetric studies

Table 5: Thermodynamic parameters for the adsorption of CV.

Studies	ΔG (kJ mol⁻¹)			ΔH	ΔS
	303 K	313 K	323 K	kJ mol⁻¹	kJ K⁻¹ mol⁻¹
Spectral	–30.7381	–37.1651	–43.5921	164	0.6427
Cyclic voltammetric	–3.4963	–4.7183	–5.9403	33.5303	0.1222

of CV. From the Fig.12, it was found that the percentage removal of dye increased from 92 to 99% with increase in temperature. This may be due to the fact that increase in temperature increases the rate of diffusion of the adsorbate molecules across the external boundary layer and in the internal pores of the adsorbent owing to decrease in the viscosity of the solution [21].

Evaluation of Thermodynamic Parameters: Thermodynamic parameters such as change in free energy change (ΔG), enthalpy change (ΔH) and entropy change (ΔS) were determined using the following equations

$$K_o = \frac{C_{Solid}}{C_{liquid}} \quad (13)$$

where K_o is the equilibrium constant, C_{Solid} is the solid phase concentration (mg.l^{-1}), C_{liquid} is the liquid phase concentration (mg.l^{-1}).

$$\Delta G = -RT \ln K_o \quad (14)$$

$$\ln K_o = \frac{-\Delta G}{RT} \quad (15)$$

$$\Delta G = \Delta H - T\Delta S \quad (16)$$

$$\ln K_o = \frac{\Delta S}{R} - \frac{\Delta H}{RT} \quad (17)$$

A plot of $\ln K_o$ vs. 1/T gives a straight line with slope is equal to ΔH/ R and intercept is equal to ΔS/ R. Knowing the value of R, ΔH and ΔS can be evaluated. From the values of ΔH and ΔS, ΔG can be determined using the equation (16). The results are presented in Table 5.

The negative values of ΔG indicated that the adsorption of CV onto PAS is a favourable and a spontaneous process. The positive values of ΔH indicated the endothermic nature of the adsorption process and positive values of ΔS indicated increased randomness of the CV at the solid solution interface. The increase in the capacity of the adsorbent to remove CV at higher temperatures may be due to activation of the adsorbent surface thereby enlarging the size of the pores [21, 30].

Statistical Analysis of the Two Methods: Statistical analysis of the respective sets of data obtained by spectral and voltammetric studies was carried out by

student's t-test. The analysis indicated that the calculated t-value (t_{calc} = 2.571) < tabulated-value (t_{tab} =3.365) at 99 % confidence level and hence it could be concluded that there is no significant difference between the two methods.

CONCLUSION

The adsorption of CV onto *PAS* was found to be an efficient process. The parameters such as pH, initial dye concentration, contact time, particle size and temperature have shown significant effect on the removal of CV from aqueous solutions. The maximum uptake of CV by *PAS* occurred at pH 8 and the equilibrium adsorption was attained after 40 min. The equilibrium adsorption data were found to fitFreundlich, Langmuir, Temkin, Harkins-Jura isotherm models. The adsorption process followed pseudo second-order kinetics. Evaluation of thermodynamic parameters indicated that the adsorption process was endothermic and there occurs increased disorder at the solid-solution interface. The various results obtained indicated that the adsorbent chosen for the study was efficient and could be used for the removal of industrial dye effluents.

ACKNOWLEDGEMENT

The authors greatly acknowledge the Management and the Department of Chemistry, Lady Doak College, for providing the necessary facilities to carry out the study.

REFERENCES

1. Babu, B.R., A. Parande, S. Raghu and T.P. Kumar, 2007. Cotton textile processing: waste generation and effluent treatment. Journal of Cotton Science, 11(141-153).
2. Asamudo, N., A. Daba and O. Ezeronye, 2004. Bioremediation of textile effluent using Phanerochaete chrysosporium. African Journal of Food, Agriculture, Nutrition and Development, 4(13): 1548-1553.
3. Robinson, T., G. McMullan, R. Marchant and P. Nigam, 2001. Remediation of dyes in textile effluent: a critical review on current treatment technologies with a proposed alternative. Bioresource technology, 77(3): 247-255.
4. Hameed, B. and M. El-Khaiary, 2008. Removal of basic dye from aqueous medium using a novel agricultural waste material: Pumpkin seed hull. Journal of Hazardous Materials, 155(3): 601-609.
5. Lin, Y., X. He, G. Han, Q. Tian and W. Hu, 2011. Removal of Crystal Violet from aqueous solution using powdered mycelial biomass of *Ceriporia lacerata* P2. Journal of Environmental Sciences, 23(12): 2055-2062.
6. Pavan, F.A., A.C. Mazzocato and Y. Gushikem, 2008. Removal of methylene blue dye from aqueous solutions by adsorption using yellow passion fruit peel as adsorbent. Bioresource Technology, 99(8): 3162-3165.
7. Hu, K., Y. Wang, C. Li and Y. Zheng, 2010. Fractal characteristics of adsorption of direct dye compounds onto modified montmorillonite particles. Acta Scientiae Circumstantiae, 30(11): 2174-2183.
8. Saeed, A., M. Sharif and M. Iqbal, 2010. Application potential of grapefruit peel as dye sorbent: kinetics, equilibrium and mechanism of crystal violet adsorption. Journal of Hazardous Materials, 179(1): 564-572.
9. Patel, H. and R. Vashi, 2010. Adsorption of crystal violet dye onto tamarind seed powder. Journal of Chemistry, 7(3): 975-984.
10. Ahmad, R., 2009. Studies on adsorption of crystal violet dye from aqueous solution onto coniferous pinus bark powder (CPBP). Journal of Hazardous Materials, 171(1): 767-773.
11. Kumar, R. and R. Ahmad, 2011. Biosorption of hazardous crystal violet dye from aqueous solution onto treated ginger waste (TGW). Desalination, 265(1): 112-118.
12. Bajpai, A.S.K. and A. Jain, 2012. Equilibrium and thermodynamic studies for adsorption of crystal violet onto spent tea leaves (STL). Water Journal, 4: 52-71.
13. Senthilkumaar, S., P. Kalaamani and C. Subburaam, 2006. Liquid phase adsorption of crystal violet onto activated carbons derived from male flowers of coconut tree. Journal of Hazardous Materials, 136(3): 800-808.
14. Hameed, B., D. Mahmoud and A. Ahmad, 2008. Quilibrium modeling and kinetic studies on the adsorption of basic dye by a low-cost adsorbent: Coconut (Cocos nucifera) bunch waste. Journal of Hazardous Materials, 158(1): 65-72.
15. Hameed, B. and M. El-Khaiary, 2008. Batch removal of malachite green from aqueous solutions by adsorption on oil palm trunk fibre: Equilibrium isotherms and kinetic studies. Journal of Hazardous Materials, 154(1): 237-244.

16. Senthilkumaar, S., P. Kalaamani, K. Porkodi, P. Varadarajan and C. Subburaam, 2006. Adsorption of dissolved reactive red dye from aqueous phase onto activated carbon prepared from agricultural waste. Bioresource Technology, 97(14): 1618-1625.
17. Chowdhury, S., S. Chakraborty and P. Das, 2013. Adsorption of Crystal Violet From Aqueous Solution by Citric Acid Modified Rice Straw: Equilibrium, Kinetics, and Thermodynamics. Separation Science and Technology, 48(9): 1339-1348.
18. Alshabanat, M., G. Alsenani and R. Almufarij, 2013. Removal of crystal violet dye from aqueous solutions onto date palm fiber by adsorption technique. Journal of Chemistry, http://dx.doi.org/10.1155/2013/210239.
19. Ali, H. and S.K. Muhammad, 2008. Biosorption of crystal violet from water on leaf biomass of Calotropis procera. J. Environ. Sci. Technol., 1(3): 143-150.
20. Madhavakrishnan, S., K. Manickavasagam, R. Vasanthakumar, K. Rasappan, R. Mohanraj and S. Pattabhi, 2009. Adsorption of crystal violet dye from aqueous solution using Ricinus communis pericarp carbon as an adsorbent. Journal of Chemistry, 6(4): 1109-1116.
21. Suyamboo, B.K. and R.S. Perumal, 2012. Equilibrium, thermodynamic and kinetic studies on adsorption of a basic dye by Citrullus lanatus rind. Iranica Journal of Energy and Environment, 3: 23-34.
22. Gandhimathi, R., S. Ramesh, V. Sindhu and P. Nidheesh, 2012. Single and tertiary system dye removal from aqueous solution using bottom ash: kinetic and isotherm studies. Iranica J. Energy Environ, 3(1): 52-62.
23. Nazari-Moghaddam, A., G.D. Najafpour, A.A. Ghoeyshi, M. Mohammadi and S.H. Sharif Zein, 2010. Removal of methylene blue from aqueous phase by pretreated walnut shell in a packed column. Iranica Journal Energy & Environment, 2(1): 137-143.
24. Banerjee, K., S. Ramesh, R. Gandhimathi, P. Nidheesh and K. Bharathi, 2012. A novel agricultural waste adsorbent, watermelon shell for the removal of copper from aqueous solutions. Iranica Journal of Energy and Environment, 3(2): 143-156.
25. Ilaboya, I., E. Oti, G. Ekoh and L. Umukoro, 2013. Performance of Activated Carbon from Cassava Peels for the Treatment of Effluent Wastewate. Iranica Journal of Energy & Environment, 4(4): 361-375.
26. Ghorbani, M., H. Eisazadeh and A. Ghoreyshi, 2012. Removal of zinc ions from aqueous solution using polyaniline nanocomposite coated on rice husk. Iran J. Energy Environ, 3(1): 66-71.
27. Radnia, H., A.A. Ghoreyshi and H. Younesi, 2011. Isotherm and Kinetics of Fe (II) Adsorption onto Chitosan in a Batch Process. Iranica Journal of Energy & Environment, 2(3): 250-257.
28. Sun, W., Y. Ding and K. Jiao, 2006. Electrochemical studies on the interaction of heparin with crystal violet and its analytical application. Journal of Analytical Chemistry, 61(4): 359-364.
29. Dada, A., A. Olalekan, A. Olatunya and O. Dada, 2012. Langmuir, Freundlich, Temkin and Dubinin-Radushkevich Isotherms Studies of Equilibrium Sorption of Zn^{2+} Unto Phosphoric Acid Modified Rice Husk. IOSR Journal of Applied Chemistry, 3(1): 38-45.
30. Annadurai, G., 2002. Adsorption of basic dye on strongly chelating polymer: batch kinetics studies. Iranian Polymer Journal, 11: 237-244.
31. Bhattacharyya, K.G. and A. Sharma, 2005. Kinetics and thermodynamics of Methylene Blue adsorption on Neem (Azadirachta indica) leaf powder. Dyes and Pigments, 65(1): 51-59.

Persia□ □□stract

□
□□□□1 □□□2 □□□□□□□□□□□2 □1 □□□□□2 □2

چکیده

جاذب سطحی موثر و مقرون به صرفه از پوست گیاه□□□ □□□□□□□□□□□□ برای حذف کریستال ویوله از فاز آبی ساخته و آماده شد. مطالعات جذب در فرآیند ناپیوسته انجام پذیرفت. در حین فرایند، وابستگی فرایند جذب به غلظت اولیه رنگ محلول ،pH ،زمان تماس ،اندازه ی ذره و دما مطالعه و بررسی گردید. در طول فرایند مشخص شد که کریستال ویوله مورد آزمایش، الکترواکتیو بوده و از این رو مطالعات الکتروشیمیایی نیز انجام گرفت. این مطالعات نشان داده است که برای غلظت های اولیه (۱۰-۳۰ mg/L) فرایند جذب در مدت زمان ۶۰ دقیقه به تعادل رسیده است. داده های جذب تعادلی به کمک مدل های مختلف ایزوترم آنالیز و بررسی شد و مشخص گردید که این داده ها در میزان دقت های مختلفی به کمک مدل های لانگمیر، فرندلیچ، تمکین و Harkins-Jura برازش می‌شود. بیشترین میزان ظرفیت ها در جذب رنگ در حالات ولتامتری چرخه ای و مطالعات طیفی در دمای ۳۰۳ درجه کلوین به ترتیب $A.g^{-1}$ ۵/۶۸۱۸×۱۰$^{-۴}$ (برحسب جریان) و $mg.g^{-1}$ ۵×۱۰^{۴} (برحسب وزن) اندازه گیری شد. داده های به دست آمده نشان داده است که سینتیک جذب، در بهترین حالت با مدل سینتیکی شبه درجه دو انطباق دارد . پارامتر های ترمودینامیکی از قبیل ΔG، ΔH و ΔS برای فرایند جذب اندازه گیری شده و نتایج این اندازه گیری ها نشان داده است که فرایند جذب، خودبخودی و گرماگیر است. ولتامتری چرخه ای و مطالعات طیفی نتایج مشابه ای را ارائه نمود. بعلاوه، در آنالیز های آماری تفاوت قابل ملاحظه ای بین دو روش بکاربرده شده مشاهده نشده است.

Iranica Journal of Energy & Environment 5 (2): 124-131, 2014
ISSN 2079-2115
IJEE an Official Peer Reviewed Journal of Babol Noshirvani University of Technology
DOI: 10.5829/idosi.ijee.2014.05.02.03

BUT

Sensitivity Analysis for Water Hammer Problem in Pipelines

Behnam Mansuri, Farzin Salmasi and Behrooz Oghati

Faculty of Agriculture, Department of Water Engineering, University of Tabriz, Tabriz, Iran

Received: February 10, 2014; **Accepted** in Revised Form: June 11, 2014

Abstract: Water hammer is a transient flow in pipes that was created by sudden changes of velocity in pipe lines. This phenomenon can cause strong positive and negative pressures in water conveyance pipes and usually it poses pipeline to danger. Overall, water hammer creates by rapidly closing valves, shutting off or suddenly restarting pumps. It has destructive hydrodynamic effects in pressurized pipelines. In this study, governing equations of water hammer is numerically simulated using MATLAB software. Then, the sensitivity analysis in negative and positive pressures by changing some variables such as pipe diameter, pipe length and also wave velocity in pipe was investigated. Numerical simulation is based on characteristic method. Sensitivity analysis help designers to have well understand of water hammer phenomenon.

Key words: Water hammer · Transient flow · Pump · Positive and negative pressure · Pipelines · MATLAB

INTORDUCTION

In some of pressurized hydraulic systems such as water conveying pipelines, water distribution networks, pipelines ending to turbine, water tunnels and pumping systems, water hammer phenomenon creates rapid and transient waves. Sometimes the power of pressure waves are too high that resulted destructive forces which caused rupturing and breaking of pipelines in conveying and distributing systems, breaking valves, control valves and pumps [1]. The velocity of such wave may exceed 1000 m/s and the values of pressure may oscillate from very high to very low values. Design and operation of any pipeline system requires that the distribution of head and flow in the system is predicted at different operating conditions. Many researchers have attempted simulation of transient flow in pipeline systems with different methods. These events in water conveying projects are usual and annually imposeextensive damages to pressurized systems [2].

Water hammer is caused by a rapid change of flow velocity in the pipe lines; that may be due tosudden valve opening or closure, starting or stopping the pumps, mechanical failure of a device, rapid changes in demand condition, etc [3]. It could result in violent change of the pressure head, which is then propagated in the pipeline in the form of a fast pressure wave leading to severe damages [4]. In a research, numerical study on an air tank in order to balance the water hammer pressure has been performed. The study has shown that increasing reservoir volume will result in decreasing negative pressure and positive pressure and decreasing water levels in the reservoir. Studies showed that the amount of control valve opening and materials of system has effects on hydraulic characteristics of flow in water hammer phenomenon that the way check valves got closed in system, has remarkable effects on transient flow characteristics of the water hammer [5]. In addition, the severe pressure fluctuation in pipelines and severe fluctuations in water volume in pipelines as a result for water hammer, plays an important role in analysis and design of water conveying systems. It is visible that changes in materials used in the pipelines have remarkable changes in downstream check valve closure process [6]. For theoretical simulation, many researchers have used hybrid models to solve water hammer problems. Among them, the method of characteristics line (MOC) is the most popular one in modeling the valve-induced water hammer equations because of its feasibility and advantage for complex systems [7]. Studding water hammer in pipelines

Corresponding Author: Farzin Salmasi, Faculty of Agriculture, Department of Water engineering, University of Tabriz, Tabriz, Iran. E-mail: salmasi@tabrizu.ac.ir

Please cite this article as: Mansuri, B., F. Salmasi and B. Oghati, 2014. Sensitivity analysis for water hammer problem in pipelines. Iranica Journal of Energy and Environment, 5(2): 124-131

using implicit method of characteristic lines (IMOC) has shown that it will be helpful to use implicit method of characteristic lines instead of the explicit characteristic lines method in order to lower and balance the limitation [8]. In another research, the effect of size in pressurized air reservoir in reducing maximum and minimum pressure due to water hammer has been studied. The research on optimization of conveying systems with pumps for water hammer using mathematical optimization method had shown that within increasing pipe diameter, effect of sudden pump stoppage especially negative pressure will be lowered. Within this method, the diameter and thickness of pipe will be optimized in order to prevent water hammer occurrence and unnecessarily expenses [9]. The hydraulic simulation study on water hammer using multiple diameters and materials of pipes showed that changes in material must be in order of the pipe with higher elasticity module to the pipe with lower elasticity module. That is,selection of closer elasticity module for pipe segments, resultsin lower pressure changes [10]. Comparison for control of transient hydraulic waves of water hammer showed that protective actions and design of expansion joints is based on low flow velocity, using check valves, control valves, balancing reservoirs and air reservoirs. In another research about water hammer in hydroelectric power plants, numerical analysis of water hammer had significant impact on the output of the actual projects. However, tolerances are visible due to simplifications and inaccessibility of some required data. Assessment of water hammer simulation using laboratory and numerical CFD models showed that numerical CFD simulation model of water hammer has high reliability and can be used as a proper numerical model to calculate maximum and minimum pressure. Mutual assessment between water hammer and centrifugal pumps showed that the centrifugal pumps especially in high energy level and velocity generate remarkable pressure fluctuations. Interaction effect can increase the effects, so that the pressure fluctuation should not be neglected [11]. Assessment of water hammer simulation using implicit method of characteristics represents high reliability of the method, which can simulate discharge and water levels in all considered cases [12].

In another study, critical hydraulic gradient for sediment transport through rockfilldam was determined [13]. Results from dynamic pressure fluctuations in stepped three-side spillway showed that the proposed form of ogee profile caused a significant reduction in turbulence intensity within the side channel. On the other hand, the stepped Ogee profiles of three-side spillways caused to simple construction and ease of operation [14].In a research, the effect of temperature and influent loadon nitrifying treatment of wastewater using CFD has been conducted [15].

In this study, the purpose is to solve the governing equations about water hammer phenomenon and analysis of the sensitivity of some hydraulic parameters. For this purpose, a program in MATLAB Environment was prepared. Fluctuations of pressure by changing of pipe diameter, length and velocity, were investigated. Sensitivity analysis of the numerical model by changing parameters, contributes to well understanding about water hammer [16, 17].

MATERIALS AND METHODS

Governing Equation: The general equation of water hammer is obtained from Newton's second law and the equation of continuity of flow. Eq. 1 is known as Euler equation or the momentum equation. This equation is used for non-compressible fluids.

$$\frac{1}{\rho}.\frac{\partial P}{\partial x}+\frac{fV|V|}{2D}+g.\sin\alpha+V\frac{\partial V}{\partial x}+\frac{\partial V}{\partial t}=0 \quad (1)$$

In Eq. 1, parameter D is internal diameter of pipe, P is pressure, x is location dimension, t is time dimension, f is friction coefficient, V is average flow velocity and L is pipe length.

Applying continuity equation considered for an element of pipe length, results in Eq. 2.

$$a^2.\frac{\partial V}{\partial x}+\frac{1}{\rho}\frac{\partial P}{\partial t}+\frac{1}{\rho}V\frac{\partial P}{\partial x}=0 \quad (2)$$

The Eq. 2 would be used simultaneously with Eq. 1 to solve water hammer phenomenon. In addition, a in Eq. 2 is velocity of pressure waves.

The Characteristic Lines Method for Numerical Solution: History of water hammer analysis is an implication for various methods development to solve Euler and continuity equation (Eqs. 1 and 2). The variety of these methods is depended on numerical analysis ability and innovation of these methods. The characteristic lines method is one of the most accurate methods to assess water hammer phenomenon because it considers minor losses and also it is customizable for various boundary conditions. In this method, the partial differential equations of flow continuity and momentum

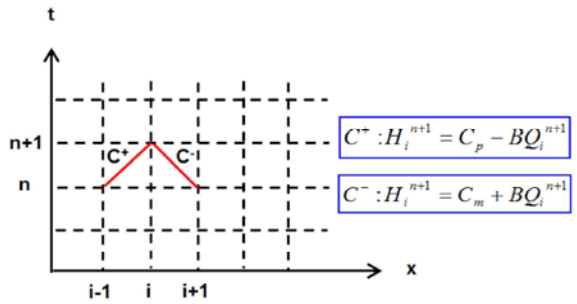

Fig. 1: Characteristic lines

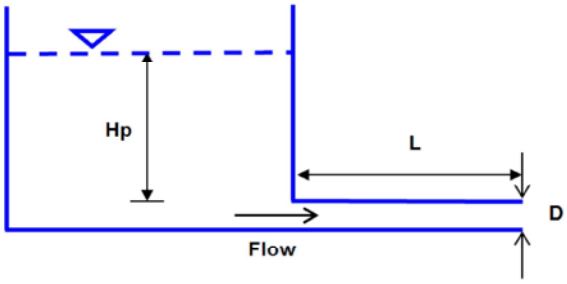

Fig. 2: The system consists of a simple pipe with a reservoir at upstream and a valve in downstream of the pipe

convert to the two ordinary differential equations and then could be solved by finite difference method [5]. By performing some mathematical operations, two ordinary differential equations are obtained as Eqs. 3 and 4.

$$\frac{\partial H}{\partial t}+\frac{c}{gA}\frac{\partial Q}{\partial t}+\frac{cf}{2gD}V|V|-\frac{Q}{A}\sin\alpha=0,\ \frac{\partial x}{\partial t}=1+c \tag{3}$$

$$\frac{\partial H}{\partial t}-\frac{c}{gA}\frac{\partial Q}{\partial t}+\frac{cf}{2gD}V|V|-\frac{Q}{A}\sin\alpha=0,\ \frac{\partial x}{\partial t}=1-c \tag{4}$$

Eqs. 3 and 4 are established on lines $\frac{\partial x}{\partial t}=1+c$ and $\frac{\partial x}{\partial t}=1-c$. Eqs. 3 and 4 on coordination screen of (x-t) are explainer of two straight lines of $1/c,-1/c$. Thus, the differential equation on these lines using finite difference method can be written as follows (Fig. 1):

B, C_m, C_p are known as coefficients based on value of H and Q in time step (n is present time). By solving these two linear equations, the two unknown values for Q_i^{n+1}, H_i^{n+1} in the next time step will be found.

In this study, a computer program in MATLAB environment was presented to solve the governing equations of water hammer (momentum and continuity of flow). The prepared program solves transient fluctuations in a simple pipeline, with an upstream reservoir and a downstream valve (Fig. 2). The valve specification places as C_DA in orifice formula (Eq.5).

$$Q_P = C_D A\sqrt{2gH_P} \tag{5}$$

Specifications of the system that MATLAB program was designed stated as follows:

[H_p=100 m, L=4800 m, D=2 m, f=0.022, a=1200 m/s]

where,H_P is reservoir water levels, L is pipe length, f is pipe's friction coefficient and a is the velocity of wave.

The datum for hydraulic levels is considered to be the geometrical axis of the pipe. The program in each time steps calculates the value of C_DA which is CV in program using linear interpolation. Simultaneously, the value of H_p and Q_p in valve would be calculated by solving Eq. 5 and characteristic equation of C^+ (Eq. 3). To specify the permanent conditions for energy equation from reservoir to valve, neglecting minor losses will expressed as follows:

$$H_R - f\frac{L}{D}\frac{Q_0^2}{2gA^2}=\frac{Q_0^2}{2gCV^2} \tag{6}$$

RESULTS AND DISCUSSIONS

In this section the behavior of water hammer on a system including a pipe within variable diameter and length and wave's variable velocity within constant 100 meters head of reservoir, would be assessed. For this purpose, a code in MATLAB language has been written which in the parameters are allowed to be replaced and plotted. Method to solve the governing equations is the characteristics method. The fluctuation of pressure is calculated in 4 statuses (pipe's full length, pipe's $\frac{3}{4}$ length, pipe's $\frac{2}{4}$ length and pipe's $\frac{1}{4}$ length). For brevity the results are mentioned for diameters of 2 and 3 meters in the Figs. 3 and 4.

According to Figs. 3 and 4, it is clear that when the diameter is considered as variable, within diameter increment, the pressure fluctuation range decreased. The reason is that in bigger diameters the cross-sectional area of pipe is bigger, so that the pressure differences would distribute on this (bigger) area.

Fig. 3 shows that the maximum pressure increment in pipe with diameter of 2 metersis about 62% of the static head of reservoir and for pressure decrement it is about

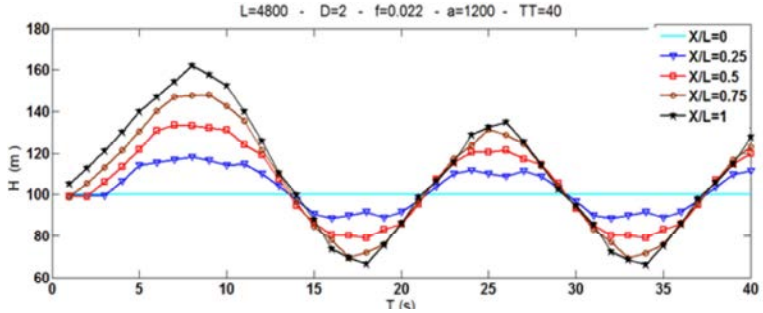

Fig. 3: Pressure fluctuations in different positions of pipe with diameter of 2 meters

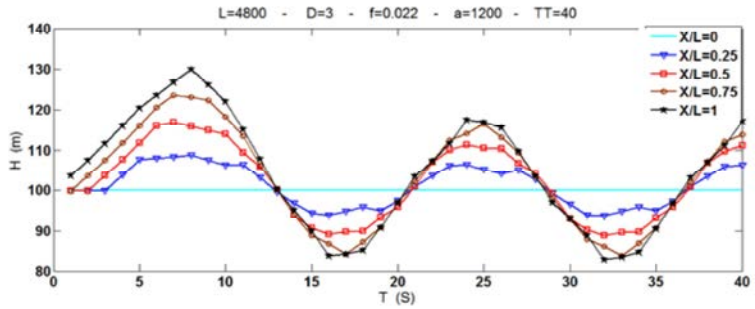

Fig. 4: Pressure fluctuations in different positions of pipe with diameter of 3 meters

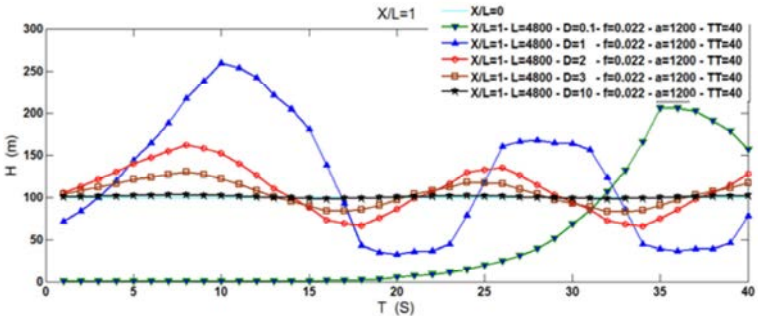

Fig. 5: Pressure fluctuations at the end of pipe for diameters of 0.1 to 10 meters

33.35% of the static head of reservoir.Thus, controlling pipe diameters in order not to break pipes and also controlling the danger of cavitation due to pressure decrement should be considered by designer [13]. In addition, according to Figs. 3 and 4, it is clear that the maximum and minimum pressure occur at the end of pipe, so that the end of pipe is considered as critical zone in design criteria.

The pressure fluctuations for middle and end of the pipes within diameters of 0.1 meter to 10 meters are presented in Figs. 5 and 6.

According to Figs. 5 and 6 it could be extracted that within diameter increment the range of pressure fluctuation decreased and as a result the energy dissipation occurred faster. In the other words, with diameter increment the transiency of flow would dissipate promptly. It is clear that the designer must consider the expenses of the bigger diameter and must prepare the optimized design for decreasing pressure and decreasing expenses of purchasing and setting up the pipeline.

In the next phase, the length is variable and other parameters are constant. For brevity the results for length of 3800 meters and 5800 meters are presented in Figs. 7 and 8.

According to Figs. 7 and 8, with length increment the range of pressure fluctuations would increase. Thus, designer must choose the shortest distance to lower expenses of pressure waves control and pipe's own expenses.

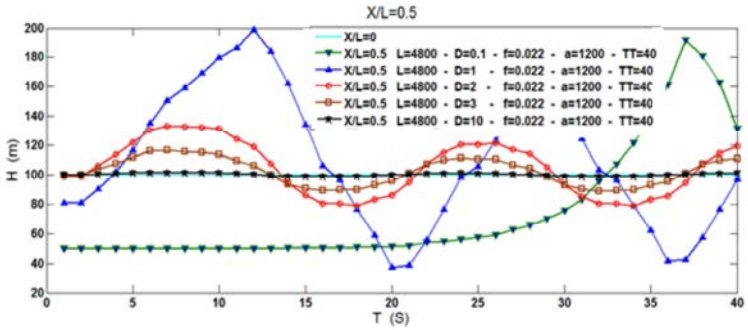

Fig. 6: Pressure fluctuations in the middle of pipe for diameters of 0.1 to 10 meters

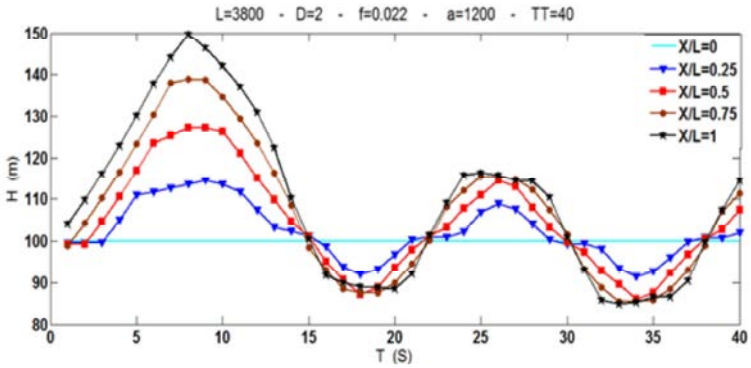

Fig. 7: The pressure fluctuations for pipe within length of 3800 meters

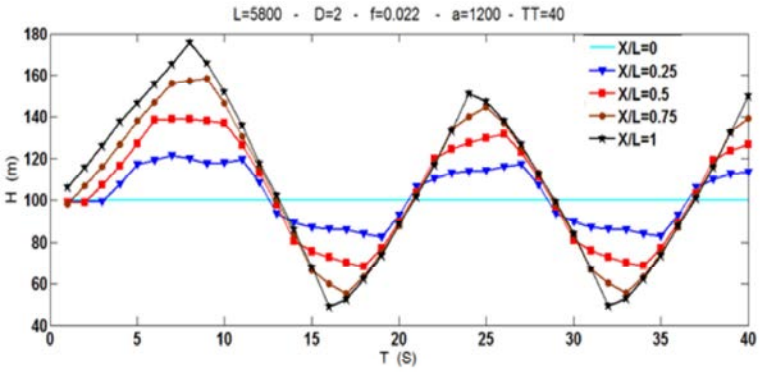

Fig. 8: The pressure fluctuations for pipe within length of 5800 meters

Accurate assessment for length effect on water hammer is presented in Figs. 9 and 10.

It is observable from Figs. 9 and 10 that with length decrement, the pressure fluctuation range decreases. The reason is that, in the shorter pipes the pressure waves sweep more and rapid and this cause to encounter the pressure waves in opposite direction, therefore it causes more dissipation of waves.

Now if the velocity of wave considered as variable, Figs. 11 and 12 are resulted.

According to Figs. 11 and 12 with velocity increment from 1000 to 1400 (m/s), the pressure fluctuation range decreases.The reason is that in higher wave velocity the wave's sweep occurs more and rapid and this could encounter waves in opposite direction.

Figs. 13 and 14 present the effect of different wave's velocity for middle and the end of the pipe.

Again within an exact look at Figs. 13 and 14, it can be seen that increasing wave velocity would results in more increasing transiency.The end of the pipe is critical

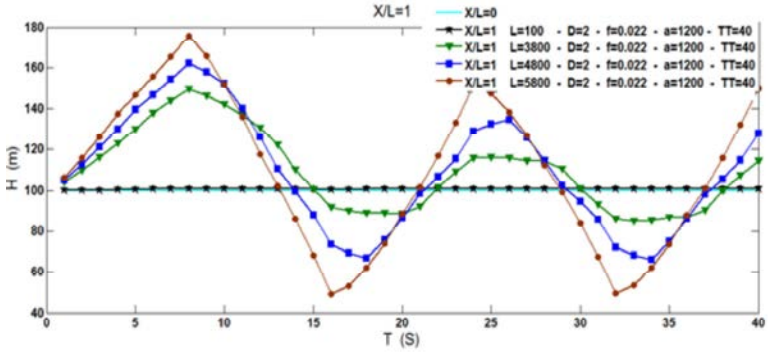

Fig. 9: Pressure fluctuations at the end of the pipe for different lengths of 100 to 5800 meters

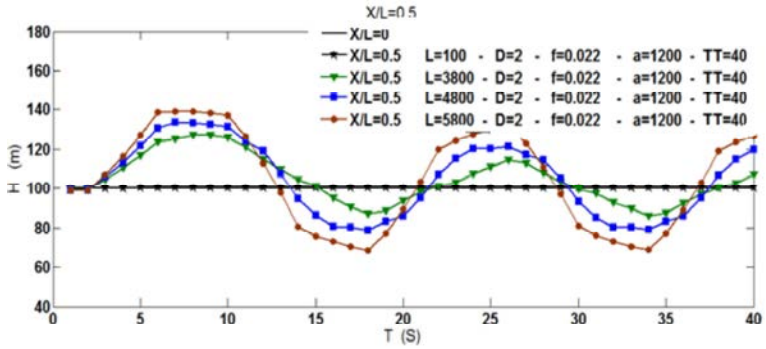

Fig. 10: Pressure fluctuations in the middle of the pipe for different lengths of 100 to 5800 meters

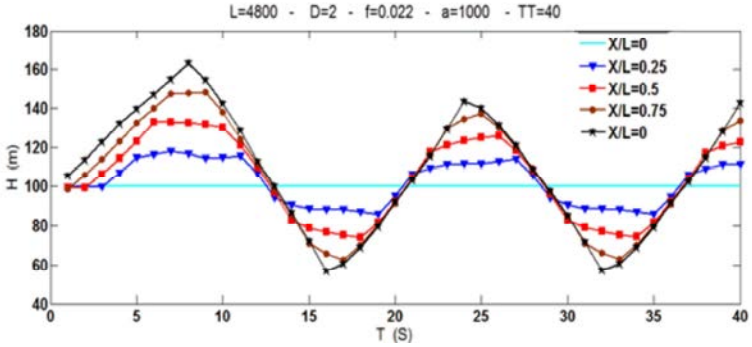

Fig. 11: Pressure fluctuation in pipe with wave's velocity of 1000 (m/s)

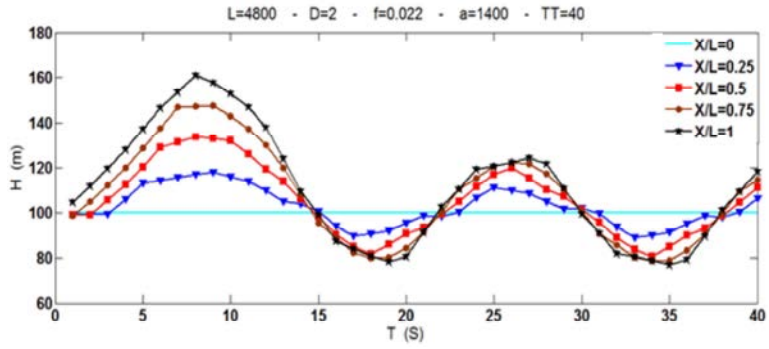

Fig. 12: Pressure fluctuation in pipe with wave's velocity of 1400 (m/s)

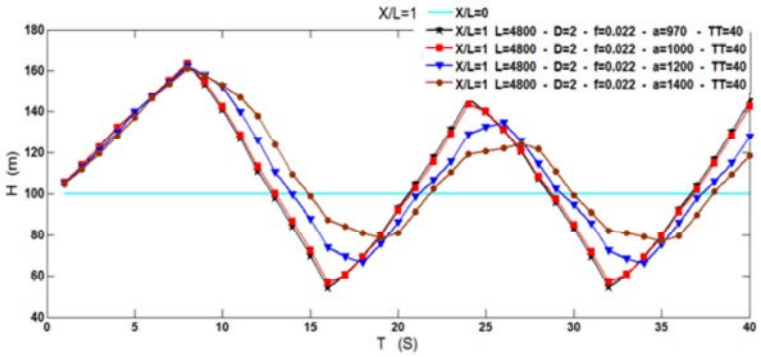

Fig. 13: Effect of different wave's velocity on positive and negative pressure at the end of pipe

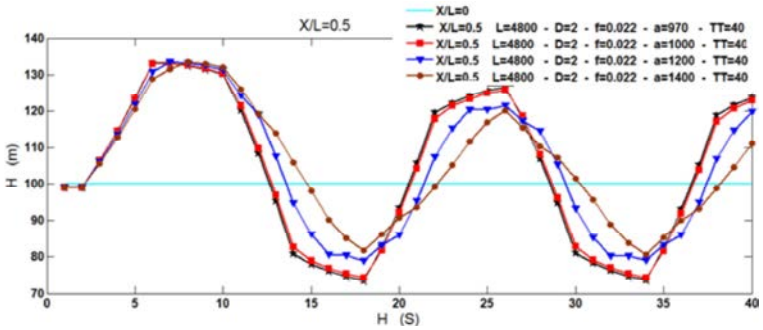

Fig. 14:Effect of different wave's velocity on positive and negative pressure in the middle of pipe

zone for water hammer phenomenon, because absolute max/min pressure in end of pipe is more. Finally, design engineer must consider it as a critical point of project.

CONCLUSION

- With increasing pipe diameter, the pressure fluctuation range would be small.In the other words the transiency of waves would be more.
- The pressure fluctuation range would remarkably decrease by using shorter pipes.
- With wave's velocity increment, the pressure fluctuation range would decrease.
- The maximum and minimum pressure occurs at the end of the pipe. Thus, end of the pipe is critical point in design criteria.

REFERENCES

1. Streeter, V.L. and W. Benjamin, Fluid Mechanics, 1960, New York: McGraw-Hill Company.
2. Afshar, M. and M. Rohani, 2008. Water hammer simulation by implicit method of characteristic. International Journal of Pressure vessels and piping, 85(12): 851-859.
3. White, F.W. Fluid Mechanics, 1979, New York: McGraw-Hill.
4. Parmakian, J., 1963. Water Hammer Analysis 1963, New York: Dover.
5. Bergant, A., A.R. Simpson and A.S. Tijsseling, 2006. Water hammer with column separation: A historical review. Journal of Fluids and Structures, 22(2): 135-171.
6. Ghidaoui, M.S., D.A. McInnis, D.H. Axworthy and M. Zhao, 2005. A review of water hammer theory and practice. Applied Mechanics Reviews, 58(1): 49-76.
7. Tian, W., G. Su, G. Wang, S. Qiu and Z. Xiao, 2008. Numerical simulation and optimization on valve-induced water hammer characteristics for parallel pump feedwater system. Annals of Nuclear Energy, 35(12): 2280-2287.
8. Tan, J., K. Ng and G. Nathan, 1987. Application of the centre implicit method for investigation of pressure transients in pipelines. International journal for numerical methods in fluids, 7(4): 395-406.
9. Vetter, G. and F. Schweinfurter. Computation of pressure pulsation in piping systems with reciprocating positive displacement pumps. in Proceedings of the First ASME Pumping Machinery Symposium. 1989.

10. Meniconi, S., B. Brunone and M. Ferrante, 2012. Water-hammer pressure waves interaction at cross-section changes in series in viscoelastic pipes. Journal of Fluids and Structures, 33: 44-58.
11. Ismaier, A. and E. Schlücker, 2009. Fluid dynamic interaction between water hammer and centrifugal pumps. Nuclear Engineering and Design, 239(12): 3151-3154.
12. Wahba, E., 2009. Turbulence modeling for two-dimensional water hammer simulations in the low Reynolds number range. Computers & Fluids, 38(9): 1763-1770.
13. Chapokpour, J. and E.A. Tokaldany, 2012. Critical Hydraulic Gradient for Sediment Transport Through Rockfill Structures. Iranica Journal of Energy & Environment, 3(2).
14. Taghizadeh, H., S.A.A. Salehi and F. Ghasemzadeh, 2012. Dynamic Pressure Fluctuations in Stepped Three-Side Spillway. Iranica Journal of Energy & Environment, 3(1): 78-87.
15. Sajjadi, B., M.K. Moraveji and R. Davarnejad, 2011. Investigation of Temperature and Influent Load on Nitrifying Treatment of Using Wastewater CFD. Iranica Journal of Energy and Environment, 2: 08-17.
16. Wylie, E. and V. Streetr, Suo Lisheng. Fluid transient in systems, 1993, Englewood Clifs. NJ. pp: 143-169.
17. Balino, J.L., A.E. Larreteguy, A.C. Lorenzo, A.G. Padilla and F.R. de Andrade Lima, 2001. The differential perturbative method applied to the sensitivity analysis for waterhammer problems in hydraulic networks. Applied Mathematical Modelling, 25(12): 1117-1138.

Persian Abstract

DOI: 10.5829/idosi.ijee.2014.05.02.03

چکیده

ضربه آب حاصل از قوچ، جریانی غیر دائمی یا گذرا در لوله‌های انتقال آب بوده که بر اثر تغییر ناگهانی در سرعت آب داخل لوله ایجاد می گردد. بر اثر وقوع این پدیده در خط لوله، فشارهای مثبت و منفی زیادی تولید می‌شود که می‌تواند باعث خطراتی مانند ترکیدگی لوله شود. عموما ضربه قوچ در خطوط لوله بر اثر بستن ناگهانی شیر فلکه، روشن و خاموش شدن موتور پمپ ها اتفاق می‌افتد که اثرات مخرب هیدرودینامیکی در لوله و تاسیسات وابسته دارد. در این تحقیق، معادلات دیفرانسیل با مشتقات جزیی حاکم بر پدیده انتقال با روش عددی توسط نرم افزار مت-لب حل گردیده است. سپس آنالیز حساسیت تولید فشارهای مثبت و منفی در لوله با تغییر برخی از پارامترها مانند قطر لوله، طول لوله و همچنین سرعت موج داخل لوله انجام گردید. روش حل عددی معادلات دیفرانسیل، بر اساس روش بررسی مشخصات است. نمودارهای ارائه شده در مورد حساسیت مدل ریاضی به تغییرات در عوامل موثر، می‌تواند به درک اصولی مهندسین طراح در مورد این پدیده پیچیده داخل لوله کمک شایانی نماید.

Iranica Journal of Energy & Environment 5 (2): 132-145, 2014
ISSN 2079-2115
IJEE an Official Peer Reviewed Journal of Babol Noshirvani University of Technology
DOI: 10.5829/idosi.ijee.2014.05.02.04

BUT

Heavy Metals and Water Quality Assessment Using Multivariate Statistical Techniques and Water Quality Index of the Semenyih River, Peninsular Malaysia

Fawaz Al-Badaii and Mohammad Shuhaimi-Othman

School of Environmental and Natural Resource Sciences, Faculty of Science and Technology, Universiti Kebangsaan Malaysia, 43600 UK, Bangi Selangor, Malaysia

Received: March 13, 2014; **Accepted** in Revised Form: June 11, 2014

Abstract: The present study was carried out to investigate and determine the water quality and the pollution sources affected on Semenyih River using multivariate statistical techniques and water quality index (WQI). Temperature, pH, dissolved oxygen (DO), conductivity, total dissolved solids (TDS), sulfate (SO_4^{2-}), nitrate (NO_3^-), nitrite (NO_2), phosphate (PO_4^{3-}), turbidity, ammonia-nitrogen (NH_3-N), total suspended solids (TSS), chemical oxygen demand (COD), biochemical oxygen demand (BOD), total hardness (TH), oil and grease (O&G), *Escherichia coli* and total *Colifor* (TC) as water quality variables and Cd, Cu, Ni, Zn, Fe, Pb, Mn, Cr and Hg as heavy metals variables have been analyzed in the collected water samples during the year 2012 from 8 sampling stations along Semenyih River. Cluster analysis (CA) categorized 8 stations into three clusters based on the similarity of water quality characteristics and categorized 27 variables analyzed to four clusters to determine the relationship among the variables and their possible sources. Principal component analysis (PCA) determined that 96.63% of the total variance was accounted for five factors which pointed to the variables responsible for deterioration of water quality attributed to anthropogenic activities associated with urbanization, industrialization, agriculture, livestock husbandry and mining activities. In addition, WQI classified the river as clean (Class I) at station 1, slightly polluted (Class II) at stations 2 and 3 and as moderately polluted (Class III) at stations 4-8; in general; however, the river falls into class III and thus is required extensive treatment before using for domestic purposes. Therefore, this study verified that the multivariate statistical techniques and water quality index are mainly required for interpreting complex data sets for the purpose of analysis of water quality variations.

Key words: Heavy metals · Water quality · Cluster analysis · Principal component analysis · Water quality index (WQI)

INTRODUCTION

The concentrations of water quality variables are known to play a main role in determining the status of aquatic systems [1, 2]. The excessive concentrations of these variables may result in diverse problems in aquatic ecosystem such as loss of oxygen, fish deaths, an increase in the extent of algal blooms and general loss of biodiversity. Pollutants enhancementc ritically deteriorates aquaticecosystems, reducing the use of water for domestic water supply, agriculture, industry, recreation and other purposes [3]. In addition, different human activities have influenced aquatic ecosystems as a result of discharge of toxic chemicals, modification in hydrology, alternations of physicochemical water characteristic as well as increase nutrient inputs [4, 5]. Activities related to urbanization and agriculture basically are main contributors to alterations in the chemical composition of

Corresponding Author: School of Environmental and Natural Resource Sciences, Faculty of Science and Technology, Universiti Kebangsaan Malaysia, 43600 UK, Bangi Selangor, Malaysia. E-mail: fawaz1980@siswa.ukm.edu.my

Please cite this article as: Al-Badaii, F. and M. Shuhaimi-Othman, 2014. Heavy metals and water quality assessment using multivariate statistical techniques and water quality index of the Semenyih river, Peninsular Malaysia. Iranica Journal of Energy and Environment, 5(2): 132-145

aquatic habitats [6, 7]. Comprehension the impacts of anthropogenic activities on aquatic ecosystems hadincreased importance because of association with contamination of essential water resources such as lakes, streams and rivers.

Recently, there has been an increasing awareness of river system contamination with different contaminants inparticular heavymetal. Essentially, rivers play more important roles in the community particularly as a source of water supply and the fishing industry, in order that rivers pollution either directly or indirectly can mostly influence humansas final consumers. Nevertheless, some of the heavy metals are essential micronutrients in their low concentrations but toxicwhen exceed the minimum requirements [8].

In Malaysia, river systems are a fundamental part of the water supply. More than 150 river systems present in Malaysia, 100 of themlocated in Peninsular Malaysia while the other 50 found in Sabah and Sarawak. These rivers are evaluated to contribute about 97% of the water supply sources [9]. However, the river's water quality is degraded by reason of the leaching of pollutants and undiscriminating disposal of anthropogenic wastes from developed area which resultsin from urbanization, increase of population and industrialization [10]. Thus, it is important to perform river quality assessment so as to detect the alterations of the water quality and the evaluation of pollution sources [11]. The state of Selangor, Malaysia, has a long history of rivers contamination problems related to urbanization and land use alterations. Semenyih River is one of the mainrivers draining a residential area and densely inhabited of Selangor. Over the past 20 years, it has supplied about one million of Selangor population and is a source of management of overflow discharges [12]. According to literature [13], Semenyih River has been classified as slightly polluted. Additionally, Semenyih River is one of the important rivers in Malaysia which from a source of domestic water supply. Therefore, study of water pollution of the river is of particular importance because of the river receives huge effluents from livestock farms, industrial and agricultural activities as well as urban runoff which cause deterioration of the river water quality [14]. In general, human activities related to land use around Semenyih River basin pose a threat to aquatic ecosystem and the provinces where the river water usually uses as domestic supply [15]. Consequently, to protect the water resources, the land use activities must be planned and controlled. A study was conducted to determine the concentration of selected water quality parameters and heavy metals in Semenyih River, and to evaluate the contamination levelusing Water Quality Index (WQI) of Malaysian rivers and the multivariate statistical methods namely cluster analysis and factor analysis in order to assess the effect of unregulated waste discharge on the quality of the river.

MATERIALS AND METHODS

Study Area and Samples Collection: The Semenyih River has area ranged from 1.37 to 35.57 km^2 and consists of 25 water catchment valleys and 36 sub-basins (Fig. 1). The river lies between longitude 101° 48'32.9 "E to 101° 52'30.5 "E and latitude 02° 54'14.9 "N to 03 ° 03'23.1 "N. The river originates from the forested areas and hilly in the western slope of BanjaranTitiwangsa, northeast of Hulu Langat [13, 15]. In addition, it flows southwards toward Hulu Langat and Sepang. The riveris negatively affected by industrialization and urbanization since the early 1990. Overall, the river is a resource of domestic water supply after the treatment for Bandar Tasek Kesuma Semenyih town and Bandar Rinching [12, 15]. Eventually, the climate of the study area is characterized by high rainfall, high average and homogeneous annual temperatures and high humidity. This climate has influenced the geomorphology and hydrology of the study area.

Sampling stations were selected along the river based on the characteristic of the water condition and anthropogenic activities along the river. Stations 1 and 2 were located in the upstream and represent clear water. Furthermore, station 3 was located in the area where mining activity and deforestation took place where the water was turbid. Station 4 was more turbid due to runoff from human activities including random settlements. Station 5 was situated in the Semenyih City in which pollution was contributed by the urban activity as well as domestic and industrial effluents. In addition, station 6 was located after livestock farms and agricultural activities that adversely impact on the water quality in this station. Station 7 was affected by deforestation and discharge from rural areas. Thelast station was located after Bangi City in JenderamHilir and characterized by turbid and contaminated water as a result of accumulated pollutants from previous stations and water treatment plant as well as erosion and human activities (Fig. 1). Water sampling has been carried out in March, July and November 2012. Water samples were collected from each station in triplicate in specific bottles based ondescription reported in literature [16].

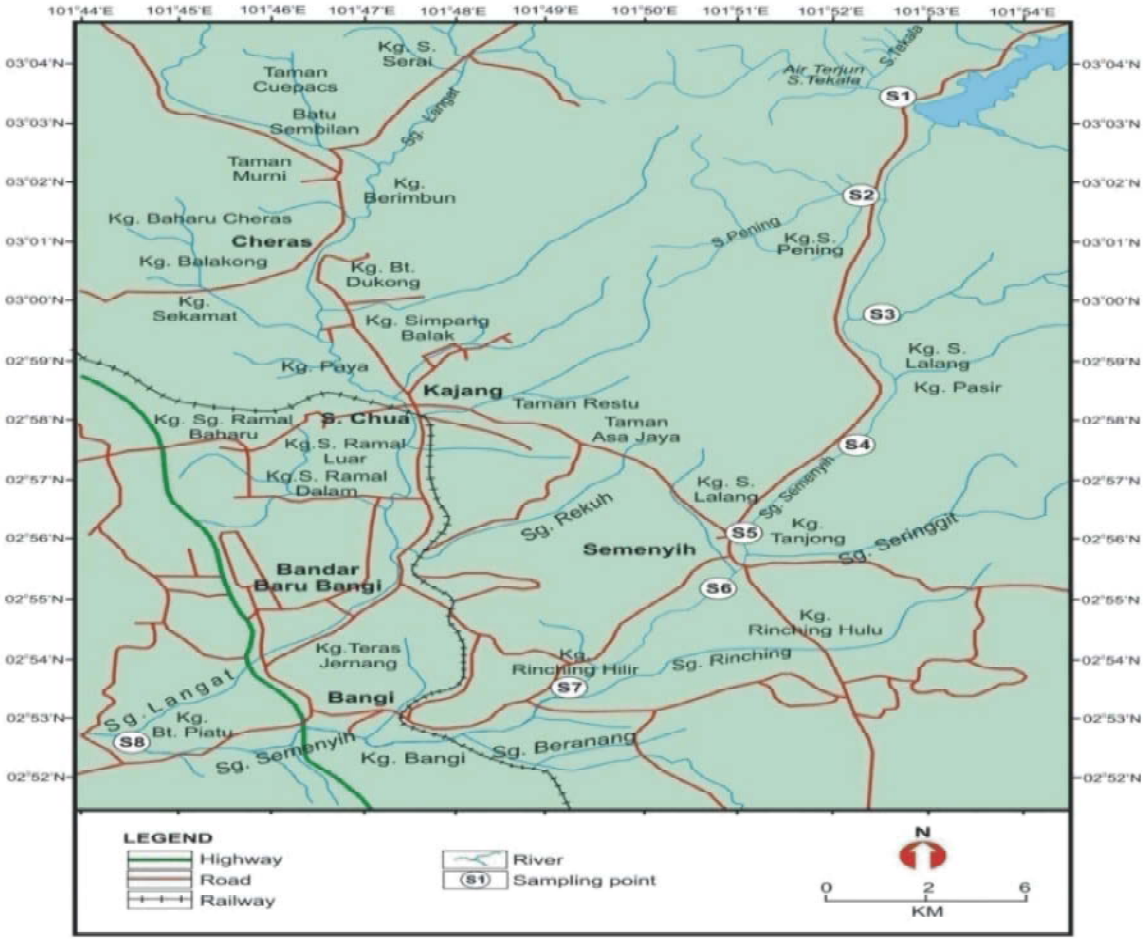

Fig. 1: Study area and sampling stations along Semenyih River

Analytical Determinations: Water quality parameters such as temperature, dissolved oxygen (DO), conductivity and pH were measured *in situ* using Multisensor probe YSI model 449D, whereas chemical oxygen demands (COD), biochemical oxygen demands (BOD_5), Total suspended solids (TSS), oil and grease (OG), turbidity, phosphate (PO_4^{3-}), sulfate (SO_4^{2-}), nitrate (No_3^-), nitrite (NO_2), ammonia nitrogen (NH_3-N), total hardness (TH), *E. coli* and total *Colifor* (TC) were analyzed in the laboratory. COD was measured by the open reflux method and BOD_5 was analyzed by 5-day test [15]. Additionally, TSS was analyzed by total solids dried at 103–105°C and O&Gwas assayed as described by liquid-liquid, partition-gravimetric method[16]. Moreover, turbidity, (PO_4^{3-}), (SO_4^{2-}), NO_2, (NO_4^-) and NH_3-N were assayed by absorptometric, acid ascorbic, SulfaVer 4®, cadmium reduction, diazotization and Nessler methods, respectively [16, 17]. Total hardness was determined by the convenient Inductive Coupled Plasma-Mass Spectrometry (ICP-MS). In addition, dissolved heavy metals (Fe, Zn, Cd, Mn, Cr, Ni, Pb, Cu and Hg) were measured by convenient Inductive Coupled Plasma-Mass Spectrometry (ICP-MS). Finally, *E.coli* and TC were determined based on the membrane filter technique [16]. All the equipments used were calibrated before use based on the manufacturer's directions.

Water Quality Index: The Water Quality Index (WQI) is attributed to quality value ofasummation set of calculated variables. It generallycontains sub-index values indicated each pre-identified variables bycomparing its measurement witha parameter-specific rating curve, optionally weighted as well as to integrate into the last index. The WQI aimed ofsummarizing amounts ofwater quality data into simple for a particular river [18]. Six variables were preferred for the WQI; Dissolved Oxygen (DO), Biochemical Oxygen Demand (BOD_5), Chemical Oxygen Demand (COD), Suspended Solids (SS), Ammoniacal Nitrogen (AN) and pH. Calculations are executed on the sub-indicesof variables. The sub-indices

Table 1: The best fit equations used for the estimation of the six sub-index values to calculate WQI

Subindices for DO (in % saturation), BOD and COD	Subindices for NH3-N, TSS and pH
SIDO = 0 for x ≤ 8	SIAN = 100.5 - 105x for x ≤ 0.3
SIDO = 100 for x ≥ 92	SIAN = 94 * exp(-0.573x) - 5 * I x – 2 I for 0.3 < x < 4
SIDO = -0.395 + 0.030x2 - 0.00020x3 for 8 < x < 92	SIAN = 0 for x ≥ 4
SIBOD = 100.4 - 4.23x for x ≤ 5	SISS = 97.5 * exp(-0.00676x) + 0.05x for x ≤ 100
SIBOD = 108 * exp(-0.055x) - 0.1x for x > 5	SISS = 71 * exp(-0.0061x) - 0.015x for 100 < x < 1000
	SISS = 0 for x ≥ 1000
SICOD = -1.33x + 99.1 for x ≤ 20	SIpH = 17.2 - 17.2x + 5.02x2 for x < 5.5
SICOD = 103 * exp(-0.0157x) - 0.04x for x > 20	SIpH = -242 + 95.5x - 6.67x2 for 5.5 ≤ x < 7
	SipH = -181 + 82.4x - 6.05x2 for 7 ≤ x < 8.75
	SipH = 536 - 77.0x + 2.76x2 for x ≥ 8.75

Source: [18]

are named SIDO, SIBOD, SICOD, SIAN, SISS and SIPH [19]. The finestequations used for the six sub-index value evaluation are shown in Table 1. Subsequently, the particular sub indices have been computed the WQI using the following equation;

WQI = 0.22*SIDO + 0.19* SIBOD +0.16 * SICOD + 0.15 * SIAN + 0.16 * SISS +0.12 * SIPH

Statistical Analysis: Statistical analysis was executed using SPSS version 20. In the cluster analysis (CA), the Ward's method and squared Euclidean distances were performed to determine water quality indicators and the variables of sampling stations [15, 20]. In addition, factor analysis (FA) orprincipal component analysis (PCA) was carried out tocategorizethe pollution factors influenced on water quality. The Bartlett's sphericity and Kaiser–Meyer–Olkin (KMO) tests were used to examine the suitability of the data regardingfactor analysis. However,all data analyzed were standardized by scale transformation to ensure normal distributions for cluster analysis and factor analysis [15, 21].

RESULTS AND DISCUSSION

Theconcentrations of Water Quality Variables: Table 2 shows the mean values of 18 variables of water quality in Semenyih River.Generally,river affectedby urbanization, agriculture, industry, mining and other human activities such as sewages from random settlements. The temperature values of the eight stations showed less variation, ranging from 25.25°C at station 1 to 27.18°C at station 8. Principally, several factors such as weather condition as well as sampling time result in variations of temperature [22]. The pH values ranged from 6.29 to 6.91, the acceptable range for aquatic life is from 6.5 to 9. Therefore, it is very significant to preserve the aquatic ecosystem within this range due tolow or high pH can causedisturbance in nature [19, 23]. The lowest DO concentration (4.77 mg/L) was found at station 8; and the DO concentrationsat stations 4,5,6 and 7 were also significantly lower than the other three stations. This attribute to the discharge of domestic effluents and industry induced serious organic contamination in the river, because of the decrease of DO was mostlyresulted from the organic compounds disintegration [24]. Further more, extremely low DO value generally pointsto the degradation of aquatic systems [25, 26]. The highest DO values were found at station 1 (6.34 mg/L). The conductivity mean values of all stations were ranged from 26.67 to 95.55 µS/cm, station 8 showed thehighest and station 1 the lowest values. This can be attributed to the effluent of domestic sewage, industrial wastewater, water treatment plant and agricultural activities, which discharge massivel evels of anions in the river system, because conductivity of surface water mainly relieson ion concentrations [27]. In addition, TDS values were ranged from 20.22 mg/L at station 1 to 61.55 mg/L at station 8. The TDS concentration in the river is essentially influenced by extreme anthropogenic activities and runoff with high suspended matter [14].The eighth station showed the highest concentrations of NO_3^- (9.51 mg/L) and PO_4^{3-} (1.01 mg/L); while showing station 7 the highest concentrations of NH_3-N (1.09 mg/L) and NO_2 (0.09 mg/L). This suggests that measures of nutrient decrease from industrial and domestic wastewater are largelyrequired to improve the water quality of Semenyih Rivertaking into consideration; that it receives highlevels of wastewater from random settlements [13]. Stations 4,5,6 and 7 showed relatively high NO_4^- and PO_4^{3-} contents; while Stations 4, 5, 6 and 8showed high NH_3-N and NO_2 concentrations. Generally, the excessive nutrients concentrations can stimulate aquatic plant and algae growth, which can lead to *eutrophication* [28]. The high nutrients and phosphorus concentrations were found in river mainlyimpacted by urbanization, industrialization and

Table 2: Mean values of water quality measurement along Semenyih River in March, July and November, 2012

Variables		Station 1	Station 2	Station 3	Station 4	Station 5	Station 6	Station 7	Station 8
Temp °C	MEAN	25.25	25.78	25.80	26.13	26.42	26.67	26.94	27.18
	SD	0.89	0.77	0.80	0.57	0.69	0.73	0.52	0.48
pH	MEAN	6.91	6.30	6.39	6.35	6.39	6.38	6.29	6.59
	SD	1.32	1.20	0.91	0.91	0.68	0.98	0.75	0.46
DO mg/L	MEAN	6.34	6.20	6.17	5.87	5.60	5.27	5.51	4.77
	SD	0.81	0.56	0.31	0.21	0.27	0.27	0.41	0.83
DO %	MEAN	77.23	72.43	72.66	68.20	65.11	60.42	63.11	52.91
	SD	6.92	5.29	6.57	6.61	5.35	5.58	5.96	2.75
Cond µS/cm	MEAN	26.67	40.78	44.55	59.89	67.78	74.22	78.00	95.55
	SD	13.50	18.95	24.50	28.34	29.18	32.85	39.18	34.62
TDS mg/L	MEAN	20.22	26.55	28.33	39.78	45.00	47.78	50.89	61.55
	SD	5.02	12.03	14.29	19.73	21.00	21.72	26.67	22.84
SO_4 mg/L	MEAN	2.30	5.87	7.51	14.81	9.90	23.21	28.44	19.69
	SD	0.82	1.83	0.34	7.76	1.84	19.79	28.28	6.54
NO_3 mg/L	MEAN	2.49	5.14	6.15	7.94	6.74	7.33	8.09	9.51
	SD	1.63	3.27	3.45	5.71	5.11	4.96	3.89	3.80
NO_2 mg/L	MEAN	0.01	0.02	0.03	0.05	0.05	0.05	0.09	0.07
	SD	0.01	0.01	0.02	0.03	0.01	0.01	0.09	0.03
PO_4 mg/L	MEAN	0.34	0.41	0.52	0.53	0.72	0.76	0.97	1.01
	SD	0.27	0.57	0.40	0.28	0.29	0.61	0.81	0.36
TUR NTU	MEAN	5.00	37.57	40.54	50.01	56.44	65.64	129.46	119.44
	SD	2.65	21.47	24.10	44.57	51.93	54.34	84.02	68.28
NH_3-N mg/L	MEAN	0.04	0.26	0.36	0.66	0.73	0.93	1.09	1.07
	SD	0.03	0.08	0.04	0.12	0.13	0.17	0.72	0.29
TSS mg/L	MEAN	17.33	38.86	67.44	87.36	70.53	74.04	264.82	93.88
	SD	10.99	9.52	20.05	74.39	35.56	59.79	198.41	41.81
BOD mg/L	MEAN	0.46	1.18	1.94	2.66	2.72	3.47	3.48	3.78
	SD	0.16	0.52	0.62	0.76	0.92	1.07	0.93	0.82
COD mg/L	MEAN	8.26	15.53	30.89	41.68	49.05	82.64	76.22	103.49
	SD	2.33	2.29	16.76	13.97	10.26	68.32	40.81	84.38
TH mg/L	MEAN	4.25	3.27	3.55	5.15	5.88	6.57	6.29	10.07
	SD	1.03	0.83	0.39	1.27	1.99	2.09	2.65	4.59
OG mg/L	MEAN	1.20	2.77	2.91	3.54	4.40	3.74	4.00	4.46
	SD	0.26	1.21	1.10	1.24	1.73	1.12	1.04	0.88
E.coli CFU//100mL	MEAN	688.9	3000	24444.4	43222.2	68666. 7	167111.1	106555. 6	135222.3
	SD	226.90	1193.04	26738.10	28636.29	46855.57	97288.99	26077.52	68350.86
T.C *CFU//100mL*	MEAN	1666.7	7855.6	68777.8	91666.7	136222.2	256000.0	203888.9	252000
	SD	218.58	2313.33	49137.37	44035.34	74765.06	61199.13	14241.31	41929.84

agricultural activities [29]. This refers to the urgent need to control pollutionsource in the river. In contrast, station 1 represented the lowest concentrations of NO_3^- (2.49 mg/L), NO_2 (0.01 mg/L), NH_3-N (0.04 mg/L) and PO_4^{3-} (0.34 mg/L). The seventh station showed the high value of SO_4^{2-} (28.44 mg/L); while station 1 recorded the lowest value (2.30 mg/L). In general, the rock weathering and human activities such as mining, fossil fuel combustion process and waste discharge are the main sources of sulfate in rivers [30]. The high turbidity values were found 129.46 NTU and 119.44 NTU at stations 7 and 8, respectively, resulted from bridge construction at station 7 which was an indicator of a high measured of turbidity. Furthermore, relatively high turbidity values were at stations 4, 5 and 6. Generally,the overland flow, stream flow and surface runoff in natural waters increase the turbidity levels in the water [15, 31]. Conversely, station 1 showed the lowest value of turbidity (5 NTU). Relatively high BOD contents were found in the stations 6 (3.47 mg/L), 7 (3.48 mg/L) and 8 (3.78 mg/L); the COD contents also showed high concentrations at stations 6 (82.64 mg/L), 7 (76.22 mg/L) and 8 (103.49 mg/L). The BOD and COD concentrations were continually increased in particular at these stations because of livestock husbandry before station 6. The BOD and COD concentrations in surface water are impacted mainly by the natural plant decomposing process andother contributors which increase the total nutrient in water bodies such as construction effluent, fertilizer, septic system and animal farms [15, 22, 32]. The seventh station

showed the highest value of TSS (264.82 mg/L). This attributed to serious erosion and drifts mud as a result of the rapidly increased flow rate along the river especially at the latest stations. Additionally, the TSS valueswere increased starting from station 3, because of deforestation, mining and palm plantation activities along the river. On the other hand, the upstream station recorded the lowest value of TSS (17.33 mg/L). TH contents were relatively low at all stations and ranged from 3.27 to 10.07 mg/L.The highest value of oil and grease (4.46 mg/L) was found in the station 8, while smaller amounts of oil and grease (1.20 mg/L) were found at station 1. Oil and grease concentratios can seriously affect the ecology of a water body [15]. These concentrations are increased along the river due to the untreated domestic and industrial wastewater from Semenyih and Bangi Cities as well as the discharges of surrounding area wastewater.All stations showed high concentrations of *E. coli* and TC. Station 6 recorded the highest concentrations of *E. coli* (167111.1 CFU/100 mL) and TC (256000 CFU/100mL). The *E. coli* and TC countswere increased drastically at station 6 that receives large amounts of effluents from livestock husbandry farms situated before station 6. Moreover, human recreational activities were also a source of *Colifor* contamination [32]. On the contrary, station 1 showed the lowest concentrations of *E. coli* (688.9 CFU/100 mL) and TC (1666.7 CFU/100mL). In general, the high counts of coliform bacteria are attributed to rapid growth of population in the basin area and the open defecation along the river banks [33, 34]. On the other hand, the mean values of temperature, pH, conductivity, TDS, SO_4 and TH werecategorized under class I, whereas DO, BOD_5 were categorized under class II based on NWQS for Malaysian rivers [20]. Consequently, these parameters were within the acceptable range. Moreover, the mean values of NO_3, NO_2, NH_3-N, TSS and COD were categorized as class III and reached the threshold limit. Likewise, the mean values ofturbidity, PO_4^{3-}, O&G, *E. coli* and TC were exceeded the allowable threshold levels of NWQS, hence, categorized as class V. Therefore, the river is slightly polluted with NO_4^{-}, NO_2, NH_3-N, TSS and COD, whereas it is extremely contaminated with turbidity, PO_4^{3-}, O&G, *E. coli* and TC.

Heavy Metals Concentrations: The heavy metals concentrations in the sampling stations of Semenyih River are shown in Table 3. For Cd, it ranged from 0.12 to 0.68 µg/L, compared to 0.06-0.98 µg/L as reported in literature [35] of the same basin. All the sampling stations recorded levels less than 10 µg/L recommended other researcher [19], to be categorized as Class II. The Cu values ranged from 0.84 to 7.33 µg/L, compared to Cu ranged from 5.96 to 21.2 µg/L reported for Semenyih River [35]. All the sampling stations recorded level less than the recommended limit(10 µg/L) by DOE in 2011. The Ni concentrations were ranging from 0.29-0.88 µg/L, compared to 0.80 to 24.72 µg/L reported [36] of the Langat river basin. All the sampling stations showed levels less than 50 µg/L recommended bythe other researcher [19]. Generally, the Ni sources are representing chemical and mining industries [37]. The values of Zn ranged from 33.10-49.19 µg/L, compared to 40-60 µg/L as reported in literature [32] of the Langat river basin. The highest Zn value was recorded at station 7, whereas the lowest at station 6. Adequate Zn is essential to neutralize the toxic influences of Cd [38]. Principally, Zn content had been shown as an example of the evolution of toxic metals related to mining pollution [39]. The Fe concentrations of water samples ranged between minimum 280.76 mg/ L at station 7 to maximum 488.60 µg/ L at station 5 and all stations had values less than 500 µg/L, compared to 340 to 1980 µg/L reported for Langat River [32]. When compared to NWQS [19], the normal criterion is 1000 µg/L for Fe. Therefore, all stations were within this range. Stations 5 and 6 received urban runoff and wastewater from Semenyih city and livestock farms that contributed to the high Fe concentration. In addition, the Pb values ranged from 0.70 to 3.08 µg/L. This study recorded lower content of Pb compared to the findings reported in literature [36], which ranged between 0.5-6.99 µg/L. Generally, Pb deposits in water partitions rapidly between the sediments and an aqueous phase, depending on pH, salt content and the presence of organic chelating agents [40]. For Mn, it ranged between minimum 30.11 µg/L at station 4 and maximum 59.79 µg/L at station 7, compared to Mn between 8.93-492 µg/L as reported in literature [30] of the same basin. Moreover, the Cr concentrations of water samples ranged between minimum 1.64 at station 2 to maximum 5.46 µg/ L at station 8. Eventually, Hg values ranged from 0.0 -0.96 µg/ L. The order of heavy metal concentrations in water samples was Fe> Zn>Mn>Cr> Cu>Pb> Ni> Cd>Hg.

Comparison with various water quality standards showed that the mean Cu, Ni, Pb, Hg and Cr were low and within the range of natural background concentrations (Table 4). Although, the mean value of Fe in the water was higher than the Canadian Standard (CCME), it was found to be lower than that of the United States Environmental Agency (USEPA (CCC)) and the Malaysian standard (NWQS). Furthermore, the mean value of Cd was also lower than the USEPA (CMC) and Malaysian standard (NWQS), while was higher than CCME and USEPA (CCC).

Table 3: Mean concentrations of heavy metals in the water samples at each station inSemenyih River during March, July and November, 2012

Heavy metal µg/L	ST1	ST2	ST3	ST4	ST5	ST6	ST7	ST8
Cd	0.64	0.35	0.26	0.68	0.61	0.12	0.15	0.29
Cu	1.99	0.84	1.70	1.78	2.03	7.33	1.81	1.95
Ni	0.86	0.29	0.33	0.37	0.88	0.53	0.38	0.72
Zn	34.80	40.13	37.79	35.16	47.55	33.10	49.19	47.41
Fe	310.17	317.67	283.98	385.06	488.60	486.79	280.76	396.98
Pb	1.20	0.76	0.70	1.50	2.18	3.08	2.10	2.49
Mn	48.73	32.35	33.72	30.11	32.16	39.38	44.40	59.79
Cr	2.90	1.64	3.97	2.62	1.99	2.57	2.34	5.46
Hg	0	0	0.01	0.14	0.96	0.12	0.17	0.15

Table 4: Criteria of heavy metals concentrations in freshwater ecosystem

Metal	*Present study µg/L*	*CCME µg/L*	*USEPA-(CMC) µg/L*	*USEPA-(CCC) µg/L*	*NWQS, Class II (µg/L)*
Cd	0.39	0.017	2.0	0.25	10
Cu	2.43	2-4	13	9.0	10
Ni	0.54	52-150	470	52	50
Zn	40.64	30	120	120	5000
Fe	368.75	300	-	1000	1000
Pb	1.75	1-7	65	2.5	50
Mn	40.8	-	-	-	100
Cr	2.94	8.9	570	87	50
Hg	0.19	-	1.4	0.77	1

Source: [19, 41, 42]

The mean value of Zn exceeded CCME, while was below USEPA (CMC and CCC) drinking water quality guidelines and Malaysian standard (NWQS). Lastly, the mean concentration of Mn was above CCME guidelines, USEPA (CMC and CCC) drinking water quality guidelines, whereas was found to be within the Malaysian standard (NWQS). It was determined that the concentrations of heavy metals in the Semenyih River were lower than the maximum permitted concentrations for protection of aquatic life, except Cd, Zn, Fe and Mn which were slightly elevated. The accumulation of heavy metals along the Semenyih River may depend largely on common sources of pollution, which are identified as industrial discharges, domestic sewage and livestock farms [12].

Cluster Analysis: Cluster analysis (CA) was used to test water quality data and determine the similarity of sampling stations as well as to classify specific areas of pollution [2, 43, 44]. H CA was executed on the standardized data set using Ward's method with Euclidean distances to the determination of similarity. CA yielded a dendrogram (Fig. 2), where all eight sampling stations were grouped into three significant different clusters at $(D_{link}/D_{max}) \times 100<40$. Cluster 1 comprised stations 1, 2 and 3. Cluster 2 encompassed stations 4 and 5, whereas Cluster 3 consisted of stations 6, 7 and 8. The classification of clusters varied with significance level due to the stations in these clusters had anthropogenic backgrounds and similar features and that influenced by parallel sources. Cluster 1 pointed out relatively low polluted stations. In cluster 1, stations were situated in the upstream thatwas surrounded by extended forest covering. The upstream area of rivers commonly is covered with intense forest covering [20, 44]. In these stations, human activitieswere limited except some recreational activities at upstream waterfall [15]. Cluster 2 corresponded to moderate polluted stations, which wereinfluenced by anthropogenic activities and land use. Station 4 receives pollutants from agricultural activities, domestic effluents and mining as well as discharge of unsewered areas, whereas station 5 was affected by surface runoff, industrial activities and wastewater from Semenyihtown [15]. Cluster 3 indicateddownstream stations which wereimpacted by palm plantation, deforestation, livestock farms particularly at station 6, runoff from agricultural fields and discharges from vehicles washing and workshops as well as water treatment plant at station 8. Additionally, the anthropogenic activities in this area included settlements and industries, which covered Rinching, Bangi, Broga and Beranang [12]. Therefore, the high deterioration of water quality was recorded at these stations that received contamination from point and non-pointsources such represented above.

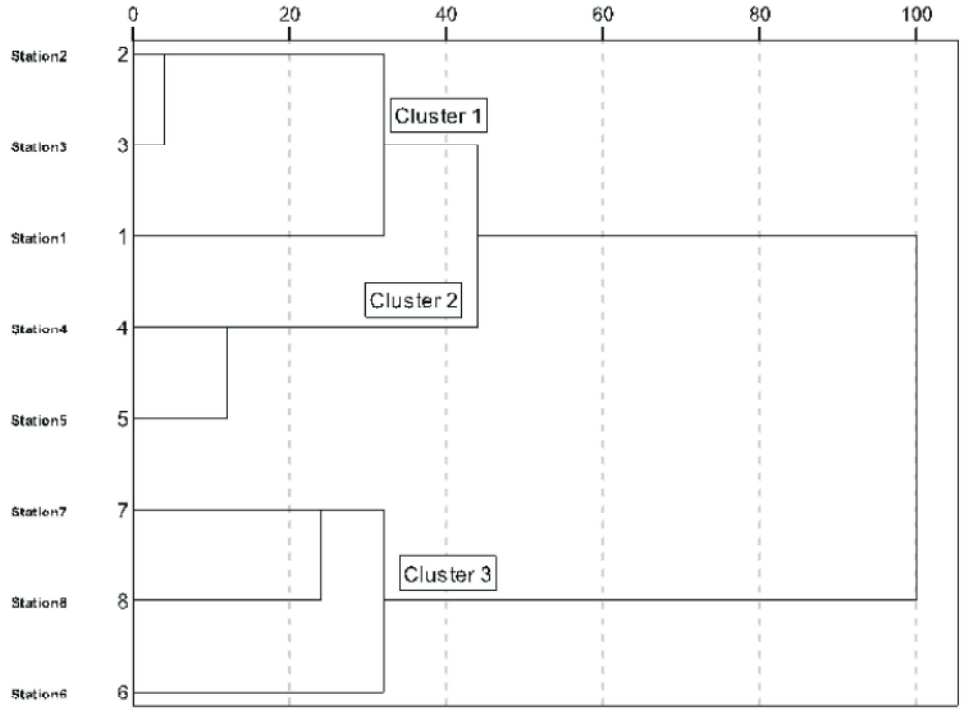

Fig. 2: Dendrogram showing clustering of sampling stations on Semenyih River

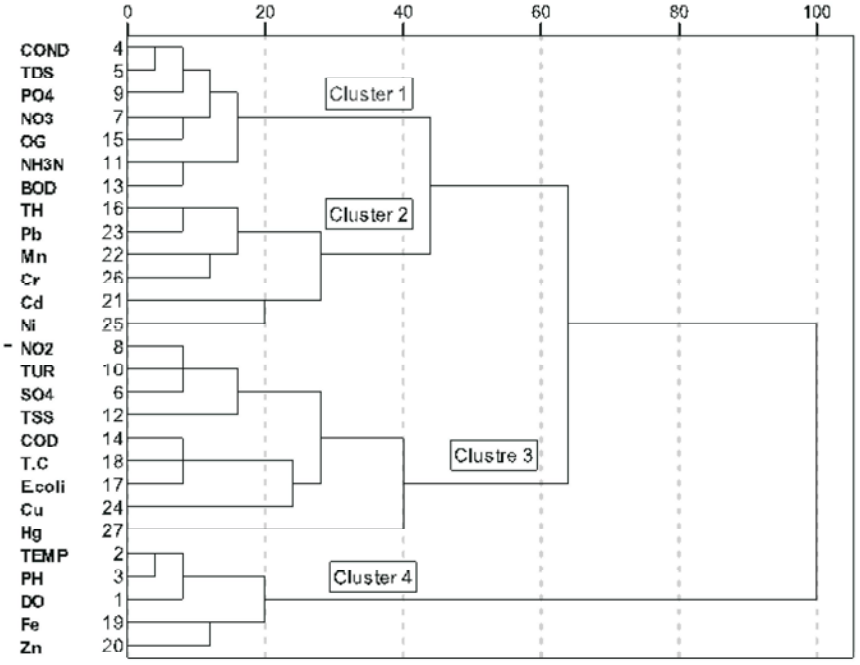

Fig. 3: Dendrogram showing clustering of the analyzed variables in water samples

Correspondingly, to confirm the associations among the variables in the total dataset, CA was carried out to classify the relationships among the analyzed variables and their possible sources [36]. CA yielded a dendrogram (Fig. 3) where all 27 variables were grouped into four statistically significant clusters at $(D_{link}/D_{max}) \times 100<40$. Cluster 1 comprised conductivity, TDS, PO_4^{3-}, NO_3^-, O&G, NH_3N and BOD which recognized as pollutants

derived from anthropogenic sources like agricultural runoff and domestic wastewater. Cluster 2 consisted of TH, Pb, Mn, Cr, Cd and Ni. Principally, Cd and Ni are derived from anthropogenic sources such as discharges of mining activities, while total hardness mostly derived from lithogenic sources as well as Cr and Mn is derived from lithogenic and anthropogenic sources (hardness is not associate with pollutant, normally cause by natural rock/sediment in the area, its significant effect is on metal toxicity). Cluster 3 contained NO_2, turbidity, SO_4^{2-}, TSS, COD, TC, *E. coli*,Cu and Hg. This cluster is primarily affected by anthropogenic sources like discharges of livestock farms and random settlements. In addition, it is greatly impacted by lithogenic sources such as erosion and surface runoff. Cluster 4 encompassed temperature, pH, DO, Fe and Zn, they are influenced by anthropogenic and lithogenic sources such as discharges of mining, agricultural activity discharges as well as surface runoff due to Fe is found in the Earth's crust. Moreover, most of these parameters reflected positive loadings of the first factor in PCA. Eventually, CA represent a useful classification of the Semenyih River basin that could be used by authorities and decision makers to design a comprehensive future monitoring network with low cost [43, 44]. According to CA results, the number of monitoring stations might be reduced and selected only from Clusters 1, 2 and 3.

Principal Component Analysis/ Factor Analysis: Factor Analysis (FA) or Principal Component Analysis (PCA) was performed on the normalized datasets for the eight sampling stations to determine the factors influenced on each water sample and to assess the composition structure among them. Five factors were obtained for the study area with total variance 96.63%, whenEigenvalues >1. The factor loadingswere classified based on the loading values to strong (>0.75), moderate (75-0.50) and weak (0.50-0.30)[45]. In this study, the data set of 28 water quality variables encompasses five factors (Table 5).

Factor 1 represents 58.19% of the total variance, showing strong positive loadings on temperature, EC, TDS, SO_4^{2-}, No_3^{-}), NO_2, PO_4^{3-}, turbidity, NH_3N, BOD, COD, O&G, TH, *E. coli* and TC, moderate positive loading on TSS, Zn and Pb. In addition, it has strong negative loadings on DO. Temperature is most possibly associated with seasonal influences. Furthermore, conductivity, TDS, TSS and turbidity can be identified to originate from both nonpoint pollution sources and water treatment plants at station 8 [13, 32]. TSS, TDS and turbidity are commonly associated with discharge from urban areas involving the erosion of road edges due to surface runoff, clearing of lands and agricultural runoff [13, 46, 47]. In addition, the conversion of forest or agricultural land to urban areas has indeed caused large negative impacts on the ecosystem of Semenyih basin in the form of mud flood, landslide and river floods [13]. The presence of NO_3^{-}, NO_2, SO_4^{2-}) and PO_4^{3-} are due to agricultural runoff such as livestock waste and fertilizers [16], as well as PO_4^{3-} is an important constituent of detergentsthat discharge into the river by municipal sewage, industrial effluents and existing water treatment plants [48]. In addition, these contaminants may also derive from nitrogen decomposition and degradation processes [27]. Positive loadings on NH_3-N, BOD, COD and O&G attributed to the anthropogenicsources, particularly the organic pollutants from point sources such as the discharge of domestic wastewater, water treatment plants, livestock farms and untreated sewage of random settlement areas as well as industrial effluents [12]. Furthermore, the positive loadings of TH is ascribed to the lithologic sources (rocks and sediments) as well as the presence of *E. coli* and TC are due to discharge into the river via surface runoff of domestic wastewater and fertilizer (animal waste) used in agricultural activities. According to [49], the transport of *Colifor* is primarily through the soil or direct input by a warm blooded animal (e.g., livestock). Moreover, strong positive loadings on *E. coli* and TC are related to municipal wastes, animal husbandry and recreation activities. The moderate positive loadings on Zn and Pb were allegedly attributed to industrial and municipal activities [13]. Furthermore, the automobile exhausts are another source of Pb, where surface runoff carries the Pb deposits into the river [32].

Factor 2, represents 11.5% of the total variance and has strong positive loadings on Cu, moderate positive loadings on *E.coli*, Fe and Pb. The presence of Cu indicates pollution from anthropogenic sources due to the discharge of domestic sewage and industrial effluents that cause Cu pollution in receiving water. On the other hand, the moderate positive loadings of *E.coli* is strongly related to municipal sewage and wastewater treatment plants [50], whereas the presence of Fe and Pb basically represents the metal group originating from industrial effluents.

Factor 3, elucidates 11.14% of the total variance, showing strong positive loadings on pH and Mn, while having moderate positive loadings on Ni and Cr. The positive loading of pH attributed to dissolved minerals, domestic wastewater and acid rain, which can affect on the pH values of the river to change any which way.

Table 5: Factor loadings of the 27 variables on varimax rotation in Semenyih River

	Rotated Component matrix				
Variables	F 1	F 2	F 3	F 4	F 5
DO	-0.921	-0.251	-0.252	-0.097	0.079
DO	0.980	0.141	0.024	0.031	0.105
pH	-0.425	0.032	0.883	0.086	0.111
COND	0.984	0.130	0.073	0.091	0.005
TDS	0.974	0.131	0.107	0.132	0.022
SO_4	0.824	0.307	-0.080	-0.181	0.377
NO_3	0.961	-0.023	-0.182	-0.070	-0.143
NO_2	0.908	-0.034	-0.046	0.021	0.350
PO_4	0.893	-0.035	0.015	-0.031	0.266
TUR	0.930	-0.100	0.075	-0.122	0.322
NH_3-N	0.958	0.194	-0.040	0.057	0.170
TSS	0.614	-0.159	-0.148	-0.157	0.691
BOD	0.959	0.229	-0.090	0.025	0.027
COD	0.941	0.278	0.184	-0.046	0.031
OG	0.920	0.007	-0.267	0.267	-0.062
TH	0.846	0.135	0.479	0.114	-0.107
E. coli	0.814	0.560	0.122	-0.003	0.085
T.C	0.890	0.421	0.123	0.006	0.082
Fe	0.347	0.582	-0.084	0.625	-0.365
Zn	0.622	-0.536	0.108	0.323	0.371
Cd	-0.457	-0.416	-0.005	0.538	-0.313
Mn	0.365	0.000	0.898	-0.187	0.110
Pb	0.693	0.622	0.189	0.286	0.102
Cu	0.187	0.977	-0.006	-0.046	-0.029
Ni	-0.085	0.098	0.667	0.730	-0.032
Cr	0.423	-0.152	0.605	-0.355	-0.471
Hg	0.232	-0.057	-0.176	0.918	0.079
Variance (%)	58.198	11.497	11.143	9.694	6.104
Cumulative (%)	58.198	69.695	80.838	90.532	96.637

Table 6: Water Quality Index (WQI) at eight stations of Semenyih River

Station	DO SI	BOD SI	COD SI	AN SI	SS SI	pH SI	WQI	CLASS
1	86	98	88	96	88	99	92	I
2	81	95	78	73	77	95	83	II
3	81	92	62	68	65	96	78	II
4	76	89	52	58	58	96	71	III
5	72	89	46	56	64	96	70	III
6	65	86	25	50	63	96	64	III
7	69	86	28	46	43	95	61	III
8	54	84	16	46	56	98	58	III
Average	73	90	44	58	58	96	70	III

Mn is associated withanthropogenic sources byeffluents from mining and mineral activities andsewage sludge as well as Mn can be released to water by discharge from industrial facilities or as leachate from landfills and soil [42]. The presence of Ni attributed to anthropogenic activities such as mining, while Cr ascribed to anthropogenic sources such as industrial effluents derived from the production of corrosion inhibitors and pigments [15], which then becomes a pollutant of aquatic ecosystems and thus harmful to aquatic organisms [32].

Factor 4, accounts for 9.69% of the total variance and has a strong positive loading on Hg, moderate positive loadings on Fe, Ni and Cd. The positive loading of Hg is related to rocks, sediments, water and soils which naturally contain small but varying amounts of mercury. The moderate positive loading of Fe is associated with iron in rocks and clay soils and argillaceous limestone as well as industrial wastes and mine drainage. Both Ni and Cd are associated with high fluxes from industrial and urban wastes including the immense urban runoff. Ni and Cd also affected by using rechargeable batteries in the region [51].

Factor 5 stands for 6.1% of the total variance and has a moderate positive loading on TSS. The TSS with moderate positive loading can be resulted from soil erosion, surface runoff and mining activities in the river [27].

Water Quality Index (WQI): The water quality index (WQI) has been considered to give criteria for surface water classification based on the use of standard variables for water characterization and mathematical instrument to transform them into a single number which represents the water quality status [52]. In this study, the values of WQI of the eight stations in the Semenyih River were fluctuated from 58 to 92; the highest value of WQI was recorded at station 1 which was the lowest pollution, while the lowest value was recorded at station 8 which showed high levels of contamination (Table 6). The WQI of the Semenyih River was classified as Class I at station 1 which was situated in the upstream, while stations 2 and 3 categorized as Class II due to receive low contaminants compared to the other stations. Moreover, stations 4, 5, 6, 7 and 8 were classified under class III, because these stations receive several pollutants from cleaning and industrial effluents, road runoff, animal and human wastewater, discharge of water treatment plant and septic system as well as agricultural activities particularly covered agriculture that affects negatively on the water quality of the river from station 4 to 8, therefore they recorded higher levels of pollution. Overall, the WQI of the Semenyih River was 70; hence it was classified as class III, which represents that the river is slightly polluted [19]. However, the river water may be required extensive treatment before using for domestic purposes.

CONCLUSION

In this study, multivariate statistical techniques and water quality index were used to investigate the water quality of the Semenyih River. Cluster analysis categorized the eight sampling stations into three clusters based on the similarity of water quality characteristics and grouped 27 variables analyzed to three clusters to identify the relationship among the variables and their possible sources. Based on obtained information, optimal sampling strategy can be designed, which could reduce the number of sampling stations and related costs. Furthermore, this analysis permitted the classification of three various regions in the river, with various water quality. Principle component analysis identifies the sources responsible for variations in river water quality. Five factors generated from the factor analysis point to that the variables responsible for deterioration of water quality are largely attributed to anthropogenic activities associated with urbanization, industrialization, agriculture and mining activities. Therefore, this study demonstrates that the multivariate statistical techniques are valuable for analysis and interpretation of data sets to evaluate water quality and identify contamination sources as well as understanding the variations in water quality for efficient river water quality management. Eventually, WQI was classified the Semenyih River as clean (Class I) at station 1, slightly polluted (Class II) at stations 2 and 3 and as moderately polluted (Class III) at stations 4-8; in general, however, the river falls into class III and thus is required extensive treatment before using for domestic purposes.

ACKNOWLEDGEMENT

The authors would like to express their appreciation to the Faculty of Science and Technology, UniversitiKebangsaan Malaysia for use of their research facilities. In addition, the authors would like to express their thanks to Thamar University, Yemen for financial support as scholarship for the first author.

REFERENCES

1. Jarvie, H., B. Whitton and C. Neal, 1998. Nitrogen and phosphorus in east coast British rivers: speciation, sources and biological significance. Science of the Total Environment, 210: 79-109.

2. Varol, M. and B. Şen, 2009. Assessment of surface water quality using multivariate statistical techniques: a case study of Behrimaz Stream, Turkey. Environmental Monitoring and Assessment, 159(1-4): 543-553.
3. Carpenter, S.R., N.F. Caraco, D.L. Correll, R.W. Howarth, A.N. Sharpley and V.H. Smith, 1998. Nonpoint pollution of surface waters with phosphorus and nitrogen. Ecological Applications, 8(3): 559-568.
4. Paul, M.J. and J.L. Meyer, 2001. Streams in the urban landscape. Annual Review of Ecology and Systematics, 32(1): 333-365.
5. Van Landeghem, M.M., M.D. Meyer, S.B. Cox, B. Sharma and R. Patiño, 2012. Spatial and temporal patterns of surface water quality and ichthyotoxicity in urban and rural river basins in Texas. Water Research, 46(20): 6638-6651.
6. Najafpour, S., S.M.V. Farabi, M. Yousefian, F.M.A. Alkarkhi and A.G. Khenary, 2010. The determination of organochlorine pesticide residues in Chalus River water by multivariate analysis. Iranica Journal of Energy and Environment, 1(3): 222-227.
7. Ahmad, K.A., I. Mushrifah and M.S. Othman, 2009. Water quality and heavy metal concentrations in sediment of Sungai Kelantan, Kelantan, Malaysia: A baseline study. Sains Malaysiana, 1(4): 435- 442.
8. Rosli, N.A., M.H. Zawawi and R.A. Bustami, 2012. Salak River Water Quality Identification and Classification According to Physico-Chemical Characteristics. Procedia Engineering, 50: 69-77.
9. Yusof, M.A., N. Hasan and M.P. Abdullah, 2002. River water quality in Langat basin, Selangor, Malaysia. Malaysian Journal of Environmental Management, 3: 125-142.
10. Abdullah, M., 0000. Water Quality Studies of Semenyih Dam, M.Sc. Thesis, UTM Malaysia.
11. Gasim, M.B., B.S. Ismail, N.A. Wan, I.Y. Muhammad and M.H. Marlia, 2005. Water Quality assessment of the Semenyih River basin Selangor, Malaysia. Journal of Bioscience, 16(1): 87-95.
12. Gasim, M.B., M.M. Jamil, S.A. Rahim and M.E. Toriman, 2009. Water-Quality Assessment of the Langat River at Kilometre 7, Jalan Kajang-Bangi, Selangor, Malaysia. The Arab World Geographer, 12(3): 188-198.
13. Al-Badaii, F., M. Shuhaimi-Othman and M.B. Gasim, 2013. Water Quality Assessment of the Semenyih River, Selangor, Malaysia. Journal of Chemistry: doi:10.1155/2013/871056.
14. APHA, Standard Methods for the Examination of Wastewater, 20th edition. America Public Health Association, Washington, DC, 1999.
15. HACH, DR/500 spectrophotometer procedure manual, Loveland, Colorado: Hach Company, 2003.
16. Saffran, K., K. Cash and K. Hallard, 2001. Canadian water quality guidelines for the protection of aquatic life. CCME water quality Index, 1(0): 200.
17. DOE, 2011. Water quality index, Department of Environment. Ministry of Science, Technology and Environment Malaysia, Kuala Lumpur, pp: 86.
18. Bu, H., X. Tan, S. Li and Q. Zhang, 2010. Temporal and spatial variations of water quality in the Jinshui River of the South Qinling Mts., China. Ecotoxicology and Environmental Safety, 73(5): 907-913.
19. Kazi, T., M. Arain, M. Jamali, N. Jalbani, H. Afridi, R. Sarfraz, J. Baig and A.Q. Shah, 2009. Assessment of water quality of polluted lake using multivariate statistical techniques: A case study. Ecotoxicology and Environmental Safety, 72(2): 301-309.
20. Al Sabahi, E., S. Abdul Rahim, W. Wan Zuhairi, F. Al Nozaily and F. Alshaebi, 2009. A Study of Surface Water and Groundwater Pollution in Ibb City, Yemen. The Electronic Journal of Geotechnical Engineering, 14: 1-12.
21. Rosli, N., S. Gandaseca, J. Ismail and M.I. Jailan, 2010. Comparative Study of Water Quality at Different Peat Swamp Forest of Batang Igan, Sibu Sarawak. American Journal of Environmental Sciences, 6(5).
22. Boyle, T.P. and H.D. Fraleigh Jr, 2003. Natural and anthropogenic factors affecting the structure of the benthic macroinvertebrate community in an effluent-dominated reach of the Santa Cruz River, AZ. Ecological Indicators, 3(2): 93-117.
23. Razmkhah, H., A. Abrishamchi and A. Torkian, 2010. Evaluation of spatial and temporal variation in water quality by pattern recognition techniques: A case study on Jajrood River (Tehran, Iran). Journal of Environmental Management, 91(4): 852-860.
24. Sayed, R.A. and S.G. Gupta, 2010. River water quality assessment in Beed district of Maharashtra: seasonal parametric variations. Iranica Journal of Energy and Environment, 1(4): 326-330.
25. Shuhaimi-Othman, M., E.C. Lim and I. Mushrifah, 2007. Water quality changes in Chini Lake, Pahang, West Malaysia. Environmental Monitoring and Assessment, 131(1-3): 279-292.

26. Rahman, M.A. and D. Al Bakri, 2010. A Study on Selected Water Quality Parameters along the River Buriganga, Bangladesh. Iranica Journal of Energy & Environment, 1(2): 81-92.
27. Abdullah, M., S. Waseem and V. Bai, 2008. Development of New Water Quality Model Using Fuzzy Logic System for Malaysia. Open Environmental Journal, 2(1): 101-106.
28. Hem, J.D., 1985. Study and interpretation of the chemical characteristics of natural water. Vol. 2254. 1985: Department of the Interior, US Geological Survey.
29. Yisa, J. and T. Jimoh, 2010. Analytical Studies on Water Quality Index of River Landzu. American Journal of Applied Sciences, 7(4).
30. Juahir, H., S.M. Zain, M.K. Yusoff, T.T. Hanidza, A.M. Armi, M.E. Toriman and M. Mokhtar, 2011. Spatial water quality assessment of Langat River Basin (Malaysia) using environmetric techniques. Environmental Monitoring and Assessment, 173(1-4): 625-641.
31. Varunprasath, K. and N.A. Daniel, 2010. Physico-chemical parameters of river Bhavani in three stations, Tamilnadu, India. Iranic Journal of Energy & Environment, 1(4): 321-325.
32. Varunprasath, K. and A.N. Daniel, 2010. Comparison Studies of Three Freshwater Rivers (Cauvery, Bhavani and Noyyal) in Tamilnadu, India. Iranica Journal of Energy and Environment, 1: 315-320.
33. Shuhaimi-Othman, M. and M.B. Gasim, 2005. Heavy metals concentrations in water of sungai Semenyih Watershed, Selangor Malaysia. Sains Malaysiana, 34(2): 49-54.
34. Lim, W.Y., A.Z. Aris and M.P. Zakaria, 2012. Spatial variability of metals in surface water and sediment in the langat river and geochemical factors that influence their water-sediment interactions. The Scientific World Journal, 2012.
35. Aziz, H.A., M.N. Adlan and K.S. Ariffin, 2008. Heavy metals (Cd, Pb, Zn, Ni, Cu and Cr (III)) removal from water in Malaysia: Post treatment by high quality limestone. Bioresource Technology, 99(6): 1578-1583.
36. Varol, M. and B. Şen, 2012. Assessment of nutrient and heavy metal contamination in surface water and sediments of the upper Tigris River, Turkey. Catena, 92: 1-10.
37. Olias, M., J. Ceron, F. Moral and F. Ruiz, 2006. Water quality of the Guadiamar River after the Aznalcollar spill (SW Spain). Chemosphere, 62(2): 213-225.
38. WHO, Guidelines for Drinking Water Quality, 3rd edition, World Health Organization, Geneva, 2004.
39. CCME, Canadian environmental quality guidelines, Canadian Council of Ministers of the Environment', Winnipeg, 1999.
40. EPA (Environmental Protection Agency, United State), National Recommended Water Quality Criteria, Office of Science and Technology, Washington, DC, 2004.
41. Vialle, C., C. Sablayrolles, M. Lovera, S. Jacob, M.C. Huau and M. Montréjaud-Vignoles, 2011. Monitoring of water quality from roof runoff: Interpretation using multivariate analysis. Water Research, 45(12): 3765-3775.
42. Singh, K.P., A. Malik, S. Sinha, V.K. Singh and R.C. Murthy, 2005. Estimation of source of heavy metal contamination in sediments of Gomti River (India) using principal component analysis. Water, Air and Soil Pollution, 166(1-4): 321-341.
43. Shen, Z., Q. Zhang, C. Yue, J. ZHAO, Z. HU, N. LV and Y. TANG, 2006. The spatial pattern of land use/land cover in the water supplying area of the Middle-Route of the South-to-North Water Diversion (MR-SNWD) Project. Acta Geographica Sinica, 6: 009.
44. Liu, C.W., K.H. Lin and Y.M. Kuo, 2003. Application of factor analysis in the assessment of groundwater quality in a blackfoot disease area in Taiwan. Science of the Total Environment, 313(1): 77-89.
45. Goonetilleke, A., E. Thomas, S. Ginn and D. Gilbert, 2005. Understanding the role of land use in urban stormwater quality management. Journal of Environmental Management, 74(1): 31-42.
46. Vega, M., R. Pardo, E. Barrado and L. Debán, 1998. Assessment of seasonal and polluting effects on the quality of river water by exploratory data analysis. Water Research, 32(12): 3581-3592.
47. Bolstad, P.V. and W.T. Swank, 1997. Cumulative impacts of landuse on water quality in a southern appalachian watershed1. JAWRA Journal of the American Water Resources Association, 33(3): 519-533.
48. Frenzel, S.A. and C.S. Couvillion, 2002. Fecal-indicator bacteria in streams along gradient of residential development. Journal of the American Water Resources Association, 38: 265-273.
49. Bai, V., R. Bouwmeester and S. Mohan, 2009. Fuzzy Logic Water Quality Index and Importance of Water Quality Parameters. Air, Soil & Water Research, 2: 51-59.
50. Štambuk-Giljanoviæ, N., 1999. Water quality evaluation by index in Dalmatia. Water Research, 33(16): 3423-3440.

Persian Abstract

DOI: 10.5829/idosi.ijee.2014.05.02.04

چکیده

در این تحقیق، بررسی و تعیین کیفیت آب و منبع آلودگی رودخانه سمنیه با استفاده از روش‌های آماری و شاخص کیفیت آب (WQI) صورت گرفته است دما، pH، اکسیژن محلول (DO)، هدایت، کل مواد جامد محلول (TDS)، سولفات (SO_4^{-2})، نیترات (NO_3)، نیتریت (NO_2)، فسفر (PO_4^{-3})، کدورت، نیتروژن آمونیاک (NH_3-N)، کل مواد جامد معلق (TSS)، اکسیژن مورد نیاز شیمیایی (COD)، اکسیژن مورد نیاز بیولوژیکی (BOD)، سختی کل (TH)، روغن و گریس (G & O)، اشریشیا کلی و کلی فرم کل (TC) به عنوان متغیر کیفیت آب؛ کادمیم، مس، نیکل، روی، آهن، سرب، منگنز، کروم و جیوه به عنوان متغیرهای فلزات سنگین در آب، در طی سال ۲۰۱۲ از ۸ ایستگاه در امتداد رودخانه سمنیه، نمونه برداری و تجزیه و تحلیل شده است. تجزیه و تحلیل خوشه ای ۸ ایستگاه بر اساس شباهت در مشخصه های کیفیت آب به سه گروه تقسیم شده و به منظور تعیین ارتباط بین متغیرها و منابع احتمالی آنها ۲۷ متغیر در چهار گروه مورد تجزیه و تحلیل قرار گرفته است. به علاوه شاخص کیفیت آب رودخانه را به تمیز (دسته ۱) در ایستگاه ۱، کاملا آلوده (دسته ۲) در ایستگاه‌های ۲ و ۳، و آلودگی متوسط (دسته ۳) در ایستگاه‌های ۴ تا ۸ تقسیم گردید. البته رودخانه در انتها به گروه ۳ منتهی می‌شود که نیاز به تصفیه کامل برای استفاده‌های شهری را دارد. این مطالعات لزوم استفاده از روش‌های آماری چند متغیره و شاخص‌های کیفیت آب برای تفسیر بهتر از داده‌های پیچیده جهت آنالیز متغیرهای کیفیت آب را مشخص می نماید.

Iranica Journal of Energy & Environment 5 (2): 146-151, 2014
ISSN 2079-2115
IJEE an Official Peer Reviewed Journal of Babol Noshirvani University of Technology
DOI: 10.5829/idosi.ijee.2014.05.02.05

BUT

Predictive Statistical Model for Indoor Manganese Airborne Particles Affected by Psychrometric Parameters

Seyedtaghi Mirmohammadi

Department of Occupational Health, Faculty of Health, Mazandaran University of Medical SciencesSari, Iran

Received: May 2, 2014; **Accepted** in Revised Form: June 11, 2014

Abstract: Commonly, there are varieties of indoor airborne particles in the foundry factories. One of the main particle with emphasize on health effect on exposed human is manganese airborne particle. The current study considered correlation between indoor psychrometric parameters and manganese concentration in the workplace. Overall, fifty samples were collected by filter based on OSHA ID-121 method in the workplaces. SPSS V.20 was used to find a predictive model using linear regression model. The mean personal exposure to manganese was 1.626 mg/m^3. The mean measured psychrometric parameters for dry temperature, relative humidity and air velocity were 29°C, 52% and 1.2m/s, respectively. The correlations between personal exposures and indoor air parameters measurements showed a high significant relationship between personal exposure, dry temperature and wind speed in the factory ($P< 0.05$). This study concluded that controlling dry temperature and air velocity is the main effective parameters on airborne manganese concentration in the workplaces and decreased the personal exposure.

Key words: Manganese · Exposure · Dry temperature · Humidity · Foundry

INTRODUCTION

The melting process involves foundry, crushing and grinding of molding materials generates particulate matters (PM) and dust in the workplaces. The process at high temperature and inside the factories helps to generate variety of dust in hot workplaces. The polishing and finishing process, using sandblasting and drilling that are both environmentally pollutants for personals and factories. Particulate matters are relatively plentiful and variable component of the indoor atmosphere in the foundry factories. It is produced and emitted naturally to the atmosphere in the melting decomposition, combustion, and finishing process [1, 2]. One of the main element as airborne particulate matter in ferrous foundries is manganese particle, the workers are exposed to manganese (Mn) in the workplaces from both naturally occurring processes and processing activities. In such factories sources of Mn include furnaces, melting process, cars, lift trucks, sanding and combustion. Because of their small particle size, it tends to remain and suspending in the air for long periods of time (weeks or months). Usually, the health effects of Manganese (Mn) airborne particles are likely to depend on several parameters, including the ingredient of melting materials, duration of and level of exposure, size of the particles, and individual characterization of the exposed subject. Manganese is a necessary element, which is essential in small quantities but in higher doses might be a neurotoxic matter. High exposure to airborne manganese may lead to accumulation of the compound in the basal ganglia of the brain [3, 4], where it may create toxic condition [5]. Researchers reported that the neurological disorder of manganese (`manganism') that bears many similarities to Parkinson's disease [6, 7]. To prevent of related disease early indicators of the clinical effects and sensitive parameters of manganese exposure are needed. A time weighted average exposure for manganese airborne particulate concentration is about 1 mg/m^3 in workplaces. The manganese preclinical adverse effects have been observed to cause in the central nervous systems in workers exposed for less than 20

Correponding Author: Seyedtaghi Mirmohammadi, Department of Occupational Health, Faculty of Health, Mazandaran University of Medical SciencesSari, Iran. E-mail: t.mirmohammadi@mazums.ac.ir

Please cite this article as: Mirmohammadi, S., 2014. Predictive statistical model for indoor manganese airborne particles affected by psychrometric parameters. Iranica Journal of Energy and Environment, 5(2):146-151.

years [8, 9]. Studies have revealed basis subclinical intoxication which has been observed in manganese exposed workers with moderate (1±4 lg/l) increases in B-Mn [10, 11]. The foundry furnace-men are potentially exposed to manganese pollution during melting, weighting, transportation of recycled manganese-alloyed iron scrap from storehouse to furnace as well as manganese fumes exposure from the furnaces, especially during melting in the foundry workplace. The non-furnace workers may be potentially exposed to manganese during the handling of manganese-alloyed iron and preparing of the production and maintenance. There is a need to find personal exposure with manganese particles in foundry factory based on local psychrometric condition; it may improve our understanding of what humans are actually exposed to and how to reduce this exposure. The indoor air study assess factory pollutant problems can effect on human health with variety study models such as regression model or multiple model for pollution estimation with emphasis on particle matter in the workplaces. Similarly, the regression model was used before by other researchers in terms of pollution predictive model [12-16]. In the workplaces some raw material used in the production process such as cement factory the generation of particulate is predictable and they pass to the atmosphere through the exhaust. In the process activity of cement industry suspended particulate matter is inborn. For instance, the process activity of cement production generates pollutants such as suspended particulate matter, CO_X and NO_X [17-19]. The objective of this research is to find correlation between Mn pollution and psychrometric parameters such as dry bulb temperature (Td), relative humidity (RH), air velocity (or wind speed) and altitude in the foundry factory.

MATERIALS AND METHODS

Fifty workstations (in furnace, melting, molding, blasting, drilling, finishing and transporting task) were chosen for the air sampling during a working shift in the current study. Sampling, data collection and results documentation were conducted in accordance with the National Institute for Occupational Safety and Health guidelines and Standards.

Study Design: The study was conducted in Iran. Based on the study objectives, the indoor manganese particles (Mn) concentration was measured during a working shift in the foundry factory.

Sampling and Analytical Method: The measurement of Mn in ambient air was performed in the selected workstations in the factory. The air-Mn concentrations in the collected samples were determined by stationary samplers. The SKC samplers equipped with cellulose mixed-esters filters (filter diameter 37 mm, pore size 0.80 µm) at a low flow rate of 2 L/min over period of 2 h. The sampler distance from the smelting department was 2 m, and for other stations the sampler was placed from 2 to 3m from the furnaces. In the iron scrap recycling plant, the samplers were fixed next to the workers station. The analytical determination of manganese on the filters was performed by atomic absorption spectrometry.

Manganese concentration was measured by graphite furnace-atomic absorption spectrometry (GF-AAS). The cellulose ester filters were suspended in 2 ml of 35% hydrochloric acid and 65% nitric acid (40:60 v/v) and tempered at 90°C for 60 min. The samples were injected into a 4100-Z-AAS spectrometer (Perkin Elmer, UÈ berlingen, Germany) (wavelength 279.5 nm, lamp current 20 mA, gap 0.2 nm, 10 ll matrix modi®er) after another 24 h at room temperature. Interferences from the matrix were minimized by the use of the Zeeman-effect background compensation and automated standard addition calibration. The detection limit for manganese in air was 2 ng/m^3 under the conditions of the above-described sampling procedure. The dry thermometer and Asman hygrometer was used to measure dry bulb temperature and relative humidity. SPSS V.20 was used for statistical analysis for current study result.

RESULTS

Lots of fifty air samples were collected by stationary sampling method from workplace. The study sampling area included all production and supervisory workstations assigned to the melting process line. The study workstations also included maintenance employees working in the workplaces. Sampling zones were selected at random from within the corresponding frequency categories, because there were many workstations which workers working in the factory.

Indoor Air Sampling and Psychrometric Parameters Measurement: The analysis of the data from Table 1 shows, Mn concentration in the factory ranged from 0.25 to 3.61 mg/m^3; the average value for Mn pollutant concentration was 1.626 mg/m^3; relative humidity ranged from 41 to 56 %; the mean relative humidity was 52 %; dry bulb temperature ranged from 22 to 27°C and the mean dry

Table 1: Mean of indoor air variables in the foundry factories

Variables		Results
Mn, concentration (mg/m^3)	Max	3.61
	Min	0.25
	Mean	1.626
Relative Humidity, (%)	Max	56
	Min	41
	Mean	52
Dry bulb temperature, (°C)	Max	27
	Min	22
	Mean	24
Air velocity, (m/s)	Max	1.5
	Min	0.9
	Mean	1.2

NIOSH permissible exposure limit for Mn: 1 mg/m^3
OEL in Iran, 0.2 mg/m^3

Table 2: Regression correlation summary of Mn particulate matters

Model	R	r^2	Adjusted r^2	SE of the Estimate
	0.964	0.982	0.982	1.352

Predictors: (Constant), Relative humidity (%), Dry bulb temperature (°C), Air velocity (m/s), Altitude (m)

Table 3: Coefficients of regression correlation for Mn particle pollution and indoor psychrometric parameters

	Coefficients			
			t	
Model	B	SE	7.707	P value.
(Constant)	11.355	3.274	3.469	0.001
Relative humidity (%)	1.35	0.06	22.564	0.0001
Dry bulb temperature (centigrade)	0.218	0.088	2.481	0.014
Air velocity (m/s)	1.121	0.07	18.243	0.92
Altitude (m)	0.89	0.051	-8.107	0.713

Dependent Variable: Mn concentration (mg/m^3)

Table 4: Regression correlation test for Mn and indoor psychrometric parameters

Model	Sum of Squares	F	P value
Regression	20098.31	3457.655	< 0.0001(α)
Residual	428.687		
Total	20526.997		

(α) Predictors: (Constant), Relative humidity (%), Dry bulb temperature (°C), Air velocity (m/s), Altitude (m)
Dependent Variable: Mn Concentration (mg/m^3)

bulb temperature was 24°C. The indoor air velocity of the factory was between 0.9 to 1.5 m/s and altitude for the factory was 1700 m.

Table 1 shows the average of Mn concentration and other parameters in the factory. The mean Mn concentration was 1.626 mg/m^3 and this corresponds with mean relative humidity of 52%. Moreover, the result of Table 1 shows the mean Mn concentration is corresponds with mean dry bulb temperature of 24°C in the factory.

Table 2 showed that 98.2% of the Mn concentration can be attributed to any some or all of the independent variables (relative humidity, dry bulb temperature, air velocity and altitude) ($r^2 = 0.982$).

The correlation between psychrometric parameters (RH and Td) also air velocity and altitude and Mn concentration were studied to understand the behavior of indoor air Mn particulate matters with respect to indoor psychrometric parameters in the foundry factory. Linear regression analysis was used to assess the interactive behavior for Mn pollution and indoor air psychrometric parameters. The extracted factors for foundry factory showed that all of the evaluated parameters correlated with Mn concentrations are well defined in Table 3.

The multiple correlation coefficients (R) and the amount of variance (r^2,) are showed in Table 2. The following equation has been employed to stand for different parameters in order to measure the predictive regression correlation between psychrometric parameters and Mn concentration of this study. According to coefficients extracted from Table 3, indoor air velocity (1.121) and altitude (0.89) were no significant in the final regression model, therefore it can be ignored to include in the model.

Results of regression model test in Table 4 demonstrate that the independent variables are significant predictors of Mn pollution situation ($P< 0.05$) in the foundry factories.

The multiple correlation coefficients (R) and the correlation of model (r^2) are illustrated in Table 2. It implies that all of the predictors (indoor air velocity, relative humidity, dry bulb temperature and altitude change 98.2% dependent variables (Mn concentration) in the foundry workplaces.

DISCUSSION

The time weighted average (TWA) of the Mn concentration in the industries according to NIOSH standards for fine particulate matters in the factories should not exceed 1 mg/m^3 (NIOSH). Therefore, the concentration Mn in the foundry factory detected (expressed in milligram per cubic meter) in the factories is 1.626, when compared to NIOSH standard appear to be extremely high. The result of this present study was slightly high compared to that of the other factories in different countries [17, 18, 20].

While duration of work in the workplaces is important factor to determine of personal exposure to particles, it is supposed that health situation of subjects

were different exposure condition compared to the general population and the exposure results are similar to other research finding in the other country [21].

A high personal exposure was found for Mn in the workplaces among subjects and it shown that there are high level of contamination of Mn compared to NIOSH permissible exposure limit, but the result of the current study is not comparable with other study was conducted by researchers [22, 23].

The correlation between the average of indoor air variables and personal exposures to indoor dust such as Mn was not strong and a straight relationship have seen between Mn pollution and condition of indoor psychrometric parameters such as relative humidity and dry bulb temperature. This finding if comparable with other results was obtained by other researchers [12, 14, 22-25].

The positive relationship between temperature and Mn n concentration can be expected as it was reported in the literature with emphasis on dust exposure [12, 15, 24, 26] where an exponential increase of fine particulate matters emission rate during curing of melting process. It was observed that in the range of typical room temperatures, 20-30°C, there was only small effect on emission. However, at temperatures greater than 30°C, a clear increase in emission was noticed. The dry bulb temperatures within the factory ranged from 22 to 27°C. The linear relationship between temperature and Mn concentration is acceptable since the indoor temperatures were not greater than 30°C where exponential increase of Mn particulate emission could occur [12, 15].

As for the effects of relative humidity on fine particulate matters concentration, researchers observed that dispersion of dusts during working process are inversely proportional to the relative humidity of the environment. The electromagnetic properties of the particle-based components studied were found to be strongly influenced by the presence of water vapor during the curing process, as evidenced by the significant difference in the real relative permittivity of samples cured in different RH environments [16].

The obtained regression predictive model in the current study is adapted with other finding that was achieved by researchers [12, 18, 21]. They illustrated that determined pollution were compared to the predictions of the thermodynamic models GFEMN [21] in order to estimate the contribution of particulate matters to water absorption. A direct comparison with the obtained particulate matters model is possible for the GFEMN and AIM models [18] calculated the amount of aerosol bound water based on the measured relative humidity and the $PM_{2.5}$ aerosol concentrations.

Researchers [3, 12, 13, 15] previously used the regression techniques to correlate pollutants indicators as a function of psychrometric parameters and other factors relevant to factory, such as dry bulb temperature, relative humidity, dimension of factory and altitude of factory. The correlation between airborne fine particulate matters and psychrometric variables can be understood better by using multiple regression correlations. The general approach is to correlate Mn concentration with independent variables, which include psychrometric data.

In this study, the use of multiple regression models to examine exposure distributions that embraced the data on a wide range of indoor air has not been previously reported in the occupational hygiene literature.

CONCLUSION

The result of this study illustrated that, the average concentration of manganese particles in the foundry factories is more than 1.626 mg/m^3 for time weighted average, this value is higher than that time weighted average of NIOSH (1 mg/m^3), it implies that the factory was studied is polluted with Mn. The obtained predictive regression model of Mn for foundry factory based on psychrometric parameters in this study shows that the relative humidity and dry bulb temperature are the main factors influenced on Mn concentration in the workplaces.

REFERENCES

1. Cheng, Y.H., 2008. Comparison of the TSI model 8520 and Grimm Series 1.108 portable aerosol instruments used to monitor particulate matter in an iron foundry. Journal of Occupational and Environmental Hygiene, 5(3): 157-168.
2. Meléndez, A., E. García, P. Carnicer, E. Pena, M. Larrión, J.A. Legarreta and C. Gutiérrez-Cañas, 2010. Fine and Ultrafine Emission Dynamics from a Ferrous Foundry Cupola Furnace. Journal of the Air and Waste Management Association, 60(5): 556-567.
3. Ansari, A.S. and S.N. Pandis, 2000. Water absorption by secondary organic aerosol and its effect an inorganic aerosol behavior. Environment Science Technology, 34(1): 71-77.

4. Dastur, D.K., D.K. Manghani and K. Raghavendran, 1971. Distribution and fate of 54 Mn in the monkey: studies of different parts of the central nervous system and other organs. Journal of Clinical Investigation, 50(1): 9.
5. Krieger, D., S. Krieger, L. Theilmann, O. Jansen, P. Gass and H. Lichtnecker, 1995. Manganese and chronic hepatic encephalopathy. The Lancet, 346(8970): 270-274.
6. Aschner, M. and J.L. Aschner, 1991. Manganese neurotoxicity: cellular effects and blood-brain barrier transport. Neuroscience and Biobehavioral Reviews, 15(3): 333-340.
7. Barbeau, A., 1984. Manganese and extrapyramidal disorders (a critical review and tribute to Dr. George C. Cotzias). Neurotoxicology, 5(1): 13-36.
8. Calne, D., N. Chu, C.M. Huang, C. Lu and W. Olanow, 1994. Manganism and idiopathic parkinsonism: similarities and differences. Neurology, 44(9): 1583-1586.
9. Grufferman, S., 1999. Complexity and the Hawthorne effect in community trials. Epidemiology (Cambridge, Mass.), 10(3): 209.
10. Lucchini, R., E. Bergamaschi, A. Smargiassi, D. Festa and P. Apostoli, 1997. Motor function, olfactory threshold and hematological indices in manganese-exposed ferroalloy workers. Environmental Research, 73(1): 175-180.
11. Mergler, D. and M. Baldwin, 1997. Early manifestations of manganese neurotoxicity in humans: an update. Environmental Research, 73(1): 92-100.
12. Mirmohammadi, M., M. Hakimi, A. Ahamd, O. Kader, M. Mohammadian and S. Mirashrafi, 2010. Evaluation of Indoor Air Pollution of Polyurethane Industries with Emphasis on Exposure with Methylene Diphenyle Diisocyanate (MDI). Iranica Journal of Energy and Environment, 1(2): 100-105.
13. Mirmohammadi, M., M.H. Ibrahim, A. Ahmad, M.O.A. Kadir, M. Mohammadyan and S. Mirashrafi, 2010. Indoor air pollution evaluation with emphasize on HDI and biological assessment of HDA in the polyurethane factories. Environmental monitoring and assessment, 165(1-4): 341-347.
14. Mirmohammadi, S., 2013. Indoor Air Quality Assessment with Emphasis on Flour Dust: A Cross-Sectional Study of a Random Sample from Iranian Bakeries Workers. Iranica Journal of Energy and Environment, 4(2): 150-154.
15. Mirmohammadi, S., S.E. Nejad, M. Ibrahim and J. Saraji, 2011. Relationships Between Indoor Air Pollution and Psychrometric and Effective Factors in the Polyurethane Factories with Emphasis on Methylene Diphenyl Diisocyanate. Iranica Journal of Energy and Environment, 2(4): 366-373.
16. Roels, H., P. Ghyselen, J.P. Buchet, E. Ceulemans and R. Lauwerys, 1992. Assessment of the permissible exposure level to manganese in workers exposed to manganese dioxide dust. British Journal of Industrial Medicine, 49(1): 25-34.
17. Clegg, S.L., J.H. Seinfeld and P. Brimblecombe, 2001. Thermodynamic modelling of aqueous aerosols containing electrolytes and dissolved organic compounds. Journal of Aerosol Science, 32(6): 713-738.
18. Demokritou, P., I.G. Kavouras, S.T. Ferguson and P. Koutrakis, 2001. Development and laboratory performance evaluation of a personal multipollutant sampler for simultaneous measurements of particulate and gaseous pollutants. Aerosol Science and Technology, 35(3): 741-752.
19. Mirmohammadi, S., M.H. Ibrahim and G. Saraji, 2009. Evaluation of Hexamethylene Diisocyanate as an Indoor Air Pollutant and Biological Assessment of Hexamethylene Diamine in the Polyurethane Factories. Indian Journal of Occupational and Environmental Medicine, 13(1): 38-42.
20. Subramanian, R., A.Y. Khlystov, J.C. Cabada and A.L. Robinson, 2004. Positive and negative artifacts in particulate organic carbon measurements with denuded and undenuded sampler configurations special issue of aerosol science and technology on findings from the fine particulate matter supersites program. Aerosol Science and Technology, 38(S1): 27-48.
21. Cabada, J.C., A. Khlystov, A.E. Wittig, C. Pilinis and S.N. Pandis, 2004. Light scattering by fine particles during the Pittsburgh Air Quality Study: Measurements and modeling. Journal of Geophysical Research: Atmospheres, (1984–2012), 109(D16).
22. Ellingsen, D.G., E. Zibarev, Z. Kusraeva, B. Berlinger, M. Chashchin, R. Bast-Pettersen, V. Chashchin and Y. Thomassen, 2013. The bioavailability of manganese in welders in relation to its solubility in welding fumes. Environmental Science: Processes and Impacts, 15(2): 357-365.

23. Sparer, J., M.H. Stowe, D. Bello, Y. Liu, R.J. Gore, F. Youngs, M.R. Cullen, C.A. Redlich and S.R. Woskie, 2004. Isocyanate exposures in autobody shop work: the SPRAY study. Journal of Occupational and Environmental Hygiene, 1(9): 570-581.
24. Baker, M.G., C.D. Simpson, B. Stover, L. Sheppard, H. Checkoway, B.A. Racette and N.S. Seixas, 2013. Blood manganese as an exposure biomarker: State of the evidence. Journal of Occupational and Environmental Hygiene, 11(4).
25. Martín-Cameαn, A., I. Molina-Villalba, A. Jos, A. Iglesias-Linares, E. Solano, A.M. Cameαn and F. Gil, 2014. Biomonitorization of chromium, copper, iron, manganese and nickel in scalp hair from orthodontic patients by atomic absorption spectrometry. Environmental Toxicology and Pharmacology, 37(2): 759-771.
26. Lohani, S.P., 2011. Biomass as a Source of Household Energy and Indoor Air Pollution in Nepal. Iranica J. Energy Environ, 2(1): 74-78.

Persian Abstract

DOI: 10.5829/idosi.ijee.2014.05.02.05

چکیده

معمولا, انواع مختلفی از ذرات معلق در هوا داخل کارخانه ریخته گری وجود دارد. یکی از ذرات مهم با تاکید بر اثر آن بر سلامتی افراد در معرض تماس با ذرات معلق حاوی منگنز است. مطالعه حاضر ارتباط بین پارامترهای شرایط جوی محیط کار را با غلظت ذرات منگنز در محوطه کار را مورد بررسی قرار داده است. در مجموع، پنجاه نمونه هوا توسط فیلتر و با استفاده از روش استاندارد OSHA ID-121 در محیط کار مورد نظر جمع آوری گردید. برای مشخص نمودن یک مدل آماری از نرم افزار SPSS V.20 و از مدل رگرسیون خطی استفاده گردید. میانگین غلظت تماس با ذرات منگنز برابر ۱/۶۲۶ mg/m^3 بوده است. میانگین پارامترهای شرایط جوی مانند دمای خشک، رطوبت نسبی و سرعت جریان هوا به ترتیب ۲۹ °C، ۵۲٪ و ۱/۲ m/s به دست آمده است. نتایج همبستگی ما بین تماس شغلی با آلودگی و پارامترهای شرایط جوی محیط کار یک رابطه معنی دار موثری را بین تماس شغلی با آلودگی و دمای خشک و سرعت جریان هوا در کارخانه نشان داده است ($P<0.05$). با استفاده از نتایج بدست آمده، با کنترل دمای خشک و سرعت جریان هوا بعنوان پارامترهای اصلی موثر بر میزان غلظت ذرات منگنز انتشار یافته در کارخانه می توان میزان تماس شغلی با این آلاینده را کاهش داد.

Iranica Journal of Energy & Environment 5 (2): 152-159, 2014
ISSN 2079-2115
IJEE an Official Peer Reviewed Journal of Babol Noshirvani University of Technology
DOI: 10.5829/idosi.ijee.2014.05.02.06

BUT

Surface Modification of Carbon Nanotubes Using Acid Treatment to Enhance Gas Separation Performance of Hybrid Nanocomposite Mixed Matrix Membrane

T.D. Kusworo and B. Budiyono

Department of Chemical Engineering, Faculty of Engineering University of Diponegoro, Jl. Prof. Sudharto Tembalang, Semarang, Indonesia

Received: March 5, 2014; **Accepted** in Revised Form: April 28, 2014

Abstract: Recently, many researchers have explored the idea of hybrid mixed matrix membranes. Membrane separation processes based on hybrid mixed matrix membrane comprising inorganic material such as zeolite and carbon nanotubes (CNTs) embedded in polymer matrix have become one of the emerging technologies and extensively discussed in membrane separation literature. The present study is performed primarily to investigate the effect of chemical modification on carbon nanotubes surface towards gas separation performance of mixed matrix membrane. Polyethersulfone (PES)-carbon nanotubes mixed matrix membrane for modified and unmodified carbon nanotubes were casted using dry/wet phase inversion technique. The modified carbon nanotubes were prepared by treating the carbon nanotubes with acid treatment to allow PES chains to be attached to carbon nanotubes surface. The results of FESEM, DSC and FTIR analysis confirmed that chemical modification on carbon nanotubes surface had taken place. Meanwhile, the nanogaps in the interface of polymer and carbon nanotubes were appeared in the PES mixed matrix membrane with unmodified of carbon nanotubes. The modified carbon nanotubes mixed matrix membrane increases the mechanical properties, the productivity and purity of gas mixture compare to neat PES and unmodified carbon nanotubes mixed matrix membrane. For PES-modified carbon nanotubes mixed matrix membrane the maximum selectivity achieved for CO_2/CH_4 are 32.59.

Key words: Mixed matrix membrane · Carbon nanotubes · Biogas · Gas separation

INTRODUCTION

In petrochemical industries, varieties of processes are being used for the removal of carbon dioxide (CO_2) and hidrogen sulfide (H_2S) from natural gas. Several basic mechanisms are involved to achieve selective separation of gas constituents. These may include physical or chemical absorption, adsorption on a solid surface, membrane separation, cryogenic separation and chemical conversion. However, membrane separation processes have emerged during the last two decades. This is due to the fact that membrane separation processes may offer more capital and energy efficiency when compared to the conventional separation processes [1-3]. In addition, advantage of membrane technology is its simplicity, *i.e.* no absorbent, which has to be regenerated; it can be easily retrofitted, modularized and scaled-up for several applications [4].

At the present, polymeric membranes dominate the membrane separation field due to the fact that they are well developed and quite competitive in separation performance and economics. Since the separation of gas mixtures depends on the relative solubility and difusivities of individual components within a particular membrane, no single material will be dictated by the nature of gas mixture to be separated. Glassy polymers such as polysulfone, polyethersulfone (PES) polyimide and ethyl cellulose which are known to have high mechanical stability and desirable inherent transport properties at high temperature are more commonly used [2].

Corresponding Author: T.D. Kusworo, Department of Chemical Engineering, Faculty of Engineering University of Diponegoro, Jl. Prof. Sudharto Tembalang, Semarang, Indonesia. Tel.:+(62)247460058, Fax: +(62)2476480675. E-mail: tdkusworo@che.undip.ac.id

Please cite this article as: Kusworo, T.D. and B. Budiyono, 2014. Surface modification of carbon nanotubes using acid treatment to enhance gas separation performance of hybrid nanocomposite mixed matrix membrane. Iranica Journal of Energy and Environment, 5(2):152-159 .

Despite concentrated efforts to tailor polymer structure to affect separation properties; current polymeric membrane materials have seemingly reached a limit in the trade-off between productivity and selectivity. Pure polymer membranes are oftentimes shows several limitations as low selectivity, high temperature instability and swelling and decomposition in organic solvents. Hybrid membranes composed organic- inorganic has attracted attention as the future membrane material. The concept of hybrid membranes or mixed matrix membrane combines the advantages of high separation capabilities of the molecular sieves and the desirable mechanical properties and economical processing capabilities of polymers [3-5]. Mixed matrix composite membranes have received world-wide attention in the field of material science in the last 2 decades [2-5]. As the consequence, it has been proposed as an alternative approach to obtain the high selectivity benefits of molecular sieve materials (e.g. carbon molecular sieves (CMS), silica and zeolites) and to counter the costly processing of purely homogeneous molecular sieving membranes through incorporating these sieves into a process able polymeric matrix. Currently, significant efforts have been devoted in fabrication of mixed matrix membrane by using carbon nanotubes as great potential filler [5-6]. The properties of polymer nanocomposites containing carbon nanotubes depend on several factors in addition to the polymer: synthetic process used to produce nanotubes; nanotube purification process (if any); amount and type of impurities in the nanotubes; diameter, length and aspect ratio of the nanotubes objects in the composite (isolated, ropes and/or bundles); nanotubes orientation in the polymer matrix. Kim et al. [7] studied the effect of incorporating of CNTs on polyimidesiloxane matrix on gas separation performance. They observed that the addition of small CNTs to the copolymer matrix will be reducing the permeability helium and hindering the diffusion of nitrogen due to the impermeable properties of CNTs. As the applications for polymer-based organic–inorganic composites membranes expand, new challenges arise. One of these challenges is to synthesize both higher performance membranes that are more durable [8]. Therefore, it is important to overcome these challenges that prevents successful introduction of inorganic molecular sieve materials into an organic polymer matrix. Many studies have been attempted to improve the interaction between the polymer and molecular sieve in order to enhance the separation performance [9-11]. Currently, different approaches are reported to improve the dispersion of CNTs in solvent or polymers in order to fabricate the composite mixed matrix membrane. As a result, extensive research have promoted upon modification,pretreatment or functionalization of their surface. The surface modification has to improve solubility of the CNTs and their ability to mix well in most organic substance. Therefore, in the present study, the feasibility fabrication and characterization result of hybrid nanocomposite membrane using carbon nanotubes particles as selective inorganic fillers was investigated. The carbon nanotubes were functionalized using acid treatment technique. The aim is to get a CNTs linked with the coupling agent having a functional group such as a double bond which can be utilized further for copolymerization. Hence, this reaction product can be chemically explored for improving their compatibility with polymer matrix to increase the separation performance.

MATERIALS AND METHODS

Polyethersulfone was supplied by Solvay Advanced Material (USA). The polymers were dried in a vacuum oven at 120°C overnight before dope preparation; N-methyl-pyrrolidinone (NMP) from Merck was used as the solvent due to its low toxicity. The multiwalled carbon nanotubes (MWCNTs) were produced using thermal catalytic chemical vapour deposition (CCVD). The particle size of CNTs was about 25.76 nm. In this study, the polymer solution consists of 25 wt % polymer, 75 % NMP and 1 wt% carbon nanotubes in the total solid. Mixed matrix membranes were prepared according to the dry/wet phase inversion technique. The solution was poured on a clear, flat and smooth glass plate that was placed on the trolley. Stainless steel support casting knife was used to spread the solution to a uniform thickness by pneumatic force. Carbon nanotubes samples were additionally modified by acid treatment. First, the CNTs were treated with hydrochloric acid to remove the impurities. The mixtures of CNTs and hydrochloric acid were stirred using magnetic stirrer for 2 h, then diluted in water, filtered, washed with deionised water and then dried overnight in vacuum at 40°C. Finally, the CNTs were again dried and pre-treated in H_2SO_4 and it is stirred at least for four hours at 40°C. After that, the resulting dispersion was diluted in water and filtered. The resulting solid washed till to neutral pH and the sample was dried overnight in vacuum at 40°C before it was ready to be used in preparation of dope solution.

The membrane sheets were coated with highly permeable elastomeric silicone polymer (Sylgard 184 Dow Corning). The membrane coating was done after the uncoated membranes were tested. The intention of coating is to fill any surface pinholes or defects on membrane surface. Membranes were submerged in a 3% w/w solution of silicone in n-hexane for 24 hours and subsequently placed in oven for 3 days at 120°C to allow curing before permeation testing. A Supra 35 VP Field Emission Scanning Electron Microscopy (FESEM) was used to ensure the asymmetric structure. The glass transition temperature of each cast film was determined using differential scanning calorimetry (Mettler Toledo DSC 822e). A small piece of membrane or pure polymer sample was first stored under vacuum at 100°C for 24 hours to remove adsorbed water; then weighed and placed into aluminium DSC pans. The scanning range was 50- 320°C with scanning rate of 10°C min^{-1} in the first DSC cycle to remove thermal history and then cooled from 320 to 25°C at the rate of 10°C min^{-1}. Finally the second cycle was carried out with the same procedure.

The permeation test involved the use of gas permeation cell in which the membrane was placed on a sintered metal plate and pressurized at the feed side. Gas permeation rates were measured by a constant pressure system using a soap bubble flow meter. Pressure normalized gas permeation flux or permeance for gas *I,* $(P/l)_i$, in (GPU), can be calculated as follows:

$$\left(\frac{P}{l}\right)_i = \frac{Q_i}{A\Delta p} \tag{1}$$

where Q_i is the volumetric flow rate of gas *i*, Δp is pressure difference across membrane (cm Hg), *A* is membrane affective surface area (cm^2) and *l* is membrane skin thickness (cm). The ideal separation factor α_{ij} can be calculated by using equation below:

$$\alpha_{i/j} = \frac{(P/l)_j}{(P/l)_j} \tag{2}$$

RESULTS AND DISCUSSIONS

Morphology of Asymmetric Polyethersulfone-nanotubes Hybrid Nanocomposite Mixed Matrix Membranes: Primarily, in this study the effect of chemical modification on surface of carbon nanotubes using sulfuric acid for fabricated hybrid nanocomposite mixed matrix membranes were examined. In order to look their characterizations, Field Emission Scanning Electron Microscopy (FESEM) and Differential Scanning Calorimetric (DSC Testing) would be used. Therefore, characterization of the membranes will be discussed after this.

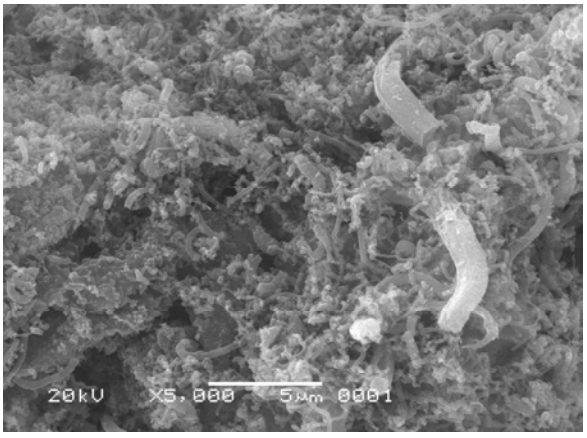

Fig. 1: Cross-sectional FESEM images of unmodified multi walled carbon nanotubes (MWNTs)

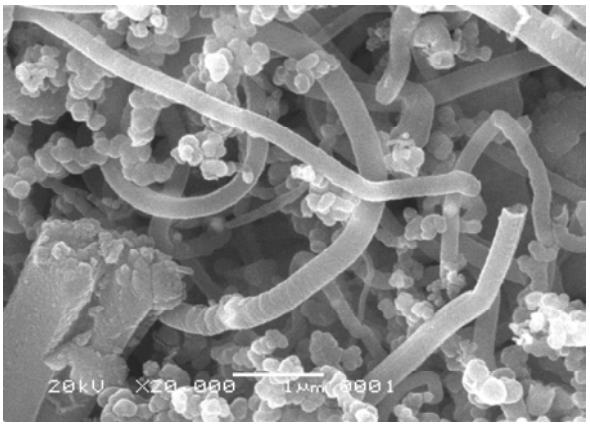

Fig. 2: Cross-sectional FESEM images of modified multi walled carbon nanotubes (MWNTs)

FESEM characterization was used in order to determine the qualitative analysis of hybrid nanocomposite mixed matrix membrane. In order to further investigate the dispersion of the functionalized MWNTs (multi walled carbon nanotubes) in hybrid nanocomposite mixed matrix membrane; careful FESEM inspections were carried out. Normally, natural or unmodified carbon nanotubes are very long tubes and flocks together as shown in the Figure 1. For the FESEM images of treated CNTs with 1 M sulfuric acid, the cross-sectional FESEM images showed a structure of treated CNTs. After CNTs be modified with sulfuric acid, the longer structure becomes shorter and the structure of treated multi walled carbon nanotubes are shown in the Figure 2.

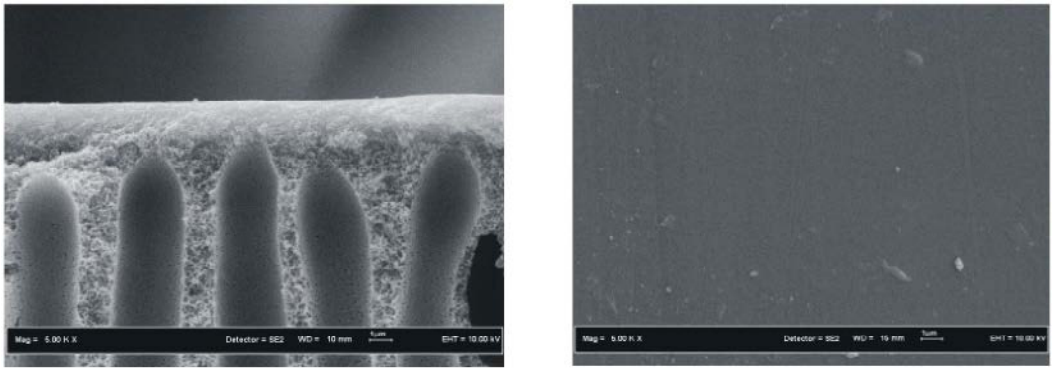

(a) (b)

Fig. 3: SEM picture of asymmetric polyethersulfone membrane at the: (a) cross section and (b) outer surface image layer.

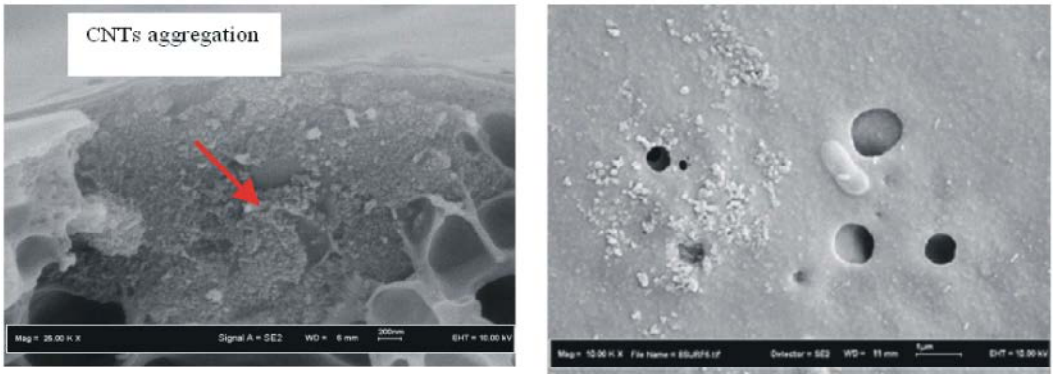

(a) (b)

Fig. 4: SEM picture of asymmetric polyethersulfone-unmodified CNTs membrane at the: (a) cross section and (b) outer surface image layer.

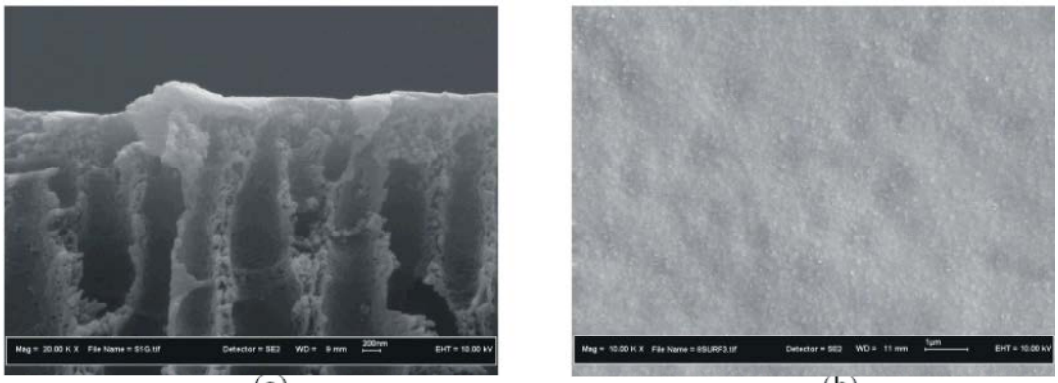

(a) (b)

Fig. 5: SEM picture of asymmetric polyethersulfone-modified CNTs membrane at the: (a) cross section and (b) outer surface image layer.

After functionalizing MWNT using sulfuric acid, the MWNTs were expected well distribute on the PES matrix. The functionalized MWNT using sulfuric acid made the carbon nanotubes having short length. Furthermore, it can be dispersed easily into polyethersulfone matrix [12-15]. Usually, carbon nanotubes are closely entangled and impurities of metal clusters originated from the catalyst stick on the surface of the ropes. These metal impurities on the tips of the ropes can block gas stream when these unpurified samples are used in the hybrid nanocomposite mixed matrix production. Samples in any part seem have to be well purified since most impurities

appear to be removed. However, these purified samples can be highly tangled with one another and are also quite long. In order to use carbon nanotubes in hybrid nanocomposite mixed matrix application, these nearly endless and highly tangled carbon ropes should be cut into short lengths of open tubes. After acid treatment using 1 M sulfuric acid in order to cut ropes, other parts which clearly showed that the length of each rope is now in the shorter lengths so that it could be easily dispersed into the polymer.

As shown in Figures 3-5, there were some differences between unmodified and modified carbon nanotubes. The FESEM micrographs of the cross-sectional and the surface of the neat PES, PES-unmodified nanotubes and PES-modified nanotubes mixed matrix membranes are shown in Figures 3-5. The structure of nanotubes composite membranes showing finger like structure which consisted of a dense skin layer supported by a spongy porous substructure. The unmodified carbon nanotubes particle seemed to good adhere with polymer matrix as shown in Figure 4. The smooth surface of the unmodified nanotubes-PES mixed matrix membrane might be due to the shape of the carbon nanotubes particles appeared to be oblong; therefore, no sharp edges that could easily perforated the active surface skin. However, in the case of unmodified carbon nanotubes, the unselective voids appeared indicated that the carbon nanotubes did not completely adhered on the surface of polymer matrix. The small surface ruptures and aggregation are also occurred on the mixed matrix membrane with unmodified carbon nanotubes as shown in Figures 4a and 4b. As demonstrated in Figures 5a and 5b, the CNTs dispersion into the polymer did not form any agglomeration. This phenomenon might be due to that the modified carbon nanotubes can be suspended and manipulated as individual macromolecules without entanglement in hybrid nanocomposite mixed matrix membrane fabrication. Previous study by Cong et al. [11] stated that the acid-SWNTs were dispersed much better than the unmodified SWNTs in the membranes such as mixed matrix membrane. The uniform nanocomposite membrane was formed and this evidence showed that, increasing loading of acid will disperse carbon nanotubes much better compared to unmodified CNTs and lower loading of acid.

The cross-section and surface of PES-modified CNTs using 1 M of sulfuric acid are shown in Figures 5a and 5b. The porous substrate of the fabricated membrane and the active skin layer can be observed in Figure 5. Cross-section of porous substrate region for PES modified CNT clearly show the compatibility between modified CNT loading with PES. Moreover, from the cross section can be seen that CNTs clearly act as the filler to in the PES polymer host. Due to the chemical and physical properties of sulfuric acid could be able to enhance the bond strength which provides a stable and strong bond between the modified CNT with PES matrix and finally reduced the presence of voids surrounded on CNT surface. Therefore, the good compatibility between polymer matrix and carbon nanotubes would finally lead to diminish gas penetrants via unselective voids of carbon nanotubes and simultaneously high gas separation performance of membrane is able to be achieved [7, 13-15]. The smooth surface of carbon nanotubes might also induce to enhance the adhesion between the nanotubes and the host of polymer.

Differential Scanning Calorymetry Analysis: The Differential Scanning Calorimetry has been done to indicate whether the CNT-PES blends were indeed miscible by observing the glass transition temperatures of the blend composition. The Tg for each membranes was determined from the heat flow versus temperature curve using an onset method. Table 1 shows the results of PES membrane, unmodified CNTs-PES membrane, PES-CNTs modified with 1 M sulfuric acid.

The influence of acid treatment modification on the glass transition temperature of PES-carbon nanotubes mixed matrix membranes are tabulated in Table 1. In the thermo-gravimetric and differential thermo-gravimetric results of pure and functionalized CNTs should reports on thermal degradation of MWNTs reveal that the on set of degradation starts at around certain temperature, which is attributed to the degradation of grapheme walls with complete degradation at around related temperature [11-12]. As summarized in Table 1, the glass transition value, the acid treatment of functionalized CNT have increased the glass transition temperature T_g. This can be seen in the effect of T_g for CNT modification with acid treatment. Increase in temperature leads to the condensation reaction between the adsorbed sulfuric acid and -OH groups present in the functionalized CNT surface and thereby eliminates water and methanol. The second and third transitions are attributed to the break down of hydrogen bonds and the bonds that present in grafted sulfuric acid leading to a major weight loss.

It can also be seen that compared to neat PES polymer, the T_g of the mixed matrix membranes increased about 3°C with the incorporating only 1 wt% modified carbon nanotubes using 1 M acid treatment into the

Table 1: Effect of acid treatment of CNTs on the glass transition temperature of PES-CNTs mixed matrix membrane

No	Membranes	Tg (°C)
1	PES	218.8
2	Unmodified CNTs	220.15
3	Modified CNTs with 1 M H_2SO_4	221.67

Table 2: Effect of sulfuric acid treatment on the gas separation performance of polyethersulfone-CNTs mixed matrix membranes at room temperature and 5 bars.

	Single gas permeance (GPU)		Selectivity
Membrane	CO_2	CH_4	CO_2/CH_4
Neat PES	20.36	0.70	28.75
Untreated membrane	25.18	1.96	12.84
Modified membrane	27.05	0.83	32.59

matrix. This phenomenon indicates that the mobility of polymer chains is reduced due to the restriction effect of carbon nanotubes. This result is in agreement with the previous study [13]. Based on Table 1, it can be concluded that the carbon nanotubes surface modification using acid treatment could induced the adherence between polymer matrix and carbon nanotubes particles. Therefore, it can be concluded that modified carbon nanotubes using chemical modification included into PES matrix makes the composite film stiffer and stronger due to strong interfacial interaction between the nanotubes and PES host matrix. Moreover, addition of the nanotubes the movement of polymer chain in polymer host matrix is restricted and this phenomenon likes physical cross-linking.

Gas Separation Performance of PES-Carbon Nanotubes Mixed Matrix Membrane: In gas separation performance, the criteria which is important in determining whether the membrane are classified as good or not was determined by the ability of the membrane to give the high enhancement in gas separation performance than others membrane. Thus, this testing was carried out in order to study the membrane effectiveness due to the effect of chemical modification on carbon nanotubes surface. The membrane effectiveness in the gas separation performance was determined by the membrane permeability and selectivity for tested CO_2 removal. In this study, we were used gas sample of CO_2 and CH_4. The gas permeation properties for each flat sheet carbon nanotubes mixed matrix membrane were measured by using variable pressure constant volume method. The permeability and selectivity for tested gases CO_2/CH_4 obtained are presented in Table 2. This table summarizes the permeability and selectivity data of neat PES, PES unmodified and PES-modified CNT.

Generally, the idea to put inorganic filler into organic polymer was enhanced gas permeability of polymer nanocomposites membranes was due to the disturbed polymer chain packing by the nanofillers. Therefore, the well dispersed and good adherence of carbon nanotubes will be effectively increased the gas permeability due to more effectively insert between polymer chains of the matrix. Addition of 1 wt% of modified carbon nanotubes loading to PES resulted in about 32.85 % increases in permeability of CO_2. The main pathways of gas transport through the mixed matrix membranes are through dense layer of PES matrix, highly selective carbon nanotubes and non-selective gaps or voids between the matrix and sieve particles. From FESEM data in Figures 5a and 5b, the carbon nanotubes are well dispersed in polymer matrix and serve as channels to transport gas molecules. The results are consistent with the previous study carried out by Chen and Sholl [16]. Moreover, the permeability for unmodified carbon nanotubes for all gases also increases compared to neat PES membrane. However, the CO_2/CH_4 selectivity was decreased for unmodified carbon nanotubes mixed matrix membrane. Therefore, the increase of permeability in the PES-unmodified carbon nanotubes was not due to the gas transportation inside the nanotubes. As shown in Figure 4, the PES- unmodified carbon nanotubes are not well distributed in polymer matrix and the severe unselective voids between carbon nano-particles and polymer matrix was appeared. Hence, the PES chains could not fall onto the carbon nanotubes walls tightly and forming a narrow gaps surrounding the carbon nanotubes. Therefore, gas molecules can easily passed through the unselective voids or the gaps. The unselective voids would be functioned as pinholes that allow all gases molecules pass rapidly without any selectivity. Thus, the permeability of all gases is increased thus reducing the gas selectivity. As results are summarized in Table 2, the acid treatment could modify carbon nanotubes filled PES polymer host mixed matrix membrane which can improved the CO_2/CH_4 selectivity.

CONCLUSION

In this study, hybrid mixed matrix membranes were produced using polyethersulfone (PES) as polymer matrix and carbon nanotubes as inorganic filler. The membrane performance was tested for CO_2 removal. The FESEM for the cross-sectional and surface area images of mixed

matrix membrane films indicated that the acid treatment can modify the surface of carbon nanotubes. Therefore, the carbon nanotubes was dispersed well in the polymer matrix. The surface ruptures are not occurred on the carbon nanotubes hybrid mixed matrix membrane might be due to the shape of carbon nanotubes appeared to be oblong. The smooth surface of carbon nanotubes might also help to enhance the adherence between the nanotubes and the host polymer. The PES-modified carbon nanotubes membranes had increased the permeability of carbon dioxide gas and the CO_2/CH_4 selectivity. The carbon nanotubes have been potentially as in organic filler for mixed matrix membrane for the future CO_2 removal membrane application i.e. biogas purification, natural gas and flue gas purification membrane.

REFERENCES

1. Lin, W.H. and T.S. Chung, 2001. Gas permeability, diffusivity, solubility and aging characteristics of 6FDA-durene polyimide membranes. Journal of Membrane Science, 186(2): 183-193.
2. Baker, R., Membrane technology and applications. 2004. England: John Wiley and Sons.
3. Hacarlioglu, P., L. Toppare and L. Yilmaz, 2003. Polycarbonate-polypyrrole mixed matrix gas separation membranes. Journal of membrane science, 225(1): 51-62.
4. Zimmerman, C.M., A. Singh and W.J. Koros, 1997. Tailoring mixed matrix composite membranes for gas separations. J. of Membrane Science, 137(1): 145-154.
5. Kusworo, T.D., A.F. Ismail, A. Mustafa and T. Matsuura, 2008. Dependence of membrane morphology and performance on preparation conditions: The shear rate effect in membrane casting. Separation and Purification Technology, 61(3): 249-257.
6. Khalili, S., A.A. Ghoreyshi and M. Jahanshahi, 2012. CO Separation from Syngas by Multiwall Carbon Nanotube 2. Iranica Journal of Energy & Environment, 3(1): 69-75.
7. Kim, S., T.W. Pechar and E. Marand, 2006. Poly (imide siloxane) and carbon nanotube mixed matrix membranes for gas separation. Desalination, 192(1): 330-339.
8. Ismail, A.F., T.D. Kusworo and A. Mustafa, 2008. Enhanced gas permeation performance of polyethersulfone mixed matrix hollow fiber membranes using novel Dynasylan Ameo silane agent. Journal of Membrane Science, 319(1): 306-312.
9. Li, Y., H.-M. Guan, T.S. Chung and S. Kulprathipanja, 2006. Effects of novel silane modification of zeolite surface on polymer chain rigidification and partial pore blockage in polyethersulfone (PES)-zeolite A mixed matrix membranes. Journal of membrane science, 275(1): 17-28.
10. Ziarani, G.M., A. Badiei, M. Azizi, P. Gholamzadeh and L. Seyedakbari, 2013. Application of Sulfonic Acid Functionalized Nanoporous Silica (SBA-Pr-SO H) in the Green Strecker Reaction under Solvent Free Condition. Reactions, 4(1): 1-7.
11. Jiang, L.Y., T.S. Chung and S. Kulprathipanja, 2006. An investigation to revitalize the separation performance of hollow fibers with a thin mixed matrix composite skin for gas separation. Journal of Membrane Science, 276(1): 113-125.
12. Cong, H., J. Zhang, M. Radosz and Y. Shen, 2007. Carbon nanotube composite membranes of brominated poly (2, 6-diphenyl-1, 4-phenylene oxide) for gas separation. Journal of Membrane Science, 294(1): 178-185.
13. Lau, A.K.T. and D. Hui, 2002. The revolutionary creation of new advanced materials-carbon nanotube composites. Composites Part B: Engineering, 33(4): 263-277.
14. Ma, P.C., J.K. Kim and B.Z. Tang, 2007. Effects of silane functionalization on the properties of carbon nanotube/epoxy nanocomposites. Composites Science and Technology, 67(14): 2965-2972.
15. Zhu, B.K., S.H. Xie, Z.K. Xu and Y.Y. Xu, 2006. Preparation and properties of the polyimide/multi-walled carbon nanotubes (MWNTs) nanocomposites. Composites Science and Technology, 66(3): 548-554.
16. Chen, H. and D.S. Sholl, 2006. Predictions of selectivity and flux for CH_4H_2 separations using single walled carbon nanotubes as membranes. Journal of Membrane Science, 269(1): 152-160.

Persian Abstract

DOI: 10.5829/idosi.ijee.2014.05.02.06

چکیده

اخیرا، بسیاری از پژوهشگران، استفاده از غشای ساختار مرکب را مورد بررسی قرار داده اند. فرآیندهای جداسازی بر اساس غشای ساختار مرکب، که متشکل از مواد معدنی مانند زئولیت و نانولوله های کربنی (CNTs) تعبیه شده درساختار شبکه پلیمر می باشد که یکی از فن آوری های نوین بوده و بطور گسترده در نشریات جداسازی غشایی مورد بحث قرار گرفته است. مقاله حاضر، به منظور بررسی اثر اصلاح شیمیایی در سطح نانولوله های کربنی، بر عملکرد جداسازی گاز، از غشای ساختار مرکب انجام شده است. غشای ساختار مرکب متشکل از نانولوله های کربنی پلی اترسولفون (PES)، با استفاده از روش واژگونی فاز خشک/ تر، برای نانولوله های کربنی اصلاح شده و اصلاح نشده، قالب گیری شد. نانولوله های کربنی اصلاح شده، با تیمار اسیدی، به منظور نشاندن زنجیره های PES، بر روی سطح نانولوله، بدست می آیند. نتایج حاصل از آنالیزهای FESEM، DSC و FTIR، نشان می‌دهد که تغییرات شیمیایی مورد نظر، بر روی سطح نانو لوله های کربنی، صورت گرفته است. همچنین، در حالتی که در غشای ساختار مرکب PES، از نانولوله کربنی اصلاح نشده استفاده شود، شکاف هایی در محدوده ابعاد نانو، در فصل مشترک پلیمر و نانولوله های کربنی، ظاهر می‌گردد. در غشای ساختار مرکب نانولوله های کربنی اصلاح شده، خواص مکانیکی، بهره وری و خلوص مخلوط گازی را نسبت به PES و غشای ساختار مرکب حاصل از نانولوله کربنی اصلاح نشده، بهبود یافته است.

Iranica Journal of Energy & Environment 5 (2): 160-166, 2014
ISSN 2079-2115
IJEE an Official Peer Reviewed Journal of Babol Noshirvani University of Technology
DOI: 10.5829/idosi.ijee.2014.05.02.07

BUT

Seasonal Variations and Sources of Heavy Metals in Free Fall Dust in an Industrial City of Western India

[1]Manju Meena, [1]Bharat Singh Meena, [1]Uttra Chandrawat and [2]Ashu Rani

[1]Department of Chemistry, Government College, Kota- 324001, Rajasthan, India
[2]Department of Pure and Applied Chemistry, University of Kota, Kota-324005, Rajasthan, India

Received: April 24, 2014; **Accepted** in Revised Form: June 11, 2014

Abstract: This study investigates seasonal variations in average concentrations of metals in free fall dust samples (350) collected at various sampling sites situated in five different zones of an industrial city Kota, India. Average concentrations of heavy metals (Cu, Cd, Zn and Pb) were higher in winter and lower in summer and reverse trend was observed for crustal metals (Fe, Ca and Mg). Overall, the order of average concentrations of heavy metals were Zn >Pb> Cu > Cd in both seasons.Seasonal differences in metal concentrationswere due to differences in wind direction, wind strength, temperature, relative humidity and anthropogenic activities at sampling sites. Enrichment factor and positive correlation between anthropogenic metal species such as Cu and Cd; Cu and Zn; Cu and Pb; Cd and Zn; Cd and Pb; Zn and Pb in both seasons indicate that their origin source iscommon i.e. coal combustion at thermal power station.

Key words: Free fall dust · Heavy metals · Wind direction · Enrichment coefficients · Thermal power station · Correlation coefficients

INTRODUCTION

Urbanization is a process which involves economic and industrial development and consequently population growth. This in turn leads to higher energy production and consumption, resulting in problems related to air pollution. As reported in previous studies [1,2], air pollution is a major problem in urban areas due to emissions from transportation and the interaction of air pollutants originating from a variety of sources and may have a significant effect on the environment. Emissions from the urban atmosphere which originate from anthropogenic activities such as the use of motor vehicles, open burning, coal burning and industrial emissions [3-5], are the major sources of air pollution in Kota city [6]. Nevertheless,airborne particles in the atmosphere have serious environmental impacts on climate [7, 8], biogeochemical cycling in ecosystems [9, 10], outside visibility [11] and health of living organisms [12, 13].

Over the last few decades, intensive monitoring programs of heavy metals in atmospheric precipitations have been carried out worldwide, which are mainly focused on the chemical characteristics, deposition fluxes and long-term temporal trends [14- 18].According to these studies, the loadings and sources of heavy metals in precipitation have great spatial variability over different locations, which is mainly caused by different meteorological conditions (prevailing wind directions and type, frequency and amount of precipitation) and the emission patterns of pollutants (emission sources, distance from emission sources and the sampling sites). Therefore, more in-depth studies, especially on the regional level, of trace metal pollution in the air are necessarily important for the assessment of impacts of heavy metals on ecosystems [19, 20]. Very few studies have reported the heavy metal load and health implications of particulate matter in Indian cities despite many citiesbeing densely populated and polluted [21].

Corresponding Author: Ashu Rani, Department of Pure and Applied Chemistry, University of Kota, Kota-324005, Rajasthan, India. Tel: +919352619059. E-mail: ashu.uok@gmail.com

Please cite this article as: Meena, M., B. Singh Meena, U. Chandrawat and A. Rani, 2014. Seasonal variations and sources of heavy metals in free fall dust in an industrial city of western India. Iranica Journal of Energy and Environment, 5(2):160-166.

City Kota has a Kota Super Thermal Power Station (KSTPS), a major coal based thermal power plant, where huge amount i.e. approximate 3000 metric tonne per day of fly ash (homogeneous mixture of several metal oxides viz. SiO_2, Al_2O_3, Fe_2O_3, CaO, MgO, CuO, CdO, MnO_2, NiO_2, ZnO, PbO etc.) is produced and released in the atmosphere. Several small and large scale industries including DCM Shriram Consolidated Limited (DSCL), Multimetals Limited, Samtel Glass Limited, Chambal Fertilizers and Chemicals Limited (CFCL), Shriram Fertilizers and Metal India, ShriramRayons and a number of Kota stone cutting polishing units further enhance the heavy metal burden of the city environment. Research studies related to atmospheric pollution in Kota city are scanty and mostly been restricted in the form of internal reports. Therefore, the present study was conducted, with the main objectives being: (1) to determine the composition offree fall atmospheric dust in terms of crustal (Fe, Ca and Mg) and anthropogenic (Cu, Cd, Zn and Pb) metals at various sampling sites located in five different zones covering entire Kota city area; (2) to identify possible sources of heavy metals associated with free fall atmospheric dust using enrichment factor and Pearson correlation coefficient; (3) to study the effect of climate on the concentration levels of heavy metals as a function of sampling sites, distance from KSTPS, seasons and meteorological parameters such as temperature, relative humidity, wind speed and wind direction.The study has indicated the influence of coal based thermal power plant and industrialization of the rapidly growing city on the concentration levels of heavy metals infree fall atmospheric dust.

Background of the Study Area: Kota is one of the major industrial cities of Rajasthan States in India. It is situated 25°11 N and 75°51 E on the eastern bank of river Chambal in the southern part of Rajasthan with an elevation of 271 meters (889 feet) abovethe sea level on the south- east of Aravali ranges. According to the 2011 census Kota district has a population of 19,50,491residents. The total geographical area of the district is 5,21,133 hectares as per land. Kota has a semi arid climate with temperature varying from minimum of 6°C in winter (January) to maximum 47°C in summer (June) and an average annual rainfall about 885.6 mm.The monsoon season follows with comparatively lower temperatures, but higher humidity and frequent, torrential downpours. The study of wind roses makes it possible to conclude that the predominate wind directions in the city during this study were north-east in winter (25.74%) and summer (15.31%). Many large and small scale industries are present due to availability of river water and power. Kota district is a power production centre of the country where coal based KSTPS is situated. A popular cost effective building stone i.e. Kota stone is being excavated, cut to various sizes and polished in more than 200 units generating huge amount of slurry waste containing mainly CaO, MgO and SiO_2.

MATERIALS AND METHODS

Sampling Sites: The sampling sites for atmospheric precipitation were chosen with the help of cartographic charts, field job and GPS (Global Positioning System). The choice of the sampling sites followed some criteria laid by ASTM D 5111 Standards [22]. These criteria were: I) distance from point source (approximately a radius of 12 km from KSTPS); ii) predominant wind direction; iii) the distance from obstacles that could interfere in sampling (twice the height of obstacles); and iv) logistics (security, access, electric power supply).The entire city area was divided into five zones (Figure 1). The location of the zones with respect to the point source KSTPS of emissions and possible source of heavy metal emission in them are presented in Table 1.

Sample Collection and Analysis: In total,350free fall dust samples (n = 1 zone x 10 samples x 7 months = 70 samples, so n= 5 zones x 10 sample x 7 months = 350 samples) were collected monthly in both summer (March, April and October) and winter (January, February, November and December) seasons during 2011-2012 at five zones (10sample per month). The sample size was estimated using the statistic formula, $n = (Z.SD/e)^2$, where Z is standard score, SD is standard deviation and e is half of the width of a 95% confidence interval on the mean [23]. The calculated number of samples was 346. Dust samples falling freely due to gravity were collected in all zones at a height of 6 m above the ground surface on plastic trays of 1 m^2 area. All free fall dust samples collected, here, represent only dry fall out, as there was no rain during the sampling period. After sampling, dry depositions were scraped off the trays and these trays were washed with milli-Q water to recover stuck particles. The water was evaporated slowly at 50 °c and the residue was mixed and homogenized with the scraped samples [24]. Then samples were digested for the analysis.

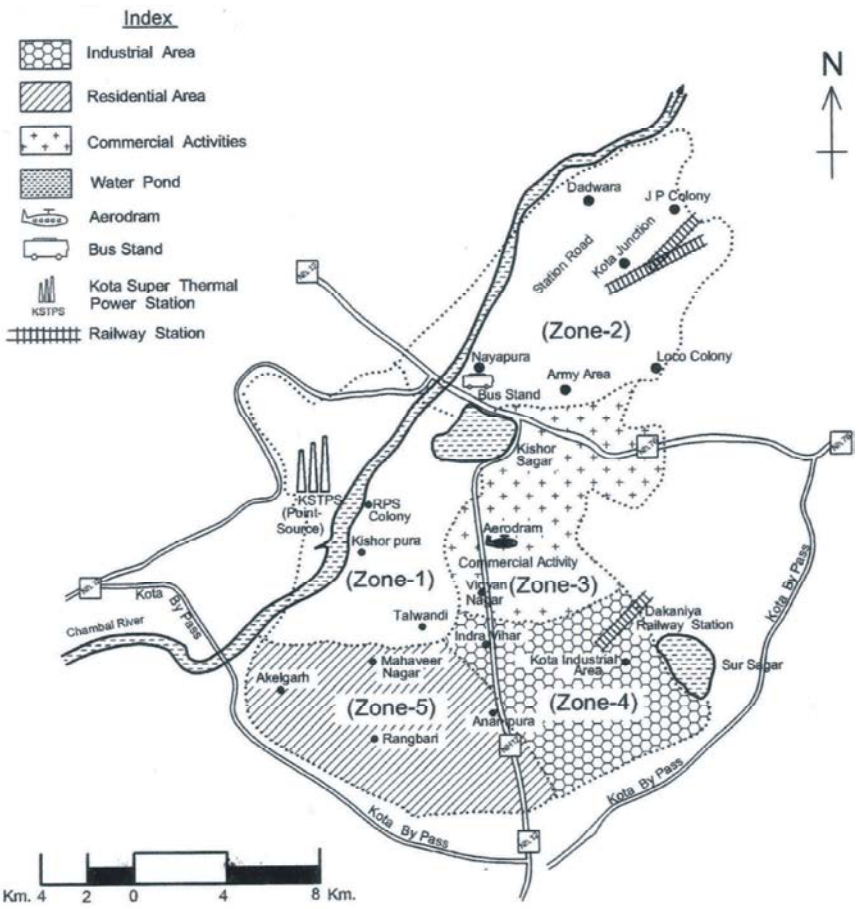

Fig. 1: Kota city map

Table 1: Location and characteristics of different zones of Kota city for present study

Zone No.	Location with reference to point source(KSTPS)	Characteristics
Zone 1	Within 2 Km. radii surrounding point source(KSTPS)	Coal dust from unloading coal; Un-burnt coal dust; Fly ash; Soil dust; High density population; High traffic load
Zone 2	2-10 Km. towards north-east direction from point source(KSTPS)	Fly ash; Soil dust; Moderate traffic dust; Railway station; Bus stand; M.B.S. hospital
Zone 3	2-7 Km. towards east direction from point source(KSTPS)	Fly ash; Soil dust; High traffic dust; Commercial activities; High population density
Zone 4	2-12 Km. towards east-south direction from point source(KSTPS)	Fly ash; Soil dust; High traffic dust; Establishment of industrial complex; High population density
Zone 5	2-8 Km. towards south direction from point source(KSTPS)	Fly ash; Soil dust; Residential area

For analysis, 1 gm of sample was placed in a covered beaker (to avoid the loss of Cd and Pb) containing a mixture of high purity HNO_3 (5 mL) and allowed to remain over night at ambient temperature. After slow evaporation to dryness, 2 mL of HNO_3 was added and the solution was extracted with 0.1 N HCl and diluted milli-Q water, filtered on pre-washed whatman filter paper no. 42 and diluted with 1% HNO_3 in a 50 mL polyethylene bottle [25].

The concentrations of 6 metals (Fe, Zn, Cu, Cd, Mg and Pb) were measured by Direct Air – Acetylene Flame method (Atomic Absorption Spectrophotometer - Shimadzu-6300) [26]. The Ca metal concentration was determined using Flame Photometer (Systronics -128) method. Certified standard solutions (CertiPUR* - MERCK) were used for calibrating the instruments.Blanks, quality control standards and stand reference materials

were inserted during the analytical measurement to detect contamination and drift. The elemental concentrations of the blanks were < 1 % of the mean analyte concentration for all metals and the precision (RSD) of the control standards and replicates were generally lower than 5%. The recovery rates for the metals in the standard material ranged from 96 to 99%. Detection limits were: 0.02 ppm for Fe; 0.005 ppm for Zn; 0.01 ppm for Cu; 0.002 ppm for Cd; 0.0005 ppm for Mg; 0.05 ppm for Pb; 0.06 ppm for Ca.

The results were summarized into a multi-elemental database using MS – Excel 2007.Analysis of variance (ANOVA) on all experimental data was performed with SPSS version 16 software.

RESULT AND DISCUSSION

Seasonal Variations of Heavy Metals Concentration: Theaverage concentrations of all the analyzed metals (Fe, Ca, Mg, Cu, Cd, Zn and Pb)of environmental concern in free fall dust collected at various sampling sites of five different zones in winter and summer seasons are given in Table 2. Average concentrations of Cd, Zn and Pb in all the studied zones are found to exceed WHO standard limits which might be due to coal combustion activity at point source KSTPS. We observe variations in the elemental concentration as a function of sampling sites, distance from sources of emissions and the wind velocity (speed and direction).

Among all the studied zones, zone 1 was found to have highest average concentrations of heavy metals i.e. Cu, Cd, Zn and Pb in bothseasons due to presence of coal based thermal power plant there while zone 5,which is a residential area,with least number of anthropogenic sources is found to have lowest concentrations of all the measured metal species in both seasons. North-east direction (21.01%) of wind blow from KSTPS encourages the worrying level of heavy metals in the study region present in fly ash. The relative abundances of these heavy metals in free fall dust samples follow the order Zn >Pb> Cu > Cd in all zones. Despite the use of lead free petrol, high concentration of Pb could be due to Pb particles in street dust accumulated from earlier vehicular exhaust for a long time due to its high residence time in environment [27].

Seasonal variation of the average concentrations of all the analysed metals were generally consistent from site to site; but were different depending on the metal species. In all the zones, concentrations of crustal metal species viz. Ca, Mg and Fe were lower in winter and higher in summer while heavy metal species viz. Cu, Cd, Zn and Pbconcentrations were higher in winter and lower in summer. The difference in concentration levels between the two seasons i.e. winter and summer can be explained by difference in meteorological conditions. During the sampling period in winter, Kota city had witnessed low average temperature (19.7 °C), high relative humidity (42.29%) and low wind speed (2 Km/h) leading to high levels of anthropogenic metal species in ambient air while summers had high average temperature (29.0 °C), low relative humidity (22.05%) and high average wind speed (4Km/h) causing decreased concentrations of anthropogenic metal species (Table 3).The high wind strength during summer is responsible for deflation or entrainment and transport of crustal metals as coarse

Table 2: Average concentrations (ppm) of analyzed metals in five zonesin winter and summer seasons of Kota cityin 350 free fall dust samples

			Average concentrations of metals in ppm				
Metal	WHO-2004 (ppm)	Season	Zone 1 (n=70)	Zone 2 (n=70)	Zone 3 (n=70)	Zone 4 (n=70)	Zone 5 (n=70)
Mg	30	Winter	11.6412	11.1502	12.5099	12.9228	13.5926
		Summer	12.8683	12.4835	14.0077	14.5591	15.2426
Ca	75	Winter	1238.38	1199.15	1452.10	1717.48	1866.11
		Summer	1627.14	1584.44	1885.23	2138.11	2320.64
Fe	0.3	Winter	68.1247	66.4600	73.6781	75.8754	78.1915
		Summer	77.4418	76.4287	81.9803	83.2715	87.1370
Cu	2.0	Winter	0.9959	0.7698	0.8422	0.7430	0.6618
		Summer	0.8961	0.5556	0.6942	0.5415	0.4501
Cd	0.003	Winter	0.1691	0.1093	0.1277	0.1039	0.0801
		Summer	0.0741	0.0552	0.0598	0.0523	0.0459
Zn	3.0	Winter	5.7631	4.5043	4.9548	4.3678	3.8493
		Summer	5.0828	3.7207	4.0352	3.4837	3.1151
Pb	0.01	Winter	3.2195	2.1639	2.6018	2.8155	1.2996
		Summer	2.5212	1.6974	1.8840	2.1298	1.0686

*n = No. Of samples

Table 3: meteorological conditions at the sampling zones during sampling periods

Meteorological parameter	Winter	Summer
Temperature (°C)	19.7 ± 3.7	29.0 ± 2.6
Humidity (RH) (%)	42.29 ± 5.4	22.05 ± 9.7
Wind speed (km/h)	2.0 ± 0.8	4.0 ± 1.0
Rain fall (mm)	9.0	0.0

Table 4: Correlation coefficients between concentrations values of analyzed metals in free fall dust in Kota city (*significant at 5% level)

Metal	Mg	Ca	Fe	Cu	Cd	Zn	Pb
Mg	1.000	0.496*	0.665*	-0.273	-0.150	-0.353	-0.346
Ca	0.563*	1.000	0.519*	-0.233	-0.370	-0.359	-0.385
Fe	0.483*	0.584*	1.000	-0.258	-0.146	-0.230	-0.398
Cu	-0.209	-0.236	-0.251	1.000	0.153	0.285*	0.259*
Cd	-0.399	-0.316	-0.288	0.442*	1.000	0.501*	0.369*
Zn	-0.278	-0.246	-0.270	0.300*	0.506*	1.000	0.542*
Pb	-0.333	-0.258	-0.395	0.472*	0.493*	0.596*	1.000

* Winter, n=200 and *Summer, n=150

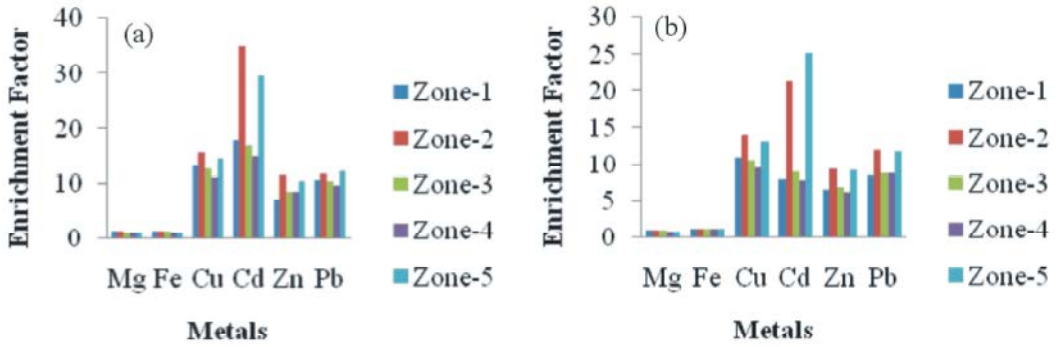

Fig. 2: Enrichment factors of metals in free fall dust at each zone in Kota city in(a) winterand (b) summerseasons

particles are influencedby gravity [28] whereas wind strength available to transport these metals drops significantly in the winter. Secondly,the stable and cold conditions during winter months favour the prolonged life of ambient particles in the atmosphere leading to elevated levels of heavy metals in free fall particulate matter.

The results obtained in the present study are in accordance with earlier studies done in India [29 - 30] and other countries [31 -32].

In winter and summer periods,the Pearson correlation coefficient (r) was calculated from the elemental concentration in order to predict the possibility of a common source (Table 4). Significant positive correlations found between Mg and Ca; Mg and Fe; Ca and Fe indicate that these metals have a common source, possibly natural soil. Similarly, significant positive correlation found between Cu and Cd; Cu and Zn; Cu and Pb; Cd and Zn; Cd and Pb; Zn and Pbin both seasons suggest their common origin i.e. point source KSTPS mainly beside other industrial activities.

Enrichment Factor: Calculation of enrichment factor (EF) helps to determine whether a certain element has an additional or anthropogenic source other thanits major or natural source. Calcium (Ca) has beenused as a reference element for an EF evaluation, assuming that the contribution from its anthropogenic sources to the atmosphere is negligible [33], this study used the EF calculation formula as follows:

$$EF = \frac{(X/C)\ \text{precipitation}}{(X/C)\ \text{reference material}}$$

Where x is the concentration of the ion of interest and *c* is the concentration of the reference ion.

Ifthe EF value approaches unity, then crustal sources are predominant while an EF > 5 indicates that a large fraction of the element can be attributed to non- crustal or anthropogenic sources [34]. Figure 2 shows the seasonal mean enrichment factors (EFs), based on average seasonal metal concentration of heavy metals identified in free fall dust collected from the five zones. EF values for Cd were the highest, followed by Cu, Pb and Zn and their EFs were much higher than 5. This indicates that the collected dust samples were extremely contaminated by

anthropogenic sources. Seasonal EF values of Cu, Cd, Zn and Pb metal species showed similar trends in both the seasons. The higher EF values of metals (Cu, Cd, Zn and Pb) during winter season than summer may be attributed to transport of fly ash from coal combustion activity from point source KSTPS and stable and cold meteorological conditions.

CONCLUSION

It is concluded that the concentrations of all anthropogenic metal species (Cu, Cd, Zn and Pb)were highest in zone 1, which is located within 2 Km radiifrom point source KSTPS while lowest in zone 5, mainly a residential area, located far away from thermal power plant and having comparatively low traffic load in both winter and summer seasons. Concentrations of anthropogenic metal species are found higher in winter and lower in summer while reverse trend is observed for crustal metal species.The high enrichment coefficients and positive correlations showed thatheavy metals viz. Cu, Cd, Zn and Pbhave similar origin source in the city and particularly can be related to point source coal based thermal power plant besides other industrial activities and traffic load.

In view of the warninglevel of heavy metals in the city environment there is an urgent need to maintain the receptive capacity of the atmosphere by adopting proper abatement procedures by industrial and mining sector for maintaining the healthy environment to breathe.

ACKNOWLEDGEMENTS

The authors are thankful to A. Mukhopadhyay and DST, New Delhi for instrumental support provided through DST – FIST project sanctioned toGovt. College, Kota and University Grants Commission, New Delhi for Minor Research Project sanctioned to ManjuMeena for this work.

REFERENCES

1. Fenger, J., 1999. Urban air quality. Atmospheric environment, 33(29): 4877-4900.
2. Cao, Z., Y. Yang, J. Lu and C. Zhang, 2011. Atmospheric particle characterization, distribution and deposition in Xi'an, Shaanxi Province, Central China. Environmental Pollution, 159(2): 577-584.
3. Ghadimi, F., M. Ghomi, M. Ranjbar and A. Hajati, 2013. Statistical Analysis of Heavy Metal Contamination in Urban Dusts of Arak, Iran. Iranica Journal of Energy and Environment, 4(4): 406-418.
4. Abdul-Wahab, S.A., 2006. Impact of fugitive dust emissions from cement plants on nearby communities. ecological modelling, 195(3): 338-348.
5. Xia, D., L. Yang, J. Ma, Y. Yu, G. Wang and F. Chen, 2007. Magnetic characteristics of dustfall in urban area of north China and its environmental significance. Science in China Series D: Earth Sciences, 50(11): 1724-1732.
6. Gujral, S., V. Sharma and A. Rani, 2001. Assessment of dispersion of ambient suspended particulate matter and meteorological conditions near Kota Thermal Power Station. Indian Journal of Environmental Protection, 21(3): 238-249.
7. Broecker, W., 2000. Abrupt climate change: causal constraints provided by the paleoclimate record. Earth-Science Reviews, 51(1): 137-154.
8. Prospero, J.M., P. Ginoux, O. Torres, S.E. Nicholson and T.E. Gill, 2002. Environmental characterization of global sources of atmospheric soil dust identified with the Nimbus 7 Total Ozone Mapping Spectrometer (TOMS) absorbing aerosol product. Reviews of geophysics, 40(1): 2-1-2-31.
9. Nriagu, J.O., 1988. A silent epidemic of environmental metal poisoning? Environmental pollution, 50(1): 139-161.
10. Nriagu, J.O. and J.M. Pacyna, 1988. Quantitative assessment of world wide contamination of air, water and soils by trace metals. Nature, 333(6169): 134-139.
11. Husar, R., J. Prospero and L. Stowe, 1997. Characterisation of tropospheric aerosols over the oceans using the NOAA advanced very high resolution radiometer optical thickness operational product. J. Geophys. Res., 102(16): 899-16.
12. Dockery, D.W., C.A. Pope, X. Xu, J.D. Spengler, J.H. Ware, M.E. Fay, B.G. Ferris Jr and F.E. Speizer, 1993. An association between air pollution and mortality in six US cities. New England journal of medicine, 329(24): 1753-1759.
13. Schwartz, J. and D.W. Dockery, 1992. Particulate air pollution and daily mortality in Steubenville, Ohio. American Journal of Epidemiology, 135(1): 12-19.
14. Gabrielli, P., G. Cozzi, S. Torcini, P. Cescon and C. Barbante, 2008. Trace elements in winter snow of the Dolomites (Italy): a statistical study of natural and anthropogenic contributions. Chemosphere, 72(10): 1504-1509.
15. García, R., R. Belmont, H. Padilla, M. Torres and A. Baez, 2009. Trace metals and inorganic ion measurements in rain from Mexico City and a nearby rural area. Chemistry and Ecology, 25(2): 71-86.

16. Halstead, M.J., R.G. Cunninghame and K.A. Hunter, 2000. Wet deposition of trace metals to a remote site in Fiordland, New Zealand. Atmospheric Environment, 34(4): 665-676.
17. Kyllönen, K., V. Karlsson and T. Ruoho-Airola, 2009. Trace element deposition and trends during a ten year period in Finland. Science of the total environment, 407(7): 2260-2269.
18. Wong, C., X. Li, G. Zhang, S. Qi and X. Peng, 2003. Atmospheric deposition of heavy metals in the Pearl River Delta, China. Atmospheric Environment, 37(6): 767-776.
19. Cong, Z., S. Kang, Y. Zhang and X. Li, 2010. Atmospheric wet deposition of trace elements to central Tibetan Plateau. Applied Geochemistry, 25(9): 1415-1421.
20. Tasiæ, M., Z. Mijiæ, S. Rajšiæ, A. Stojiæ, M. Radenkoviæ and J. Joksiæ, 2009. Source apportionment of atmospheric bulk deposition in the Belgrade urban area using positive matrix factorization. in Journal of Physics: Conference Series. IOP Publishing.
21. Tiwari, K., A. Pandey and J. Pandey, 2008. Atmospheric deposition of heavy metals in a seasonally dry tropical urban environment (India). Journal of Environmental Research And Development Vol, 2(4).
22. ASTM., 1996a. Standard Guide for Choosing Locations and Sampling Methods to Monitor Atmospheric Deposition at Non-Urban Locations: D 5111, West Conshohocken, PA.
23. Zhang, C., 2007. Fundamentals of environmental sampling and analysis: John Wiley and Sons.
24. Yadav, S. and V. Rajamani, 2006. Air quality and trace metal chemistry of different size fractions of aerosols in N–NW India-implications for source diversity. Atmospheric Environment, 40(4): 698-712.
25. Rashed, M.N., 2008. Total and extractable heavy metals in indoor, outdoor and street dust from Aswan City, Egypt. Clean - Soil, Air, Water, 36(10-11): 850-857.
26. APHA, W., 1998. AWWA, 1995. Standard Methods for the Examination of Water and Wastewater. Amer. Pub. Health Association. Washington DC.
27. Kulshrestha, A., P.G. Satsangi, J. Masih and A. Taneja, 2009. Metal concentration of $PM_{2.5}$ and PM_{10} particles and seasonal variations in urban and rural environment of Agra, India. Science of the Total Environment, 407(24): 6196-6204.
28. Moja, S. and J. Mnisi, 2013. Seasonal variations in airborne heavy metals in Vanderbijlpark, South Africa. Journal of Environmental Chemistry and Ecotoxicology, 5(9): 227-233.
29. Savant, A. and G. Pandey, 1993. Deposition of toxic metals on surface soil in the vicinity of a steel plant. Indian Journal of Eenvironmental Protection, 13: 168-168.
30. Sandhu, R.S. and H. Gehlan, 1992. Estimation of Some Metal in the Ambient Air of Amritsar. Indian Journal of Environmental Protection, 12(10): 773-739.
31. Lee, B.K. and N.T. Hieu, 2011. Seasonal variation and sources of heavy metals in atmospheric aerosols in a residential area of Ulsan, Korea. Aerosol and Air Quality Resarch, 11(6): 679-688.
32. Krolak, E., 2000. Heavy metals in falling dust in Eastern Mazowieckie province. Polish Journal of environmental studies, 9(6): 517-522.
33. Yaroshevsky, A., 2006. Abundances of chemical elements in the Earth's crust. Geochemistry International, 44(1): 48-55.
34. Wu, Y.S., G.C. Fang, W.J. Lee, J.F. Lee, C.C. Chang and C.Z. Lee, 2007. A review of atmospheric fine particulate matter and its associated trace metal pollutants in Asian countries during the period 1995-2005. Journal of hazardous materials, 143(1): 511-515.

Persian Abstract

DOI: 10.5829/idosi.ijee.2014.05.02.07

چکیده

در این مطالعه تغییرات فصلی غلظت متوسط فلزات در نمونه های گرد و غبار (۳۵۰) جمع آوری شده ، از ایستگاه‌های نمونه گیری مختلف واقع در پنج نقطه از شهرک صنعتی کوتا، در کشور هند بررسی شده است. میانگین غلظت فلزات سنگین (مس، کادمیم، روی و سرب) در فصل زمستان بالا و در فصل تابستان پایین بوده اما در مورد فلزات پوسته‌ای (آهن، کلسیم و منیزیم) این روند معکوس می‌باشد. به طور کلی، ترتیب غلظت متوسط فلزات سنگین در هر دو فصل به صورت $Zn > Pb > Cu > Cd$ بوده و تغییرات فصلی غلظت این فلزات ناشی از تفاوت در جهت و قدرت باد، دما، رطوبت نسبی و فعالیت های انسانی در ایستگاه‌های نمونه‌گیری بوده است. عامل تغلیظ و رابطه مثبت بین گونه های فلزی آنتروپوژنیک: مانند مس و کادمیم، مس و روی، مس و سرب، کادمیم و روی، کادمیم و سرب، و روی و سرب در هر دو فصل حاکی از منبع و منشاء مشترک حاصل از احتراق زغال سنگ در نیروگاه حرارتی می‌باشد.

Iranica Journal of Energy & Environment 5 (2): 167-172, 2014
ISSN 2079-2115
IJEE an Official Peer Reviewed Journal of Babol Noshirvani University of Technology
DOI: 10.5829/idosi.ijee.2014.05.02.08

BUT

Effects of Binding Ratios on Some Densification Characteristics of Groundnut Shell Briquettes

[1]O.A. Oyelaran, [2] B.O. Bolaji, [3]M.A. Waheed and [4]M.F. Adekunle

[1]Department of Research and Development, Hydraulic Equipment Development Institute, Kano, Nigeria
[2, 3]Department of Mechanical Engineering, Federal University of Agriculture, Abeokuta, Nigeria
[4]Department of Forestry, Federal University of Agriculture, Abeokuta, Nigeria

Received: March 30, 2014; **Accepted** in Revised Form: June 11, 2014

Abstract: This study has revealed that groundnut shell can be compacted to a stabled state with binding material. The densification of the groundnut shells aid in transporting and storing, making it more economically than is possible at unprocessed state. The effects of binder (cassava starch gel) show that the highest lateral and axial expansion was 1.91 and 6% respectively. Maximum density, relax density, relaxation ratio ranges between 411 to 441 kg/m^3, 201 to 202 kg/m^3, 2.03 to 2.19, respectively. Other results are durability in the range of 69.89 to 93.52%, while the calorific value ranges between 19.82 to 21.97 MJ/kg. The overall, briquettes performances showed that 20% binder have the most outstanding resultin terms of durability. It was found that the amount of binder used have significant influence on the properties of the briquettes.

Key words: Briquettes · Groundnut shell · Binder · Cassava starch gel · Durability · Density

INTRODUCTION

Biomass is defined as the biological degradable fraction of products, waste and residues from agriculture (including animal and vegetable materials), forestry and the biological degradable fraction of industrial and household waste [1]. The usage of biomass for the production of energy is one of the various means of reacting to the problems associated to energy crisis. The use of biomass as a source of energy is a matter of growing importance and discuss as agreed by Ana [2], Fernando [3] and Kaygusuz [4].

Several kinds of promising fuel-biomass such as swine manure[5], coconut oil [6], cashew shell waste [7], soft wood waste [8], algae [9], maize cob [10], coconut shell and waste paper admixture [11] were investigated. Tonnes of groundnut shellare produced annually in developing countries. The disposal of these shellsin the fields hasbeen by burning, sometimes disposed indiscriminately most especially in the rural areas of developing countries, thereby causing health hazard. Because of the highheating value of groundnut shell demonstrated when compressed to arelatively high density with binder. Experiments have shown that groundnut shell can becompressed and stabilized to a high density.

Biomass briquetting is the process of increasing the density of biomass into higher density, energy concentrated, storable and transportable solid fuel called briquette. Process of translating biomass into solid fuel involves drying, cutting, grinding and pressing with or without the aid of a binder. Therefore, attemptshave been made towards improved, efficient and sustainable utilization of biomass. Densification of agricultural residues in the form of briquettes is therefore a promising technique for this purpose. Densification improves heating value, handling and transportation characteristics of agricultural residues by increasingits density. The aim of this workis to study the effects of binding ratios on some densification characteristics of groundnut shell briquettes.

MATERIALS AND METHODS

Groundnut shells were collected from the processing sites at Dawanu, Kano, Nigeria. The shells were hammer milled and sieved. Particles that passed

Corresponding Author: O.A. Oyelaran, Department of Research and Development, Hydraulic Equipment Development Institute, Kano, Nigeria. Tel: +2348028253912, E-mail: ajanioyelaran@gmail.com

Please cite this article as: Oyelaran, O.A. , B.O., Bolaji, M.A. Waheed and M.F. Adekunle, 2014. Effects of Binding Ratios on Some Densification Characteristics of Groundnut Shell Briquettes. Iranica Journal of Energy and Environment, 5(2):167-172.

through the 850µm sieves and were retained on the 600µm sieves were used. The groundnut shell was sundried for three days before stocking. Cassava starch was used as the binder in this study. The reason for choosingcassava starch in this research is because of relative availability, ease of preparation and cost of binder.

The groundnut shell and binder were thoroughly mixed in order to obtain a uniformly blended mixture. Mixtures were prepared with four different percentages (5, 10, 15 and 20) of binder with fixed weight of groundnut shell. In each case, fixed quantities of the samples were hand-fed into the design and produced press and compacted. The dwell time of 5 minutes as in Olorunnisola [11] was used. The machine is a motorized briquetting machine, According to the design of the moulds, twelve (12) briquettes were produced per batch.

Briquette stability was measured in terms of its dimensional changes when exposed to the atmosphere [12]. The stability of briquettes produced from the groundnut shell with varying binding ratio examined in this study was determined in terms of dimensional expansion in the axial and lateral directions. Immediately after extrusion from the mould, the briquette length, breath and height were measured using vernier caliper. Briquette mass was also determined with a digital scale. Therefore, the (initial) density of each and every newly formed briquette was evaluated for the defined combination of material. Additionally, the dimensions of each briquette formed were measured after 5, 10, 30, 60, 1440 minutes, 7[12] and 19 day period to determine the diametral and longitudinal expansion, along with the relaxed density of briquette.

The compressed density also called maximum density (density immediately after compression) of the briquette was determined immediately after ejection from the moulds as the ratio of measured weight to the calculated volume. The relaxed density (density determined when dried) and relaxation ratio (ratio of compressed density to relaxed density) of the briquette were determined in dry condition of the briquette after about 19 days of sun drying to a constant weight. The relaxed density was calculated as the ratio of the briquette weight (g) to the new volume (cm^3). This gave an indication of the relative stability of the briquette after compression.

Durability signifies the measure of shear and impact forces a briquette could withstand during handling, storage and transportation processes [13]. The durability test was carried out according to Al-Widyan *et al.*[14] method, where the briquettes were drop from a height of 1.85 m on a flat steel plate four times. The durability (%) was calculated as the ratio of the final weight of the briquette retained after four drops to the initial weight of the briquette. The fraction of the briquette that remained unshattered was used as an index of briquette durability. The durability rating of the briquette was expressed as a percentage of the initial mass of the material remaining on the metal plate and this gave an indication of the ability of the briquette to withstand mechanical handling [15].

Leco AC-350 Oxygen Bomb Calorimeter interfaced with a microcomputer was used to assess the heat values of the produced briquettes. Two grams of the briquettes was measured and the screw mould bracket was used to re-mould the briquette to the appropriate calorimeter bucket size. Ten (10) ml distilled water was poured into the bomb and the industrial oxygen cylinder was connected to the bomb and the valves were opened and bomb was filled slowly at pressure range of 2.5-3.0 Mpa for a minute. The bomb was placed inside a canister bracket containing distilled water and the bomb lid was covered. The switch was turned on and the microcomputer was set for the determinations which automatically calibrate and measure the energy values and display the values on the screen for recording after feeding the necessary data on the briquettes. The data and result of the experiment are displayed on computer screen [16]. The result of the test is shown on Table 3.

RESULTS AND DISCUSSION

Figure 1 shows dimensional change of briquettes in the axial and lateral directions. The results of the stability test reflect the trend observed in compressed and relaxed density of the briquettes. The observed linear expansions were relativelysmaller compared to the axial expansion. When the stability tendency was viewed along the blending ratios, briquettes sample A produced with 5% binder in both axial and lateral directions were observed to mexhibit the best stability. Thus, sample 5% blend produced the most stabilising effect, followed by briquettes with 10% binder blend. This validates that stability of the briquette is a function of the binder levels and compressed density [17].

The stability of the briquettes, which is expressed in terms of percentage axial and lateral expansions, is presented in Figure 1. From the figure, it was observed that briquettes expanded largely in the axial direction than in the lateral direction. The change in briquette dimensions in the axial direction was up to 6% compared to maximum of 1.91 % in the lateral direction.

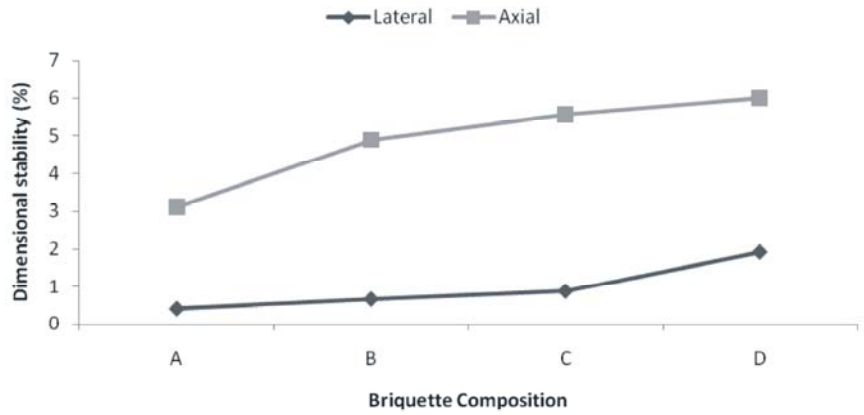

Fig. 1: Comparative result of dimensional stability of briquettes

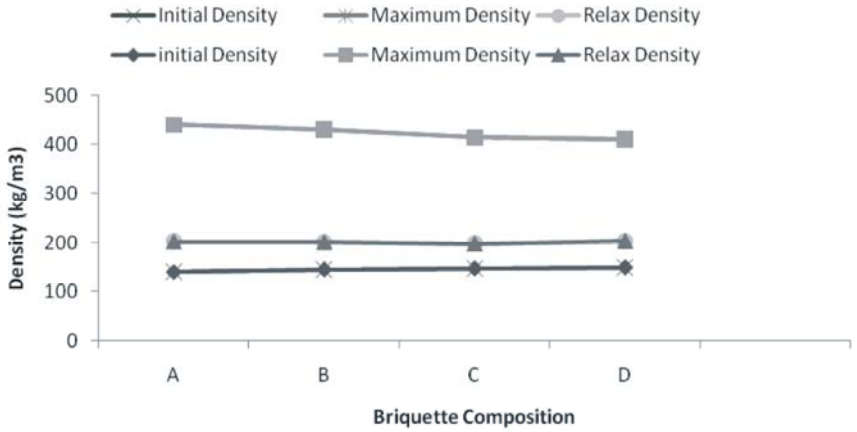

Fig. 2: Comparative result of densities of briquettes

Table 1: Result of compaction ratios of briquetteswith binder

Sample	Maximum density (kg/m^3)	Initial density (kg/m^3)	Compaction Ratio
A	441.08	142	3.11
B	430.75	147	2.93
C	414.56	149	2.78
D	411.01	151	2.72

Table 2: Result of durability testof briquettes

Sample	Weight before test (kg) m_b	Weight after test (kg) m_a	Durability (%)
A	0.146	0.102	69.89
B	0.142	0.126	88.90
C	0.141	0.129	91.55
D	0.144	0.135	93.52

Table 3: Result of bomb calorimeter test result of fuel samplesof briquettes

Samples	Calorific Value (kJ/kg)
A	19,820.43
B	20,545.35
C	21,456.13
D	21,968.32

A similar expansion result was also reported byresearcher [14] during briquetting of olive cake. Oladeji [18] in his work investigationed the effects of different binding ratios on some densification characteristics of corncob briquettes reported a similar trend change in briquette dimensions in the axial direction of up to 4.15%

compared to maximum of 1.76 % in the lateral direction. The axial expansion of briquettes increased as the percentage binder ratio increased. The lowest percentage binder ratio by weight A (5%) has the least axial and lateral expansions of 3.11 and 0.42, respectively. The implication of this is that, the lower the percentage binder ratio, the more stable are the briquettes produced.

Densities of Briquettes: Figure 2 shows the initial, maximum and relaxed densities of briquettes produced from groundnut shell under four different percentage binder ratios. The mean initial densities of the briquette with the percentage binder ratio A, B, C and D were 142, 147, 149 and 151 kg/m^3 respectively. The maximum densities for percentage binder ratio by weight A, B, C and Dwere 441.08, 430.75, 414.56 and 411.01 kg/m^3 respectively (see Figure 2). The values of the maximum densities are higher than the initial density of the uncompressed briquettes. It was observed that the higher the percentage of binder ratio by weight, the lower the maximum density *i.e*. that the maximum density decreased with increasing percentage binder ratio by weight. The same thing could be true for relaxed density for A, B, C and D were 201.41, 200.35, 197.41 and 202.45 kg/m^3 respectively. The values of maximum densities obtained with percentages of binders were less than the minimum value of 600 kg/m^3 recommended by Mani et al. [19] and Gilbert et al. [20] for efficient transportation and safe storage. The implication of this is that using percentage binder ratio up to 20 % may result in briquettes of good quality in term of density.

Table 1 shows the compaction, density and relaxation ratios obtained from the groundnut shell briquettes under four different percentage binder ratios. The values for compaction ratios of A, B, C and Dare 3.11, 2.93, 2.78 and 2.72, respectively. For the four weight percentages of binder examined in this study with percentage binder ratio A (5%) having the highestvalue. Higher compaction ratio implied more void in the compressed materials. Higher figure indicates more volume displacement, which is good for packaging, storage and transportation and above all, it is an indication of good quality briquettes [21]. From Table 1, it was observed that the compaction ratio decreased with increasing percentage binder ratio by weight and in this regards, the lowest percentage binder ratio exhibited the best result of 4.03. Furthermore, the values of compaction ratio obtained in this study compare and compete favourably well with notable biomass residues. For example, compaction ratio of between 3.20 and 9.70 was obtained by Boluwafi [22] during briquetting of guinea corn residue. In the similar manner, compaction ratios of 4.2 and 3.5 were obtained during briquetting of groundnut and melon shells, respectively [23]. While Oladeji, [24] obtained a compaction ratio of 3.80 during briquetting of rice husk.

The mean values of density ratio with percentage binder ratio by weight A, B, C and D are 0.46, 0.47, 0.48 and 0.49, respectively. The higher the value of the density ratio for a given mass, the less relaxed the briquettes are. There is practically little differences in the value of density ratio obtained for the four percentage binder ratios examined in this study.

The mean relaxation ratios of briquettes produced were found to be 2.19, 2.15, 2.10 and 2.03, for percentage binder ratio by weight A, B, C and D respectively (Table 1). Lower value of percentage binder ratio indicates a more stable briquette, while higher value indicates high tendency towards relaxation *i.e*. less stable briquette. The values of relaxation ratio obtained in this study indicate that briquettes produced with binder ratio are more stable than briquettes produced with the three other percentages binder ratios. A reciprocal relationship was observed between density ratio and relaxation ratio of the briquettes

Durability Resistance of Briquettes: The decisive factor regarding durability of briquettes reflect on the severity of handling, transportation and storage and weather conditions of the locations where the products are transportedor exported [25]. Therefore, the measurement of durability is critical indescribing briquette quality, in view of the fact that it predicts briquette performance in transportation, storage and handling. However, Karunanithy e*t al*. [26] and Dobie [27] suggested that fines up to 5% (by weight) would be an acceptable level and greater than 5% would reduce storage capacity and create problems in flow characteristics. It has been reported thatAdapa *et al*, [28]; Tabil and Sokhansanj, [29] classified the durability into high (> 0.8), medium (0.7-0.8) and low (< 0.7) depending upon the values. Table 2 shows that durability of the briquettes varied between 69.89 and 93.52 % while the losses vary between 6.48 and 30.11%. From the obtainedvalue it can be concluded that an addition of 10 to 20% of binder will give a good briquette in terms of durability.

The shattering resistance depends upon amount of concentration of binders. It increased with

increase in amount of binder. The differences in durability between briquettes might be due to chemical composition including lignin, extractive, cellulose and hemicelluloses[26]. For briquettes formed with 5% binder, the shattering resistance was the minimum of 69.89%. The maximum was recorded by the briquettes with the highest percentage of binderat 20% binder as 93.52 %.These are relatively high values, even higher than the range of reported values of 46.5 and 88.4% by Wamukonya and Jenkins [30] for sawdust and wheat straw briquettes. The observed increased in briquette durability with increase in starch content could also be attributed to the adhesive role the starch played in the briquettes[11].

Calorific Values: From Table 3, Calorific values increases with increase in concentration of binders. Based on the figure below, it is found that most of the briquettes fulfil the minimum requirement of calorific value for making commercial briquette (>17500 J/g), as stated by DIN 51731 [31]. From the result, it is found that briquette D having the highest binder ratio by weight (20%) has the highest gross calorific value of21,518kJ/kg; while briquette A that with the lowest value of binder (5%) has the lowest value of 18,220 kJ/kg. This proved that the gross calorific value is most influenced by the composition of briquette.

CONCLUSIONS

Cassava starch gelas binder in groundnut shell briquettes has enhanced the heating value, durability rating and densities of the briquettes as evident in this research work. The effect of binder (cassava starch gel) shows that the highest lateral and axial expansionswere 1.91 and 6%, respectively. Maximum density, relax density, relaxation ratio were in the range of 411 to 441 kg/m^3, 201 to 202 kg/m^3, 2.03 to 2.19, respectively. Other results are durability of between 69.89 to 93.52%, while the calorific value ranged between 19,820 to 21,968 kJ/kg. The overall performances showed 20% binder have the most outstanding result. It was found that the amount of binder used have significant influence on the properties of the briquettes. So the groundnut shell briquettes provide better alternatives to fossil fuel for firing heating and melting devices in the areas where groundnut is grown. The increasingly use of these wastes in composite briquette form, will help in solving disposal problem; apart from providing good alternatives to fossil fuel.

REFERENCES

1. Patel, B. and B. Gami, 2012. Biomass Characterization and its Use as Solid Fuel for Combustion. Iranica Journal of Energy and Environment, 3: 123-128.
2. Gómez-Loscos, A., M.D. Gadea and A. Montañés, 2012. Economic growth, inflation and oil shocks: are the 1970s coming back? Applied Economics, 44(35): 4575-4589.
3. Galembeck, F., 2010. Synergy in food, fuels and materials production from biomass. Energy and Environmental Science, 3(4): 393-399.
4. Kaygusuz, K. and S. Keleş, 2008. Use of biomass as a transitional strategy to a sustainable and clean energy system. Energy Sources, Part A: Recovery, Utilization and Environmental Effects, 31(1): 86-97.
5. Xiu, S., A. Shahbazi, L. Wang and C.W. Wallace, 2010. Supercritical ethanol liquefaction of swine manure for bio-oils production. American Journal of Engineering and Applied Sciences, 3(2): 494.
6. Singh, P., J. Khurma and A. Singh, 2010. Coconut oil based hybrid fuels as alternative fuel for diesel engines. American Journal of Environmental Sciences, 6(1): 71.
7. Mohod, A., S. Jain and A. Powar, 2010. Energy option for small scale cashew nut processing in India. Energy Research Journal, 1(1): 47.
8. Khalil, A.M., A.F. Al-Shawabkeh, A.S. Mazahreh, M.S. Al-Damanhoory and J.M. Quasem, 2009. Utilization of soft wood wastes as a feed stock to produce fuel ethanol. American Journal of Engineering and Applied Sciences, 2(2): 451.
9. Sharif Hossain, A., A. Salleh, A.N. Boyce, P. Chowdhury and M. Naqiuddin, 2008. Biodiesel fuel production from algae as renewable energy. American Journal of Biochemistry and Biotechnology, 4(3): 250-254.
10. Wilaipon, P., 2007. Physical Characteristics of Maize Cob. Briquette under Moderate Die Pressure. American Journal of Applied Sciences, 4(12): 995-998.
11. Olorunnisola, A., 2007. Production of fuel briquettes from waste paper and coconut husk admixtures. Agricultural Engineering International: CIGR E. Journal., IX: 1-11.
12. Sotannde, O., A. Oluyege and G. Abah, 2010. Physical and combustion properties of briquettes from sawdust of Azadirachta indica. Journal of Forestry Research, 21(1): 63-67.

13. Adapa, P., L. Tabil and G. Schoenau, 2009. Compaction characteristics of barley, canola, oat and wheat straw. Biosystems engineering, 104(3): 335-344.
14. Al-Widyan, M., H. Al-Jalil, M. Abu-Zreig and N. Abu-Hamdeh, 2002. Physical durability and stability of olive cake briquettes. Canadian Biosystems Engineering, 44: 341-346.
15. Sah, P., B. Singh and U. Agrawal, 1980. Compaction Behavior of Straw. Journal of Agricultural Engineering-India, 18(1): 89-96.
16. Obi, O.F., C.O. Akubuo and W.I. Okonkwo, 2013. Development of an Appropriate Briquetting Machine for Use in Rural Communities. International Journal of Engineering and Advanced Technology, 2(4): 578-582.
17. Chaiklangmuang, S., S. Supa and P. Kaewpet, 2008. Development of fuel briquettes from biomass-lignite blends. Chiang Mai J. Sci., 35(1): 43-50.
18. Oladeji, J., 2011. The Effects of some processing parameters on physical and combustion characteristics of corncob briquettes. An Unpublished Ph. D Thesis of the Department of Mechanical Engineering, Ladoke Akintola University of Technology, Ogbomoso, Nigeria.
19. Mani, S., S. Sokhansanj, X. Bi and L.G. Tabil, 2004. Compaction of corn stover. ASAE/CSAE Meeting, Paper No.041160, St. Joseph, MI.
20. Gilbert, P., C. Ryu, V. Sharifi and J. Swithenbank, 2009. Effect of process parameters on pelletisation of herbaceous crops. Fuel, 88(8): 1491-1497.
21. Davies, R.M. and U.S. Mohammed, 2013. Effect of Processing Variables on Compaction and Relaxation Ratio of Water Hyacinth Briquettes. International Journal of Scientific Research in Knowledge, 1(9): 308-316.
22. Bolufawi S.J., 2008. Briquetting Characteristics in Relation to Fuel Values of Guinea Corn (Sorghum bicolor) Residue, An Unpublished Ph.D Thesis of the Department of Agricultural and Environmental Engineering, University of Ibadan, Nigeria.
23. Oladeji, J., 2010. Fuel characterization of briquettes produced from corncob and rice husk resides. Pacific Journal of Science and Technology, 11(1): 101-106.
24. Oladeji, J., 2012. Comparative Study of Briquetting of Few Selected Agro-Residues Commonly Found in Nigeria. Pacific Journal of Science and Technology, 13(2): 80-86.
25. Khoush Taghaza, M., S. Sokhansanj and B. Gossen, 1999. Quality of alfalfa cubes during shipping and storage. Applied Engineering in Agriculture, 15(6): 671-676.
26. Karunanithy, C., Y. Wang, K. Muthukumarappan and S. Pugalenghi, 2011. Physiochemical characterization of briquettes made from different feedstock. Biotechnology Research International, ID 165202, pp: 1-9.
27. Dobie, J.B., 1961. Materials-handling systems for hay wafers. Agricultural Engineering, 42(12): 692-697.
28. Adapa, P., G. Schoenau, L. Tabil, S. Sokhansanj and B. Crerar. Pelleting of fractionated alfalfa products. in 2003 ASAE Annual International Meeting, Las Vegas, Nevada.
29. Tabil Jr, L. and S. Sokhansanj, 1996. Process conditions affecting the physical quality of alfalfa pellets. Applied Engineering in Agriculture, 12(3): 345-350.
30. Wamukonya, L. and B. Jenkins, 1995. Durability and relaxation of sawdust and wheat-straw briquettes as possible fuels for Kenya. Biomass and Bioenergy, 8(3): 175-179.
31. Yuhazri, M., H. Sihombing, N. Umar, L. Saijod and P. Phongsakorn, 2012. Solid Fuel from Empty Fruit Bunch Fiber and Waste Papers Part 1: Heat Released from Combustion Test. Global Engineers and Technologists Review, 2(1): 7-13.

Persian Abstract

DOI: 10.5829/idosi.ijee.2014.05.02.08

چکیده

مطالعات نشان داده است پوست بادام زمینی می تواند با استفاده از مواد چسبنده، به حالت پایدار و ثابتی فشرده شود. فشرده سازی پوست های بادام زمینی به حمل و نقل و ذخیره سازی کمک می کند که تولید آن از لحاظ اقتصادی نسبت به حالت فشرده نشده، مقرون به صرفه تر است. بررسی اثر چسب نشاسته کاساوا نشان داده است که بیشترین انبساط عرضی و محوری به ترتیب ۱/۹۱ و ۶ درصد می‌باشد. محدوده حداکثر دانسیته، چگالی آزاد و نسبت انعطاف پذیری به ترتیب بین ۴۱۱ تا ۴۴۱ کیلو گرم بر متر مکعب، ۲۰۱ تا ۲۰۲ کیلو گرم بر متر مکعب و ۲/۰۳ تا ۲/۱۹ می‌باشد. محدوده پایداری آن ۶۹/۸۹ تا ۹۳/۵۲ درصد، در حالی که ارزش گرمایی آن بین ۱۹/۸۲ تا ۲۱/۹۷ مگاژول بر کیلوگرم بوده است. در حالت کلی راندمان بریکت (قالب فشرده) نشان داده است که استفاده از ۲۰ درصد چسب، نتایج مطلوبی در دوام و پایداری محصول دارد. در نهایت مقدار چسب استفاده شده اثر قابل توجهی بر روی خواص بریکت دارد.

Iranica Journal of Energy & Environment 5 (2): 173-183, 2014
ISSN 2079-2115
IJEE an Official Peer Reviewed Journal of Babol Noshirvani University of Technology
DOI: 10.5829/idosi.ijee.2014.05.02.09

BUT

The Potential and Characteristics of Solar Energy in Yazd Province, Iran

[1, 2]H. Khorasanizadeh, [1, 2]K. Mohammadi and [1, 2]A. Aghaei

[1]Faculty of Mechanical Engineering,
University of Kashan, Kashan, Iran, Post Code: 87317-51167
[2]Energy Research Institute, University of Kashan, Kashan, Iran

Received: March 28, 2014; **Accepted** in Revised Form: June 11, 2014

Abstract: In this study, utilizing the obtained data from four distributed locations known as Abarkuh, Behabad, Halvan and Yazd, the solar energy potential and its characteristics in Yazd province of Iran have been evaluated. For the data, daily horizontal global radiation (HGR) and clearness index also their monthly, seasonal and yearly averaged values have been obtained. The results indicate that the four locations enjoy from 300, 294, 289 and 311 sunny and very sunny days; their yearly averaged daily clearness indexes are 0. 66, 0. 66, 0. 64 and 0. 67 and their yearly averaged daily global radiations are 20. 74, 20. 78, 19. 52 and 20. 60 MJ/m^2, respectively. In overall, Yazd province enjoys from sunshine hours in almost 76% of the whole day times and its annually averaged daily HGR and clearness index are 20. 41 MJ/m^2 and 0. 66, respectively. Making comparison between the four nominated locations of Yazd province and 7 other selected cities around the globe, but at the same latitude, except Arizona, revealed that, their monthly mean daily global radiation and clearness index are higher than those of other six selected cities. Due to the great potential of Yazd province more funds and endeavors for solar energy development have to be devoted.

Key words: Solar energy assessment · Global solar radiation · Clearness index · Yazd province · Sunshine duration

INTRODUCTION

Due to pollution problems related to fossil fuels, such as being non-renewable, their impact on environment and increasing their pricedue to uncertainties in future, the global investment to utilize renewable energy sourcesis rapidly growing. The total global investment in renewable energy from $220 billion in 2010 reached to $257 billion in 2011. Also by the end of 2011 the total renewable energy capacity reached to 1, 360 GW with the most contribution belong to hydro power and wind power summing up to 970 GW and 238 GW, respectively [1]. Nonetheless, among various types of renewable resources, solar energy is more attractive due to its almost even distribution in most parts of the world. Solar energy is clean, environmentally friendly and inexhaustible. Nowadays different kinds of solar energy technologies such as solar photovoltaic (PV), concentrating solar thermal power (CSP), solar hot water/space heating systems, solar dryers, solar stills and solar ovens are becoming widespread. By the end of 2011, the global capacity of PV, CSP and solar hot water/space heating reached to 70 GW, 1. 76 GW and 232 GW, respectively [1]. Aligned with augmented utilization of these technologies in the recent years, many studies have been undertaken to enhance the performance of such technologies [2-6].

Due to placement in the solar belt region of the world, Iran enjoys considerable solar radiation, so that the amount of solar radiation in different parts of Iran is estimated in the range of 1800-2200 KWh/m^2 per year[1]. However, in order to design a solar energy system in every region, having accurate information about the potential of solar radiation, clearness index and optimum tilt angle of solar collectors are very essential.

[1]SEIA (Iranian Solar Energy Industries Association). http://www.irseia.com.

Corresponding Author: H. Khorasanizadeh, Faculty of Mechanical Engineering, University of Kashan, Kashan, Iran. Post Code: 87317-51167. Tel: +98-3615912449, Fax: +98-3615912424, E-mail: khorasan@kashanu.ac.ir

Please cite this article as: Khorasanizadeh, H., K. Mohammadi and A. Aghaei, 2014. the potential and characteristics of solar energy in Yazd province, Iran. Iranica Journal of Energy and Environment, 5(2):173-183.

Extensive researches have been conducted to analyze measured solar radiation data at various parts of the globe [7-12]. Besides, several investigations have been performed to enlighten different aspects of solar radiation in Iran, from which references are made here only to some of them. Yaghoubi and Sabzevari [13] analyzed global solar radiation on horizontal surface and clearness index using data of seven years for the city of Shiraz. Noorian *et al*. [14] examined the performance of 12 different models to estimate hourly diffuse solar radiation on inclined surfaces based on measured data on horizontal surface in Karaj. Moeeni *et al*. [15] utilized the long term measured solar radiation data and established the Angström model for prediction of the monthly averaged daily global radiation in the city of Yazd. Salvatipour *et al*. [16] theoretically determined the optimum tilt angles for the south facing solar collectors in city of Isfahan for monthly, seasonal and yearly adjustments. They also investigated the effect of earth reflectivity on optimum slope angle and maximum total solar radiation. Behrang *et al*. [17] proposed some newglobal solar radiation models using relative sunshine hours for 17 selected cities across Iran by employing particle swarm optimization (PSO) technique. Dehghan [18] presented a review paper to discuss the status and potential of renewable energies, in particular solar and wind energies, in Yazd province. As for solar energy, his study only involved reviewing the experiences of installing the solar energy technologies in Yazd province, but it has lack of assessment of solar energy and exploration of its characteristics. Khorasanizadeh and Mohammadi [19] tested performance of 11 empirical models from 3 different categories to predict the monthly mean daily global solar radiation over six major cities of Iran. They presented the suitable model for each city, in which the sunshine hours was an important variable. In another study Khorasanizadeh and Mohammadi [20] utilized long-term global solar radiation data to test 6 days of the year based empirical models for prediction of daily global solar radiation in four Iranian cities of Bandarabass, Isfahan, Kerman and Tabass. They employed the statistical non-linear regression technique and were able to establish the best model for every city. In a recent study, Khorasanizadeh *et al*. [21] established a proper model for estimation of horizontal diffuse radiation in Tabass, Iranand determined the optimum tilt angle for south-facing solar surfaces in Tabass region for the fixed monthly, seasonal, semi-yearly and yearly adjustments.

In order to know and evaluate the potential of solar energy in Yazd province of Iran, this study presents an analysis of horizontal global solar radiation (HGR), clearness index (CI), sunshine duration (SD) and ambient temperature (AT) in four very well distributed locations in this province.

The Study Region and Data Collection: Yazd province with an area of 131, 575 km^2 is located in the central part of Iran approximately between 30-35°N latitudes and 52-58°E longitudes. This province is divided to eleven districts; one of them is the city of Yazd, the center of Yazd province. Based on 2011 statistical survey, the total population of Yazd province is1, 074, 428 residents. Yazd province is subjected to the rain shadow effect due to its location east of Zagros Mountain such that its annual average participation is about 100 mm, most of it falling in winter months[2]. Low precipitations as well as high rate of evaporation in summer are two important parameters which make much of this province one of the driest areas of Iran. Based on the Köppen classification, the climate condition in this province is categorized ashot desert climate (BWh), which relates to hot arid desert [22]. This is because of its annual participation which is less than 250 mm and its mean annual temperature which is above 18°C.

For analyzing the status of solar radiation and assessing the solar potential of this province, four station locations of Abarkuh, Behabad, Halvan and Yazd have been selected, which are geographically distributed across the province. Figure 1 displays Yazd province on the map of Iran and placement of the selected siteson this province. Abarkuh and Behabad are small towns and Halvan is a rural area. The geographical locations of these four places and time period of data used in this study are given in Table 1. For the city of Yazd, long-term (five years) measured daily data provided by Iranian Meteorological Organization (IMO) was available, but for the other three locations only one year every ten minute measured data was available. These one-year data were obtained in a survey study by Iranian Renewable Energy Organization, locally called SUNA. As part of this survey study and in order to measure different meteorological parameters such as horizontal global radiation, temperature, relative humidity and wind speed at different heights many temporary stations were positioned at various parts of the country, in particular in Abarkuh, Behabad and Halvan.

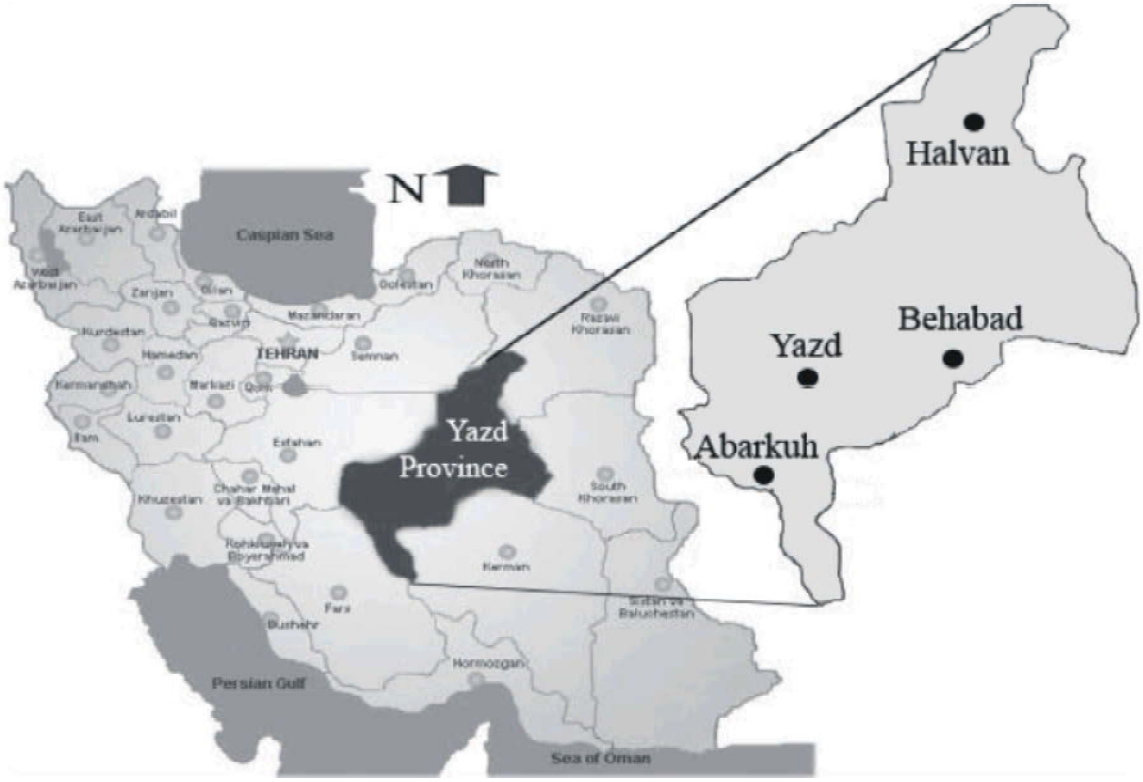

Fig. 1: The position of Yazd province, Abarkuhh, Behabad, Halvan and the city of Yazd on the map of Iran

Table 1: Geographical locations of four nominated locations inYazd province and period of data series

City	Latitude (°N)	Longitude (°E)	Period of data series
Abarkuh	31°30′	53°66′	2007
Behabad	31°77′	56°11′	2007
Halvan	33°96′	56°29′	2007
Yazd	31°53′	54°37′	2003, 2004 & 2007-2009

Caculation Procedure: To analyze solar data some useful parameters are needed. Clearness index is the ratio of terrestrial HGR to extraterrestrial horizontal radiation. The daily clearness index is [23]:

$$K_T = \frac{H}{H_o} \tag{1}$$

where, H is the daily global solar radiation on a horizontal surface and H_oi s the extraterrestrial solar radiation on a horizontal surface at the same geographical location. The extraterrestrial solar radiation on a horizontal surface, H_o, is represented in literature [23]:

$$H_o = \frac{24\times 3600}{\pi} G_{sc}\left(1+0.033\cos\frac{360 n_{day}}{365}\right) \times\left(\cos\varphi\cos\delta\sin\omega_s + \frac{\pi\omega_s}{180}\sin\varphi\sin\delta\right) \tag{2}$$

where, G_{sc} is the solar constant equal to 1367 W/m^2, n is the day number of the year, φ is the latitude of the location, δ is the solar declination angle and ω_s is the sunrise hour angle. The solar declination and the sunrise hour angles are [23]:

$$\delta = 23.45\sin\left(\frac{(n+284)360}{365}\right) \tag{3}$$

$$\omega_s = \cos^{-1}\left(-\tan\varphi\tan\delta\right) \tag{4}$$

For Abarkuh, Behabad and Halvan the ten-minute recorded solar and temperature data were averaged to get hourly HGR. Then these hourly values were used to obtain daily HGR. For Yazd the five years measured daily HGR data were utilized to obtain an average for every day of the year. Moreover, the monthly, seasonal and yearly mean values of daily HGR were obtained by getting average from the daily HGR values, correspondingly.

For every selected location, in order to obtain the daily clearness index the daily extraterrestrial solar radiation for the corresponding φ, δ and ω_s was utilized. For each month the monthly mean clearness index was obtained by dividing the monthly averaged daily HGR to the daily extraterrestrial radiation of the average day of that month. The monthly average temperature was obtained by averaging all of the hourly measured temperatures. In addition the monthly average minimum and maximum temperatures were obtained by averaging all of the measured daily minimum and maximum values, respectively. Toderive the seasonal and the yearly averaged daily HGR and clearness index their monthly values were also averaged, correspondingly.

RESULTS AND DISCUSSIONS

In this section the daily sunshine hours, HGR and clearness index are presented, analyzed and discussed first. Due to climatic changes occurring in different days of each month and throughout the year, daily analysis is not conclusive; hence, monthly seasonal and yearly studies are required. The monthly results are discussed in the next subsection and the seasonal and yearly results are discussed together in another subsequent subsection.

Daily Results: To determine the potential of a region for installing solar energy systems one important factor is the amount of sunshine hours. According to a particular definition proposed by the World Meteorological Organization (WMO) [24], sunshine duration during a day, n, is the sum of periods for which the beam (direct) solar irradiance exceeds 120 W/m^2.

Due to lack of measured data for the three other locations, the study of sunshine duration was done only for the city of Yazd. However, because of similar weather condition in all of the considered locations, the results can be extended to make conclusion about the whole Yazd province. For the city of Yazd, daily sunshine hours, based on averaged values obtained in the five years of measurement, as well as the day length, N, throughout the year are shown in Figure 2. The total sunshine duration in a whole year for the city of Yazd is 3342 hours; which is 19% higher than the average estimated sunshine duration of 2800 hours for the whole Iran. It should be noted that the total day lengths for a whole year in Yazd province are 4380 hours. Thus, Yazd province enjoys from sunshine hours in almost 76% of the whole day times.

The ratio of sunshine hours in a day to the maximum possible sunshine hours (the day length) is defined as relative sunshine hours (n/N). One classification for the daily weather condition proposed by the World Meteorological Organization [25] is:

Cloudy sky: $0 \leq n/N < 0.3$
Scattered clouds: $0.3 \leq n/N < 0.7$
Fair weather: $0.7 \leq n/N \leq 1.0$

On this basis, the city of Yazd in 269 days (74% of a whole year) enjoys from fair weather condition, whereas only in 5 and 91 days there exist cloudy sky and scattered clouds, respectively.

To obtain daily characteristics of radiation, particularly the maximum values, study of daily HGR throughout the year is important. For Abarkuh, Behabad, Halvan and the city of Yazd the daily HGRin different days of yearis shown in Figure 3. In Abarkuh the maximum daily HGR of 32.03 MJ/m^{2}has occurred on 3rd July. For Behabad and Halvan the maximum values of HGR are 31.38 and 30.68 MJ/m^2 on May 28 and May 21, respectively. For Yazd, the highest HGR is 35.06 MJ/m^2 happened on May 31, 2009 whereas the lowest HGR is 1.93 MJ/m^2 occurred on December 3, 2008. However, for the city of Yazd and based on the five years averaged values the maximum and minimum daily HGR are 29.69 and 6.15 MJ/m^2, respectively. A general comparison of plots related to different locations showsa similar trend during the year, although fewer fluctuations are observed for the city of Yazd. This isdue to the fact thatfor Abarkuh, Behabad and Halvan only one year measured data have been used, whereas for the city of Yazd five years averaged values of daily HGR have been utilized.

In the design of solar energy systems, clearness index is a very crucial factor. Clearness of sky directly influences the beam (direct) radiation which is essential for concentrating solar systems. The extraterrestrial solar radiation in every geographical location is a constant value for each specific day, irrespective of change of year. However, solar attenuation occurs as radiation passes through the atmosphere due to atmospheric phenomenon such as, aerosol extinction, cloud extinction, permanent gas absorption, ozone absorption, Rayleigh scattering and water vapor absorption. According to Figure 4, which shows the daily clearness index in the four nominated locations, for most of the days the clearness index is high indicating high level of beam (direct) radiation. Nevertheless, low values of HGR and clearness index in some of the days refer to the lessening due to the above mentioned atmospheric incidents.

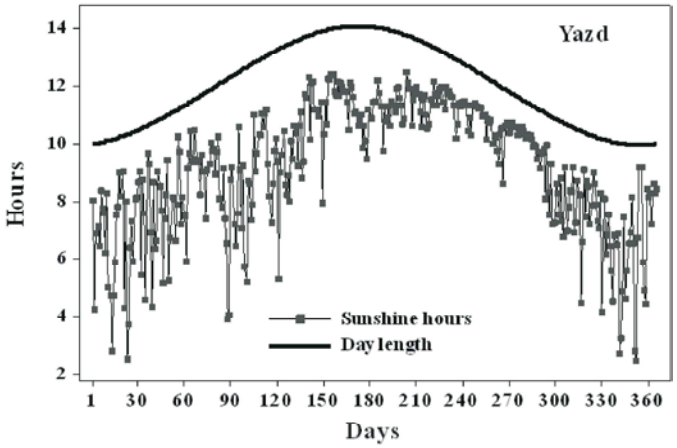

Fig. 2: Daily sunshine hours and day length in the city of Yazd

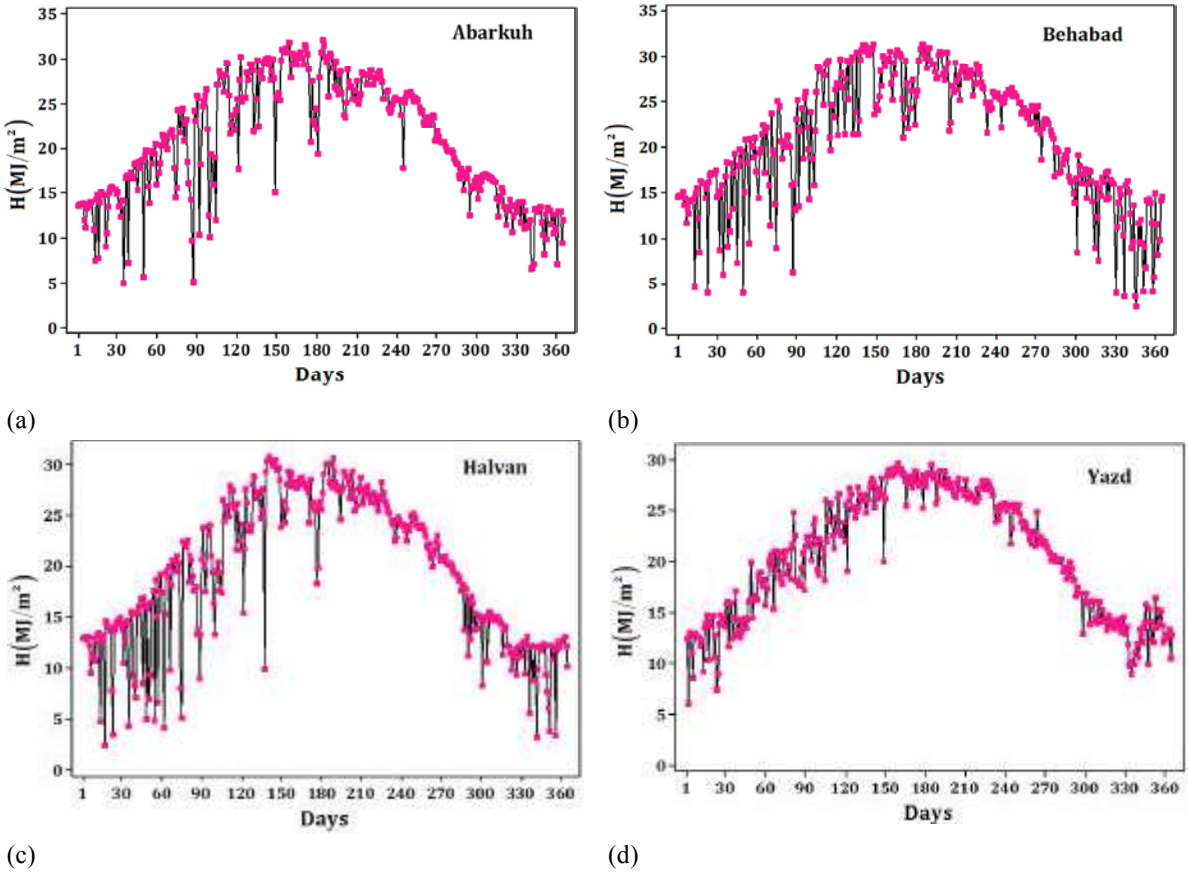

Fig. 3: Daily global solar radiation at different locations in Yazd province

For Abarkuh, Bahabad, Halvan and the city of Yazd the maximum daily clearness indexes are 0. 79, 0. 85, 0. 77 and 0. 88 and the minimum ones are 0. 15, 0. 13, 0. 13 and 0.32, respectively.

Another important parameter that can be helpful to find and understand the characteristics of solar energy is the frequency distribution of daily HGR and clearness index at some specified intervals throughout the year. These two are important parameters inde signing solar systems like PV or solar concentrators. An analysis was conducted for daily HGR from 0 to 35 MJ/m^2 with interval of 5 MJ/m^2, also for daily clearness index from 0 to 1 with interval of 0. 1 andthe results are presented in Tables 2 and 3, respectively.

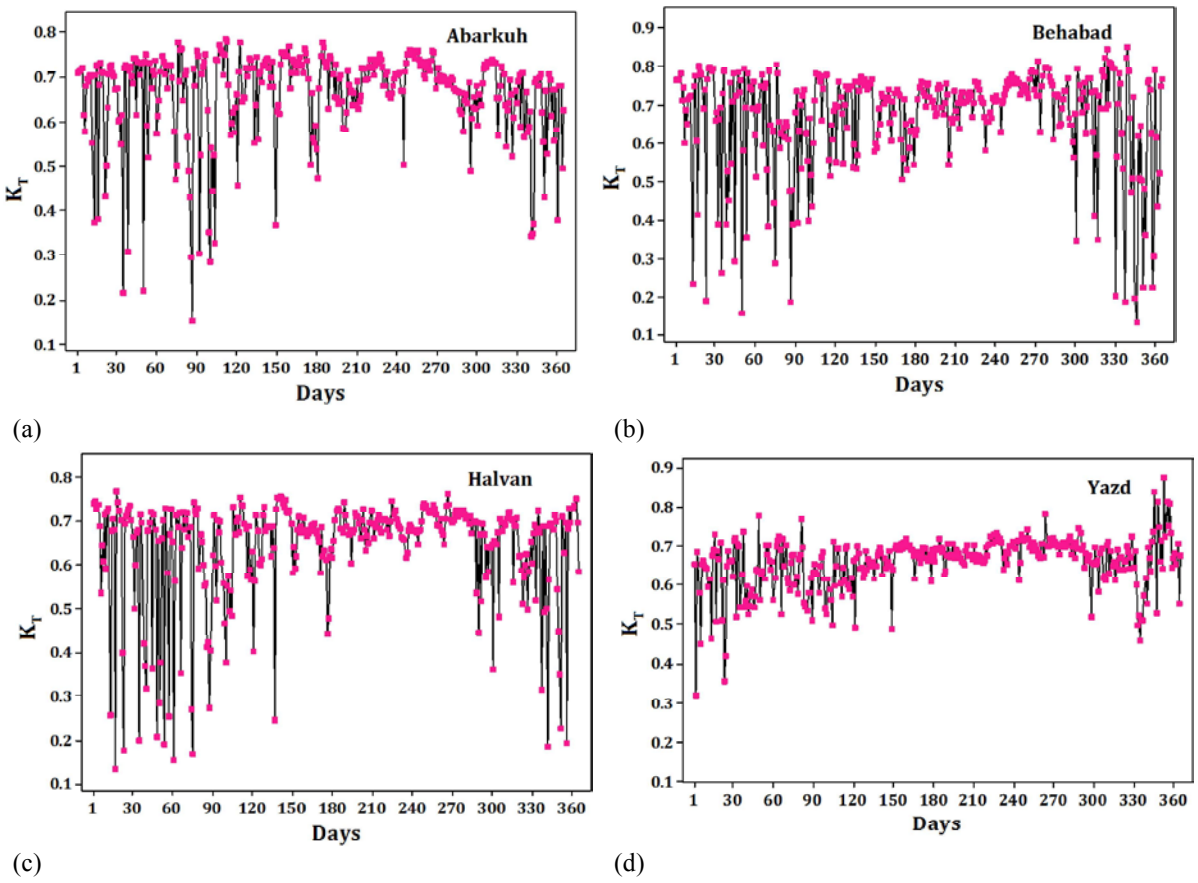

Fig. 4: Daily clearness index in different locations of Yazd province

Table 2: The frequency distribution of days of a year at different intervals ofglobal solar radiation (MJ/m^2)

City/interval	0-5	5-10	10-15	15-20	20-25	25-30	30-35
Abarkuh	1	14	75	80	63	109	23
Behabad	9	20	51	82	77	99	27
Halvan	9	26	83	59	79	100	9
Yazd	0	10	85	69	78	123	0

Table 3: The frequency distribution of days of a year at different intervals of clearness index

City/interval	0.0-0.1	0.1-0.2	0.2-0.3	0.3-0.4	0.4-0.5	0.5-0.6	0.6-0.7	0.7-0.8	0.8-0.9	0.9-1.0
Abarkuh	0	1	4	11	11	38	124	171	0	0
Behabad	0	6	7	11	10	37	90	187	11	0
Halvan	0	8	8	9	17	34	164	125	0	0
Yazd	0	0	0	2	8	44	221	85	5	0

In another classification, Yousif *et al*. [26] proposed four different intervals of K_T for the level of clearness of sky, which are:

Cloudy: $0 < K_T < 0.2$
Partly cloudy: $0.2 \leq K_T < 0.6$
Sunny: $0.6 \leq K_T < 0.75$
Very sunny: $0.75 \leq K_T < 1$

According to this classification, with clearness index more than 0. 6, Abarkuh, Behabad, Halvanand the city of Yazd enjoy from 295, 288, 289 and 311 days, respectively. Figure 5 shows the comparison of frequency distribution of clearness index at different intervals in four nominated locations of Yazd province. It can be concluded that the whole Yazd province has more or less the same status in terms of clearness of sky. Additionally, Yazd province

Table 4: The monthly mean daily HGR (MJ/m^2), clearness index and temperature (°C) of four nominated locations in Yazd province

City		Jan	Feb	Mar	Apr	May	Jun	Jul	Aug	Sep	Oct	Nov	Dec
Abarkuh	$\overline{H}$	13.38	16.13	19.69	22.88	27.02	28.40	27.65	26.64	23.61	17.60	14.54	11.36
	$\overline{K}_T$	0.65	0.64	0.63	0.63	0.68	0.69	0.68	0.70	0.72	0.65	0.67	0.59
	$\overline{T}$	4.6	9.2	12.3	18.7	24.7	31.3	32.6	30.1	25.4	21.3	14.1	7.5
Behabad	$\overline{H}$	13.06	15.42	18.55	23.80	27.59	27.19	28.60	26.57	24.75	18.74	14.67	10.43
	$\overline{K}_T$	0.65	0.62	0.60	0.65	0.69	0.66	0.71	0.70	0.75	0.70	0.69	0.55
	$\overline{T}$	5.6	9.0	12.0	20.2	23.8	30.0	30.0	27.7	23.0	22.0	12.3	4.1
Halvan	$\overline{H}$	11.97	12.89	17.17	22.52	26.61	26.80	28.06	25.69	22.69	16.69	12.80	10.40
	$\overline{K}_T$	0.63	0.54	0.57	0.62	0.67	0.65	0.69	0.69	0.71	0.65	0.64	0.59
	$\overline{T}$	7.9	11.8	14.6	23.8	28.3	34.7	34.8	32.8	28.5	26.4	17.3	8.0
Yazd	$\overline{H}$	12.48	15.58	19.56	23.01	25.98	28.18	27.55	26.19	23.04	18.22	14.59	12.79
	$\overline{K}_T$	0.61	0.62	0.63	0.63	0.65	0.68	0.68	0.69	0.70	0.68	0.68	0.67
	$\overline{T}$	7.3	10.1	15.2	21.1	26.1	30.6	33.0	31.3	27.6	21.5	13.2	8.7

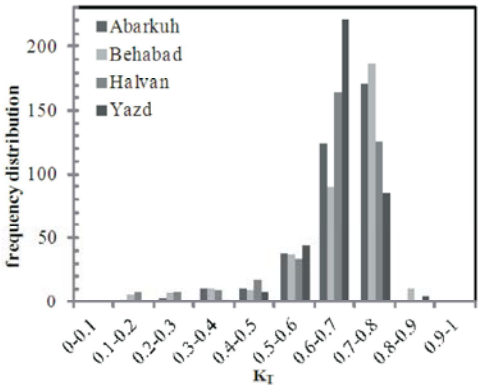

Fig. 5: Comparison of frequency distribution of clearness index at different intervals in the four nominated locations of Yazd province

enjoys from sunny and very sunnydays at least in more than 79% of the days of a whole year. Although the clearness index does not exclusively provide information on the accessibility of beam radiation, desirable level of beam radiation suitable for concentrating solar systems in Yazd province seems inevitable.

Monthly Results: Table 4 represents monthly mean daily HGR, clearness index and average temperature in different months for Abarkuh, Behabad and Halvan and the city of Yazd. For Abarkuh and the city of Yazd, the maximum monthly mean HGR occur in June were 28. 40 and 28. 18 MJ/m^2, respectively. While for Behabad and Halvan the maximum mean HGR in occur in July were 28. 60 and 28. 06 MJ/m^2, respectively. On the other hand, for Abarkuh, Behabad and Halvanthe minimum monthly mean HGR occur in December were 11. 37, 10. 43 and 10.40 MJ/m^2, respectively. Whereas for the city of Yazd the minimum HGR happens in January is 12. 48 MJ/m^2. For Abarkuh, Behabad, Halvan and the city of Yazd the maximum monthly mean daily clearness index occur in September were 0. 72, 0. 75, 0. 71 and 0. 70, respectively. For Abarkuh and Behabad, the minimum monthly clearness indexes, happening on December are 0.59 and 0.55 , respectively; while for Halvan the minimum is 0.54 belonging to February and for the city of Yazd, the minimum is 0. 61 belonging to January. The results denote that the monthly averaged daily HGR and clearness index in all of the locations ofYazd province are high throughout the year. A further comparison of the monthly averaged daily HGR and clearness index in different locations of Yazd province at the same months express that the status of solar radiation across this province is more or less the same.

To study the comparison of the status of solar radiation in Yazd province with some other places around the globe, 7 cities in different continents but all located in almost the same latitude asYazd province (Table 5) have been selected. Table 6 presents the monthly averaged daily HGR, clearness index and average temperature in these designated cities.

A comparison between the data in Tables 4 and 6 for all of the months reveals that, except Arizona, the monthly mean daily HGR and clearness index in different locations of Yazd province are higher than those of other six designated cities. Arizona is considered as one of the sunniest locations across the world [23]. However, in the last and first months of the year Yazd province enjoys from higher HGR and clearness index than Arizona does. The high values of HGR and clearness index indicate that Yazd province isa suitable region for investment in solar systems utilized by solar concentrators or PV.

In designing solar systems, the ambient temperature is an important parameter. The monthly mean maximum, minimum and average temperatures for all of the nominated locations are shown in Figure 6. The results indicate that Halvan and the city of Yazd compared with Abarkuh and Behabad have a bit higher minimum, average

Table 5: Geographical locations of the 7 nominated cities around the globe

City	Country (Continent)	Latitude	Longitude
Arizona	USA (North America)	33.89 °N	112.10 °W
Baghdad	Iraq (Asia)	33.32 °N	44.39 °E
Cairo	Egypt (Africa)	30.00 °N	31.20 °E
Casablanca	Morocco (Africa)	33.60 °N	7.62 °W
Georgia	USA (North America)	32.96 °N	83.11 °W
Jerusalem	Israel (Asia)	31.78 °N	35.22 °E
Texas	USA (North America)	30.30 °N	97.50 °W

Table 6: The monthly mean daily HGR (MJ/m^2), clearness index and temperature (°C) in 7 nominated cities around the globe [8, 23]

City		Jan	Feb	Mar	Apr	May	Jun	Jul	Aug	Sep	Oct	Nov	Dec
Arizona	$\overline{H}$	11.60	15.60	20.59	26.73	30.38	31.10	28.23	26.02	22.88	17.90	13.06	10.57
	$\overline{K}_T$	0.60	0.65	0.68	0.74	0.76	0.75	0.69	0.69	0.71	0.69	0.64	0.59
	$\overline{T}$	11	13	15	20	25	29	33	32	29	22	15	11
Baghdad	$\overline{H}$	10.80	13.68	17.28	20.52	23.4	26.28	25.92	23.76	20.52	15.84	11.88	9.72
	$\overline{K}_T$	0.55	0.59	0.58	0.53	0.58	0.65	0.62	0.64	0.61	0.54	0.52	0.52
	$\overline{T}$	9.77	11.5	16.2	23	29.1	33.3	36.1	35.7	32	26.2	17.8	11.5
Cairo	$\overline{H}$	11.84	15.60	19.32	23.15	26.32	27.95	27.10	25.23	21.97	17.86	13.24	11.12
	$\overline{K}_T$	0.56	0.60	0.61	0.63	0.66	0.68	0.67	0.66	0.66	0.65	0.59	0.56
	$\overline{T}$	14	15	17	25	27	28	28	28	26	24	19	15
Casablanca	$\overline{H}$	9.72	11.88	16.20	19.44	22.68	23.40	23.04	21.04	18.00	13.68	9.72	8.64
	$\overline{K}_T$	0.51	0.61	0.63	0.66	0.64	0.66	0.67	0.68	0.64	0.57	0.52	0.48
	$\overline{T}$	11.6	13.1	16.5	20.6	25.8	30.5	33.0	32.9	28.3	23.4	17.5	13.1
Georgia	$\overline{H}$	8.14	11.00	14.80	19.14	21.05	21.73	20.57	19.39	16.14	13.62	10.02	7.66
	$\overline{K}_T$	0.43	0.46	0.49	0.53	0.53	0.52	0.51	0.52	0.50	0.53	0.50	0.43
	$\overline{T}$	6	7	11	16	21	24	26	25	22	17	11	6
Jerusalem	$\overline{H}$	9.72	12.24	18.00	21.60	24.84	27.36	27.36	25.92	21.96	17.28	12.60	9.36
	$\overline{K}_T$	0.49	0.50	0.54	0.59	0.62	0.67	0.66	0.63	0.61	0.55	0.52	0.49
	$\overline{T}$	10.6	11.3	14.1	18.8	22.1	24.2	26.0	26.3	25.0	21.7	17.0	12.3
Texas	$\overline{H}$	9.81	12.77	16.22	18.22	20.81	23.52	23.90	21.92	18.23	15.13	11.20	9.37
	$\overline{K}_T$	0.47	0.50	0.52	0.50	0.52	0.57	0.59	0.58	0.55	0.55	0.51	0.47
	$\overline{T}$	10	12	15	20	24	28	29	29	26	21	15	11

and maximum temperatures throughout the year. However, the overall condition in terms of temperature is not much different across the province.

Seasonal and Yearly Results: In the northern hemisphere the seasons consist of: (1) Winter: December, January and February; (2) Spring: March, April and May; (3) Summer: June, July and August; (4) Autumn: September, October and November. The seasonal and yearly averaged daily HGR, clearness index and average temperature for Abarkuh, Behabad, Halvanand the city of Yazd are presented in Table 7. Apparently, they are high and despite distribution of the geographical locations are not much different; so thatthe relative difference of yearly averaged daily HGR and clearness indexfor Abrakuh, Behabad, Halvan and the city of Yazdat most is 6%. Therefore, in order to present mean values for the whole province, it is possible to average the yearly values related to the four nominated locations. In this regard the annually averaged daily HGR and clearness index for Yazd province would be 20.41 MJ/m^2 and 0. 66, respectively.

To make comparison, the seasonal and the yearly averaged daily HGR, the clearness index and the average temperature for the seven selected cities around the globehave been listed in Table 8. Comparison among the corresponding values in Tables 7 and 8 indicates that, except Arizona, the averaged seasonal and yearly HGR and clearness indexin different locations of Yazd province are higher than those of the internationally selected cities. In addition, in autumn and winter all of the nominated locations in Yazd province, except Halvan, enjoy from higher HGR and clearness index values compared to those of Arizona. This conclusion highlights the great potential of solar energy inall of the selected locations, which are geographically distributed in Yazd province.

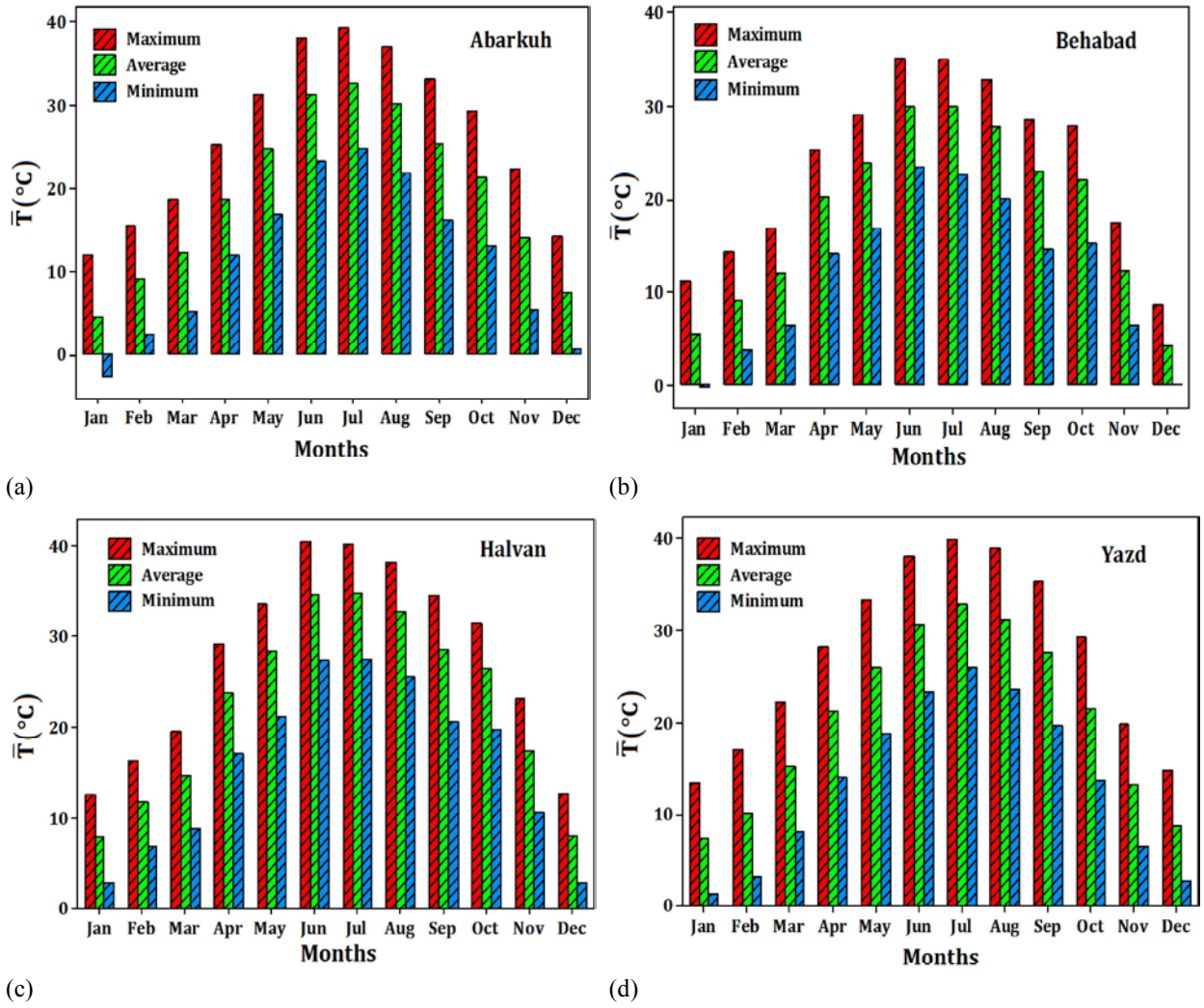

Fig. 6: Monthly maximum, average and minimum temperatures for different locations in Yazd province

Table 7: The averaged seasonal and annual daily HGR (MJ/m^2), clearness index and temperature (°C) in four locations of Yazd province

City		Winter	Spring	Summer	Autumn	Annual
Abarkuh	$\overline{H}$	13.62	23.20	27.57	18.58	20.74
	$\overline{K}_T$	0.63	0.64	0.69	0.68	0.66
	$\overline{T}$	7.2	18.6	31.3	20.3	15.5
Behabad	$\overline{H}$	12.97	23.31	27.46	19.39	20.78
	$\overline{K}_T$	0.61	0.65	0.69	0.71	0.66
	$\overline{T}$	6.2	18.7	29.2	19.1	18.3
Halvan	$\overline{H}$	11.75	22.10	26.85	17.39	19.52
	$\overline{K}_T$	0.59	0.62	0.67	0.67	0.64
	$\overline{T}$	9.2	22.2	34.1	24.1	22.4
Yazd	$\overline{H}$	13.62	22.85	27.31	18.62	20.60
	$\overline{K}_T$	0.63	0.64	0.68	0.69	0.67
	$\overline{T}$	8.7	20.8	31.6	20.7	20.5

Table 8: The mean seasonal and yearly daily HGR (MJ/m^2), clearness index and temperature (°C) in the 7 selected cities around the globe [8, 23]

City		Winter	Spring	Summer	Autumn	Yearly
Arizona	$\overline{H}$	12.59	25.90	28.45	17.95	21.22
	$\overline{K}_T$	0.61	0.73	0.71	0.68	0.68
	$\overline{T}$	11.7	20.0	31.3	22.0	21.3
Baghdad	$\overline{H}$	11.40	20.40	25.32	16.08	18.30
	$\overline{K}_T$	0.55	0.56	0.64	0.56	0.58
	$\overline{T}$	10.9	22.8	35.0	25.3	23.5
Cairo	$\overline{H}$	12.85	22.93	26.76	17.69	20.06
	$\overline{K}_T$	0.57	0.63	0.67	0.63	0.63
	$\overline{T}$	14.7	23.0	28.0	23.0	22.2
Casablanca	$\overline{H}$	10.08	19.44	22.49	13.80	16.45
	$\overline{K}_T$	0.53	0.64	0.67	0.58	0.61
	$\overline{T}$	12.6	21.0	32.1	23.1	22.2
Georgia	$\overline{H}$	8.93	18.33	20.56	13.26	15.27
	$\overline{K}_T$	0.44	0.52	0.52	0.51	0.50
	$\overline{T}$	6.3	16.0	25.0	16.7	16.0
Jerusalem	$\overline{H}$	10.44	21.48	26.88	17.28	19.02
	$\overline{K}_T$	0.49	0.58	0.65	0.56	0.57
	$\overline{T}$	11.4	18.3	25.5	21.2	19.11
Texas	$\overline{H}$	10.65	18.42	23.11	14.85	16.76
	$\overline{K}_T$	0.48	0.51	0.58	0.54	0.53
	$\overline{T}$	11.0	19.7	28.7	20.7	20.0

CONCLUSION

Every ten-minute global solar radiation and temperature data measured from January to December 2007 in Abarkuh, Behabad, Halvanand the long term daily measured data in the city of Yazd, all placed in Yazd province of Iran, were utilized to evaluate the potential of solar energy in this province. Results indicated that the yearly averaged daily HGR for Abarkuh, Behabad, Halvan and Yazd are 20. 74, 20. 78, 19. 52 and 20. 60 MJ/m^2, respectively. From the obtained data, the mean value for the whole province Yazd is 20. 41 MJ/m^2. Comparison of the status of solar radiation in Yazd province with those of some other world wide places at the same latitude showed that, except Arizona, the rank of Yazd province is superior. The yearly averaged clearness indexes for the four nominated locations are 0. 66, 0. 66, 0. 64 and 0. 67, respectively; which resultsin the mean value of 0. 66 for the whole province. In addition, the number of sunny and very sunny days, for which the daily clearness index is more than 0. 6, is 295, 288, 289 and 311, respectively. On the other word, Yazd province enjoys from sunshine hours in almost 76% of the whole day times. Due to the fact that this province has a great potential for solar investment, it is hoped that the local and central authorities will pay enough attention for providing funds and supporting installation of solar technologies in the region.

ACKNOWLEDGMENTS

The authors are grateful to the Energy Research Institute of University of Kashan for supporting present research [Grant No. 158576/9]. Our thanks are also extended to Iranian renewable energy organization (SUNA) and Iranian meteorological organization (IMO) for providing the solar data.

REFERENCES

1. Sawin, J.L., Renewables 2012 Global Status Report., 2012.
2. Panchal, H. and P. Shah, 2011. Char performance Analysis of Different Energy Absorbing Plates on Solar Stills., 2(4): 297-301.
3. Azimi, A., T. Tavakoli, H.K. Beheshti and A. Rahimia, 2012. Experimental Study on Egg plant Drying by an Indirect Solar Dryer and Open Sun Drying. Iranica Journal of Energy and Environment, 3(4): 347-353.
4. Khalil, M.H. and M. Ramzan, 2012. Development and Evaluation of a Solar Thermal Collector Designed for Drying Grain. Iranica Journal of Energy & Environment, 3(4): 380-384.
5. Mehrpooya, M. and S. Daviran, 2013. Dynamic modeling of a hybrid photovoltaic system with hydrogen/air PEM fuel cell. Iranica Journal of Energy & Environment, 4(2): 104-109.
6. Shah, N.A., M. Abbas, W.A. Syed and W. Mahmood, 2014. Physical Properties of Silver Doped ZnSe Thin Films for Photovoltaic Applications. Iranica Journal of Energy & Environment, 5(1): 87-93.
7. Oğulata, R.T. and S.N. Oğulata, 2002. Solar energy potential in Turkey. Energy Sources, 24(12): 1055-1064.
8. Islam, M., I. Kubo, M. Ohadi and A. Alili, 2009. Measurement of solar energy radiation in Abu Dhabi, UAE. Applied Energy, 86(4): 511-515.
9. De Souza, J.L., R.M. Nicácio and M.A.L. Moura, 2005. Global solar radiation measurements in Maceió, Brazil. Renewable Energy, 30(8): 1203-1220.
10. Sahin, A.Z., A. Aksakal and R. Kahraman, 2000. Solar radiation availability in the northeastern region of Saudi Arabia. Energy Sources, 22(10): 859-864.
11. Zawilska, E. and M. Brooks, 2011. An assessment of the solar resource for Durban, South Africa. Renewable Energy, 36(12): 3433-3438.
12. El Chaar, L. and L.A. Lamont, 2010. Global solar radiation: Multiple on-site assessments in Abu Dhabi, UAE. Renewable Energy, 35(7): 1596-1601.

13. Yaghoubi, M. and A. Sabzevari, 1993. Solar radiation for Shiraz, Iran: a comparative study for two periods. Renewable Energy, 3(6): 725-729.
14. Noorian, A.M., I. Moradi and G.A. Kamali, 2008. Evaluation of 12 models to estimate hourly diffuse irradiation on inclined surfaces. Renewable Energy, 33(6): 1406-1412.
15. Moeeni, S., S. Javadi, M. Dehghan Menshady and E. Esmaeeli, 2010. Estimation of solar radiation potential in the city of Yazd. Iran Energy Journal, 13(1): 71-78. In Persian.
16. Salvatipour, H., M. Abdolzadeh, H. Beheshti and M. Rahnama, 2011. Solar Energy Enhancement of a Solar Collector by an Optimum Slope Angle in Isfahan, Central Region of Iran. Energy Sources, Part A: Recovery, Utilization and Environmental Effects, 33(17): 1625-1635.
17. Behrang, M., E. Assareh, A. Noghrehabadi and A. Ghanbarzadeh, 2011. New sunshine-based models for predicting global solar radiation using PSO (particle swarm optimization) technique. Energy, 36(5): 3036-3049.
18. Dehghan, A., 2011. Status and potentials of renewable energies in Yazd Province-Iran. Renewable and Sustainable Energy Reviews, 15(3): 1491-1496.
19. Khorasanizadeh, H. and K. Mohammadi, 2013. Introducing the best model for predicting the monthly mean global solar radiation over six major cities of Iran. Energy, 51: 257-266.
20. Khorasanizadeh, H. and K. Mohammadi, 2013. Prediction of daily global solar radiation by day of the year in four cities located in the sunny regions of Iran. Energy Conversion and Management, 76: 385-392.
21. Khorasanizadeh, H., K. Mohammadi and A. Mostafaeipour, 2014. Establishing a diffuse solar radiation model for determining the optimum tilt angle of solar surfaces in Tabass, Iran. Energy Conversion and Management, 78: 805-814.
22. Kottek, M., J. Grieser, C. Beck, B. Rudolf and F. Rubel, 2006. World map of the Koppen-Geiger climate classification updated. Meteorologische Zeitschrift, 15(3): 259-263.
23. Duffie, J.A. and W.A. Beckman, 2006. Solar Engineering of Thermal Processes, 2006, John Wiley & Sons, INC. NY.
24. World Meteorological Organization (WMO), 2003. Manual on the global observing system. Volume I-Global Aspects (Annex V to the WMO Technical Regulations), WMO-No. 544.
25. World Meteorological Organization (WMO), 2008. Guide to meteorological instruments and methods of observation, Seventh edition. WMO-No. 8.
26. Yousif, C., G.O. Quecedo and J.B. Santos, 2013. Comparison of solar radiation in Marsaxlokk, Malta and Valladolid, Spain. Renewable Energy, 49: 203-206.

Persian Abstract

DOI: 10.5829/idosi.ijee.2014.05.02.09

چکیده

در این مطالعه، با استفاده از داده‌های اندازه‌گیری‌شده در چهار منطقه توزیع شده جغرافیایی ابرکوه، بهاباد، حلوان و شهر یزد در استان یزد پتانسیل انرژی خورشیدی و مشخصات آن در این استان ارزیابی شده است. برای این مناطق تابش خورشیدی کل روزانه روی سطح افقی و شاخص روزانه صافی هوا و همچنین مقادیر متوسط ماهانه، فصلی و سالانه آن‌ها بدست آمده است. نتایج نشان می‌دهند که این مناطق به‌ترتیب از ۳۰۰، ۲۹۴، ۲۸۹ و ۳۱۱ روز آفتابی بهره می‌برند و همچنین متوسط سالانه شاخص صافی هوای روزانه آن‌ها به‌ترتیب ۰/۶۶، ۰/۶۶، ۰/۶۴ و ۰/۶۷ و متوسط سالانه تابش کل روزانه آن‌ها به‌ترتیب ۲۰/۷۴، ۲۰/۷۸، ۱۹/۵۲ و ۲۰/۶۰ مگاژول بر مترمربع است. در استان یزد ۷۶ درصد از کل طول روزهای سال آفتابی هستند و متوسط سالانه تابش کل روزانه ۲۰/۴۱ مگاژول بر مترمربع و متوسط سالانه شاخص صافی هوای روزانه ۰/۶۶ است. مقایسه شرایط این چهار منطقه از استان یزد با هفت شهر انتخاب شده دنیا در عرض جغرافیایی مشابه، نشان می‌دهد که به‌جز آریزونا متوسط ماهانه تشعشع کل روزانه و متوسط ماهانه شاخص روزانه صافی هوای این مناطق بیشتر از شهرهای منتخب دیگر است. با توجه به پتانسیل بالای انرژی خورشیدی در استان یزد، تلاش و سرمایه‌گذاری بیشتری در زمینه توسعه استفاده از انرژی خورشیدی ضروری به‌نظر می‌رسد.

Iranica Journal of Energy & Environment 5 (2): 184-191, 2014
ISSN 2079-2115
IJEE an Official Peer Reviewed Journal of Babol Noshirvani University of Technology
DOI: 10.5829/idosi.ijee.2014.05.02.10

BUT

Characterisation of Liquid Derived from Pyrolysis Process of Charcoal Production in South of Thailand

Abdulrahim Saad and S.B. Ratanwilai

Department of Chemical Engineering, Faculty of Engineering,
Prince of Songkla University, Hat Yai, Songkhla 90112, Thailand

Received: April10, 2014; **Accepted** in Revised Form: June 6, 2014

Abstract: Pyrolysis liquid obtained from local suppliers in Phatthalung Province, Thailand was separated in conventional vacuum distillation into light and heavy fractions. The physiochemical characteristics and thermal behaviour of the fractionated pyrolysis liquid were investigated. It was found that light fraction had higherwater content and stronger acidity than heavy fraction and pyrolysis liquid. The heating value of light fraction was lower than those of the pyrolysis liquid and heavy fraction. The heating value of heavy portion was almost double that of the light fraction. The thermal behaviours of the pyrolysis liquid and the two fractions were determined. The light fraction had the highest decomposition rate and the lowest residual yield; in contrast to heavy fraction had slow weight loss through a wide range of temperatures and it had the highest residual yield. The chemical composition of the pyrolysis liquid and the two fractions were analysed by GC-MS. The chemical distribution differed for the fractions and the pyrolysis liquid. The light fraction was dominated by acetic acid and the heavy fraction was mainly composed phenolic compounds.

Key words: Pyrolysis liquid · Vacuum distillation · Light fraction · Heavy fraction · Physiochemical characterization

INTRODUCTION

Biomass represents a potential alternative source of energy to replace fossil fuels. It has attracted great attention as a renewable energy source after the global oil crisis in 1970s [1, 2]. In addition, biomass is considered the only current sustainable source to produce energy-related products, including electricity, heat and valuable chemicals, such as resins, flavourings and other materials [3, 4]. Furthermore, biomass is an environmentally-friendly candidate because it contains a low content of sulphur [5, 6].

The pyrolysis of biomass has been used for ages to produce charcoal and currently the slow-pyrolysis process is widely used for producing so-called biochar [7, 8]. However, extensive attention has been focused recently on fast pyrolysis to obtain pyrolysis liquid (pyrolysis oil) [9]. Pyrolysis oil is a complex, oxygenated compound with a wide range of boiling temperatures that contains nearly 400 known compounds, primarily of phenolic compounds, organic acids, aldehydes, ketones, esters and water [10, 11].

Currently, pyrolysis oil has attracted considerable interest due to its several applications in industry. Althoughit has been proven to be a promising alternative to petroleum fuels, it also has potential for use in producing value-added chemicals for the pharmaceutical, food and paint industries [2, 12].

The pyrolysis oil mixture is quite complex and there has been significant interest in studying its chemical composition and thermal behaviour. Hence, its chemical and physical properties have been extensively discussed in literature [13-15].

A great deal of work has been done on fractionation and characterization of pyrolysis oil and different methods and techniqueshave been used. Garcia-Perezet *et al*. [16] used different solvents to fractionate pyrolysis oil into six fractions, which were characterized by GC-MS,

Corresponding Author: Abdulrahim Saad, Department of Chemical Engineering, Faculty of Engineering,
Prince of Songkla University, Hat Yai, Songkhla 90112, Thailand.
Tel: +66874755690, E-mail: abdorahim@hotmail.com

Please cite this article as: Saad A. and S.B. Ratanwilai, 2014. Characterisation of liquid derived from pyrolysis process of charcoal production in south of Thailand. Iranica Journal of Energy and Environment, 5(2):184-191.

hermogravimetric techniques (TG) and gel permeation chromatography (GPC). A similar investigation was conducted by Sipila *et al*. [17] and they have reported the physiochemical properties and fuel characteristics of the water-soluble and water-insoluble fractions of flash pyrolysis oil. They also compared the properties and characteristics of these two fractions with those of the whole pyrolysis oil.

Apart from solvent extraction techniques, Wang, *et al*. [18-20] used molecular distillation techniques to separate pyrolysis oil into several fractions using different operational parameters and then studied the physiochemical characteristics of the fractions.

To a great extent, Thailand is an agriculture-based country and it has the potential for producing energy from biomass equivalent to about 25-30% of its primary energy needs; in addition, rubber wood is regarded as one of the most important sources of biomass and it is planted extensively in the peninsular area in southern Thailand [21]. Rubber wood has been utilised to a great extent by local farmers and small plants to produce charcoal, which is carried in conventional, slow-pyrolysis process. The pyrolysis liquid, called 'wood vinegar' locally, is produced as a by-product from the production of charcoal and it is used extensively by farmers in growing and protecting plants as well as to improve the quality of the soil [22].

To the best of our knowledge, few studies have been conducted on the physiochemical properties of pyrolysis liquid produced from the slow pyrolysis of wood in the process of charcoal production. Most of the studies focused on the fast pyrolysis oil; hence, the purpose of our work was to use vacuum distillation to separate the liquid produced by the slow pyrolysis of wood into fractions and then determine the chemical and physical properties of the fractions.

Pyrolysis liquid was collected from different producers in Phatthalung, one of the southern provinces in Thailand and conventional vacuum distillation was conducted to fractionate the liquid into two fractions. The pyrolysis liquid and its fractions were analysed using GC-MS. The physical properties of the pyrolysis liquid and its two fractions were investigated, including heating value, pH, colour and thermal stability.

MATERIALS AND METHODS

Crude Pyrolysis Liquid: The crude pyrolysis liquid was obtained from local suppliers in Phatthalung Province. The suppliers produced the liquid as a by-product from the slow pyrolysis of wood in the process of making charcoal. The biomass source they used for making charcoal was mainly rubber wood. First, the crude pyrolysis liquid was treated to reduce water and remove the fine particles using evaporation and filtration, respectively.

Pyrolysis Liquid Fractionation: After the crude pyrolysis liquid was treated as described, the treated liquid was fractionated into two fractions. The fractionation was conducted in a conventional, vacuum-distillation facility at 60-70°C and 60-10 mmHg. The fractions collected from the distillation process were labelled as the light fraction (LF) and the heavy fraction (HF). The LF, which contained the light components, was vaporized, condensed and collected at room temperature. The HF, which contained the heavy components,could not be vaporized and collected as a residual fraction.

GC-MS Analyses: The compounds in the pyrolysis liquid and its fractions were identified with a Trace GC Ultra/ISQMST equipped with a capillary column of 30 m long×0.25 mm × 0.25 µm film thickness. The oven temperature was programed to increase from 35 to 245°C. The data were acquired with Xcalibur software using the Wiley mass spectra library's.

Thermogravimetric Analysis and Physical Characteristics: The physical properties were measured to determine heating value, pH, water content

Table 1: Analysis methods and instruments used for physical characterisation

Physical Property	Method and Instrument
Heating value	CHNS/O Analyser, Flash EA 1112 Series
	Automatic calculation of GHV (Gross Heat Value) and NHV (Net Heat Value) using Eager 300 software.
pH	pH meter
	Water content Coulometric Karl Fischer titration method
	First, the sample was diluted with methanol and then analysed using a Karl Fischer titrator. A mass balance was used to determine the water content of the sample.
Appearance	Visual observation

and appearance of the pyrolysis liquid, light and heavyfractions. They were analysed according to the methods listed in Table 1. Thermogravimetry (TG) and Derivative thermogravimetric (DTG) profiles of the pyrolysis liquid, light fraction and heavy fraction were assessed by a thermogravimetric analyser (Perkin Elmer TGA 7). The conditions were controlled under a nitrogen purge gas at temperatures ranging from 50 to 1000°C with a heating rate of 10°C/min.

RESULTS AND DISCUSSION

GC-MS Characterization of the Pyrolysis Liquid and its Fractions: Several compounds were identified by the GC-MS analyses. The total ion chromatogram of the pyrolysis liquid in Figure 1 and Table 2 show the top 20 compounds of the pyrolysis liquid. Acetic acid had the highest concentration and it was followed by a group of abundant phenolic compounds. Among the phenolic compounds, syringol was the most abundant and it was followed by ketones, pyridines, sugars and acids in that order. Generally, the chemical composition was almost in agreement with that reported by Branca e*t al*. [23] for pyrolysis liquid. In addition, Noor et al. conducted similar work using slow pyrolysis of cassava wastes for biochar production [8].

Figure 2 shows the GC-MS total ion chromatograms of the two fractions obtained from the vacuum distillation of the pyrolysis liquid. It was obvious that the distributions of the components differed in the two fractions and in the pyrolysis liquid. As illustrated in Figure 3, the compounds in the fractions were classified into different groups, such as acids, esters, phenols and ketones, according to their chemical structures.

Table 3 shows that the light fraction was dominated by acetic acid, followed by acetol. Some phenols were partially distilled during the distillation process and they were present in trace amounts in the light fraction, although the rest of the phenolic compounds were not present. Table 4 shows that the heavy fraction was composed mainly of 2, 6-dimethoxyphenol, followed by high-molecular weight phenols, ketones, pyridines, sugar and some acids.

Furthermore, it was noted that more compounds were detected in the two fractions than in the pyrolysis liquid due to thermal cracking process of conventional distillation that had a long residence time and a relatively high temperature. As a result, the thermo-sensitive pyrolysis liquid was not completely vaporized and as a result, some compounds reacted, producing additional compounds [24].

Physical Characteristics of the Pyrolysis Liquid and its Fractions: Table 5 presentsthe principal physical properties of the pyrolysis liquid and its fractions. The pyrolysis liquid was a light-black liquid with a 30% water content, a pH value of 3.72 and a heating value of about 21 MJ/kg. The light fraction, which had good fluidity, was dark yellow with a high water content of 60%; in contrary, the heavy fraction had poor fluidity, was dark black with a relatively low water content of 1.5%. Moreover, the heating value of the light fraction was much lower than that of the heavy fraction. The heating value heavy fractionwas almost double that of the light fraction. Earlier work has proven that the heating value depends mostly on the chemical composition and the water content [5]. In addition, it was noted that the light fraction had the lowest pH value due to its content of acids, particularly acetic acid, which had the highest concentration among all of the components in the light fraction.

Thermogravimetric Analysis: In our study, we used thermogravimetric analysis (TGA) to investigate the thermal stability of the pyrolysis liquid and its fractions. The results of TGA were useful in studying and predicting the properties of the pyrolysis liquid and its fractions. Figure 4 shows the thermal behaviour of the pyrolysis liquid and its fractions at a heating rate of 10°C/min. The pyrolysis liquid was evaporated and decomposed over the temperature range of 25-1004°C; it had its maximum weight loss at 120°C (DGT plot) and its final residue yield at 1004°C was 2%. However, the light fraction, which had the highest rate of decomposition, evaporated mostly in the range of 25-186°C; its maximum weight loss occurred at 161°C (DGT plot) due to the release of water vapour (moisture content was 60%) and compounds that had low boiling points. The yield of the final residue was 0.1% at 1004°C. The heavy fraction had a different thermal behaviour from the light fraction. It had slow weight loss over a wide range of temperatures, *i.e*., 35-110°C, due to the presence of compounds with higher boiling points and it had its maximum weight loss at 227°C (DGT plot). The yield of the final residue was 20% at 110°C.

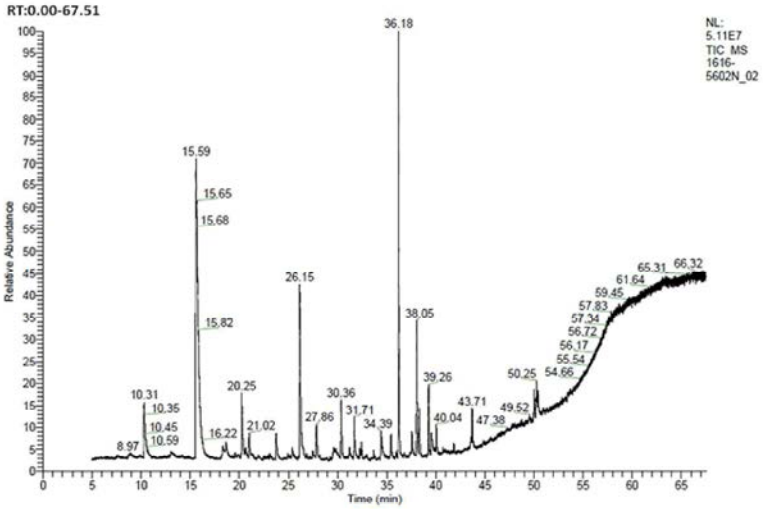

Fig. 1: Total ion GC-MS chromatograms of the pyrolysis liquid

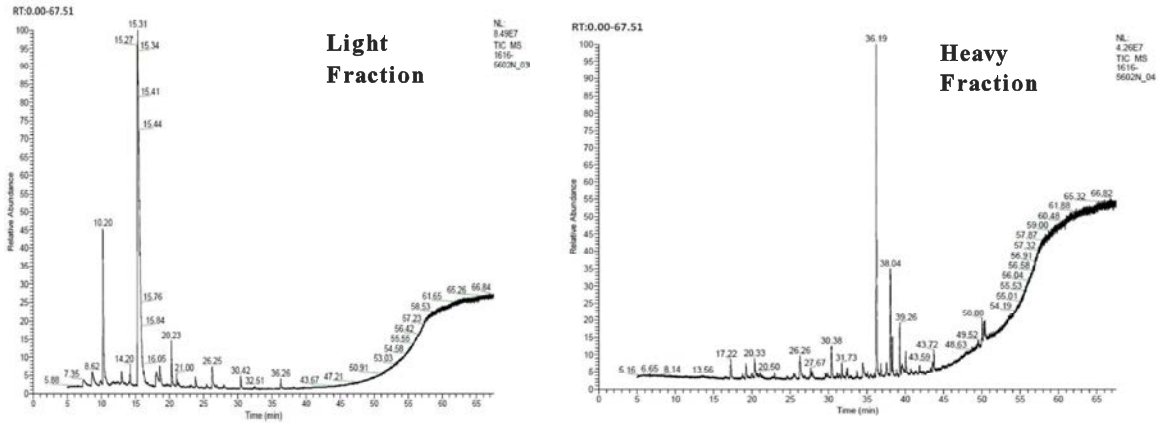

Fig. 2: Total ion GC-MS chromatograms of the two fractions obtained from the pyrolysis liquid using conventional vacuum distillation at 60-70°C and 60-10 mmHg

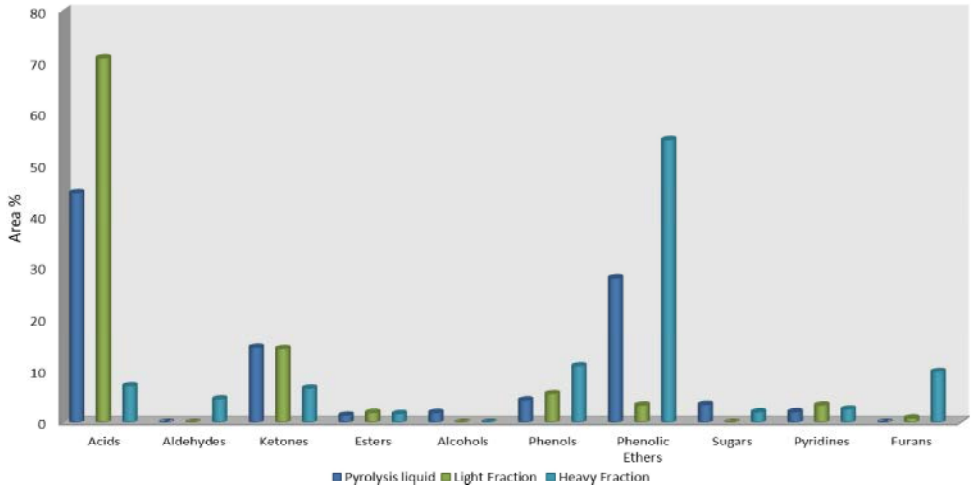

Fig. 3: Chemical distribution of the pyrolysis liquid and its two fractions

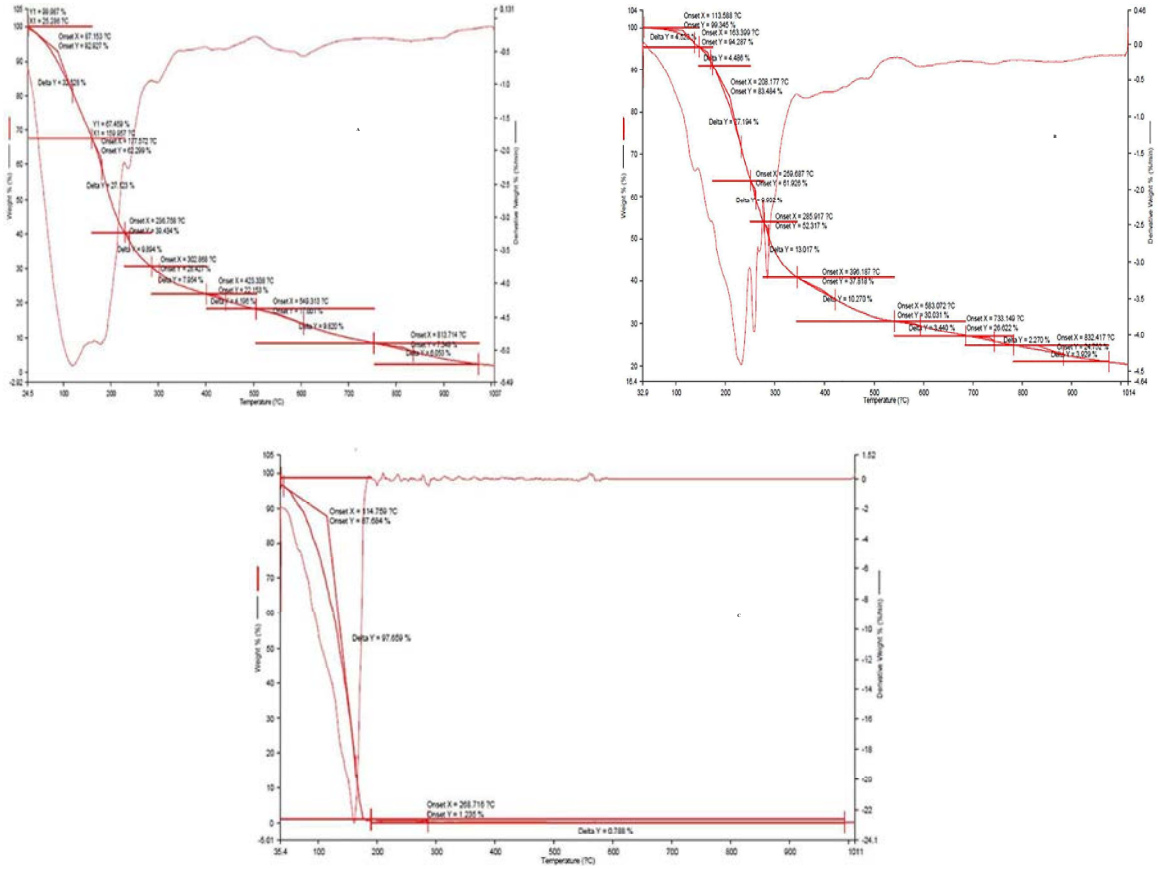

Fig. 4: TG and DTG at a heating rate of 10°C/min for (A) pyrolysis liquid, (B) heavy fraction and (C) light fraction

Table 2: Main chemical composition of the pyrolysis liquid identified by GC–MS

	Composition	MW	Formula	Peak area %[a]
1	Acetic acid	60	$C_2H_4O_2$	37.30
2	Syringol	154	$C_8H_{10}O_3$	15.27
3	Corylon	112	$C_6H_8O_2$	9.85
4	4-Methoxy-3-(methoxymethyl)phenol	168	$C_9H_{12}O_3$	4.89
5	Acetol	74	$C_3H_6O_2$	4.66
6	4-Chlorobutyric acid	122	$C_4H_7ClO_2$	3.53
7	Phenol	94	C_6H_6O	2.43
8	2,6-Dihydroxy-4-methoxyacetophenone	182	$C_9H_{10}O_4$	2.31
9	Butyryl oxide	158	$C_8H_{14}O_3$	2.19
10	Anhydro - sugar	132	$C_5H_8O_4$	1.96
11	3-Pyridinol	95	C_5H_5NO	1.87
12	3,4,8-Trimethyl-2-none-1-ol	182	$C_{12}H_{22}O$	1.84
13	Syringyl acetone	126	$C_7H_{10}O_2$	1.47
14	Ethyl cyclopentenolone	180	$C_{10}H_{12}O_3$	1.81
15	1-(4-Hydroxy-3-methoxyphenyl)acetone	166	$C_{10}H_{14}O_2$	1.70
16	p-Butoxyphenol	210	$C_{11}H_{14}O_4$	1.55
17	3,4-Anhydro-d-galactosan	144	$C_6H_8O_4$	1.39
18	Levulinic acid	116	$C_5H_8O_3$	1.35
19	à-Furanone	84	$C_4H_4O_2$	1.35
20	2-hydroxy-4 6-dimethoxy acetophenone	196	$C_{10}H_{12}O_4$	1.28

The composition of the pyrolysis liquid estimated by the peak area% of GC-MS

Table 3: Main chemical composition of the light fraction identified by GC–MS

	Composition	Mw	Formula	Peak area %[a]
1	Acetic acid	60	$C_2H_4O_2$	67.96
2	Syringol	154	$C_8H_{10}O_3$	0.48
3	Corylon	112	$C_6H_8O_2$	1.88
4	4-Methoxy-3-(methoxymethyl)phenol	168	$C_9H_{12}O_3$	2.9
5	Acetol	74	$C_3H_6O_2$	11.36
6	4-Chlorobutyric acid	122	$C_4H_7ClO_2$	2.88
7	Phenol	94	C_6H_6O	0.73
8	Pyridine, 4-methyl	93	C_6H_7N	2.67
9	Hydrazine, n-propionyl-N-methyl-	102	$C_4H_{10}N_2O$	1.99
10	Trimethylorthoacetate	120	$C_5H_{12}O_3$	1.11
11	1-Hydroxy-2-butanone	88	$C_4H_8O_2$	1.08
12	4-Hydroxybut-2-enoic acid lactone	84	$C_4H_4O_2$	0.8
13	2-Hydroxyethyl acetate	104	$C_4H_8O_3$	0.74
14	3,5-Dimethylpyridine	107	C_7H_9N	0.37
15	Pyridine	79	C_5H_5N	0.34
16	1,3,5-Trimethyl-2-octadecylcyclohexane	378	$C_{27}H_{54}$	0.26

The composition of the light fraction estimated by the peak area% of GC-MS

Table 4: Main chemical composition of the heavy fraction identified by GC–MS

	Composition	Mw	Formula	Peak area %[a]
1	Syringol	154	$C_8H_{10}O_3$	34.22
2	Corylon	112	$C_6H_8O_2$	4.47
3	4-Methoxy-3-(methoxymethyl)phenol	168	$C_9H_{12}O_3$	11.52
4	4-Chlorobutyric acid	122	$C_4H_7ClO_2$	3.44
5	Phenol	94	C_6H_6O	3.9
6	2,6-Dihydroxy-4-methoxyacetophenone	182	$C_9H_{10}O_4$	5.58
7	Butyryl oxide	158	$C_8H_{14}O_3$	2.61
8	Anhydro– sugar	132	$C_5H_8O_4$	1.76
9	3-Pyridinol	95	C_5H_5NO	2.75
10	3,4,8-Trimethyl-2-none-1-ol	182	$C_{12}H_{22}O$	4.18
11	Syringyl acetone	126	$C_7H_{10}O_2$	2.4
12	Tetrahydro-2-methyl-2-Furanol	102	$C_5H_{10}O_2$	3.66
13	1,4-Benzenediol	110	$C_6H_6O_2$	3.6
14	3,4,5-Trimethoxybenzaldehyde	196	$C_{10}H_{12}O_4$	3.51
15	Dihydro-5-(hydroxymethyl)-2(3h)-furanone	116	$C_5H_8O_3$	2.91
16	Tetrahydrofuran, 2-hexyl-	102	$C_5H_{10}O_2$	2.31
17	Butanoic acid, butyl-1,1-d2 ester	144	$C_8H_{14}D_2O_2$	1.53
18	m-Cresol	108	C_7H_8O	1.21

The composition of the heavy fraction estimated by the peak area % of GC-MS

Table 5: Physical properties of pyrolysis liquid and its fractions

		Heating value (MJ/kg)			
Sample	Appearance	GHV	NHV	Water content (% w/w)	pH value
Pyrolysis liquid	Light black	22	21	30	3.72
Light fraction	Dark yellow	14	12	60	2.67
Heavy fraction	Dark black	28	27	1.5	4.50

CONCLUSIONS

Vacuum distillation was used to fractionate a woody pyrolysis liquid obtained from local suppliers in Phatthalung Province. Fractionation has shown to be a useful technique to assess the whole pyrolysis liquid with respect to physiochemical characteristics of its fractions. The compositions of the pyrolysis liquid, its light fraction and its heavy fraction were experimentally determined and classified into different groups according to their chemical structures. It was obvious that the chemical compositions of the pyrolysis liquid and its two fractions were all different. The light fraction had high water content and strong acidity;

however, the pyrolysis liquid and its heavy fraction had relatively low acidity and low water content. The heating value of the light fraction was lower than those of the pyrolysis liquid and its heavy fraction, whereas the heavy fraction's heating value was almost double that of the light fraction. The thermal behaviour results that were obtained indicated that the light fraction had the highest rate of decomposition and the lowest residual yield; in contrast, the heavy fraction had a slow weight loss over a wide range of temperatures and it had the highest residual yield.

The results of this study demonstrated that the pyrolysis liquid produced during the process of charcoalproductionhas the potentialfor more extensive and beneficial use. For instance, the light fraction, which has high acetic acid and water contents, can be used as a feedstock for producing pure acetic acid, whereas the heavy fraction can be directed to further processing and upgrading for use as a fuel. It also could be used as the raw material for producing a number of valuable chemicals, which could be more attractive and beneficial than using it to make fuels.

ACKNOWLEDGEMENTS

The authors are thankful for the financial support granted from graduate school of Prince of Songkla University and very grateful to the scientists of scientific equipment centre, who performed some of theanalysis, reported in this paper.

REFERENCES

1. Demirbas, A., 2007. Progress and recent trends in biofuels. Progress in energy and combustion science, 33(1): 1-18.
2. Bridgwater, A.V. and G. Grassi, 1991. Biomass pyrolysis liquids: upgrading and utilisation: Springer.
3. Huber, G.W., S. Iborra and A. Corma, 2006. Synthesis of transportation fuels from biomass: chemistry, catalysts and engineering. Chemical reviews, 106(9): 4044-4098.
4. Dodds, D.R. and R.A. Gross, 2007. Chemicals from biomass. Science, 318(5854): 1250-1251.
5. Jenkins, B., L. Baxter, T. Miles Jr and T. Miles, 1998. Combustion properties of biomass. Fuel Processing Technology, 54(1): 17-46.
6. Patel, B. and B. Gami, 2012. Biomass Characterization and its Use as Solid Fuel for Combustion. Iranica Journal of Energy and Environment, 3: 123-128.
7. Noor, N.M., A. Shariff and N. Abdullah, 2012. Slow Pyrolysis of Cassava Wastes for Biochar Production and Characterization. Iranica Journal of Energy and Environment, 3(5): 60-65.
9. Bridgwater, A. and G. Peacocke, 2000. Fast pyrolysis processes for biomass. Renewable and Sustainable Energy Reviews, 4(1): 1-73.
10. Mohan, D., C.U. Pittman and P.H. Steele, 2006. Pyrolysis of wood/biomass for bio-oil: a critical review. Energy and Fuels, 20(3): 848-889.
11. Czernik, S. and A. Bridgwater, 2004. Overview of applications of biomass fast pyrolysis oil. Energy and Fuels, 18(2): 590-598.
12. Chiaramonti, D., A. Oasmaa and Y. Solantausta, 2007. Power generation using fast pyrolysis liquids from biomass. Renewable and Sustainable Energy Reviews, 11(6): 1056-1086.
13. Elliott, D.C., Analysis and comparison of biomass pyrolysis/gasification condensates: Final report, 1986, Pacific Northwest Lab., Richland, W.A. (USA).
14. Peacocke, G., P. Russell, J. Jenkins and A. Bridgwater, 1994. Physical properties of flash pyrolysis liquids. Biomass and Bioenergy, 7(1): 169-177.
15. Oasmaa, A. and P. Koponen, 1997. Physical characterisation of biomass-based pyrolysis liquids: Espoo.
16. Garcia-Perez, M., A. Chaala, H. Pakdel, D. Kretschmer and C. Roy, 2007. Characterization of bio-oils in chemical families. Biomass and Bioenergy, 31(4): 222-242.
17. Sipilä, K., E. Kuoppala, L. Fagernäs and A. Oasmaa, 1998. Characterization of biomass-based flash pyrolysis oils. Biomass and Bioenergy, 14(2): 103-113.
18. Guo, X., S. Wang, Z. Guo, Q. Liu, Z. Luo and K. Cen, 2010. Pyrolysis characteristics of bio-oil fractions separated by molecular distillation. Applied Energy, 87(9): 2892-2898.
19. Guo, Z., S. Wang, Y. Gu, G. Xu, X. Li and Z. Luo, 2010. Separation characteristics of biomass pyrolysis oil in molecular distillation. Separation and Purification Technology, 76(1): 52-57.
20. Wang, S., Y. Gu, Q. Liu, Y. Yao, Z. Guo, Z. Luo and K. Cen, 2009. Separation of bio-oil by molecular distillation. Fuel Processing Technology, 90(5): 738-745.
21. Krukanont, P. and S. Prasertsan, 2004. Geographical distribution of biomass and potential sites of rubber wood fired power plants in Southern Thailand. Biomass and Bioenergy, 26(1): 47-59.

22. Chalermsan, Y. and S. Peerapan, 2010. Wood-vinegar: by-product from rural charcoal kiln and its roles in plant protection. Asian Journal of Food and Agro-Industry, 2: 189-195.
23. Branca, C., P. Giudicianni and C. Di Blasi, 2003. GC/MS characterization of liquids generated from low-temperature pyrolysis of wood. Industrial and Engineering Chemistry Research, 42(14): 3190-3202.
24. Bridgewater, A.V., 2004. Biomass fast pyrolysis. Thermal Science, 8(2): 21-50.

Persian Abstract

DOI: 10.5829/idosi.ijee.2014.05.02.10

چکیده

مایع پیرولیز به دست آمده از منابع محلی در ایالت فتالونگ تایلند، بوسیله روش متداول تقطیر جزء به جزء (سبک و سنگین) در خلاء تفکیک گردید. خصوصیات فیزیکوشیمیایی و رفتار حرارتی مایع پیرولیز مورد بررسی قرار گرفت. مشخص شد که جزء سبک تر میزان آب بیشتر و اسیدیته قوی تری از جزء سنگین و مایع پیرولیز دارد. ارزش حراراتی جزء سبک تر کمتر از مایع پیرولیز و جزء سنگین بوده و ارزش حراراتی جزء سنگین تقریبا دو برابر جزء سبک بوده است. رفتار حرارتی مایع پیرولیز و دو جزء سبک و سنگین نیز محاسبه گردیده که جزء سبک دارای بالاترین سرعت تجزیه و پایین ترین بازده مواد باقیمانده بود؛ در مقابل آن، جزء سنگین آهنگ کاهش وزن کند در طیف گسترده ای از دما، و حداکثر بازده مواد باقیمانده را دارد. ترکیب شیمیایی مایع پیرولیز و دو جزء توسط جذب اتمی مورد تجزیه و تحلیل قرار گرفت. توزیع شیمیایی برای دو جزء و مایع پیرولیز متفاوت بوده و جزء سبک تر از اسید استیک و جزء سنگین تر عمدتا از ترکیبات فنلی می‌باشد.

Iranica Journal of Energy & Environment 5 (2): 192-201, 2014
ISSN 2079-2115
IJEE an Official Peer Reviewed Journal of Babol Noshirvani University of Technology
DOI: 10.5829/idosi.ijee.2014.05.02.11

BUT

Degradation of Water Resources by Agricultural Pesticides and Nutrients, Weruweru, Tanzania

[1]Jokha Mohamed, [1]Shadrack Murimi and [2]Charles Kihampa

[1]Department of Geography, Kenyatta University, P.O. Box 43844-00100, Nairobi, Kenya
[2]School of Environmental Science and Technology,
Ardhi University, P.O. Box 35176, Dar es Salaam, Tanzania

Received: May 8, 2014; **Accepted** in Revised Form: June 6, 2014

Abstract: Agrochemicals nutrients and residues of pesticides in surface water and sediments samples of Weruweru sub-catchment were investigated to determine their concentrations and quality of water for human consumption. Plant nutrients NO_3^-, NO_2^-, NH_3 and PO_4^{-3} concentrations ranging from 0.005 to 0.96 mg/L were detected in surface water samples. Pesticides residues cyanazine, α-chlordane, endosulfan sulphate, *p,p'*-DDT, *p,p'*-DDD, *p,p'*-DDE, lindane and cypermethrin concentrations ranging from below detection limit to 45.7 µg/l and below detection limit to 157 µg/kg dw were detected in surface water samples and sediments samples, respectively. In most sites, nutrients and pesticides residues concentrations were below the maximum limits as per WHO and national limits for drinking water. The agrochemical contaminants were considered to originate from agricultural runoff and weathered agricultural soils. All parameters were measured by standard methods.

Key words: Agrochemicals · Nutrients · Pesticides · Surface water · Sediments

INTRODUCTION

Agrochemical is a common term encompassing various chemical products that are used in agricultural activities. It refers to the wide range of pesticides, synthetic fertilizers, hormones and other chemical growth agents as well as concentrated stores of raw animal manure. The majority of agrochemicals are pesticides and plant nutrients, which are used to control pests' invasion, control of vectors of human and animal diseases and improve soil fertility [1]. The widespread use of these chemicals over the past half-century has led to their detection in many hydrological systems of many countries [2]. Despite the fact that pesticides and nutrients pollution in aquatic environment can also originate from other sectors, agriculture is undoubtedly seen as the most important source of this contamination [3]. The major concerns are the ways in which they are applied and handled that pose threat of diffuse water pollution. Farmers have inadequate knowledge in pesticides and nutrients use and they rely on the directives given by pesticides dealers. Other problems include use of repackaged products, lack of safety equipments, unsafe storage facilities, unlabelled, or labeled in unfamiliar languages and complex instructions that are difficult to apply [4]. Pesticides and nutrients from areas under agriculture activities can therefore reach the aquatic environment through direct runoff, leaching, careless disposal of empty containers and equipment washings.

In addition to reducing the ecological status of river systems, pesticides and nutrients can have significant social and economic costs through polluting drinking and bathing waters, degrading fisheries and potentially increasing food risks [5]. Excess nitrogen and phosphates in rivers, lakes, reservoirs and ponds can lead to massive overgrowth of algae and deplete the oxygen levels that fish, shellfish and other aquatic organisms need to survive. High level of nitrogen in drinking water can pose particular risk to infants and children. For example, the blue baby syndrome is a common health effect in children arising from high levels of nitrogen in drinking water. Galloway and Cowling [6] reported that chemicals used to disinfect drinking water such as chlorine can react with

Corresponding Author: Charles Kihampa, School of Environmental Science and Technology, Ardhi University, P.O. Box 35176, Dar es Salaam, Tanzania. Tel: +255 713 269069, Fax: +255 22 2775391, E-mail: kihampa@yahoo.com.

Please cite this article as: Jokha M., S. Murimi and C. Kihampa, 2014. Degradation of water resources by agricultural pesticides and nutrients, Weruweru, Tanzania. Iranica Journal of Energy and Environment, 5(2):192-201.

algae in water to form disinfection byproducts that have been associated with reproductive and developmental health problems. Pesticides are poisonous by nature and are intended to kill, destroy or control animals and plant species which interfere with agricultural processes or are vectors of human diseases. Environmental contamination of natural waters by pesticide residues is of great concern. Water pollution by pesticides can affect many non-targeted biological systems, such as fish, birds, beneficial insects and plants. They may take very long time to clear and can pose danger of bioaccumulation [7]. Some pesticides are endocrine disruptors that mimic or antagonise natural hormones in the body. Such pesticides are linked to human health effects such as immune suppression, hormone disruption, diminished intelligence, reproductive abnormalities and cancer [8]. Assessment of organochlorine pesticides in water and sediments of rivers from agricultural areas of most countries shows that pesticides and other toxic agriculture chemicals are increasingly polluting the aquatic environments [9-11]. Thus, with continuously high influx of agriculture products from increased population in Weruweru sub-catchments the magnitude of the problem cannot be underestimated. Unfortunately, there is lack of information related to pesticide and nutrients contamination levels in the sub-catchment of Pangani river basin, in Tanzania. The study was therefore undertaken in order to ascertain the levels of plants nutrients and pesticides residues in selected surface water and sediments of Weruweru sub-catchment. An understanding of the effects of pesticides and nutrients contaminations is a positive step towards addressing the imminent problems posed to biological organisms and proposes some remedial approaches in Weruweru sub-catchment area.

Findings of this study can be used as baseline information towards management of water quality in the study area and may be replicated other watersheds with similar agricultural activities and population scenarios.

MATERIALS AND METHODS

Study Area: MapWindow GIS version 4.3, software delineated the watershed and drainage network of Weruweru sub-catchment from Enhanced Thematic Mapper (+ETM, 2006) Landsat imagery. The computed watershed was then draped over Shuttle Radar Topographic Mission (srtm, 30 x 30m^2) satellite 3DEM through 3DEM software (Figure 1). Figure 2 depicts the 3D perspective view of 432 FCC of Weruweru River watersheds showing the 3 zones. The computed watershed covers an area of 250.646 km^2, located at the southern base of Mount Kilimanjaro in the north-western part of Pangani River Basin (PRB), Kilimanjaro region, Tanzania (Figure 3). It is situated at latitudes 3°00' to 3°30'S and longitudes 36° 30' to 37°15'E. The altitude above sea-level ranges between approximately 700 m at the confluence with Kikafu River to over 4,360 m at the snowline of Mount Kilimanjaro. The sub-catchment is characterized by steep slope valleys to gentle slopes, lowlands and in a few areas valley side slopes (Figures 1 and 2). Weruweru sub-catchment is estimated to have a total population of 196,800 people, distributed in upper, middle and lower zones. The upper zone supports production of coffee; middle zone supports maize and vegetables, while the lower zone supports production of vegetables and tropical fruits. The three zones also support livestock rearing that includes dairy and beef cattle, sheep, poultry, goats and pigs.

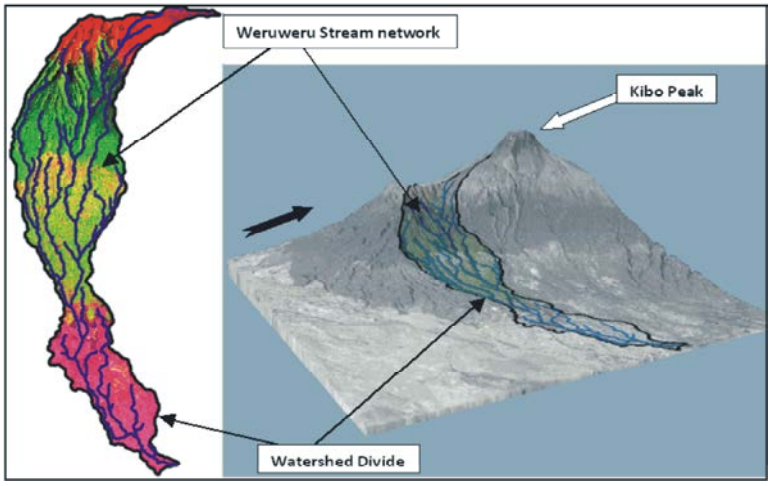

Fig 1: Delineated watershed and stream network of Weruweru River

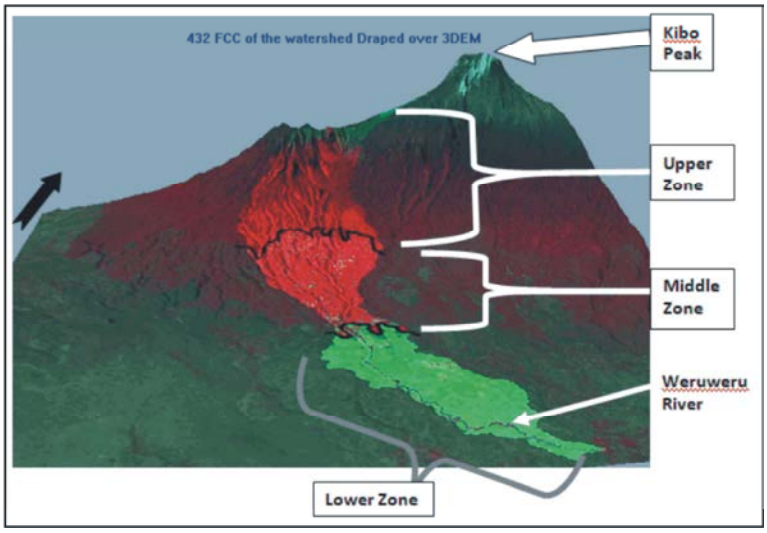

Fig 2: 3D perspective view of 432 FCC of Weruweru River watersheds showing the 3 zones

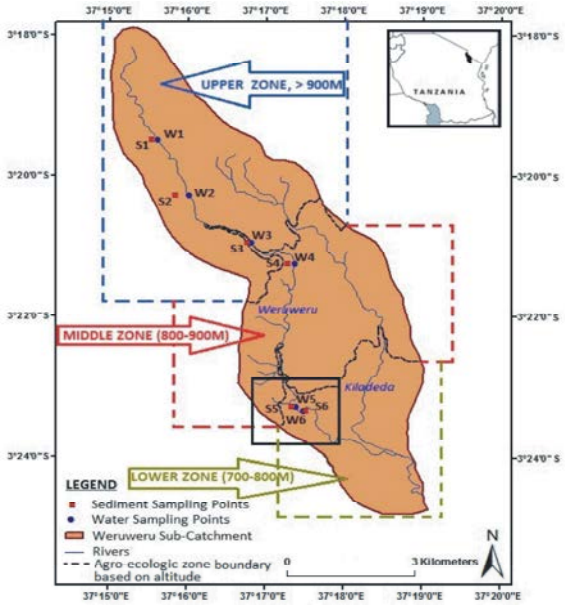

Fig 3: Map of Weruweru sub-catchment showing sampling points in the three zones

The length of Weruweru River starting from the upper zone to the confluence of Kiladeda is about 17.9 km and about 19.0 km to the sub-catchment. The river is a tributary of the large PRB and it joins the Pangani River through Kiladeda River [12].

Sample Collection: Water and sediments samples were concurrently collected from 6 selected sampling sites (two from each zone) during the dry (February 2013) and rainy (April 2013) seasons. The sites were selected based on the qualitative information obtained from key stakeholders and 3DEM software algorithms. The locations were divided into three zones based on their respective heights above sea-levels (a.s.l.). The zones lower zone (below 800 m), middle zone (between 800 – 1200 m) and upper zone (above 1200 m) were assumed to approximate agro-ecological units in the study area (Figure 2). Details of sampling sites are described in Table 1 and indicated in the sub-catchment map in Figure 3. The indication of sampling sites in the sub-catchment map was enabled by Global Position System (GPS) points that were measured during sampling campaigns.

Table 1: Description of the Sampling Sites in Weruweru Sub-catchment

Site	Sampling Site	Coordinates	Site characteristics
W1&S1	Upper zone (1)	03°19' 8.13''S 37°15' 9.26''E	Human settlements, farming activities (coffee), domestic activities (fetching water and washing)
W2&S2	Upper zone (2)	03°19' 8.32''S 37°15' 9.15''E	Human settlements, farming activities (coffee and livestock) and domestic activities (fetching water and washing). Water flows to middle zone of the river
W3&S3	Middle zone (1)	03°21' 3.37''S 37°17' 5.07''E	Human settlements, farming activities (maize, banana and vegetables such as cucumbers, tomatoes, green vegetables), fetching water and animals drinking
W4&S4	Middle zone (2)	03°21' 0.3''S 37°17' 5.23''E	Human settlements, farming activities (maize, banana and vegetables) and domestic activities (fetching water) and livestock. Water flows to the lower zone of the river
W5&S5	Lower zone (1)	03°23' 10.3''S 37°17'11.33''E	Human settlements, farming activities (tropical fruits, beans and vegetables such as tomatoes, green vegetables, cucumbers, onions) and livestock, domestic activities (fetching water, bathing and washing)
W6&S6	Lower zone (2)	03°23'11.23''S 37°17' 11.7''E	Human settlements, farming activities (beans, green vegetables, tomatoes, onions and millet and tropical fruits) and (poultry and livestock) and domestic activities (fetching water, bathing and washing). Lower zone of Weruweru River discharges water to Kifaru river

W1-W2 = water sampling sites, S1-S2 = sediment sampling sites

Water samples were collected by grabbing technique, preserved, kept in cool boxes and later transported to the laboratory for analysis. In the laboratory, water samples for pesticide analysis were stored in temperatures between 0-4°C prior to extraction and analysis, while samples for nutrients were analyzed immediately upon arrival. Water samples for pesticides analysis were collected in one liter sampling bottles with Teflon stop cork. After sampling, samples were measured for physico-chemical parameters temperature, pH, DO, TDS and EC using hand-held potable water quality monitor and later preserved by 10% of 1000 g of NaCl salt as described by Akerblom [13]. Water samples for nutrients analysis were collected in 500 mL plastic bottles. The samples were filtered and preserved with concentrate H_2SO_4. The physico-chemical parameters already measured in water samples for pesticide analysis were deemed to be adequate for the nutrient samples.

Bed sediment samples were taken by using a stainless spoon, wrapped in aluminium foil, labeled, placed in air-tight bags, kept in ice-coolers and transported to the laboratory where they were kept at 20°C before extraction and analysis. Two field points were selected randomly at 0–20 cm depths per sampling site in each zone because sediments at this depth level are expected to be the most contaminated and have the greatest potential for exchange with the water column [14].

Pesticides Analysis

Sediment Samples Extraction and Clean up: Three sub-samples (20, 10 and 5 g) were measured in analytical balance. The first sub-sample of 5 g was used for measuring sediment pH values. The sediment sample was mixed with 5 mL of deionised water (pH 7.0) in a small clean container and gently stirred by a scoop into slurry. The mixture was then left to settle for approximately 15 min before recording the pH value using a calibrated pH meter. Another sub-sample of 10 g was taken in a pre-weighed petri dish for dry weight and organic matter determinations. It was later dried in an oven at 105°C for 12 hours and 400°C for 3 hours for determination of moisture and organic contents, respectively.

The third sub-sample (20 g) was grinded with 30 g anhydrous sodium sulphate in the mortar and more sodium sulphate were added to make the sample free floating powder to bind the water. The mixture was poured into a column and eluted with 120 mL dichloromethane in a beaker while shaking the beaker and left to settle for 15 min. The contents were then decanted through a plug of glasswool into an evaporation flask. The remaining sodium sulphate was rinsed with 20-30 mL dichloromethane mixture and decanted through the same glasswool. The resulting extract was concentrated in a rotary evaporator and the solvent was changed to cyclohexane and concentrated to 2 mL ready for clean up.

Clean up of sediment samples were done by column chromatography using florisil (magnesium silicate). A glass column of 5 g (60 cm x 22 mm) packed with florisil, glasswool and anhydrous sodium sulphate was used. 50 mL of cyclohexane was added into the glass column and allowed to pass through drop by drop until very little was left on the upper part of the column. The sample concentrate was poured into the column and drained to make 2 mL of the sample, then transferred into Teflon cork vial and stored at 4°C until analysis was done.

Water Samples Extraction and Clean up: Unfiltered water samples, previously preserved with 10% sodium chloride, were extracted by Liquid-Liquid Extraction (LLE) method. Each water sample 1000 mL was quantitatively transferred to a 1 liter separating funnel and the sampling bottle was rinsed with 30 mL dichloromethane, which was then transferred to the separating funnel containing the water sample. The combined contents were then successively extracted with dichloromethane (3 x 50 mL). The organic layer was filtered through plugwool containing anhydrous sodium sulphate (30 g) for drying. Sodium sulphate was later rinsed with dichloromethane (2 x 3 mL) and the combined extract concentrated in *vacuo* at 30°C and the solvent changed to cyclohexane. The volume was adjusted in a stream of air to 2 mL in 9:1 cyclohexane:acetone (v/v) in vials ready for analysis. The water extract appeared clean and were not subjected to further clean up [13].

Analytical Quality Assurance

Analytical Quality Assurance for Sediment Samples: A 100 mL aliquot of each n-hexane, dichloromethane, cyclohexane, ethyl acetate and acetone was concentrated to 2 mL and used to check contamination from the solvents used. Two matrices blank from bed sediments were obtained from a virgin land where the water passes and the same procedure of extraction and analysis as that of sediment samples was performed. The result showed that no significant peaks appeared in the chromatograms of the blanks. Recoveries were estimated by spiking the matrix blank with four OCls pesticides standard at concentrations ranging from 0.01-1.1 ìg/mL of each analyte. The average of percentage recoveries ± SD (n=4) were α-chlordane 81.7±3.6%, *p,p'*-DDE 89±1.5%, *p,p'*-DDD 80±1.7%, *p,p'*-DDT 95±2.7% and endosulfan sulphate 87±0.4%. The results were not corrected for recoveries since all were with the normal acceptable range of 70-120% [15].

Analytical Quality Assurance for Water Samples: A 100 mL aliquot of each n-hexane, dichloromethane, cyclohexane, ethyl acetate and acetone was concentrated to 2mL and used to check contamination from the solvents used. 1 L of distilled water was extracted the same way as water sample. The results showed no significant peaks appeared in the chromatograms of the blanks. Recoveries were estimated by spiking the matrix blank with four OCls pesticides standards at concentration ranging from 0.01-1.1ìg/mL of each analyte. The average of percentage recoveries ± SD (n= 4) were α-chlordane 87±0.3%, *p,p'*-DDE 98±0.2%, *p,p'*-DDD 99±0.7%, *p,p'*-DDT 99±1.2% and endosulfan sulphate 97±0.9%. The results were not corrected for recoveries since all were with the normal acceptable range of 70-120% [15]. ill, 2000).

Gas Chromatography Analysis: Pesticide residue analyses were determined as described by Akerblom [13]. GC-Varian CP-3800 gas chromatography equipped with ^{63}Ni Electron Capture (EC) detector was used for analysis. The GC capillary column WCOT FUSED SILICA 30 mm x 0.32 mm, coated with CP-SIL 8CB DF 0.2 ìg/mL was used. Nitrogen was used as both a carrier and make up gas in the Electron Capture Detector (ECD) at a flow rate of 30 ± 1 mL/min. The temperature programme was held at 70°C for 1min, 15°C/min to 180°C, 4°C/min to 230°C for 15 min. The injection and detector temperatures were 240 and 250°C, respectively. Identification of residues was effected by running samples and external reference standards in GC and then comparing the chromatograms [16].

Nutrients Analysis: Nutrients in water samples were analysed following the methods outlined by APHA/AWWA/WEF [17]. For ammonia-nitrogen determination, colorimetric method using Nessler's reagent was used. The detection limit for this method was 0.02 mg/L. Nitrate-nitrogen and phosphoros were determined by the cadmium reduction method and ascorbic acid method, respectively. Methods detection limit for both methods were 0.01 mg/L. The quality of the data was assured by the analysis of blank and duplicate samples according to the standard operating procedures of the analytical laboratory at the Department of Chemistry, University of Dar es Salaam.

Data Analysis: The analyses of data were performed using descriptive statistics including frequencies, percentages, mean and histograms. These were computed through the use of Microsoft excel computer software.

RESULTS AND DISCUSSION

Nutrient Concentrations in Weruweru River: Nitrate (NO_3^-), nitrite (NO_2^-), ammonia (NH_3) and orthophosphate (PO_4^{-3}) compounds were analyzed in water samples and results tabulated as shown in Figure 4. These compounds are the most significant inorganic forms of two elements; nitrogen and phosphorus that commonly limit the productivity of plants. The concentration of NH_3-N was

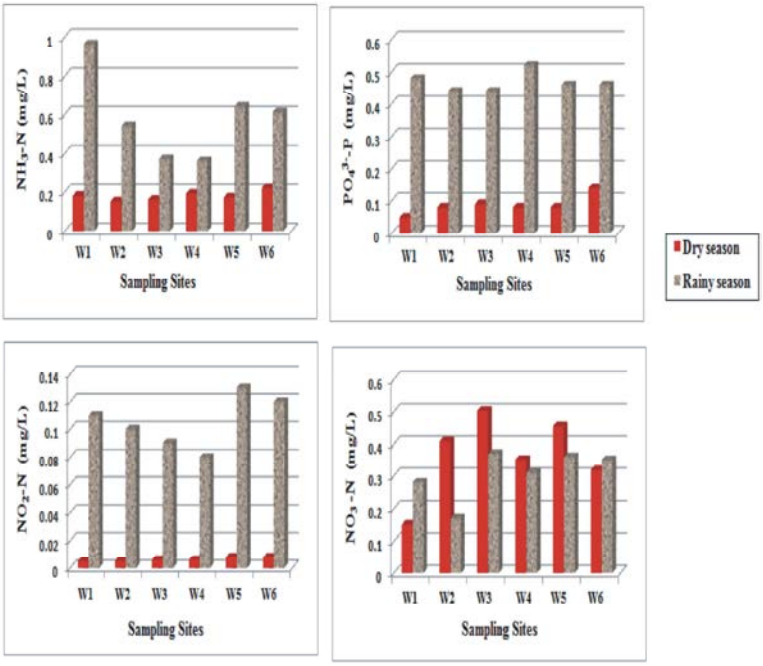

Fig 4: Concentration of the Nutrients in Weruweru water samples measured at six sampling sites

low during the dry season (0.15–0.22 mg/L, range) than during the rainy season (0.37–0.96 mg/L, range). NH_3-N is pH and temperature dependent, such that at high pH and temperatures high values of NH_3-N are expected. Results from the study indicate that the pH and temperature were high during the dry season than rainy season. This means that pH and temperature cannot be the cause of high NH_3-N during the rainy season. A possible source of high NH_3-N contamination during rainy season is expected to be runoffs containing fertilizers from upstream. This was attributed to the fact that both sampling stations are located close to farm lands where extensive agriculture is conducted.

The concentrations of NO_2^--N during the dry and rainy seasons range from 0.005 to 0.008 mg/L and from 0.08 to 0.13 mg/L, respectively. Both concentrations were below the maximum limits in drinking water quality of 1 mg/L as per Tanzania standards [18]. The concentration for NO_3^--N during the dry season ranged from 0.15 to 0.454 mg/L and rainy season range from 0.17 to 0.37 mg/L. The high range of NO_3^--N than NO_2^--N is normally expected because nitrite is the unstable form of nitrogen and is easily oxidized into nitrate [6]. Exposure to higher levels of nitrites or nitrates has been associated with cancer, brain tumors, leukemia and asopharyngeal. In infants and children, nitrate and nitrite bind to hemoglobin and cause chemically altered hemoglobin (methemoglobinemia) that impairs oxygen delivery to tissues, resulting in the blue colour of the skin "blue baby syndrome". The normal background range of nitrate concentration in natural waters is normally below 5 mg/L, any value above this level is an indication of manmade nitrate pollution [19]. The World Health Organization has set limits of 50 mg/L for NO_3^--N concentration in potable water [20]. In this study concentrations of NO_3^--N in all sampling stations and in both seasons were within the allowable limits for WHO potable water quality and normal range of natural water.

Concentration of PO_4^{3-}-P during the dry season range from 0.05 to 0.14 mg/L, while during the rainy season it ranges from 0.44 to 0.52 mg/L. These concentrations were higher than the natural background levels of PO_4^{3-}-P in river waters which usually range from 0.005 to 0.02 mg/L [21]. High values of phosphorous in rivers can speed up eutrophication and reduction of dissolved oxygen of the river water due to increased minerals and organic nutrients [22]. Therefore, low level of DO observed during the rainy season could partly be associated with high level of phosphorous.

Pesticide Residue in Water and Sediment Samples: Concentration of eight different types of organochlorine pesticides residues cyanazine, α-chlordane, endosulfan sulphate, *p,p'*-DDT, *p,p'*-DDD, *p,p'*-DDE, lindane and cypermethrin were measured in water and sediment samples collected from six different sites in Weruweru

Table 2: Types and Concentrations of Pesticides Residues Detected in Water (µg/L) and Sediment (µg/kg dw) Samples in Dry and Rainy Seasons

Season	Site	Cyanazine	α-Chlordane	Endosulfan Sulphate	*p,p'*-DDT	*p,p'*-DDD	*p,p'*-DDE	Lindane	Cypermethrin
Dry	W1-W3								
	(S1-S3)	bdL	bdL	bdL	bdL	bdL	bdL	bdL	bdL
	W4 (S4)		0.084 (bdL)	bdL	bdL	bdL	bdL	bdL	bdL
	W5 (S5)	bdL	bdL	12.7(bdL)	bdL(19.0)	bdL	bdL	3.66(bdL)	bdL(157)
	W6 (S6)	45.7 (0.115)	0.816(64)	12(bdL)	bdL(5.63)	0.481(bdL)	0.74(bdL)	bdL	bdL
Rainy	W1-W2								
	(S1-S2)	bdL	bdL	bdL	bdL	bdL	bdL	bdL	bdL
	W3 (S3)	bdL	bdL	bdL(13)	bdL	bdL	bdL	bdL	bdL(5.2)
	W4 (S4)	bdL	0.081(bdL)	bdL	bdL	bdL	bdL	bdL	bdL
	W5 (S5)	bdL	0.028(bdL)	bdL	bdL	bdL	bdL(81)	bdL	bdL
	W6 (S6)	bdL	0.23(bdL)	bdL(0.433)	bdL	0.506(bdL)	bdL	bdL	bdL

bdL = below detection limit, w1-w6 = water samples, s1-s6 = sediment samples, values in brackets represent sediment concentrations where there is no brackets all water and sediment concentrations were bdL

sub-catchment. Results of the various concentrations are indicated in Table 2. The computation reveals that most pesticide residues in water and sediment samples were below detection limits. Concentration range for both dry and rainy seasons in water samples was bdL to 4.7 µg/L and in sediment samples ranges from bdL to 157 µg/kg dw.

Endosulfan sulphate, a major degradation of endosulfan was the most detected pesticide residues. It was detected in about 33% of the samples analysed during the dry and rainy season. Its concentration in water and sediment samples ranged from bdL to 12.7 µg/L and bdL to 13 µg/kg dw, respectively during the dry season and rainy season. Although endosulfan sulphate is susceptible to photolysis in the environment, it is expected to have a high occurrence in cultivated areas [23]. Dem and coworkers [24] also reported high occurrences of endosulfan sulphate in soil samples, which were 74% of the sample analysed. Endosulphate is known to be toxic as parent compound endosulfan [25]. Because of their high toxicity, technical endosulfan was restricted in many countries including Tanzania. In the study area however, it was found to be in use under trade name thionex/thiodan.

Percentage detection of DDT metabolites in water samples were 33.4% during the dry season and 16.7% during rainy season. In the lower zone of Weruweru river, *p.p'*-DDD was detected for both seasons and the concentrations ranged bdL-0.506 µg/L. Then, *p,p'*-DDE was only detected in the lower zone of the river during the dry season with concentrations ranging from bdL to 0.81 µg/L. The concentrations of the DDT metabolites were within the acceptable limits in water 2 µg/L as per WHO guidelines [26]. *p,p'*-DDT was detected during the dry season in the sediment samples analysed with concentrations ranging from bdL to 19.0 µg/kg dw. DDT can be degraded into DDD under anaerobic conditions and into DDE in aerobic environments. Normally, ratios of (*p,p'*-DDT)/(DDT metabolite) greater than 0.5 indicate recent DDT usage [27]. In the current research study, ratios of *p,p'*-DDT to *p,p'*-DDE was 0.23, suggesting previous inputs of DDT into Weruweru river sediments. The ratio also agrees with the results from farmer's survey that indicated use of DDT up to the late 1990s. DDE may last in the sediment for a very long time, potentially for hundreds of years sticking strongly to sediments and thus may remain in the sediment surfaces for a long span of time. The persistence in the environment of this organochlorine has also been reported in others parts of the world. For instance DDE have been reported to be widely distributed in soils in China despite the fact that its use has been discontinued since 1983 [28].

Lindane was only detected in water samples from one site (W5) during the dry season with concentration of 3.66 µg/L. This concentration is above the acceptable limits for drinking water 2 µg/L as per WHO guidelines [26]. The small percentage of detection indicates the possibility of past usage. Use of lindane was restricted by the United State Environmental Protection Agency (U.S EPA) due to concerns raised over its potential to causing cancer and birth defects in animals [29]. It is highly persistent in soils and sediments, with a half life of approximately 15 months.

Cyanazine was detected in the lower zone of the river during the dry season with concentrations ranging from bdL to 45.7 µg/L. This is higher than acceptable limit in drinking water of 10 µg/L as per WHO guidelines [26]. Concentrations of cyanazine during the rainy season were below detection limits. This could be due to the fact that cyanazine takes 2 to 14 weeks to disappear completely, although it could also have been washed away by runoff

from one point to another. High concentrations of cyanazine during the dry season in the study area correlate with a similar study in USA where cyanazine was detected in surface water and groundwater at maximum concentrations of 1300 and 3500 µg/L, respectively. Cyanazine is restricted by U.S EPA because of its persistence and teratogenicity effects [30].

Alfa-chlordane was detected in 33% of water samples analysed during the dry season and 50% of samples for the rainy season. The concentrations ranged from bdL to 0.82 µg/L. α-chlordane does not biodegrade and is highly persistent in soils with a half-life of about 4 years. Chlordane has been detected in surface water, groundwater and sediments. Concentrations detected in surface water have been very low, while those found in suspended solids and sediments are always higher [30]. In this study, α-chlordane was detected only during the dry season in lower zones of the River, with concentrations ranging from bdL to 64 µg/kg dw. Such values are above the fresh water sediment quality assessment guidelines for alfa-chlordane 4.5 µg/kg dw [31].

CONCLUSION

Results emanating from the current research study reveal that surface water and sediments in Weruweru sub-catchment are contaminated with pesticides and nutrients. The concentrations of contaminants in most of the sites were within the recommended international and national limits for drinking waters. However if such contaminations are not controlled can lead to heavy contamination of the sediments. Sediments normally act as a sink of pollutants that eventually releases into water reserves. It can hence be concluded that, if taken up through plant roots and bioaccumulate in the food chain beyond acceptable limits may cause chronic adverse health effects to consumers.

ACKNOWLEDGEMENTS

We gratefully acknowledge the support by the German Academic Exchange Service (DAAD) for a study grant extended to Jokha Mohamed. We thank Mr Charles Riwa and Engineer Arafa Magidi from Pangani River Basin Water Office (PBWO) and Mr. Godwin Masumbuko of Ngurudoto Defluoridation Research Station, Arusha for location of the sampling sites and their constructive ideas that were useful in analysing the data. The authors are also grateful to Mr. Lutufyo Mwamtobe for his excellent technical assistance during sample extractions and analyses of pesticides and nutrients at the Department of Chemistry, University of Dar es Salaam.

REFERENCES

1. Ecobichon, D.J., 2001. Pesticide use in developing countries. Toxicology, 160(1): 27-33.
2. Kolpin, D., 2000. Importance of the Mississippi River Basin for investigating agricultural–chemical contamination of the hydrologic cycle. Science of the Total Environment, 248(2): 71-72.
3. Sattler, C., H. Kächele and G. Verch, 2007. Assessing the intensity of pesticide use in agriculture. Agriculture, ecosystems & environment, 119(3): 299-304.
4. Ngowi, A., 2003. A study of farmers' knowledge, attitude and experience in the use of pesticides in coffee farming. African Newsletter on Occupational Health and Safety, 13(3): 62-64.
5. Bhanti, M. and A. Taneja, 2007. Contamination of vegetables of different seasons with organophosphorous pesticides and related health risk assessment in northern India. Chemosphere, 69(1): 63-68.
6. Galloway, J.N. and E.B. Cowling, 2002. Reactive nitrogen and the world: 200 years of change. AMBIO: A Journal of the Human Environment, 31(2): 64-71.
7. Dalvie, A.M., E. Cairncross, A. Solomon and L. London, 2003. Contamination of rural surface and ground water by endosulfan in farming areas of the Western Cape, South Africa. Environment Health: A Global Access Science Source, 2: 1-15.
8. Brouwer, A., M.P. Longnecker, L.S. Birnbaum, J. Cogliano, P. Kostyniak, J. Moore, S. Schantz and G. Winneke, 1999. Characterization of potential endocrine-related health effects at low-dose levels of exposure to PCBs. Environmental Health Perspectives, 107(Suppl 4): 639.
9. Najafpour, S., S.M.V. Farabi, Y.M., F.M. Abbas Alkarkhi and A. Ganjian Khenary, 2010. The Determination of Organochlorine Pesticides Residues in Chalus River Water by Multivariate Analysis. Iranica Journal of Energy & Environment, 1(3): 222-227.
10. Bouraie, M.M.E. and A.A. El Barbary, 2011. Assessment of Organochlorine Pesticide in Water and Sediment Samples Collected from El-Rahawy Drain, Egypt. Iranica Journal of Energy & Environment, 2(3): 191-200.

11. El Bouraie, M.M., A. Ahmed and M.M. Yehia, 2011. Examining the Concentration of Organonitrogen Pesticides in Water at Nile Delta, Egypt. Iranica Journal of Energy & Environment, 2(4): 331-338.
12. Pangani Basin Water Office (PBWO), 2010. Report. Tanzania.
13. Akerblom, M., 1995. Guideline for environmental monitoring of pesticide residues for the SADC Region. SADC/ELMS, Monitoring Techniques Series.
14. Nowell, L.H., P.D. Capel and P.D. Dileanis, 1999. Pesticides in stream sediment and aquatic biota: distribution, trends and governing factors, 4: CRC Press.
15. Hill, A., 2000. Quality Control Procedures for Pesticide Residues Guidelines for Residues Monitoring in the European Union. Document No. SANCO/3103/2000, European Commission.
16. Martens, D., K. Schramm and A. Kettrup, 1999. Standard operation procedures for the determination of chlorinated hydrocarbons in sediments, suspended solids and surface waters. On the Presence of Polychlorinated Organic Compounds in the Liao River and the Yangtse River in Eastern China, European Commission EUR-Report, 18702: 21-28.
17. APHA/AWWA/WPCF, 2005. Standard Methods for the Examination of Waters and Wastewaters, 21st ed. Washington, DC, USA.
18. Tanzania Bureau of Standards (TBS), 2003. Drinking (potable) water: Specification (TZS 789:2003), National Environmental Standards Compendium, Tanzania Bureau of Standards.
19. Bruning-Fann, C.S. and J. Kaneene, 1993. The effects of nitrate, nitrite and N-nitroso compounds on human health: a review. Veterinary and human toxicology, 35(6): 521-538.
20. World Health Organization (WHO), 2004. Guideline for drinking water quality: recommendations, 3rd Ed, Vol.1, Geneva.
21. Chapman, D., 1992. Water quality assessment. A guide to the use of biota, sediments and water in environmental monitoring. Chapman on Behalf of UNESCO, WHO and UNEP, Chapman & Hall, London, England.
22. Perlman, H., 2013. The effects of urbanization on water quality: Phosphorus http://ga.water.usgs.gov/edu/phosphorus.html, Accessed 06th June, 2013.
23. Manikariza, P., O. Akinbamijo, A. Covaci, R. Pitonzo and P. Schepens, 2003. Assessment of organochlorine pesticides residues in West Africa farms: Banjul and Dakar case study. Archives of Environmental Contamination and Toxicology, 44: 171-179.
24. Dem, S., J. Cobb and D. Mullins, 2007. Pesticide residues in soil and water from four cotton growing areas of Mali, West Africa. Journal of Agricultural, Food and Environmental Sciences, 1(1): 16.
25. Jiang, Y.F., X.T. Wang, Y. Jia, F. Wang, M.H. Wu, G.Y. Sheng and J.M. Fu, 2009. Occurrence, distribution and possible sources of organochlorine pesticides in agricultural soil of Shanghai, China. Journal of Hazardous Materials, 170(2): 989-997.
26. World Health Organization (WHO), 1993. Drinking water standards. WHO's Guidelines for Drinking-water Quality, set up in Geneva.
27. Montgomery, J.H., 2000. Groundwater Chemicals Desk Reference, third ed. Lewi Publishers and CRC Press, Boca Raton.
28. Wu, N., S. Zhang, H. Huang, X. Shan, P. Christie and Y. Wang, 2008. DDT uptake by arbuscular mycorrhizal alfalfa and depletion in soil as influenced by soil application of a non-ionic surfactant. Environmental pollution, 151(3): 569-575.
29. Gandhi, R. and S. Snedeker, 2010. Pesticides and Breast Cancer Risk: Lindane http://envirocancer.cornell.edu/FactSheet/Pesticide/fs15.lindane.cfm, Accessed on 20th June, 2013.
30. Extoxnet, 1996. Pesticide Information profiles, http://extoxnet.orst.edu/pips/cyanazin.htm, Accessed on 5th October, 2012.
31. MacDonald, D.D., C.G. Ingersoll and T. Berger, 2000. Development and evaluation of consensus-based sediment quality guidelines for freshwater ecosystems. Archives of Environmental Contamination and Toxicology, 39(1): 20-31.

Persian Abstract

DOI: 10.5829/idosi.ijee.2014.05.02.11

چکیده

مواد مغذی شیمیایی کشاورزی و باقی مانده های آفت کش ها در آب های سطحی و نمونه های رسوبات حوزه آبریز فرعی ورو_ورو به منظور تعیین غلظت و کیفیت آب برای مصارف انسانی مورد بررسی قرار گرفت. غلظت های مواد مغذی گیاهی PO_4^{-3} , NO_2^-, NH_3، NO_3^- در محدوده ۰/۰۰۵ تا ۰/۹۶ mg/l در نمونه های آب سطحی مشخص گردید. غلظت های باقی مانده آفت کش های سیانازین ، آلفا کلردان، سولفات اندوسولفان، ددت، ددد، ددی، لیندان و سایپرمترین به ترتیب در نمونه های آب سطحی و نمونه های رسوبات، در محدوده زیر حد تشخیص تا ۴۵/۷ g/l و زیر حد تشخیص تا ۱۵۷ µg/l تعیین گردید. در اغلب مکان ها، غلظت مواد مغذی و باقی مانده های آفت کش ها کمتر از میزان حداکثری WHO و حد ملی برای آب آشامیدنی بوده است. آلاینده های شیمیایی کشاورزی از نشت آب‌های کشاورزی و فرسایش خاک های کشاورزی ، نشأت گرفته اند. کلیه پارامترها با روش های استاندارد اندازه گیری گردید.

Iranica Journal of Energy & Environment 5 (2): 202-208, 2014
ISSN 2079-2115
IJEE an Official Peer Reviewed Journal of Babol Noshirvani University of Technology
DOI: 10.5829/idosi.ijee.2014.05.02.12

BUT

Chemical Analysis and Utilization of *Sargassum* sp. as Substrate for Ethanol Production

[1]*Jelynne P., Tamayo and* [2]*Ernesto J. Del Rosario*

[1]Food Science Cluster, College of Agriculture, University of the Philippines Los Baños, Laguna, Philippines
[2]Institute of Chemistry, College of Arts and Sciences,
University of the Philippines Los Baños, Laguna, Philippines

Received: May13, 2014; **Accepted** in Revised Form: June 11, 2014

Abstract: The brown seaweed *Sargassum sp.* is a promising feedstock for ethanol production because of its relatively high content (41.6% dry basis) of holocellulose. Chemical pretreatment of the seaweed was carried out with 1% (v/v) H_2SO_4 solution at 5% solid loading for 15 min at 121°C prior to saccharification with commercial cellulase. The cellulose-to-glucose conversion efficiency after 72 hours incubation was 49.84% and 61.54% for the untreated and chemically treated biomass, respectively.The algal residue after pretreatment with dilute acid was subjected to either simultaneous enzymatic saccharification and fermentation (SESF) or separate enzymatic hydrolysis and fermentation (SEHF). *Saccharomyces cerevisiae* was used for ethanol fermentation. The cellulose to ethanol conversions forSESF and SEHF were 66.9 and 34.1%, respectively.

Key words: Bioethanol · *Sargassum* sp. · Ethanol fermentation · Algal saccharification · Brown seaweed

INTRODUCTION

Due to escalating price of petroleum-based fuels, extensive research has been done towards the development of alternative, renewable and cost-effective energy sources with lower greenhouse gas emissions [1, 2]. One promising energy source is biofuel, which is derived from plant biomass. One the most important biofuel is ethanol which can be produced from abundant supplies of cellulosic biomass, both terrestrial and marine. The leading countries in the world in terms of bioethanol production are Brazil, US and Canada [3]. Bioethanol production can reduce green house gas levels since biomass assimilation by feedstock crops can utilize atmospheric carbon dioxide. In addition, ethanol is less toxic and is readily biodegradable and its use producesless air borne pollutants compared to petroleum fuel.

Ethanol fuel can be produced from terrestrial feedstocks that produce sugar, starch and cellulose. In addition, use of agricultural wastes and palm trees residual wastes to ethanol in tropical regions created great potential for ethanol production from wastes and outcomes are encouraging as alternative sources of energy [4,5].However, the use of feedstock crops for ethanol production has raised issues on its possible impact on food supply and security. Because of these drawbacks on the use of food crops as bioethanol feedstock, several species of algae with high content of fermentable carbohydrates are now being investigated. Thus, algae are now gaining wide attention as biomass source for the production of bioethanol and biodiesel, which are known asthird-generation of biofuels.

Marine algae consist of macroalgae (seaweeds) and microalgae. Seaweeds are classified as green, brown and red. They are good sources of colloidal substances which are useful as gelling agents, emulsifiers and stabilizers in pharmaceutical, cosmetics and food products. Most seaweed research has dealt with chemical analysis because of seaweeds contain unique carbohydrates. *Sargassum*is one of the important brown seaweed that is distributed in temperate and tropical oceans of the world. It is utilized as animal feed, fertilizer and as source of alginate which has various used in industries. In Philippines, 72 *Sargassum* species have been recorded [6].

Corresponding Author: Jelynne P., Tamayo, Food Science Cluster, College of Agriculture, University of the Philippines Los Baños, Laguna, Philippines. Tel: + 063 5362303. E-mail: jelptamayo@yahoo.com

Please cite this article as: Tamayo, J.P. And E.J. Del Rosario, 2014. Chemical analysis and utilization of Sargassum sp. as substrate for ethanol production. Iranica Journal of Energy and Environment, 5(2):202-208.

Production of ethanol from biomass requires two steps: (1) hydrolysis of polysaccharides to sugars; and (2) fermentation by yeast or bacteria to convert fermentable sugars into ethanol. At present, hydrolysis has been done using acid or enzyme. One advantage of the latter is high specificity of the enzyme and the saccharification can be done under mild conditions with minimal formation of side products that can be potential inhibitors in the fermentation process[7].

The present study deals with chemical characterization of the brown seaweed, *Sargassum* sp., as source of fermentable sugars for bioethanol production. Proximate chemical analysis was done on the seaweed and its contents of holocellulose, alpha-cellulose and alginate were also determined. Dilute acid pretreatment was conducted on the dried seaweed followed by enzymatic hydrolysis and yeast fermentation of the resulted sugars into ethanol. The efficiencies for saccharification and sugar to ethanol conversion were determined.

MATERIALS AND METHODS

Preparation of Biomass: *Sargassum sp*. was obtained from Real, Quezon; it was washed with running water to remove salts, sun-dried and then oven-dried at 50°C. The ground samples were stored in plastic containers at room temperature.

Proximate Analysis: Contents of crude protein, crude fat, crude fiber, ash and moisture of the ground algal biomass were determined according to standard methods. The moisture content was determined by drying to constant weight in an oven at 105°C. Crude protein was analyzed by the Kjeldahl method and ash was determined gravimetrically. Crude lipid was extracted using petroleum ether in a Soxhlet extractor and measured gravimetrically after oven-drying.

Determination of Alginate and Holocellulose

Alginate: The extraction procedure for alginate was adapted from Fenoradosoa, *et al*. [8]. The seaweed (25 g) was suspended and stirred in 800mL of 2% formaldehyde for 24 hours, then washed with deionized water prior to acidification (800 mL 0.2M HCl, 24 hours). The algal sample was then washed with deionized water prior to alginate extraction by stirring in 800mL 2% Na_2CO_3 for 3 hours at room temperature. After filtration, the alginate was precipitated with 95% ethanol (1:2 v/v) as sodium salt. The precipitate was washed with ethanol, then acetone and dried for 24 hours at 40°C.

Holocellulose and alpha-cellulose. Cellulose was isolated from the seaweed using the method of Siddhanta with some modifications [9]. Dried algal powder was placed in a Soxhlet extractor with ethanol for a period of 16 hours to remove the extractives. The holocellulose portion of the biomass was isolated using sodium chlorite, $NaClO_2$. Alpha-cellulose was then obtained as the residue which was insoluble in 17.5% sodium hydroxide solution from the isolated holocellulose.

Enzymatic Hydrolysis: Enzymatic hydrolysis was carried out on the chemically-pretreated samples. Chemical pretreatment is carried out with 1.0 % v/v H_2SO_4 at a solid-to-liquid ratio of 1:20. The effect of pretreatment was assessed in order to determine the potential sugar yield prior to enzymatic hydrolysis. Chemical treatment was done in an autoclave at 121°C (15 psi) for 15 min. After treatment, the pretreated solids were filtered and washed with distilled water until neutral pH prior to store in the refrigerator.

A commercial enzyme mixture was used in the experiments. The activity of the enzyme was determined prior to saccharification of the pretreated substrates. The procedure for measurement of cellulase activity was based on the NREL method [10]. Cellulase activity was expressed in terms of "filter paper units" (FPU) per milliliter of original (undiluted) enzyme solution. One unit of FPU is defined as the amount of enzyme that produces 1μmol of glucose per minute under the assay conditions.

The enzymatic digestibility of the pretreated sample was examined at constant enzyme loading of 25 FPU/g and substrate loading of 5%. All enzymatic hydrolysis experiments were done at 50°C for 72 h in 125 mL Erlenmeyer flasks using an incubator shaker. Samples were withdrawn after 0 h, 24 h, 48 h and 72 h and analyzed for reducing sugars content, which was determined using the DNS method.

Fermentation: Ethanol fermentation was carried out in flask experimentson the enzymatic hydrolysates obtained as described above. *Saccharomyces cerevisiae,* which was used in all fermentation processes. The organism was inoculated into fresh slant culture medium in a test tube and cultivated at 30°C for 1 day, until yeast growth appeared on the slant culture and was distributed evenly. To maintain the purity and activity of the *S. cerevisiae*, the sample was streaked on a slant of sterile YEPG (1% yeast extract, 2% peptone, 2% glucose and 2% agar dissolved in distilled water). After 24 hours of incubation at room temperature, the slant was inoculated into the pre-culture medium.

Two fermentation processes were performed, namely (1) separate enzymatic hydrolysis and fermentation (SEHF) and (2) simultaneous enzymatic saccharification and fermentation (SESF). In both SEHF and SESF experiments, enzyme hydrolysates obtained from untreated (raw) and acid-pretreated biomass were used. Samples were withdrawn after 0 h, 24 h, 48 h and 72 h and analyzed for ethanol content which was determined by Gas Chromatography with a Flame Ionization Detector.

RESULTS AND DISCUSSION

Proximate Composition of *Sargassum sp:* The results of proximate analysis of *Sargassum* sp. used in present study are presented in Table 1. It should be noted that seaweed composition generally varies with algal age and species, season, geographic location and temperature [11].

The appreciable amount of ash in the seaweed sample indicates residual mineral salts in the sample that were not completely removed by washing with water. The varying ash content of each type of seaweed shows differences in the amount of minerals salts that attach to the algal surface [12].The mineral salt content of seaweed depends on the type, age and condition of hydrology. Based on the results, it was found that the biomass used in present work was a good source of carbohydrates for the commercial production of monosaccharides. These rich sources of carbohydrates could be utilized as substrates for the production of bioethanol.

Alginate and Holocellulose Contents of Seaweed: Alginate is the major structural polysaccharide present in brown seaweeds. The seaweed was soaked first in a formaldehyde solution overnight before it was extracted with alkali. Formaldehyde kills microorganisms in seaweeds which could contribute to the degradation of alginates [13]. Also, the presence of transition metal ions such as Fe^{2+} or Fe^{3+} together with phenolic compounds enhances free radical formation which causes depolymerization of the phycocolloids. Therefore, removal of phenolic compounds prior to extraction by Na_2CO_3 solution was done in order to reduce the degradation of alginates.

After the sample was soaked overnight in formaldehyde solution, it was mixed with HCl solution. The alginic acid was extracted with Na_2CO_3 (with stirring for 3 hours) that gave a thick brownish slurry. Addition of 95 % ethanol (1:2 v/v) precipitated the alginic acid as sodium alginate which was jelly-like. The sodium alginate obtained was yellowish and the calculated yield was 32.2%; this is the same as that obtained by Omar *et al.* [13].

Table 1: Proximate composition* of *Sargassum sp*

Composition	Values (%)
Moisture	13.93 ± 0.06
Ash	27.11 ± 0.62
Crude Fiber	12.50 ± 0.39
Crude Fat	0.54 ± 0.02
Crude Protein	6.99 ± 0.03
Nitrogen-free extract	51.43 ± 0.73

*Based on dry-weight basis and average of three replicates.

Table 2: Holocellulose, alpha-cellulose and alginate contents* of *Sargassum sp*

Component	Values (%)
Alginate	32.2± 0.4
Holocellulose	41.6± 0.3
Alpha-cellulose	22.0± 0.8
Hemicellulose	19.6± 0.9

*On dry-weight basis and average of three replicates.

The amounts of holocellulose and alpha-cellulose fractions in the algal sample are listed in Table 2. Holocellulose consists of cellulose and hemicellulose after all the extractives have been dissolved by ethanol in a Soxhlet extractor for 16 hours. Then the holocellulose in the sample was extracted with sodium chlorite. Traditionally, acidified sodium chlorite is commonly used to delignify wood as an initial step in the isolation of pure cellulose [14]. Sodium chlorite is a moderately strong oxidizing agent; its use does not allowheavy metal contamination and yields pure cellulose with no residual lignin. The alpha-cellulose was then obtained by adding 17.5% NaOH to the isolated holocellulose. Alpha-cellulose (or true cellulose) is the insoluble residue after treatment with alkali. The hemicellulose in the biomass was not isolated but was calculated as the difference between the holocellulose and alpha-cellulose contents.

The relatively high cellulose content of *Sargassum* makes it a promising source of fermentable sugars for ethanol production. However, the alginate, which cannot be fermented to ethanol, is a valuable by-product with useful applications.

Enzymatic Hydrolysis: Enzymatic hydrolysis using commercial cellulase was done to yield sugars prior to fermentation into ethanol. Chemical pre-treatment was done in order to enhance enzymatic saccharification because of the recalcitrance of native cellulose to the enzyme due to the crystalline structure and low surface area of the cellulose matrix [15].

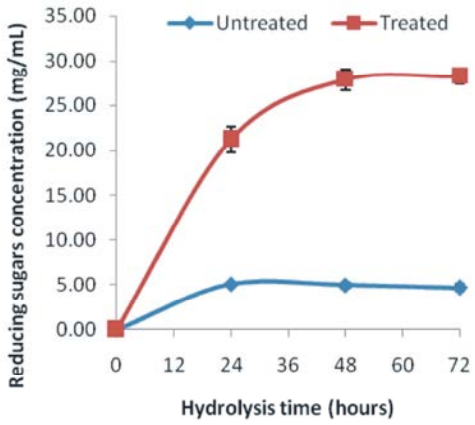

Fig. 1: Enzymatic saccharification of *Sargassum sp.* using a commercial enzyme.

Enzymatic saccharification was done at a substrate loading of 5% (w/v). An increased substrate loading allowed a higher sugar yield. Figure 1 showsthe concentration profiles with respect to time of enzymatic saccharification for the untreated and pretreated algal samples. The reducing sugar yield for the untreated sample was appreciably lower than that of the treated sample. The amount of sugars released increased up to 48 hours and remained constant until 72 hours of hydrolysis for the pretreated sample. The maximum amount of sugars released (326.89 mg/g dry biomass) was observed after 72 hours hydrolysis for the acid-pretreated sample. The untreated sample gave only 91.93 mg/g dry biomass.

Various factors have been found to affect the enzymatic hydrolysis of the pretreated material including (a) accessibility and adsorption characteristics of the cellulose, (b) reactivity of the cellulose and (c) adsorption characteristics of the lignin, if present [16].

These factors are influenced by biomass composition and pretreatment method [17]. Previous studies have reported that cellulose hydrolysis improved with increasing lignin removal, although differences have been reported in the degree of lignin removal needed [18]. Since seaweeds have no lignin, the pretreatment step can be omitted prior to saccharification. However, in the present study acid pretreatmentwas observed to improvesaccharification of the material; this is probably due to the alginate-cellulose matrix present in the cell wall of brown seaweeds. The cellulose matrix may be exposed upon acid pretreatment making it more accessible to the enzyme resulted in greater saccharification.

The cellulose to glucose conversion efficiencies for the untreated (raw) and pretreated *Sargassum sp*. after 72 hours incubation were 49.84% and 61.54%, respectively. Generally, pretreated biomass had higher saccharification efficiencies than the untreated ones.

Fermentation: Ethanol fermentation was done on the enzymatic hydrolysates of the acid-pretreated algal sample. Two types of fermentation experiments were considered: (1) Simultaneous Enzymatic Saccharification and Fermentation (SESF) and (2) Separate Enzymatic Hydrolysis and Fermentation (SEHF).

Simultaneous Enzymatic Saccharification and Fermentation (SESF): Simultaneous production of ethanol and consumption of glucose was observed during the first 12 hours of fermentation (Figure 2). A sudden drop in total sugar concentration was observed during the first 24 hours of fermentation which remained almost constant for the 48th up to the 72nd hour. This indicated that there was no end-product inhibition of the enzyme

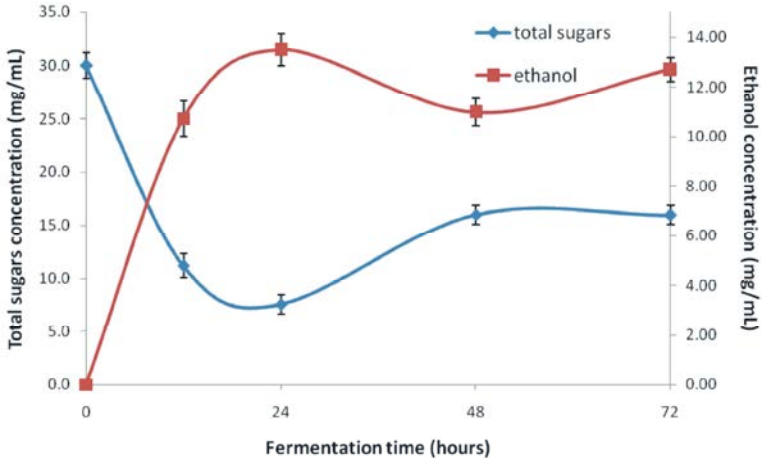

Fig. 2: Time profile of simultaneous enzymatic saccharification and fermentation (SESF) for pretreated*Sargassum sp*.

Table 3: Ethanol concentration obtained from SESF.

		Final Ethanol Concentration*	
Treatment	Initial Conc. of Total Sugars, mg/mL	% v/v	mg/mL
Untreated	5.63 ± 0.92	0.52 ± 0.12	4.10 ± 0.26
1% H_2SO_4, 15 min, 121°C	30.01 ± 1.03	1.60 ± 0.25	12.70 ± 0.54

* Concentration obtained after 72 hours fermentation based on three replicates

Table 4: Ethanol concentration obtained from SEHF.

		Final Ethanol Concentration*	
Treatment	Initial Conc. of Total Sugars, mg/mL	% v/v	mg/mL
Untreated	8.95 ± 0.26	0.53 ± 0.16	4.14 ± 0.73
1% H_2SO_4, 15 min, 121°C	29.41 ± 1.41	0.82 ± 0.17	6.47 ± 0.94

* Concentration obtained after 72 hours fermentation based on three replicates

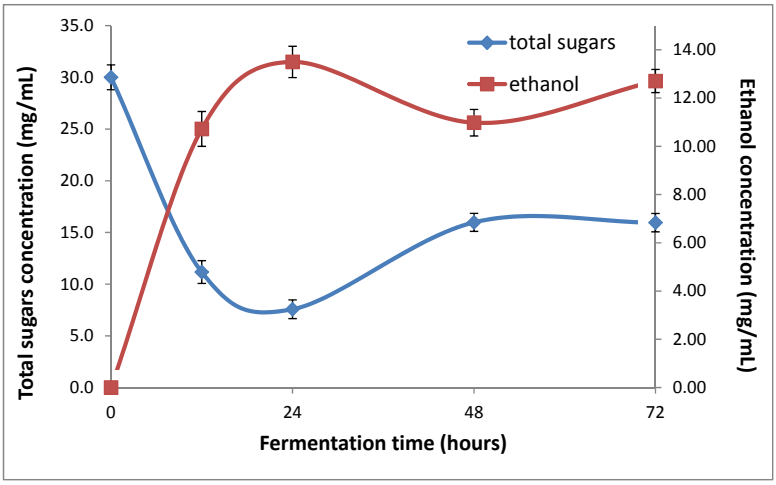

Fig. 3: Time profile of separate enzymatic hydrolysis and fermentation (SEHF) for pretreated *Sargasssum sp*.

as the glucose produced was immediately converted to ethanol.The ethanol concentrations of the untreated and pretreated biomass are presented in Table 3.

The maximum ethanol concentration for SESF of acid-pretreated *Sargassum sp*. after 72 hours of fermentation was 12.70 mg/mL.

There are two fundamental problems with Simultaneous Enzymatic Saccharification and Fermentation. Hydrolysis and fermentation both require specific temperature ranges for optimal operation. *Saccharomyces cerevisiae* ferments best at about 30°C and pH range of 4-5. A temperature during fermentation which is lower than 20 °C or greater than 40°C results in a lower concentration of ethanol for most yeast strains. The enzymatic hydrolysis process, however, performs best at temperatures of about 50°C and at 30°C enzymatic hydrolysis proceeds at a much lower rate.

Ethanol produced from glucose during SESF could inhibit fermentation of the glucose by yeast. Both enzyme and yeast undergo plasma degradation as the ethanol concentration increases. Eventually, a high ethanol concentration could cause enzyme denaturation and yeast cell death.

Separate Enzymatic Hydrolysis and Fermentation (SEHF): Concentrated enzymatic hydrolysates of the untreated and pretreated biomass were used as substrates (at 8% substrate loading) for the separate enzymatic hydrolysis and fermentation (SEHF). The initial total sugar concentrations are listed in Table 4 and the time profile for fermentation of the pretreated alga is shown in Figure 3. A rapid drop in total sugar concentration was observed after 24 hours which was accompanied by an increase in ethanol concentration. After 24 hours, the amount of ethanol produced remained constant which may be due to

Table 5: Cellulose to ethanol conversion efficiency for pretreated algae using different strategies

Fermentation Strategy	Cellulose to Ethanol Conversion Efficiency (%)
SESF	66.93
SEHF	34.10

the low amount of available sugars present in the fermentation broth. The maximum ethanol concentration for SEHF of pretreated biomass after 72 hours of fermentation was 6.47 mg/mL.

The advantage of the separate process (SEHF) over the simultaneous one (SESF) is the possibility of separate optimization, namely enzymatic hydrolysis at 50°C and fermentation at about 32°C. However, the disadvantage of this method is the inhibition of cellulase and α-glucosidase by glucose which is released during hydrolysis; this requires lower solids loadings and higher enzyme loadings in order to achieve reasonable yields [19].

The calculated cellulose to ethanol conversion efficiencies for the two bioconversion strategies are given in Table 5. The efficiency value depends on the glucose yield after saccharification. SESF gave a higher efficiency for the fermentation step compared to SEHF.

The cellulose-to-ethanol conversion efficiency value was based on glucose liberated from cellulose; the conversion of pentose (resulting from hydrolysis of hemicellulose) was not considered. Also, the yeast (*S. cerevisiae*) is not capable of fermenting pentose into ethanol. A fermentation strategy wherein both five-carbon and six-carbon sugars can be converted into ethanol involves simultaneous saccharification and co-fermentation using *S. cerevisiae* and a pentose-fermenting microorganism. Alternatively, a genetically-engineered yeast or bacterium can be used which can ferment both hexose and pentose into ethanol.

The ethanol yields (g ETOH/g dry biomass) for the treated *Sargassum* sp. are 0.112 and 0.057 for SEHF and SEHF, respectively.

CONCLUSION

Production of ethanol from brown seaweeds has received little attention because of alginate, the main carbohydrate fraction in brown seaweed, cannot be utilized directly as a substrate for ethanol production. Nonetheless, results of the present studyshowed that *Sargassum* sp. is a promising raw material for bioethanol production in addition to being a source of valuable by-products, especially alginate.

ACKNOWLEDGEMENT

The authorswould like to thank Department of Science and Technology-Accelerated Science and Technology Human Resources Development Program (ASTHRDP) with the supervision of the Philippine Council for Agriculture, Aquatic and Natural Resources Research and Development (PCAARRD) for the full time scholarship grant to accomplishpresent research.

REFERENCES

1. Wi, S.G., H.J. Kim, S.A. Mahadevan, D.J. Yang and H.J. Bae, 2009. The potential value of the seaweed Ceylon moss (Gelidium amansii) as an alternative bioenergy resource. Bioresource technology, 100(24): 6658-6660.
2. Subbaiah, G.V., K.R. Gopal and S.A. Hussain, 2010. The Effect of Biodiesel and Bioethanol Blended Diesel Fuel on the Performance and Emission Characteristics of a Direct Injection Diesel Engine. Iranica Journal of Energy and Environment, 1(3): 211-221.
3. Taylor, G., 2008. Biofuels and the biorefinery concept. Energy Policy, 36(12): 4406-4409.
4. Nahar, K., 2011. Sweet sorghum: an alternative feedstock for bioethanol. Iranica J of Energy and Environment, 2: 58-61.
5. Samsudin, M.D.M. and M.M. Don, 2014. Batch Fermentation of Bioethanol from the Residues of Elaeis guineensis: Optimization and Kinetics Evaluation. Iranica Journal of Energy and Environment, 5(1): 1-7.
6. Silva, P.C., E.G. Menez and R.L. Moe, 1987. Catalog of the benthic marine algae of the Philippines. Smithsonian Contributions to the Marine Sciences, 27: 179.
7. Hii, S.L., D.T.Y. and O.L.G.A., 2010. Comparative Evaluation of Pretreatment Strategies on Enzymatic Saccharification of Hylocereus polyrhizus's Pericarps for Bioethanol Production. Iranica Journal of Energy and Environment, 1(4): 275-279.
8. Fenoradosoa, T.A., G. Ali, C. Delattre, C. Laroche, E. Petit, A. Wadouachi and P. Michaud, 2010. Extraction and characterization of an alginate from the brown seaweed Sargassum turbinarioides Grunow. Journal of applied phycology, 22(2): 131-137.

9. Siddhanta, A., K. Prasad, R. Meena, G. Prasad, G.K. Mehta, M.U. Chhatbar, M.D. Oza, S. Kumar and N.D. Sanandiya, 2009. Profiling of cellulose content in Indian seaweed species. Bioresource technology, 100(24): 6669-6673.
10. Adney, B. and J. Baker, 1996. Measurement of cellulase activities. LAP-006. National Renewable Energy Laboratory, Golden, CO.
11. Kaehler, S. and R. Kennish, 1996. Summer and winter comparisons in the nutritional value of marine macroalgae from Hong Kong. Botanica Marina, 39(1-6): 11-18.
12. Mushollaeni, W., 2011. The physicochemical characteristics of sodium alginate from Indonesian brown seaweeds. African Journal of Food Science, 5(6): 349-352.
13. Omar, S., N. Ahmad and F. Ahmad, 1988. Composition of Aiginates from Brown Seaweeds, Sargassum and Padina spp. Pertanika, 11(1): 79-85.
14. Bono, A., P. Ying, F. Yan, C. Muei, R. Sarbatly and D. Krishnaiah, 2009. Synthesis and Characterization of Carboxymethyl Cellulose from Palm Kernel Cake. Advances in Natural and Applied Sciences, 3(1): 5-11.
15. Dale, B.E., 1987. Lignocellulose conversion and the future of fermentation biotechnology. Trends in biotechnology, 5(10): 287-291.
16. Converse, A.O. 1993. Substrate factors limiting enzymatic hydrolysis. In Bioconversion of forest and agricultural plant residues edited by Saddler, J.N. Wallingford, UK: CAB International, pp: 93-106.
17. Hsu, T.A., 1996. Pretreatment of biomass. Handbook on bioethanol, Edited by C.E. Wyman, Washington DC, Taylor and Francis.
18. Lu, Y., B. Yang, D. Gregg, J.N. Saddler and S.D. Mansfield, 2002. Cellulase adsorption and an evaluation of enzyme recycle during hydrolysis of steam-exploded softwood residues. Applied biochemistry and biotechnology, 98(1-9): 641-654.
19. Silverstein, R.A., Y. Chen, R.R. Sharma-Shivappa, M.D. Boyette and J. Osborne, 2007. A comparison of chemical pretreatment methods for improving saccharification of cotton stalks. Bioresource Technology, 98(16): 3000-3011.

Persian Abstract

DOI: 10.5829/idosi.ijee.2014.05.02.12

چکیده

جلبک دریایی قهوه ای، گونه ی سارگاسوم به خاطر محتوای نسبتاً غنی از هالوسلولوز (۴۱/۶٪ بر اساس وزن خشک)، یک ماده اولیه مناسب برای تولید اتانول می‌باشد. پیش از ساکاریفیکاسیون توده جلبک با سلولاز تجاری، پیش تیمار شیمیایی جلبک با محلول H_2SO_4 ۱٪(v/v) و میزان ماده جامد ۵٪ به مدت ۱۵ دقیقه در ۱۲۱°C صورت گرفت. بازده تبدیل سلولوز به گلوکز بعد از ۷۲ ساعت انکوباسیون برای بایومس هیدرولیز نشده و هیدرولیز شده به ترتیب ۴۹/۸۴ و ۶۱/۵۴٪ می‌باشد. باقی مانده های جلبک پس از پیش تیمار با اسید رقیق با تخمیر همزمان با ساکاریفیکاسیون آنزیمی (SESF)، و تخمیر مجزا پس از هیدرولیز آنزیمی (SEHF) مورد آزمایش قرار گرفت. ساکارومایسیس سرویسیه برای تخمیر اتانول مورد استفاده گرفت و تبدیل سلولز به اتانول با فرآیند SESF وSEHF به ترتیب ۶۶/۹ و ۳۴/۱٪ به دست آمد.

Iranica Journal of Energy & Environment 5 (2): 209-217, 2014
ISSN 2079-2115
IJEE an Official Peer Reviewed Journal of Babol Noshirvani University of Technology
DOI: 10.5829/idosi.ijee.2014.05.02.14

BUT

Application of Partial-Mixed Semi-Continuous Anaerobic Reactor for Treating Palm Oil Mill Effluent (POME) Under Mesophilic Condition

Chou Kian Weng, Norli Ismail, Anees Ahmad

Environmental Technology Division, School of Industrial Technology,
Universiti Sains Malaysia, 11800 USM, Penang, Malaysia

Received: February 11, 2014; **Accepted** in Revised Form: June 11, 2014

Abstract: Partially mixed semi-continuous reactor was used to examine the effect of organic loading rate (OLR) and hydraulic retention time (HRT) on the mesophilic anaerobic digestion of palm oil mill effluent (POME). The performance of the reactor was evaluated with emphasis on biodegradability of POME, methane gas (CH_4) production rate and methane yield under different organic loading rates. The OLR of the anaerobic reactor increased stepwise from 1.0 to 6.0 g COD/L/day and HRT ranged from 13.3 to 80.0 days. The total chemical oxygen demand (TCOD) utilized was higher than 75% and the CH_4 percentage of the biogas was 62.00-63.00% for the OLRs studied. The methane yield coefficient (Y_{CH4}) was inversely proportional to the OLR due to the loss of biomass with effluent. The experimental observations proved that partially mixed semi-continuous reactor could perform similar to complete-mixed reactors.

Key words: Anaerobic Digestion · Mesophilic · Semi-Continuous · Palm Oil Mill Effluent (POME) · Methane Yield.

INTRODUCTION

Palm oil extraction process generates a massive amount of non-toxic but high organic strength liquid effluents, such as palm oil mill effluent (POME). Under proper operation, approximately 2.5 m^3 of POME is generated per ton of crude palm oil produced. POME is mainly contributed by a sterilization (0.9 m^3) and clarification process (1.5 m^3), in which a large amount of steam and hot water are used, along with washing water from hydrocyclone (1.0 m^3) [1]. It is a hundred times more polluted compared to domestic sewage. Anaerobic digestion is considered an effective treatment method for POME. This biological process disintegrates organic matter while generating green energy, specifically, methane gas (CH_4). The recovery of this renewable energy not only conserves cost by fuel displacement, it also represents a more acceptable alternative under the Kyoto Protocol, which aims to reduce greenhouse gas (GHG) emissions. Previous lab-scale anaerobic reactors were operated in continuous mixing mode [2-4]. The contents of most anaerobic reactors are completely mixed to ensure intimate contact between microorganisms and organic matter; prevent precipitation of dense particles and release biogas bubbles trapped in the medium. These results may enhance the anaerobic digestion process.

However, continuous mixing is not necessary in terms of attaining optimum performance; inhibitory factors are observed at higher organic loading rates (OLRs) [5]. Kim *et al*. [6] reported that non-mixed anaerobic reactors show higher gas production, given that non-mixing reactor configurations have closer microbial consortia proximity than others do. Sulaiman *et al*. [7], who conducted anaerobic digestion of POME in a semi-commercial closed digester tank, reported that vigorous mixing inhibits CH_4 production and causes a high concentration of total volatile fatty acids (TVFAs) in the system.

Corresponding Author: Chou Kian Weng, Norli Ismail, Environmental Technology Division, School of Industrial Technology, Universiti Sains Malaysia, 11800 USM, Penang, Malaysia. Tel.: +604 6532824; Fax: +604 6573678. E-mail: norlii@usm.my

Please cite this article as: Weng, C.K., N. Ismail and A. Ahmad, 2014. Application of Partial-Mixed Semi-Continuous Anaerobic Reactor for Treating Palm Oil Mill Effluent (POME) Under Mesophilic Condition. Iranica Journal of Energy and Environment, 5(2):209-217.

Seengenyoung *et al*. [8] have investigated the effect of alkaline and acid pretreatment on solubilization of solid organic matter in palm oil mill effluent (POME) and hydrogen production using enriched sludge; they have successfully converted the volatile organic compound of POME to hydrogen. Chelliapan *et al*. [9] have converted paper mill effluent to methane in anaerobic digester at OLR of 1.56 kg COD/m^3.d. Stafford [10] reported no improvement in gas yield for mixing speed between 140 and 1000 rpm; a slight reduction in biogas production at high speeds was observed due possibly due to shear forces separating hydrolytic bacteria from their polymer substrates. Mixing appears to inhibit the syntrophic oxidation of volatile fatty acids, possibly by disrupting the spatial concurrence of syntrophic bacteria and their methanogenic partners [5]. In addition, mixing systems not only affect the anaerobic efficiency, they are also often expensive to install, maintain and operate. Although many lab-scale investigations show the excellent performance of completely mixed anaerobic reactors at agitation speeds ranging from 70 to 260 rpm [2-4, 11, 12], high-speed, continuous mixing systems seem to be impractical in conventional digester tanks, since the operating volume may be up to a few thousand cubic meters, as stated by Tong and Jaafar [13]. Therefore, an efficient mixing system will be advantageous in terms of productivity and cost effectiveness [14].

Few studies evaluate the anaerobic digestion of POME using reactors with minimal mixing. To fill this information gap, this study aims to i) develop a partially mixed semi-continuous mesophilic anaerobic reactor that provides minimal disturbance (mixing) on the anaerobic process; and ii) evaluate the performance of the anaerobic reactor in treating POME. For this purpose, an intermittently mixed lab-scale reactor is used and operated at different OLRs.

MATERIALS AND METHODS

Equipment: A 3 L glass flask with a working volume of 2 L was used as the mesophilic (35°C) anaerobic reactor. The reactor was placed in a water-bath to maintain a corresponding fixed temperature. The operation cycle was based on the draw and fill principle (fed-batch mode) via a peristaltic pump. The liquid in the anaerobic reactor was in mixing condition during the effluent withdrawal to obtain homogenous (mixed) effluent. An equal volume of POME was then immediately fed after effluent withdrawal and the reactor was mixed again to enhance the contact between the newly fed POME and anaerobic biomass. The reactor was mixed for 5 min twice per day, with the aid of manual shaking to guarantee complete mixing. In addition, manual shaking minimized the tendency of the substrate to stick to the reactor wall due to scum formation.

Table 1: The characteristics of inoculum and POME used in the experiment

Parameters	Inoculum	POMEa (mean)
pH	7.4	3.7
TCOD	1.650×10^4	8.000×10^4
SCOD	0.125×10^4	2.660×10^4
PCOD	1.525×10^4	5.340×10^4
TS	2.410×10^4	4.955×10^4
VS	1.255×10^4	4.228×10^4
TSS (MVSS)	1.525×10^4	2.518×10^4
VSS (MLVSS)	1.234×10^4	2.346×10^4
TDS	0.885×10^4	2.437×10^4
VDS	0.021×10^4	1.882×10^4
TVFA	0.12×10^3	1.98×10^3

* Unit for all parameter is mg/L except pH [a]n = 30

POME: POME was collected from Malpom Industries Sdn Bhd, located in Nibong Tebal, Penang, Malaysia; and was kept in a freezer at -20°C until further detailed analysis or experiments were conducted. POME was warmed to room temperature before chemical analysis and feeding. This storage had no noticeable effect on the composition during the experimental period. The POME used in experiment is characterized and shown in Table 1.

Inoculum: The inoculum for the mesophilic reactor, taken from a scum-sludge mixture of a facultative-anaerobic pond treating POME, was obtained from a laboratory-scale anaerobic reactor operated under mesophilic condition (35 °C). Table 1 summarizes the characteristics of the inoculum.

Experimental Operation: Prior to start an experiment, 2 L of mesophilic anaerobic sludge was loaded into the reactor and then purged with nitrogen gas for 5 min to achieve anaerobic condition. The inoculum sludge was incubated at 35 °C for two weeks before the start up of the experiment. The preliminary incubation step was followed by a series of semi-continuous flow experiments using stepwise increase OLR to minimize the organic shock in the reactor. The mesophilic reactor was operated at a hydraulic retention time (HRT) of 80.0, 40.0, 32.0, 26.7, 20.0, 16.0 and 13.3 days, which corresponded to OLRs of 1.0, 2.0, 2.5, 3.0, 4.0, 5.0 and 6.0 g COD/L/day, respectively. Decreased HRT was achieved by increasing the OLR, as well as by increasing the feed flow rate (Q). The reactor

was fed and the effluents were chemically analyzed every two days. The volumetric feed applied was equivalent to 0.050, 0.100, 0.125, 0.150, 0.200, 0.250 and 0.300 L, respectively. Since the reactor was not equipped with a biomass separator or support medium, the OLR was gradually increased once a steady state was achieved, allowing for acclimatization of the microbial biomass. The steady-state value of a given parameter was defined as the mean of the consecutive measurements (n=3) for that parameter when the deviations between the observed values were less than 10% in all cases.

Analytical Methods: Different parameters of the samples were analyzed according to American Public Health and Association (APHA) standard methods for water and wastewater analysis [15]. The parameters studied were pH, total chemical oxygen demand (TCOD), soluble chemical oxygen demand (SCOD), total solids (TS), volatile solids (VS), total suspended solids (TSS), volatile suspended solids (VSS) and TVFA. TCOD and SCOD were analyzed according to the closed reflux, colorimetric method (5220 D). The particulate COD (PCOD), defined as non-soluble COD, was calculated by subtracting SCOD from TCOD. The samples were dried at 105 °C (methods 2540 B and 2540 D) to determine TS and TSS and ignited at 550 °C to measure VS and VSS (method 2540 E). TVFA (as acetic acid) was determined by distillation method (5560 C), which is a routine control test for the anaerobic digestion process. The biogas generated was collected in 5 L Tedlar gas sampling bags and the composition of CH_4 was analyzed using a portable gas analyzer (GA 2000, GEOTECH); the total volume of biogas was measured with a volumetric plastic syringe. The volumes of biogas and CH_4 were corrected to volume under standard temperature and pressure (STP).

Performance Parameters: Other than the aforementioned analytical parameters, other performance parameters were included to evaluate the start-up process, such as the fraction of organics utilized by microorganisms ($TCOD_{utilized}$) and methane yield (Y_{CH4} and B_{CH4}) of the anaerobic suspended growth reactors. $TCOD_{utilized}$, defined as the percentage of organic matter utilized by microorganisms for anaerobic metabolisms, was calculated by the following equation:

$$TCOD_{utilized} = \frac{(TCODi - TCODe)}{TCODi} x100\% \quad (1)$$

where $TCOD_i$ and $TCOD_e$ represent the TCOD concentration of raw POME and mixed effluent, respectively.

Methane yield, Y_{CH4}, was the methane conversion tool based on the organics utilized, while B_{CH4} is based on organic load:

$$Y_{CH4} (L\ CH_4/g\ COD_{utilized}) = \frac{Q_{CH4}}{Q*(TCOD_i - TCOD_e)} \quad (2)$$

$$B_{CH4} (L\ CH_4/g\ COD_{added}) = \frac{Q_{CH4}}{Q*TCOD_i} \quad (3)$$

where Q_{CH4} is the volume of methane generated per day (L CH_4/day) and Q is the volumetric feed rate of POME (L POME/day).

RESULTS AND DISCUSSION

Process Stability: The experimental results obtained at steady-state conditions for different analyzed parameters and performance parameters; calculations are summarized in Table 2. The mesophilic anaerobic digestion was carried out using progressive OLRs; the OLR of 1.0 g COD/L/day was the first and 6.0 g COD/L/day was performed at the end of this research. The influence of OLR on the pH and TVFA concentration in the mesophilic reactor were observed, as illustrated in Fig. 1. The pH remained practically constant, with values ranging between 7.3 and 7.4, which is near the inoculum pH. Previous investigations on different types of wastewater proved that the pH of a steady-state process ranged between 6.9 and 7.5 [16, 17]. The TVFA concentration was kept below 250 mg/L when OLR was increased stepwise from 1.0 to 5.0 g COD/L/day. The effective methane conversion did not allow for the accumulation of high TVFA concentration in the system. However, the pH value (4.3) significantly decreased when OLR reached the maximum value studied (6.0 g COD/L/day). For the lowest HRT studied (13.3 days), TVFA sharply increased to 8.2×10^3 mg/L. Low pH value and high TVFA concentration symbolized the destabilization and acidification of the anaerobic reactor, which may be due to the loss of biomass and sudden decrease in alkalinity. Rincon *et al*. [17] observed an appropriate buffering capacity (alkalinity) and high stability of the anaerobic digestion before the system was acidified due to high OLR. They have stated that the high buffering capacity reduced the possible acidification of the reactor by giving an

Table 2: Reactor performance at different OLR and HRT during steady state.

OLR (g COD/L/day)	1.0	2.0	2.5	3.0	4.0	5.0	6.0
HRT (days)	80.0	40.0	32.0	26.7	20.0	16.0	13.3
Process stability							
pH	7.4	7.4	7.4	7.4	7.3	7.3	4.3
TVFA, mg/L	140	170	190	200	220	250	8200
Digester effluent							
TCODe, mg/L	1.800×10^4	1.800×10^4	1.650×10^4	1.690×10^4	1.750×10^4	1.980×10^4	7.000×10^4
SCODe, mg/L	0.150×10^4	0.160×10^4	0.180×10^4	0.190×10^4	0.225×10^4	0.320×10^4	2.050×10^4
PCODe, mg/L	1.650×10^4	1.640×10^4	1.47×10^4	1.500×10^4	1.525×10^4	1.660×10^4	4.950×10^4
PCODe/TCODe, %	91.67	91.11	89.09	88.76	87.14	83.84	70.71
$TCOD_{utilized}$ (biodegradability) %	77.50	77.50	79.38	78.88	78.13	75.25	12.50
MLVSS, mg/L	1.220×10^4	1.259×10^4	1.037×10^4	0.936×10^4	0.905×10^4	$0.90^4 \times 10^4$	1.89×10^4
Biogas production & methane yield							
CH^4 composition, %	62.95	63.00	62.60	62.50	62.70	62.00	0
CH^4 production rate, L/L/day	0.348	0.673	0.799	0.936	1.187	1.267	0
Substrate utilization rate, g COD/L/day	0.775	1.550	1.984	2.366	3.125	3.763	0.750
Y CH^4, L CH^4/g COD removed	0.449	0.439	0.403	0.395	0.380	0.337	0
B CH^4, L CH^4/g COD added	0.348	0.337	0.320	0.312	0.297	0.253	0
Y/Y_o, %	95.25	92.13	85.38	83.88	80.55	71.41	-
B/B_o, %	98.35	95.13	90.29	88.14	83.84	71.59	-

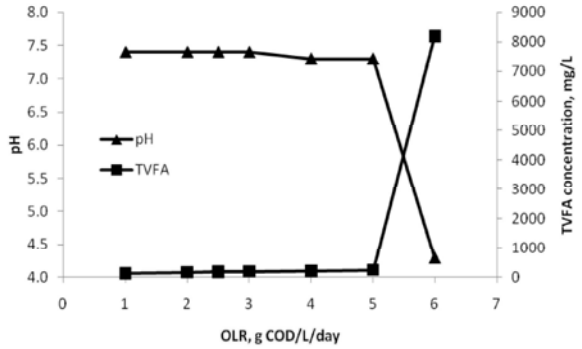

Fig. 1: Evolution of pH and TVFA with the OLR.

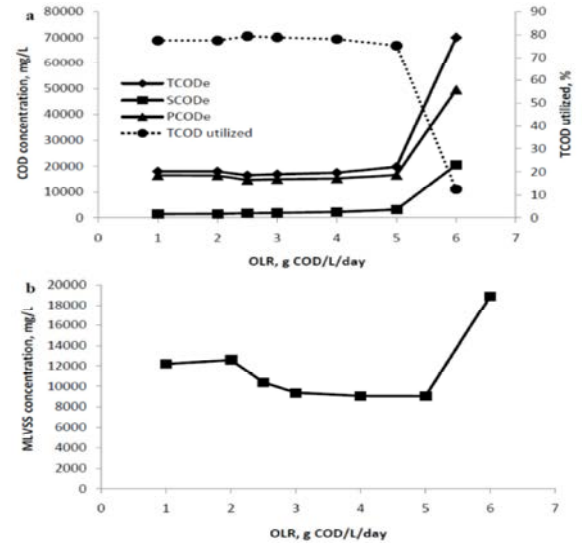

Fig. 2: Variation of the characteristics of the mixed effluent with OLR: a) $TCOD_e$, $SCOD_e$, $PCOD_e$ concentration and $TCOD_{utilized}$ and b) MLVSS

optimal pH for methanogens. The process with a TVFA/alkalinity ratio of less than 0.3-0.4 was considered one that operated favorably without acidification risk. Although the alkalinity and the TVFA/alkalinity ratio in this study were not measured, continuous monitoring on pH and TVFA was enough to examine the stability of the process.

Process Performance: As illustrated in Fig. 2a, $TCOD_e$, $PCOD_e$ and $SCOD_e$ were virtually steady when OLR increased from 1.0 to 5.0 g COD/L/day. However, $TCOD_e$ was 1.800×10^4 mg/L at an OLR of 1.0 g COD/L/day; then decreased to a minimum value of 1.650×10^4 mg/L at an OLR of 2.5 g COD/L/day; followed by a gradual increase with a further increase in OLR (Table 2). $PCOD_e$ displayed a similar development trend as $TCOD_e$. The unusual finding, high $TCOD_e$ and $PCOD_e$ observed at a low OLR, was probably due to the application of 100% inoculum to initiate anaerobic digestion. The undiluted inoculum had a high TCOD value of 1.650×10^4 mg/L, where 92.42% were in particulate form (Table 1). The excess sludge and refractory materials (PCOD) in the inoculum only washed out slowly by increasing OLR in the experiment. On the other hand, $SCOD_e$ showed a steady increase but remained at a low concentration, from 0.150×10^4 to 0.320×10^4 mg/L. All values showed a sharp increase at an OLR of 6.0 g COD/L/day. $TCOD_e$ increased from 1.980×10^4 to 7.000×10^4 mg/L; $PCOD_e$ increased from 1.660×10^4 to 4.950×10^4 mg/L; and $SCOD_e$ increased from 0.320×10^4 to 2.050×10^4 mg/L. $TCOD_{utilized}$ measured the total COD utilized by the mixed consortium of bacteria in anaerobic metabolisms, where organic load was equal to organic

effluent plus organics converted to biogas. $TCOD_{utilized}$ generally remained steady (ranged from 75.25 to 79.38%) until OLR reached 5.0 g COD/L/day. Further increase in OLR caused a marked decrease in efficiency to a minimum level of 12.50%. Although CH_4 production ceased at OLR of 6.0 g COD/L/day, a small fraction of organic matter was utilized under acidic condition for the growth of hydrolytic and acidogenic bacteria. The performance of the anaerobic reactor became virtually independent on the OLR provided the OLR of the reactor was maintained below 5 g COD/L/day. Before the inhibition of methanogenesis, $PCOD_e/TCOD_e$ fractions ranged from 83.84 to 91.67% when HRT decreased from 80.0 to 16.0 days (see Table 2). Thus, major organic matter left in the effluent was in particulate form, mainly contributed by the undigested solids and small fraction of washed out biomass. Pretreatment may be required to solubilize solids in POME prior to feeding to anaerobic digestion.

The mixed liquor volatile suspended solids (MLVSS), determined by the same method as VSS, provided a crude measurement of the biomass within the reactors; since differentiating viable cells and inert materials are extremely difficult with the mixed culture of bacteria associated with hydrolyzed intermediates and undigested POME. As shown in Fig. 2b, MLVSS was slightly high at low OLR, gradually decreasing and achieving steady concentration of 0.904×10^4 mg/L at an OLR of 5.0 g COD/L/day. This implied that a significant fraction of biomass and inert materials, already present in the reactor during start-up, were gradually washed out with increased OLR. MLVSS concentrations at OLRs of 4.0 and 5.0 g COD/L/day were similar, indicating that the amount of biomass growth was the same as the amount of biomass flushed out. Higher OLRs would have resulted in excessive loss of biomass, but MLVSS was high (1.890×10^4 mg/L) due to the contamination of TSS from feeding POME.

CH_4 Production: As shown in Fig. 3, variations were observed in the CH_4 production and substrate utilization rates. The CH_4 production rates increased almost linearly, from 0.348 to 1.187 L CH_4/L/day, with OLR up to 4.0 g COD/L/day. Then, CH_4 production rates followed a slower increment, reaching 1.267 L CH_4/L/day at an OLR of 5.0 g COD/L/day; it ceased at a higher OLR. The decrease in CH_4 production might be due to the loss of methanogens that caused a sudden increase in effluent TVFA concentration (Fig. 1). Before the inhibition of methanogenesis, the detected CH_4 compositions varied between 62.00 and 63.00% (Table 2), similar to those reported by Tong and Jaafar [13]. A linear relationship

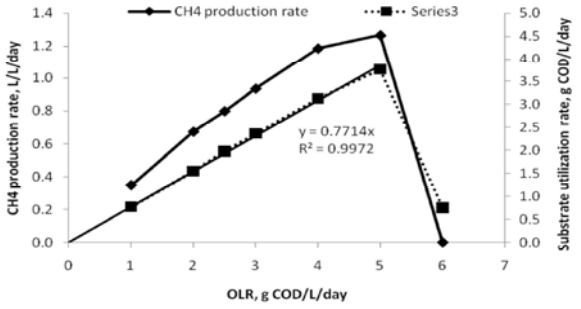

Fig. 3: Methane (CH_4) production rate and substrate utilization rate on different OLRs.

between the substrate utilization rate and OLR are presented in Fig. 3. A linear fit of all data points corresponding to OLRs in the range of 1.0 to 5.0 g COD/L/day gave a gradient of 0.7714, with a high correlation coefficient (R^2=0.9972). Thus, on average, 77.14% of input organics was biodegraded during the anaerobic digestion of POME at mesophilic temperature. However, at high OLR, a drastic decrease in efficiency was observed, coinciding with the deterioration of other parameters previously discussed.

Methane Yield Coefficient (Y_{CH4}): To understand further the relationship between substrate utilization rate and CH_4 production, the CH_4 yield coefficient (L CH_4/g $COD_{utilized}$), Y_{CH4} must be determined. The following typical equation was obtained by balancing TCOD around the anaerobic reactor:

$$Q * (TCOD_i) = Q * (TCOD_e) + Q_{CH4} * (1/Y_{CH4}) + m.V.X. \quad (4)$$

where m is the biomass maintenance coefficient (g $COD_{consumed}$/g MLVSS/d); V is the working volume of the mesophilic reactor (L); and X is the concentration of microorganisms, also known as MLVSS. Organic matter (TCOD) fed into the reactor was mostly utilized by microorganisms for CH_4 generation and cellular maintenance and a small portion will leave the reactor without any biotransformation. Thus, $TCOD_e$ also included biomass washed out from the reactor. Eq. (4) can be converted into the following equation:

$$Q * (TCOD_i - TCOD_e) = Q_{CH4} * (1/Y_{CH4}) + m.V.X. \quad (5)$$

Eq. (5) was applied by Rincon *et al*. [12] to determine the CH_4 yield coefficient and cellular maintenance coefficient for the methanogenic step of a

two-stage anaerobic digestion process treating olive mill solid residue. The following assumptions were made.

- Constant volumetric flow (Q), which is the volume of POME fed into the reactor at every experimental day, was the same as the volume of effluent withdrawn.
- Constant biomass concentration, where the biomass from the feeding substrate, POME, was too low to be determined, can therefore be ignored.

However, a significant variation of MLVSS concentration was observed in this study; and it was inversely proportional to the increase in OLR. Therefore, applying Eq. (5), by assuming a constant biomass concentration for the calculation, would be inappropriate. As proof, Fig. 4a was plotted using Eq. (5), showing the relationship between daily substrate utilization and the corresponding CH_4 production. The data points were adjusted to a straight line and the correlation coefficient (R^2) obtained was 0.9780. The CH_4 yield coefficient, Y_{CH4}, determined by the reciprocal of the slope (3.1326), was 0.319 L CH_4/g $COD_{utilized}$. However, the interception point was a negative value (-0.9189), which contradicted Eq. (5) and was therefore unable to determine the biomass maintenance coefficient (*m*). To solve the problem, Fig. 4b was plotted to demonstrate the experimental Y_{CH4} corresponding to different OLRs. The Y_{CH4} was inversely proportional to the OLRs applied. It started at 0.449 L CH_4/g $COD_{utilized}$, before gradually decreasing to 0.337 L CH_4/g $COD_{utilized}$ when OLR increased from 1.0 to 5.0 g COD/L/day. The horizontal line (0.319) corresponds to the Y_{CH4} calculated by using Eq. (5) and the value is significantly lower than all experimental Y_{CH4}. The reduction of Y_{CH4} was due to losses of biomass with effluent, as well as reduced HRT and the different experimental system configurations of previous research [12]. Thus, Eq. (5) would not be appropriate to determine the Y_{CH4} of a partially mixed semi-continuous anaerobic system without support media of immobilized biomass or recycled sludge. A second-order polynomial regression curve was then plotted (Fig. 4a) and the fitted model expressed the experimental data (R^2=0.9910) better. The curve intercepted at the y axis had a value of 0.5046 g COD/day, which can indicate the daily consumption of organic matter by the microorganisms inside the reactor. The *m* value calculated was 0.0279 g $COD_{consumed}$/g MLVSS/day, on the assumption that the MLVSS concentration was 0.904×10^4 mg/L (lowest value obtained). The low calculated value showed the low

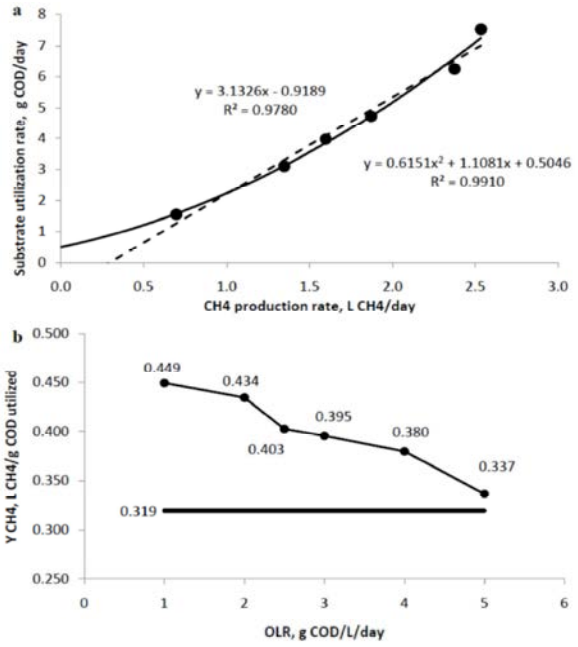

Fig. 4: Methane yield coefficient (Y_{CH4}): a) Application of typical liner regression, Eq. (10) and b) Variation of Y_{CH4} on different OLRs.

requirement of biomass for cellular maintenance. However, *m* is a combined coefficient of two distinct bacteria populations, the acidogenic and methanogenic populations. This value could be compared to the result from Rincon *et al*. [12], concluding the *m* value as 0.016 g $COD_{consumed}$/g MLVSS/day. They further pointed out that the actual value of *m* should be relatively higher than the calculated value because due to the *X* included both active biomass and non-biological solids in the reactor. The real biomass concentration, X_{real} is lower and can be determined only if the non-biological solids are removed from *X*.

Ultimate CH_4 Yield ($Y_{o\,CH4}$ and $B_{o\,CH4}$): The ultimate CH_4 yield, $Y_{o\,CH4}$, is defined as the maximum Y_{CH4} at infinite HRT, while $B_{o\,CH4}$ represents the maximum CH_4 yield at infinite HRT based on the organic loaded. Both values were determined by plotting a graph of the corresponding values versus the reciprocal of the HRT applied (Fig. 5a). The data points were fitted to a polynomial regression. By using the value of the intercepts, the $Y_{o\,CH4}$ and $B_{o\,CH4}$ determined were 0.4715 L CH_4/g $COD_{utilized}$ and 0.3539 L CH_4/g COD_{added}, respectively. The gap between the two curves implied the refractory portion of POME. Therefore, the biodegradability of POME can also be determined by the following formula:

Table 3: Performance comparison of anaerobic digestion treating different wastewater.

Wastewater	Reactor	HRT, days	OLR(g COD/L/day)	CH_4 production rate, L/L/day	TCO Dutilized, %	Reference
POME	Completely mixed, continuous flow, 35 °C	8.3	5.784	0.965	52.9	[2]
Condensation water	Completely mixed, continuous flow, 35 °C	2.7	2.088	0.573	86.7	[2]
TPOP	Stirred, daily fed, 35 °C	10.0	3.45	0.910	88.7	[17]
		12.5	6.49	1.545	88.5	[17]
		12.5	9.05	1.870	89.8	[17]
		12.5	12.02	2.120	88.4	[17]
TPOP	Completely mixed, daily fed, 35°C	20	9.5	0.9	46.8	[18]
OMSR	Stirred, daily fed, 35°C	17	9.2	1.700*	77	[15]
Acidified OMSR	Stirred, daily fed, 35°C	5	20	3.24	61.3	[16]
POME	Partial-mixed, fed per two days, 35°C	16.0	5.0	1.267*	75.25	This study

TPOP = two-phases olive pomace

OMSR = olive mill solid residue

* Values are corrected to STP conditions.

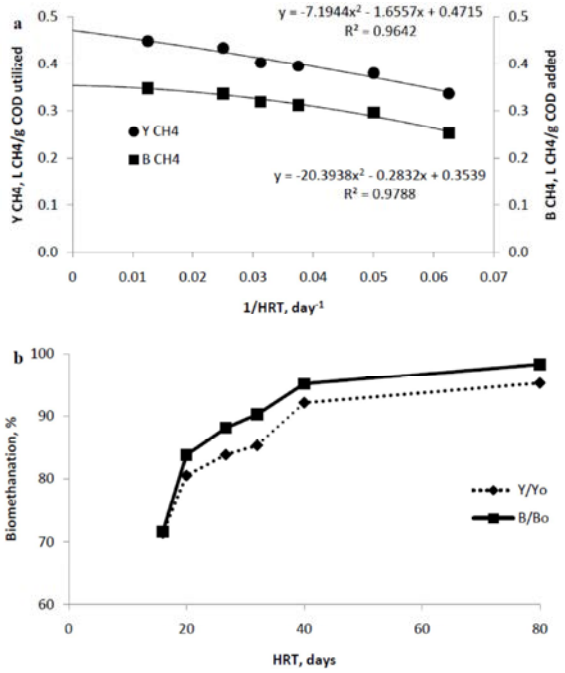

Fig. 5: Methane production efficiency: a) Determination of the ultimate methane yield coefficient based on organic utilized (Yo CH_4) and organic load (Bo CH_4) and b) Effect of HRT on biomethanation of POME.

$$\text{Biodegradability} = \frac{B}{Y} x100\% \quad (9)$$

where the calculated values are the same as those $TCOD_{utilized}$ declared previously and ranges from 75.25 to 79.38%. The biomethanation of POME based on substrate utilized (Y/Y_o) and substrate added (B/B_o) are shown and summarized in Fig. 5b. At HRT of 80.0 days (OLR=1.0 g COD/L/day), the Y/Y_o and B/B_o were very high, at 95.25 and 98.35%, respectively. The performance kept decreasing with shorter HRT, remaining at 71.51 and 71.59%, respectively, at day 16.0 of HRT. Thus, the partially mixed, semi-continuous anaerobic system only achieved good biomethanation (>70%) at HRT of 16.0 days or longer, when there was less biomass washed out.

Overall Performance: The mesophilic anaerobic reactor was operated for 100 days until the production of CH_4 ceased. The activity of methanogenic microorganisms was not impaired up to OLR of 5.0 g COD/L/day because of appropriate stability. The corresponding operation conditions at higher OLRs produced a high TVFA concentration of 8.2×10^3 mg/L, which could be applied to develop a hydrolytic-acidogenic reactor in a two-stage anaerobic digestion system. The experimental results were comparable to those of Borja *et al*. [2], who reported on the maximum CH_4 production rate for anaerobic digestion of POME at OLR near 5.8 g COD/L/day. The digester performances of previous investigations are summarized in Table 3. The experimental observations proved that partially mixed semi-continuous reactor could perform similar to complete-mixed reactors. However, reactor performance may be affected by the mixing mode. The contact between microorganisms and POME was possibly reduced by the rapid formation of scum, since the reactor was only mixed twice per day. Therefore, frequent intermittent mixing (e.g. mixing every few hours) might be a better mixing mode to enhance the microorganism-substrate contact without significantly disturbing the microbial consortia proximity. Moreover, the feeding frequency was another factor that affects the anaerobic process. For example, in this study, the anaerobic reactor was fed every two days instead of daily, which was used

in previous investigations [12, 17-20]. Given that the feeding interval was doubled, the volumetric feed rate doubled as well. The higher volumetric feed rate implied that more biomass will be washed out with the effluent and the reactor pH was affected by the higher feeding volume of acidic POME (pH=3.7). As the biomass inside the reactor was not immobilized, the slow growth of methanogenic bacteria was gradually flushed out as the volumetric feed rate, Q, increased with increased OLR. Nevertheless, the acidogenic bacteria seemed less sensitive to high OLRs. The oxygen consumption measurement in 20 hour biodegradation was a very good indicator of inhibitory effects. Inhibition started at an $OD_{20} > 17$ - 18g-O_2/kg [21].

Thus, the continuous decline in Y_{CH4} was affected by the considerable biomass loss with the effluent. In turn, the system became unable to support higher OLRs. A separation device for sludge recycling [4] or a support media for biomass immobilization [12] may be suitable to ensure sufficient and constant microorganism concentration inside the reactor.

CONCLUSIONS

The partially mixed semi-continuous mesophilic reactor prevailed at the methanogenic condition at OLR of =5.0 g COD/L/day (HRT=16.0), while the system shifted to acidogenic condition at higher OLRs and shorter HRT. CH_4 production stopped at an OLR of 6.0 g COD/L/day. The biodegradability of POME was previously more than 75%, with CH_4 compositions varying from 62.00 to 63.00%. The experimental results concurred with previous studies. In conclusion, continuously mixing in anaerobic digestion is not necessary; intermittent mixing is be preferable in continuous operation, in terms of cost saving. The application of typical linear regression to determine the Y_{CH} of present system is inappropriate, as well. The Y_{CH4} observed was inversely proportional to OLR, which may be linked to the loss of biomass with a higher OLR and lower HRT.

ACKNOWLEDGEMENT

The authors gratefully acknowledge the research facilities by School of Industrial Technology and Universiti Sains Malaysia for granting RUI grant (1001/PTEKIND/814147) for the financial support of this study.

REFERENCES

1. Ma, A. and A.S. Ong, 1985. Pollution control in palm oil mills in Malaysia. Journal of the American Oil Chemists' Society, 62(2): 261-266.
2. Borja, R., C. Banks, A. Martin and B. Khalfaoui, 1995. Anaerobic digestion of palm oil mill effluent and condensation water waste: an overall kinetic model for methane production and substrate utilization. Bioprocess Engineering, 13(2): 87-95.
3. Borja, R., A. Martin, C. Banks, V. Alonso and A. Chica, 1995. A kinetic study of anaerobic digestion of olive mill wastewater at mesophilic and thermophilic temperatures. Environmental Pollution, 88(1): 13-18.
4. Şentürk, E., M. Ince and G. Onkal Engin, 2010. Kinetic evaluation and performance of a mesophilic anaerobic contact reactor treating medium-strength food-processing wastewater. Bioresource Technology, 101(11): 3970-3977.
5. Stroot, P.G., K.D. McMahon, R.I. Mackie and L. Raskin, 2001. Anaerobic codigestion of municipal solid waste and biosolids under various mixing conditions—I. Digester performance. Water Research, 35(7): 1804-1816.
6. Kim, M. and R. Speece, 2002. Aerobic waste activated sludge (WAS) for start-up seed of mesophilic and thermophilic anaerobic digestion. Water Research, 36(15): 3860-3866.
7. Sulaiman, A., M.A. Hassan, Y. Shirai, S. Abd-Aziz, M. Tabatabaei, Z. Busu and S. Yacob, 2009. The effect of mixing on methane production in a semi-commercial closed digester tank treating palm oil mill effluent. Australian Journal of Basic & Applied Sciences, 3(3): 1577-1583.
8. Seengenyoung, J., P. Prasertsan and S.O. Thong, 2013. Biohydrogen Production from Palm Oil Mill Effluent Pretreated by Chemical Methods Using Thermoanaerobacterium-Rich Sludge. Iranica Journal of Energy & Environment, 4(4): 312-319.
9. Chelliapan, S., S.B. Mahat, M.F.M. Din, A. Yuzir and N. Othman, 2012. Anaerobic digestion of paper mill wastewater. Iranica Journal of Energy & Environment, 3(2): 85-90.
10. Stafford, D., 1982. The effects of mixing and volatile fatty acid concentrations on anaerobic digester performance. Biomass, 2(1): 43-55.
11. Choorit, W. and P. Wisarnwan, 2007. Effect of temperature on the anaerobic digestion of palm oil mill effluent. Electronic Journal of Biotechnology, 10(3): 376-385.

12. Rincón, B., R. Borja, M. Martín and A. Martín, 2010. Kinetic study of the methanogenic step of a two-stage anaerobic digestion process treating olive mill solid residue. Chemical Engineering Journal, 160(1): 215-219.
13. Tong, S. and A.B. Jaafar, 2004. Waste to energy: methane recovery from anaerobic digestion of palm oil mill effluent. Energy Smart, 4: 1-8.
14. Ward, A.J., P.J. Hobbs, P.J. Holliman and D.L. Jones, 2008. Optimisation of the anaerobic digestion of agricultural resources. Bioresource technology, 99(17): 7928-7940.
15. APHA. Standard Methods for the Examination of Water and Wastewater, 21st ed. American Public Health Association. Washington DC, USA (2005).
16. Faisal, M. and H. Unno, 2001. Kinetic analysis of palm oil mill wastewater treatment by a modified anaerobic baffled reactor. Biochemical Engineering Journal, 9(1): 25-31.
17. Rincón, B., R. Borja, J. González, M. Portillo and C. Sáiz-Jiménez, 2008. Influence of organic loading rate and hydraulic retention time on the performance, stability and microbial communities of one-stage anaerobic digestion of two-phase olive mill solid residue. Biochemical Engineering Journal, 40(2): 253-261.
18. Rincón, B., R. Borja, M. Martín and A. Martín, 2009. Evaluation of the methanogenic step of a two-stage anaerobic digestion process of acidified olive mill solid residue from a previous hydrolytic-acidogenic step. Waste management, 29(9): 2566-2573.
19. Borja, R., A. Martín, B. Rincón and F. Raposo, 2003. Kinetics for substrate utilization and methane production during the mesophilic anaerobic digestion of two phases olive pomace (TPOP). Journal of Agricultural and Food Chemistry, 51(11): 3390-3395.
20. Borja, R., A. Martin, E. Sánchez, B. Rincón and F. Raposo, 2005. Kinetic modelling of the hydrolysis, acidogenic and methanogenic steps in the anaerobic digestion of two-phase olive pomace (TPOP). Process Biochemistry, 40(5): 1841-1847.
21. Evans, E.A., K.M. Evans, A. Ulrich and S. Ellsworth, 2011. Anaerobic processes. Water Environment Research, 83(10): 1285-1332.

Persian Abstract

DOI: 10.5829/idosi.ijee.2014.05.02.13

چکیده

راکتور نیمه پیوسته اختلاط جزیی برای ارزیابی تاثیر نرخ بار آلی (OLR) و زمان ماند هیدرولیکی (HRT) جهت تصفیه بیهوازی مزوفیلیک پساب کارخانه روغن نخل (POME) مورد استفاده قرار گرفت. کارایی راکتور توسط زیست تخریب پذیری POME، نرخ تولید گاز متان (CH_4)، و بازده تولید متان تحت نرخهای بار آلی متفاوت ارزیابی گردید. بار آلی راکتور بیهوازی از ۱ به ۲ g COD/L/day و HRT از ۱۳ به ۸۰ افزایش یافت. تمامیت اکسیژن مورد نیاز شیمیایی (TCOD) مورد استفاده از ۷۵٪ بیشتر شده و در صد متان بیوگاز ۶۳-۶۲٪ به دست آمد. ضریب بازده متان (Y_{CH4}) رابطه معکوس با OLR داشته که این به علت کاهش میزان بایومس با جریان پساب بوده است. مشاهدات آزمایش‌ها نشان می‌دهد که راکتور نیمه پیوسته اختلاط جزیی می‌تواند عملکردی مشابه با راکتورهای اختلاط کامل داشته باشد.

Iranica Journal of Energy & Environment 5 (2): 218-223, 2014
ISSN 2079-2115
IJEE an Official Peer Reviewed Journal of Babol Noshirvani University of Technology
DOI: 10.5829/idosi.ijee.2014.05.02.15

BUT

Rice Husk Silica Adsorbent for Removal of Hexavalent Chromium Pollution from Aquatic Solutions

[1]Seyed Mahmoud Mehdinia, [1]Khalilollah Moeinian and [2]Tayyabeh Rastgoo

[1]Department of Environmental Health Engineering, Damghan Faculty of Health, Semnan University of Medical Sciences, Semnan, Iran
[2]Department of Environmental Health Engineering, Damghan Faculty of Health, Semnan University of Medical Sciences, Semnan, Iran and Department of Environment Engineering, Faculty of Environment and Energy, Science and Research Branch, Islamic Azad University,Tehran, Iran

Received: May 13, 2014; **Accepted** in Revised Form: June 8, 2014

Abstract: The present study investigates the effectiveness of a new adsorbent prepared from agricultural wastes, namely rice husk silica as well as raw rice husk and rice bran to remove Cr^{+6} from aquatic solutions. The raw rice husk was collected from North of Iran. But rice husk silica was prepared by burning of clean rice husk inside a muffle furnace at a temperature of 800°C for 4 hours after acid leaching. The effects of four parameters: contact time (30 to 90 min), pH values (2 to 9), adsorbents dosages (0.5 to 1.5 g/L) and initial concentration (1.0 to 15 mg/L) were investigated to remove Cr^{+6}. The silica derived from rice husk showed a high percentage of SiO_2 up to 94.24%. But carbon was the highest element in raw rice husk up to 35.92%. The maximum removal efficiency (RE) of Cr^{+6} was obtained by rice bran up to 98.8% at 5.0 mg/L initial concentration of Cr, 60 min of contact time, pH = 2 and adsorbents dosage of 1.0 g/L. However, at the same condition the maximum RE by raw rice husk and rice husk silica were 82.3 and 88.4%, respectively. Moreover, a negative strong significant correlation between increasing of initial concentration of Cr^{+6} and RE was detected by the three adsorbents ($p<0.01$). In conclusion, raw rice husk and adsorbents prepared from it such as rice husk silica could be considered as effective and inexpensive adsorbents for removal of $Cr^{+6}$from aquatic solutions.

Key words: Environmental pollution · Heavy metals · Hexavalent chromium · Removal efficiency · Rice husk silica

INTRODUCTION

Heavy metals are considered as important environmental pollutants, because of their toxicity for environment and human [1, 2]. Hexavalent chromium (Cr^{+6}) is a usual and very toxic pollutant introduced into different water sources from a variety of industrial process [3]. Chromium is in either Cr (III) or Cr (VI) oxidation statuses, as all other oxidation conditions are not stable in aquatic environment. The Cr^{+6} is 100-1000 times more toxic to organisms than Cr^{+3} and more readily transported into soils [4]. Commercial activated carbons and carbon nanotube have been extensively used for removal of heavy metals from aquatic environment and other adsorption processes [5]. Because using commercial activated carbon is expensive to remove pollutants; thus, today a large and considerable study are finding inexpensive adsorbents instead of expensive one[6]. Today, especial attention has been devoted to the study of elimination of heavy metals from water and wastewater by adsorption using agricultural wastes [7-19]. The main goal of this study was to synthesis and application of an inexpensive adsorbent derived from rice husk and its application to remove hexavalent chromium pollutant. Hence, present study investigated the effectiveness of a new adsorbent prepared from agricultural wastes, namely rice husk silica as well as raw rice husk and rice bran to remove hexavalent chromium from aquatic solutions.

Corresponding Author: Khalilollah Moeinian, Department of Environmental Health Engineering, Damghan Faculty of Health, Semnan University of Medical Sciences, Semnan, Iran.
Tel: +989133105012, Fax: +982335239778, E-mail: khalilollah@yahoo.com

Please cite this article as: Mehdinia, S.M. K. Moeinian, T. Rastgoo, 2014. Rice husk silica adsorbent for removal of hexavalent chromium pollution from aquatic solutions. Iranica Journal of Energy and Environment, 5(2):218-223.

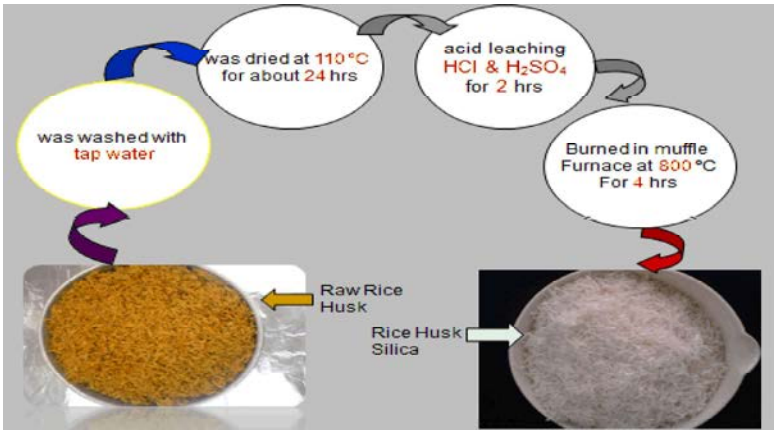

Fig. 1: A schematic process to preparation of silica from raw rice husk

MATERIALS AND METHODS

The batch removal of Cr^{+6} from aqueous solution using three low-cost adsorbents: raw rice husk, rice bran and rice husk silica under different experimental conditions were investigated. The raw rice husk and rice bran was collected from North of Iran and the rice husk silica was prepared according to the method proposed by Jamwal and Mantri [20]. Base on this method, the raw rice husk was first washed with tap water to remove the contaminants and then it was dried in an oven at 110°C for 24 hrs. After that, it was subjected to acid leaching by refluxing it in 3% (v/v) chloridric acid (HCL) and 10% (v/v) sulphuric acid (H_2SO_4) for 2 hours and at a ratio of 50 g husk/L. The husk was thoroughly washed with distilled water and then dried in an air oven at 100°C. Finally, it was burned inside a muffle furnace at temperature of 800°C for 4 hours in static air. A schematic process to preparation of silica from raw rice husk is showed in Figure (1).

In this study, the effects of four parameters: contact time (30, 45, 60, 75 and 90 min), pH values (2, 3, 4, 5, 6, 7, 8 and 9), adsorbents dosages (0.5, 1.0 and 1.5 g/L) and initial concentration of Cr^{+6} (1.0, 5, 10 and 15 mg/L) were investigated by varying any of the process parameters and keeping the other parameters constant. The experiments were carried out in batch reactors and at room temperature of 25±2°C. The synthetic solution containing chromium was ready by dissolving the known amount of analytical-grade potassium dichromate in distilled water. The concentrations of chromium were measured using a standard method of atomic adsorption. The Eq. (1) was used to determination of removal efficiency:

$$RE(\%) = \frac{(C_0 - C)}{C_0} \times 100$$

where RE is the removal efficiency (%), C_o and C are the inlet and outlet concentration of hexavalent chromium (mg/L) [21-24].

RESULTS AND DISCUSSION

The physico-chemical characteristics of the adsorbents showed that carbon is the highest element percentage of the CHN analysis in the raw rice husk, but the silica derived from rice husk showed a high percentage of SiO_2 up to 94.24%. Some of the important physico-chemical characteristics of the rice husk silica and raw rice husk used in this study are summarized in Table 1.

The Scanning Electron Microscope (SEM) of the adsorbents showed that, when the raw rice husk goes under on the acid leaching and combustion processes at high temperature, it reduces the crystallization cells and increases its porosity. This issue can increase the adsorption rate of the adsorbents (Figure 2).

For the investigation of the effect of pH, hexavalent chromium removal experiments at various values of pH 2, 3, 4, 5, 6, 7, 8 and 9 while keeping the other parameters constant (initial concentration of hexavalent chromium = 5.0 mg/L, adsorbents dosage = 1.0 g/L and contact time = 60 min) were studied. The results of removal efficiency of hexavalent chromium at different values of pH by the three adsorbents are shown in Figure 3.

The removal efficiency of Cr^{+6} at different contact times (30, 45, 60, 75 and 90 min), pH=2, adsorbents dosage = 1.0 g/L, initial concentration of Cr^{+6} = 5.0 mg/L by the three adsorbents is shown in Figure 4.

Effects of the adsorbents dosages (0.5, 1.0 and 1.5 g/L) on removal efficiency of hexavalent chromium at pH = 2, initial concentration of hexavalent chromium = 5.0 mg/L and contact time = 60 min are shown in Figure 5.

Table 1: Some of the important physico-chemical properties of the rice husk silica and raw rice husk used in this study

Raw Rice Husk			Rice Husk Silica		
Physico-chemical characteristics	Unit	Value	Physico-chemical characteristics	Unit	Value
Density	(g/L)	93.3	Density	(g/L)	44.5
pH	-	6.7	pH	-	7.5
C	(%)	35.92	C	(%)	0.09
H	(%)	4.84	H	(%)	0.16
N	(%)	0.42	N	(%)	0.14
SiO_2	(%)	NM*	SiO_2	(%)	94.24

NM* = not measured

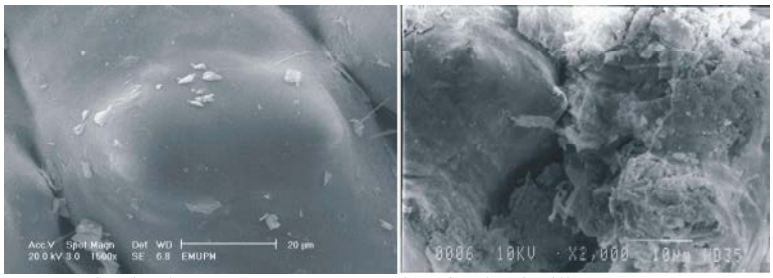

a) Raw rice husk b) Rice husk silica

Fig. 2: Scanning Electron Microscope (SEM), a) raw rice husk and b) rice husk silica

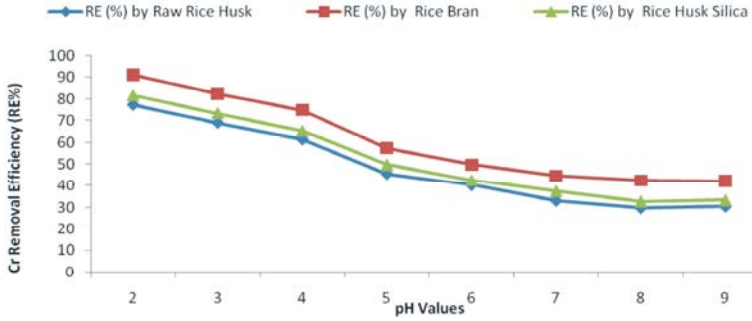

Fig. 3: Cr^{+6} removal efficiency by raw rice husk, rice bran and rice husk silica at variable pH values, adsorbents dosage of 1.0 g/L, 5.0 mg/L initial concentration of Cr^{+6} and 60 min of contact time.

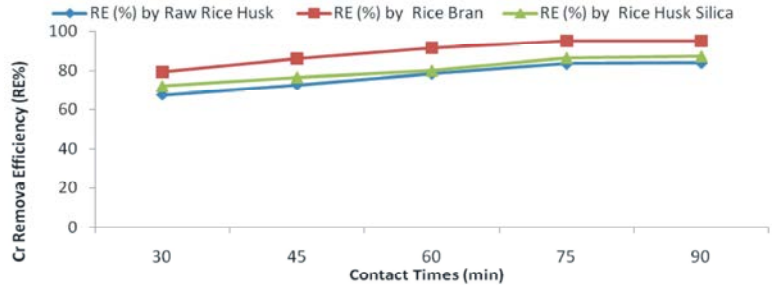

Fig. 4: Removal efficiency of $Cr^{+6}$with variable contact times at pH = 2, adsorbent dosage = 1.0 g/L and initial concentration = 5.0 mg/L by three adsorbents.

In addition, in this research the correlation between increasing of initial concentration of Cr^{+6} and removal efficiency was studied using the Pearson correlation analysis. For this purpose the correlation between increasing of initial concentration of Cr^{+6} (1, 5, 10 and 15 mg/L) at pH = 2, adsorbents dosage = 1.0 g/L and contact time = 60 min were studied. The results are illustrated in Figure 6.

The experimental data were also fitted using two adsorption models including Freundlich and Longmuir. The constants coefficients for Freundlich and Langmuir adsorption isothermsare summarized in Table 2.

The value of media pH is very important to remove Cr^{+6}, which is the toxic type of chromium. The result of this study showed that the adsorption of hexavalent chromium is highly pH-dependent and the best pH for

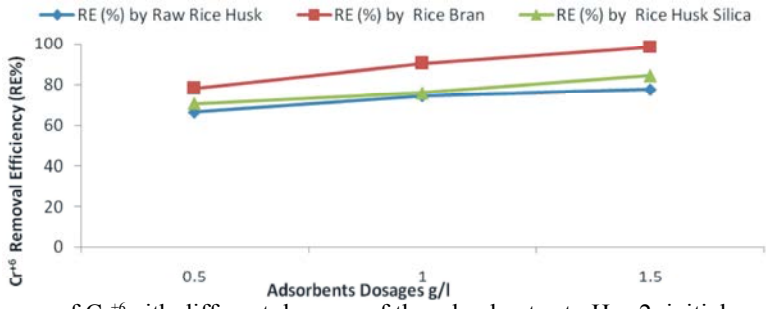

Fig. 5: Removal efficiency of $Cr^{+6}$with different dosages of the adsorbents at pH = 2, initial concentration of Cr^{+6}= 5.0 mg/L and contact time = 60 min by the three adsorbents.

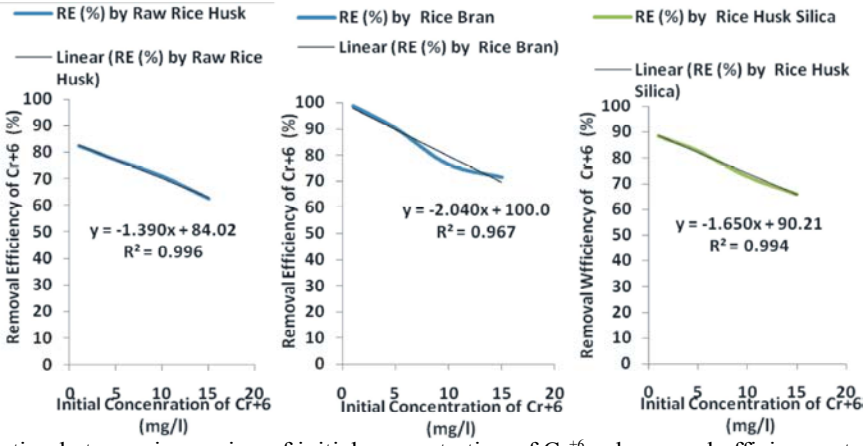

Fig. 6: The correlation between increasing of initial concentration of $Cr^{+6}$and removal efficiency at pH = 2, adsorbents dosage of 1.0 g/L and contact time of 60 min by the three adsorbents.

Table 2: Constants coefficients for Freundlich and Langmuir adsorption isotherms

	Langmuir Coefficients			*Freundlich Coefficients*		
Adsorbents	q_{max}(mg/g)	b (l/mg)	R^2	K (mg/g)	n	R^2
Raw rice husk	*13.30*	*0.38*	*0.9978*	*3.87*	*1.39*	*0.9865*
Rice bran	*7.13*	*16.28*	*0.9884*	*5.85*	*2.60*	*0.9966*
Rice husk silica	*9.18*	*0.98*	*0.9386*	*3.82*	*1.57*	*0.9801*

q_{max} = Amount adsorbed on the surface; b = Isotherm constant; K, n = Isotherm constants

the removal of hexavalent chromium was found to be acidic condition at pH value of 2 for the three adsorbents. This result is in agreement with reported data by Khazaei *et al*. [14] which showed the optimum initial pH was observed at pH = 2.0 to remove hexavalent chromium using agricultural waste. Demirbas *et al*. [8] reported an optimum pH of 1.0 for adsorption of hexavalent chromium ions from aqueous solutions using activated carbons prepared from agricultural wastes. However to remove cadmium, zinc and lead, Kafika *et al*. [16] have reported an increasing of heavy metals adsorption with increasing of pH.

In this study, the maximum removal efficiency of hexavalent chromium was obtained by rice bran up to 98.8% at 5.0 mg/L initial concentration of hexavalent chromiun, 60 min of contact time, pH = 2 and adsorbents dosage of 1.0 g/L. However, at the same condition the maximum removal efficiency by raw rice husk and rice husk silica obtained 82.3 and 88.4%, respectively. A removal efficiency of hexavalent chromium up to 42% with 30 min contact time using activated carbon derived from rice husk was obtained. However, a maximum removal efficiency of hexavalent chromium up to 61% with 180 min contact time was reported[25]. Moreover, a negative strong significant correlation between increasing of initial concentration of hexavalent chromium and removal efficiency was detected by the three adsorbents ($p<0.01$). Khazaie *et al*. [14] reported a decreasing removal adsorption of hexavalent chromium with increasing of initial concentration. They pointed out that "at low

concentrations the ratio of available surface to initial hexavalent chromium is larger; therefore, the removal becomes independent of initial concentrations. However, in the case of higher concentrations this ratio is low; the percentage removal then depends upon the initial concentration" [14].

CONCLUSION

Based on obtained results, raw rice husk and adsorbents prepared from it such as rice bran and rice husk silica could be considered as effective and inexpensive adsorbents for the removal of hexavalent chromium from aquatic solutions. High removal efficiency, easy and inexpensive way to preparation of the adsorbents from raw rice husk could be the advantages of their application in removal of heavy metals.

ACKNOWLEDGEMENTS

Authors would like to acknowledge Semnan University of Medical Sciences for the financial support through research project no.: 418.

REFERENCES

1. Kobya, M., E. Demirbas, E. Senturk and M. Ince, 2004. Adsorption of heavy metals ions from aqueous solutions by activated carbon prepared from apricort Stone, Bioresource Technology, 96(13): 1518-1521.
2. Ghaneian, M.T., B. Jamshidi, M. Amrollahi and M. Dehvari, 2014. Application of biosorption process by pomegranate seed powder in the removal of hexavalent chromium from aquatic environment, Koomesh, 15(2): 206-211.
3. Donmez, D. and Z. Aksu, 2002. Removal of chromium (VI) from saline wastewaters by dualilla species, Process Biochemistry, 38(5): 751-762.
4. Karthikeyan, T., S. Rajgopal and L.R. Miranda, 2005.Chromium (VI) adsorption from aqueous solution by Hevea Brasilinesis sawdust activated carbon, Journal of Hazardous Materials, (124): 192-199.
5. Monemtabary S., M. Shariati Niasar, M. Jahanshahi and A.A. Ghoreyshi, 2013. Equilibrium and Thermodynamic Studies of Methane Adsorption on Multi-Walled Carbon Nanotube. Iranica Journal of Energy & Environment 4 (1) Special Issue on Nanotechnology, pp: 17-23.
6. Abdel-Ghani, N.T., M. Hefny and G.A.F. El-Chaghaby, 2007. Removal of lead from aqueous solution using low cost abundantly available adsorbents. International Journal of Environmental Science, 4(1): 67-73.
7. Mahvi, A.H., B. Bina and A. Saeidi, 2002. Heavy metal removal from industrial effluents by natural fibers, Water and Wastewater, (43): 2-5.
8. Demirbas, E., M. Kobya, E. Elif Senturk and T. Ozkan, 2004. Adsorption kinetics for the removal of chromium (VI) from aqueous solutions on the activated carbons prepared from agricultural wastes. Water SA., 30(4): 533-540.
9. Gueu, S., B.A. yao, K. douby and G. Ado, 2007. Kinetics and thermodynamics study of lead adsorption on to activated carbons from coconut and seed hull of the Palm trees. Environmental Science & Technology, 4(1): 11-17.
10. El-Ashtoukhy, E.S.Z., N.K. Amin and O. Abdelwahab, 2008. Removal of lead (II) and copper (II) from aqueous solution using pomegranate peel as a new adsorbent, Desalination, (223): 162-173.
11. Shamohammadi, Z., H. Moazed, N. Jaafarzadeh and P. Haghighat Jau, 2008. Removal of Low Concentrations of Cadmium from Water using Improved Rice Husk.Water and Waste Wáter, (67): 27-33.
12. Montazeri, N., E. Baher, Z. Barami and M. Ghochi-Baygi, 2009. Kiwi role in eliminating environmental pollution and its affecting factors. Journal of Sciences and Techniques in Natural Resources, 5(1): 118-128.
13. Blazquez, G.M.A. and M. Martin-Calero, 2011. Batch biosorption of lead (II) from aqueous solutions by olive tree pruning waste: Equlibrrum ,Kinetics and thermodynamic study. Chemical Engineering Journal, (168): 170-177.
14. Khazaei, I., M. Aliabadi and H.T. Hamed –Mosavian, 2011. Use of Agricultural Waste for Removal of Cr (VI) from Aqueous Solution. Iranian Journal of Chemical Engineering, 8(4): 11-23.
15. Egila, J.N., B.E.N. Daudu, Y.A. lyak and T. Jimoh, 2012. Agricultural waste as a low cost adsorbent for heavy metal removal from waste wáter. International Journal of the Physical Sciences, 6(8): 2152-2157.
16. Kafia, M. and S. shareef, 2012. Atrieultural wastes as low cost adsorbent for Pb removal: Kinnetice, Equilibrium and Thermodynamlcs. International Journal of Chemistry, 3(3): 103-112.

17. Salari, B. and M. Shahmohammadi, 2012. Examination of kinetic the removal of nickel from aqueous solutions by Rafsanjan Pistachio Shell. Journal of Environmental Studies, (60): 149-156.
18. Ghorbani M., H. Eisazadeh and A.A. Ghoreyshi, 2012. Removal of Zinc Ions from Aqueous Solution Using Polyaniline Nanocomposite Coated on Rice Husk. Iranica Journal of Energy & Environment, 3(1): 66-71.
19. Ilaboya I.R., E.O. Oti, G.O. Ekoh and L.O. Umukoro, 2013. Performance of Activated Carbon from Cassava Peels for the Treatment of Effluent Wastewate. Iranica Journal of Energy & Environment, 4(4): 361-375.
20. Jamwal, R.S. and S. Mantri, 2007. Utilisation of rice husk for derivation chemicals. nandini consultancy, global information source for chemical, pharmaceutical and allied industries. 2007. Available from: http:// www.nandinichemical.com/ 2007febjournal.html.
21. Kun, E., 2005. Development of a Foamed Emulsion Bioreactor for Air Pollution Control. Ph.D Thesis in Chemical and Environmental Engineering, University of California Reverside, USA.
22. Taghipour, H., M.R. Shahmansoury, B. Bina and H. Movahdian, 2006. Comparison of the biological NH_3 removal characteristics of a three stage biofilter with a one stage biofilter. International Journal of Environmental Science and Technology, 3(4): 417-424.
23. Mehdinia, S.M., P. Abdul- Latif, A. Makmom-Abdullah and H. Taghipour, 2011. Synthesize and characterization of rice husk silica to remove the hydrogen sulfide through the physical filtration system. Asian Journal of Scientific Research, (4): 246-254.
24. Mehdinia, S.M., P. Abdul-Latif, H. and Taghipour, 2013. Removal of Hydrogen Sulfide by Physico-biological Filter, Using mixed Rice Husk Silica and Dried Activated Sludge, Clean Soil, Air, Water, 41(10): 949-954.
25. Dabrowski, A., 2000. Adsorption from Theory to Practice. Adventure Colloid Interface Science, 93: 135-224.

Persian Abstract

DOI: 10.5829/idosi.ijee.2014.05.02.14

چکیده

مطالعه حاضر، تاثیر یک جاذب جدید تهیه شده از ضایعات کشاورزی بنام سیلیکای شلتوک برنج و نیز شلتوک خام و سبوس برنج را در حذف کروم شش ظرفیتی از محلول های آبی مورد بررسی قرار می دهد. شلتوک خام از کارخانجات شالیکوبی شمال ایران و سیلیکای شلتوک برنج از طریق مراحل اسیدشویی و سپس حرارت دادن در کوره با دمای ۸۰۰ درجه سانتی گراد به مدت ۴ ساعت ، تهیه گردیده است. اثرات ۴ فاکتور شامل: زمان تماس (۳۰ تا ۹۰ دقیقه)، مقادیر pH (۲ تا ۹)، دزهای جاذب (۰/۵ تا ۱/۵ گرم در لیتر) و غلظت اولیه (۱ تا ۱۵ میلی گرم در لیتر) برای حذف کروم شش ظرفیتی بررسی گردید. سیلیکای حاصل از شلتوک برنج درصد بالایی از سیلیس به مقدار ۹۴/۲۴ درصد را نشان داده است اما در شلتوک خام بالاترین درصد عناصر، مربوط به کربن و به میزان ۳۵/۹ درصد بوده است. بالاترین میزان حذف کروم شش ظرفیتی در شرایط ۵ میلی گرم در لیتر غلظت اولیه کروم، زمان تماس ۶۰ دقیقه، pH برابر ۲ و جرم جاذب ۱ گرم در لیتر توسط سبوس برنج و به میزان ۹۸/۸ درصد و در شرایط مشابه، ماکزیمم حذف توسط شلتوک خام و سیلیکای شلتوک برنج به ترتیب برابر ۸۲/۳ و ۸۸/۴ درصد بوده است. علاوه بر این، همبستگی قوی و معنی دار منفی بین افزایش غلظت اولیه کروم و کارایی حذف کروم توسط هر سه جاذب مشاهده شده است ($P<0.01$). نتایج حاصل از این تحقیق نشان می دهد که شلتوک خام و جاذب های تهیه شده از آن نظیر سیلیکای حاصل از شلتوک برنج می توانند بعنوان جاذب های ارزان و مؤثر در حذف کروم شش ظرفیتی از محلولهای آبی مورد توجه قرار گیرند.